Santos Figueroa, LE.; Moragues Pons, ME.; Climent Terol, E.; Agostini, A.; Martínez Mañez, R.; Sancenón Galarza, F. (2013). Chromogenic and fluorogenic chemosensors and reagents for anions. A comprehensive review of the years 2010-2011. Chemical Society Reviews. 42(8):3489-3613. doi:10.1039/C3CS35429F.

Chromogenic and fluorogenic chemosensors and reagents for anions. A comprehensive review of the years 2010-2011

Luis E. Santos-Figueroa,[a,b,c] María E. Moragues,[a,b,c] Estela Climent,[a,b,c] Alessandro Agostini,[a,b,c] Ramón Martínez-Máñez,[a,b,c] Félix Sancenón [a,b,c]

[a] Centro Interuniversitario de Reconocimiento Molecular y Desarrollo Tecnológico, (IDM), Unidad Mixta Universidad Politécnica de Valencia – Universitat de València, Spain.

[b] Departamento de Química. Universidad Politécnica de Valencia. Camino de Vera s/n. E-46022, Valencia, Spain.

[c] CIBER de Bioingeniería, Biomateriales y Nanomedicina (CIBER-BBN).

This review focuses on examples reported in the years 2010-2011 dealing with the design of chromogenic and fluorogenic chemosensors or reagents for anions.

1.- Introduction

The supramolecular chemistry of anions is still one fertile area of research in the supramolecular chemistry field.[1,2,3,4,5,6] Nowadays, most reported examples of chemosensors or reagents for anions still use one of the following three main approaches: (i) the "binding site-signaling subunit" protocol, (ii) the "displacement" approach and (iii) the "chemodosimeter" paradigm. In the first approach, "binding sites" and the optical "signaling subunit" are covalently bonded in such a way that the interaction of the anion with the binding

site induces electronic modulations in the signaling unit, resulting in color or emission changes.[7,8,9] In the displacement protocol, "binding sites" and "signaling subunits" are not covalently bonded but form a molecular ensemble.[10,11] In this case, the coordination of a certain anion to the binding site results in the displacement of the signaling subunit, which is usually accompanied with optical changes. Finally, the "chemodosimeter" approach takes advantage of anion-induced chemical reactions, usually irreversible, which results in changes in fluorescence or color.[12,13] Moreover, increasing interest is shown in the development of new sensing paradigms, most of which usually involve the use of nanomaterials.

This review aims to be a complete compilation of the examples published in 2010 and 2011 relating to the design of chromogenic and fluorogenic chemosensors or reagents for small anions. Moreover, although they are not strictly anions, the review also includes chromo-fluorogenic systems for the detection of amino acids.[14] We have not included examples of probes to recognize large anionic macromolecules such as DNA, etc. This review is a continuation of previous comprehensive reviews reported by us recently.[15] It was our aim to include a scheme of the probe and a short comment on chemosensor performance for each example. Diagrams of the coordination or reaction occurring between the probe and the corresponding anion have been included in some examples for clarity. The review is divided into two main sections: (a) chromogenic and (b) fluorogenic chemosensors and reagents. Moreover, each section is divided into examples following (i) the binding site – signalling unit protocol, (ii) the displacement approach, (iii) the chemodosimeter paradigm and (iv) the use of hybrid materials.

2.- Chromogenic anion chemosensors and reagents

2.1.- The binding site-signalling subunit approach

This is still a very popular approach for the development of chromogenic and fluorogenic anion probes. The examples included here have been especially designed to offer color changes, whereas most examples in which an emission modulation is also observed are included in the "Fluorogenic anion chemosensors and reagents" section (*vide infra*). The examples below are organized according to a classification based on the signaling unit. A weak point in this approach is that the interaction of the anion with binding sites usually relies on relatively weak hydrogen bonding interactions or anion-induced deprotonation and, in most cases, optical modulations are observed only in organic solvents.

2.1.1.- Containing nitroaromatic derivatives

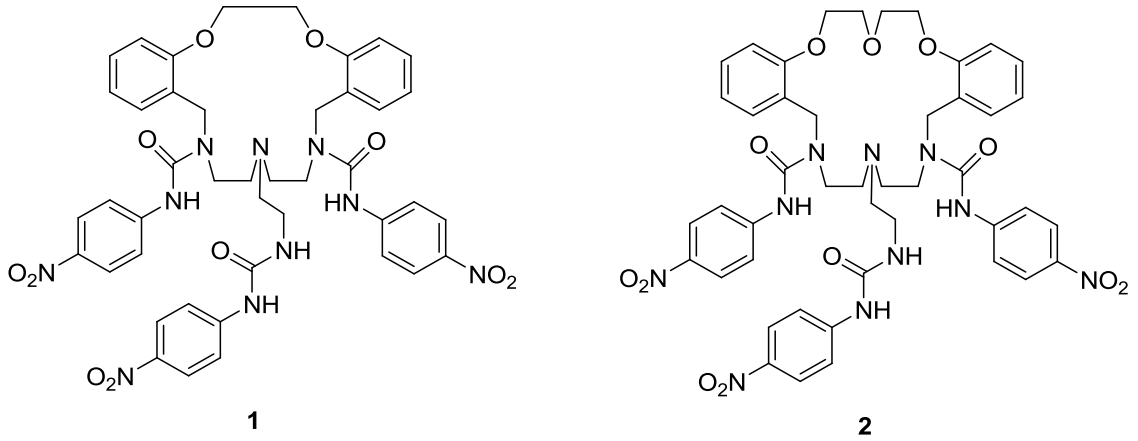

Fig. 1 Structures of receptors **1** and **2**.

This section describes chromogenic probes based on the use of nitroaromatic groups as the signaling unit which, in most cases, are coupled to the urea or thiourea coordinating units. Ligands **1** and **2** (see Fig. 1), containing the macrocyclic structures linked to three nitrophenylurea groups, showed changes in color in the presence of F^-, OH^-, CN^- and $H_2PO_4^-$ in DMSO.[16] The interaction of the urea H atoms with these anions enhanced π delocalization and red shifted the π-π* transition (decreasing the band centered at 348 nm), therefore inducing the formation of a charge transfer band in the visible region (at ca. 480 nm). This resulted in the generation of orange or intense yellow solutions depending on the anion. No change occurred upon the addition of the less basic NO_3^-, ClO_4^-, Cl^-, Br^- and I^- anions. Addition of 1 equiv. of F^- to the solutions of receptors **1** and **2** sufficed to promote the complete deprotonation of NH protons as proved by ^{1}H-NMR studies. The authors suggested that the larger stability constants calculated for chemosensor **2** ($F^- > OH^- > CN^- > H_2PO_4^-$) were in agreement with the strongest interaction expected for **2** which contains a bigger cavity and provides more flexibility.

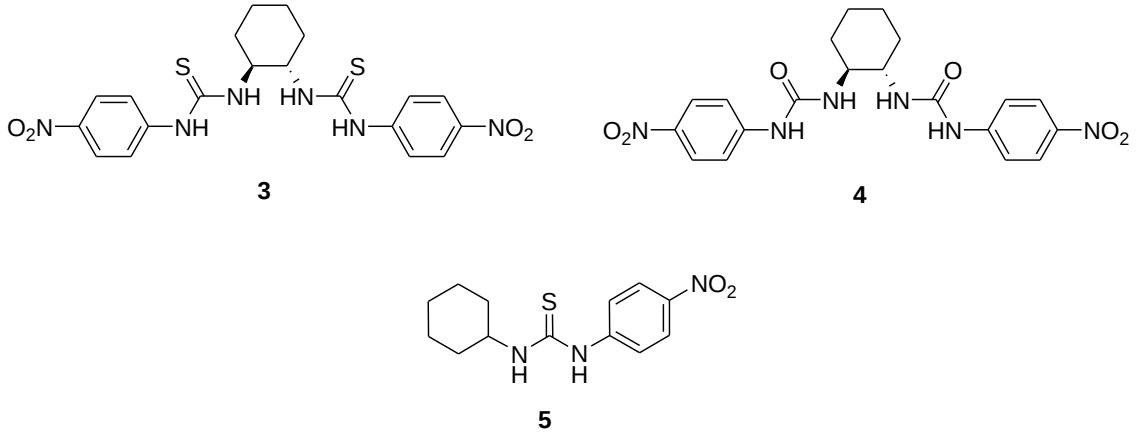

Fig. 2 Chemical structures of receptors **3**, **4** and **5**.

The simple thiourea-based sensor **3** was reported to selectively detect CN^- in DMSO (Fig. 2).[17] In the presence of CN^-, F^-, AcO^- and BzO^-, the original absorption band of **3** at 360 nm decreased and a new band at 475 nm emerged to some extent depending on the anion. A selective distinct colour change from yellow to wine-red was observed for CN^-. In the presence

of this anion, the extent of the intramolecular charge transfer (ICT) from the thioureido N atom in **3** was enhanced due to deprotonation of the thiourea proton by CN^- ions. Furthermore **3** was faintly responsive to $H_2PO_4^-$, while the other anions (i.e., Cl^-, Br^-, I^-, ClO_4^-) did not show any noticeable change. Upon the addition of H_2O or of other competitive protic solvents, the deprotonation of the NH group of receptor **3** by CN^- reversed. In comparison, no colour or absorption changes were observed for receptor **4**. However, similar results were found for **5** (a monomeric analogue of **3**). ^{1}H-NMR titrations revealed the formation of 1:2 complexes for receptor **3** with CN^-, and confirmed the NH hydrogen-bonding interaction of **3** with AcO^- and deprotonation of the NH groups by CN^-.

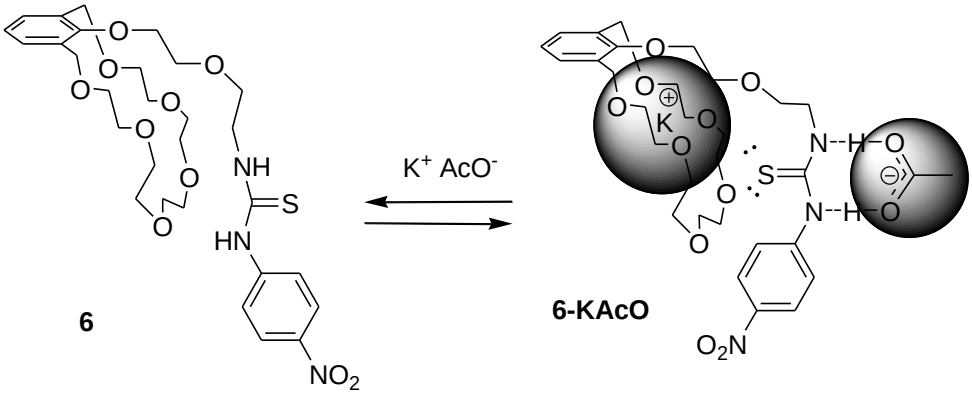

Fig. 3 Schematic representation of the binding mode between receptor **6** and KAcO.

The binding properties of heteroditopic molecule **6,** which features both a cation binding site, in the form of benzocrown ether, and an anion binding site/chromophore in the form of a nitrophenylthiourea group, were investigated in CH_3CN.[18] Probe **6** was able to bind (causing dramatic upfield shifts of the thiourea NH signals, $\Delta\delta > 4$ ppm) and to optically detect AcO^- and BzO^- anions (red shift from 344 nm to 367 nm showing solution changes from colourless to yellow). Interestingly in the presence of K^+, the affinity of **6** for both AcO^- and BzO^- increased, suggesting that cation and anion were coordinated to the receptor in a cooperative fashion (see Fig. 3). Moreover, the authors found that the addition of Na^+ to yellow solutions of **6** in CH_3CN containing AcO^- resulted in the disappearance of colour because the Na^+ cation was able to sequester the carboxylate anion from **6**. No changes in the UV-Vis spectrum of **6** were observed upon the addition of Cl^-, Br^-, NO_2^-, HSO_4^- or BF_6^- ions in either the presence or the absence of metal cations. The authors suggested that **6** allows for the chromogenic detection and discrimination of Na^+ and K^+ acetates.

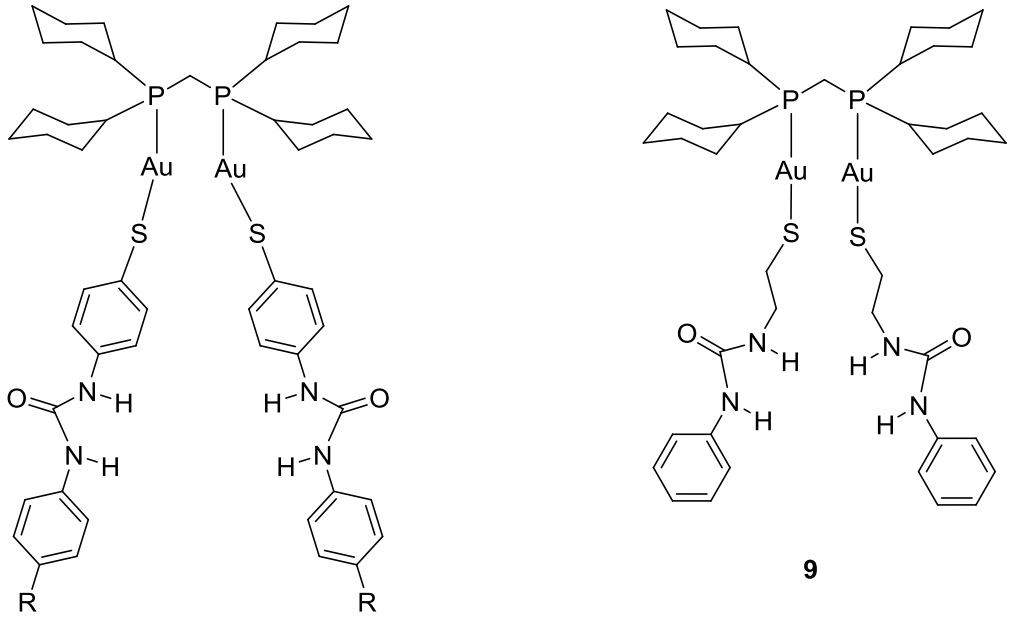

Fig. 4 Structures of receptors **7**, **8** and **9**.

Distinct UV-Vis spectral changes in DMSO solutions of **7-9** (see Fig. 4) were observed upon the addition of basic anions, such as F^-, AcO^-, or $H_2PO_4^-$, whereas the addition of Cl^-, Br^- or I^- led to negligible variations.[19] Complexes **7** and **8** showed the same anion selectivity trend of $F^- > AcO^- > H_2PO_4^- > Cl^- \approx Br^- \approx I^-$. In contrast, complex **9** bound very weakly to the anions in DMSO, although interactions with F^- were observed in CH_2Cl_2 (a less competitive solvent). The most pronounced UV-Vis spectral change, accompanied by a drastic colour modification from yellow to red, was observed upon the addition of F^- to complex **7**, probably due to the deprotonation resulting from the higher acidity of the urea groups in this receptor.

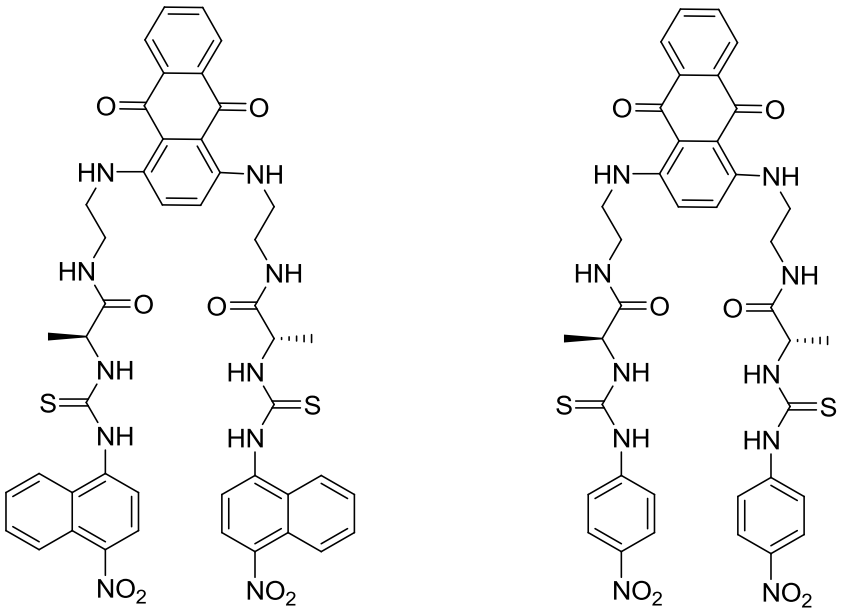

Fig. 5 Structures of receptors **10** and **11**.

The alanine-based derivatives **10** and **11** (see Fig. 5) were described as chiral colourimetric probes for the enantioselective recognition of the aspartate and malate anions in DMSO:H_2O 4:1 v/v.[20] Solutions of **10** showed three absorption bands at 384,595 and 639 nm. Addition of D-aspartate induced the progressive decrease of these bands with the increase of a new absorption at 520 nm (change of color from sky blue to dark magenta). However, L-aspartate induced almost the same changes, but the band at 520 nm was less intense (change in color from sky blue to medium purple). These color modulations were ascribed to a deprotonation of the N-H moiety adjacent to the 4-nitronaphthyl group induced by the added amino acid. Practically the same changes in the absorption bands and in colour were obtained upon the addition of D- and L-malate to **10**. On the other hand, the DMSO:H_2O 4:1 v/v solutions of **11** exhibited absorption bands at 354, 580 and 650 nm. Addition of D-aspartate induced loss of intensity in these bans and the concomitant growth of a new absorption at 471 nm (change in colour from blue to green), whereas addition of L-aspartate also induced the appearance of the 471 nm band, but with less intensity (change in color from blue to cornflower blue). These changes were ascribed to the formation of hydrogen bonding complexes between **11** and the D- and L-aspartate amino acids. The same results were obtained upon the addition of D- and L-malate to the DMSO-H_2O 4:1 v/v solutions of **11**.

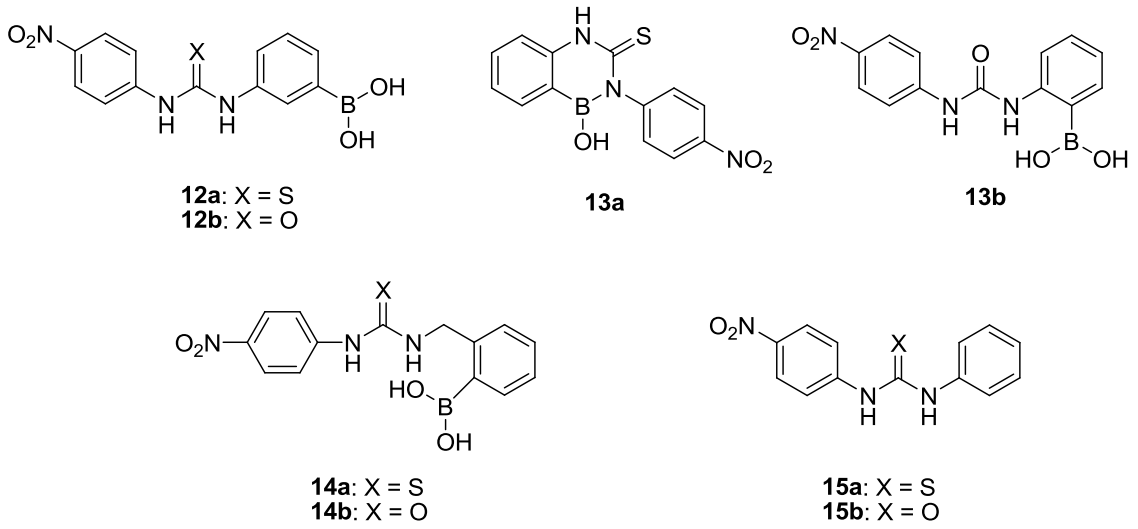

Fig. 6 Structures of receptors **12(a-b)**, **13(a-b)**, **14(a-b)** and **15(a-b)**.

A series of receptors (i.e., **12a-15b**, see Fig. 6) containing phenylboronic acid groups and urea or thiourea units were used for the simultaneous recognition of the carboxylate groups.[21] The binding of the eight receptors with AcO^- (as a model for the carboxylate function) was followed by means of spectrophotometric titrations in DMSO solutions. Upon the addition of AcO^- to **12a**, the intensity of the band at 362 nm progressively decreased, while three new bands with maxima at 290, 398 and 470 nm developed and were characteristic of the deprotonation of the receptor. Unlike **12a** (and **15a**), thiourea **14a** did not undergo deprotonation and a bathochromic 30 nm-shift of the absorption maximum at 360 nm was observed indicating AcO^- recognition through hydrogen bonding interactions. Furthermore the spectral variations observed in ureas **12b**, **13b**, **14b** and **15b** were even less pronounced (minimum bathochromic shifts of the absorption maximum) as no deprotonation occurred. Thiourea receptors displayed stronger H-bond interactions with AcO^- than urea ones, and the logarithm of the binding constants was determined in this order: **15a** > **13a** > **12a** > **14a** >> **12b** > **14b** > **15b** > **13b**.

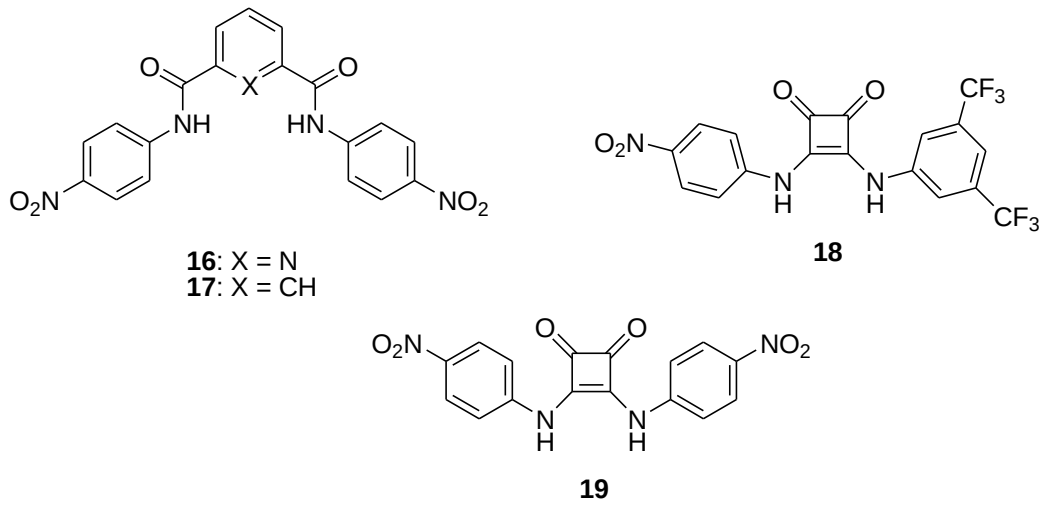

Fig. 7 Structures of receptors **16, 17, 18** and **19**.

The anion-sensing properties of bis(*p*-nitroanilide)s of dipicolinic **16** and isophthalic **17** acids were studied by UV-Vis spectroscopy (Fig. 7).[22] Titration of **16** with F^- in $CH_3CO_2CH_2CH_3$ resulted firstly in the diminished absorbance of the maximum at 322 nm (due to the formation of 1:1 coordination complexes), followed by a shift of the maximum absorption from 322 to 343 nm (due to deprotonation in the presence of excess F^-). Moreover in the presence of Cl^- or Br^-, complexation was preferred. When **17** was titrated with $H_2PO_4^-$, the intensity of the peak centred at 330 nm reduced which occurred with the development of a second peak in the 400-500 nm region. Both **16** and **17** changed colour from colourless to yellow and brownish-yellow when F^- and $H_2PO_4^-$ were added, respectively.

The *p*-nitroaniline-derived squaramide **18** (Fig. 7) displayed distinct a colorimetric behaviour as an anion probe in comparison to the well-explored ureas because of the enhanced acidity of the former.[23] Addition of excess F^- to **18** in DMSO resulted in the formation of an intense blue colour attributable to the dianion $[\mathbf{18}]^{2-}$ formed as a result of two sequential deprotonations. In both DMSO and CH_3CN, the presence of excess TsO^- resulted in the protonation of $[\mathbf{18}]^-$ to form the **18-TsO**$^-$ complex, accompanied by a colour change from pink to yellow (appearance of an absorption peak at 395 nm and the disappearance of the peak at 500 nm). In both DMSO and CH_3CN, the addition of excess AcO^-, HSO_4^-, $H_2PO_4^-$, Cl^-, Br^- and I^- resulted in the persistence of the pink color which was characteristic of $[\mathbf{18}]^-$.

The solutions of receptor **19** (Fig. 7) in CH_3CN showed two absorption bands at 272 and 395 nm which were weakly red-shifted upon the addition of Cl^-, Br^-, I^-, NO_2^-, NO_3^-, $H_2PO_4^-$ and HSO_4^-.[24] These changes were ascribed to the formation of hydrogen bonding 1:1 complexes between **19** and the cited anions. The UV-Vis behaviour noted in the presence of F^- and AcO^- was quite different because the addition of small amount of both anions induced a red shift of ca. 30 nm of the 395 nm band in **19**, with the appearance of a new absorbance at 500 nm. This change was ascribed to an anion-induced deprotonation of the receptor.

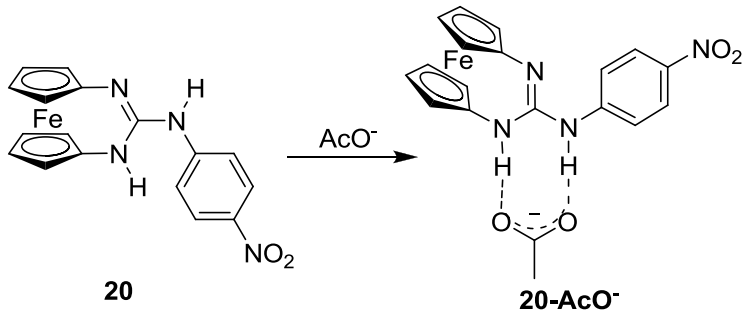

Fig. 8 Binding mode of receptor **20** with AcO^-.

Upon the addition of the Y-shaped anion AcO^- to the solution of **20** (see Fig. 8) in CH_3CN, the band at 350 nm progressively decreased, while a new absorption at 374 nm developed.[25] For BzO^- and F^-, similar spectral changes were found, whereas no variation was observed for NO_3^-, HSO_4^-, $H_2PO_4^-$ and $HP_2O_7^{3-}$, and a slight red-shift ($\Delta\lambda$ = 6 nm) of the absorption band of **20** was observed for Br^- and Cl^-. Addition of OH^-, however, induced the appearance of another low-energy band at 481 nm ($\Delta\lambda$ = 131 nm) with the development of a deep orange-red colour attributable to deprotonated species. The corresponding monoprotonated form [**20**·H^+] was

able to selectively sense the less basic Cl^-, Br^- and NO_3^- anions; in this case, the low-energy band of the absorption spectrum became red-shifted (Δλ = 8 nm) upon complexation.

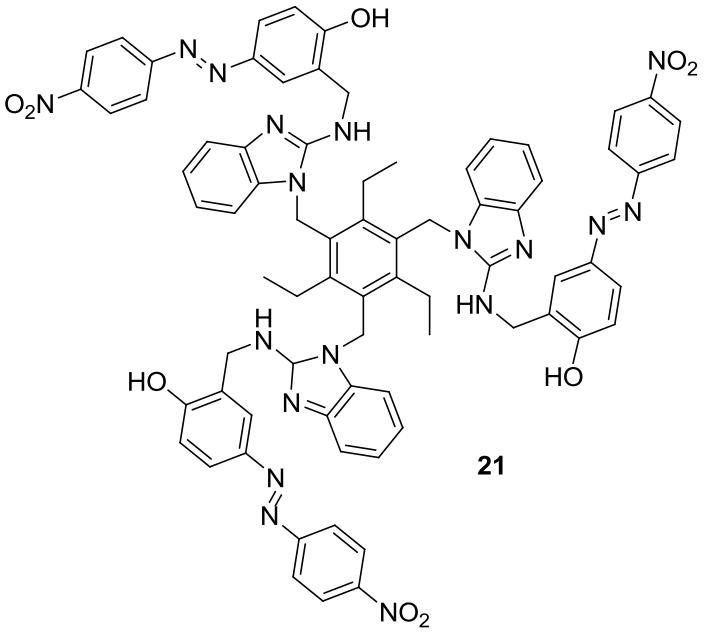

21

Fig. 9 Structure of receptor **21**.

CH_3CN:DMSO:H_2O 93:1:6 v/v/v (HEPES pH 7.1) solutions of tripodal receptor **21** (Fig. 9) presented an absorption band at 375 nm, which shifted to 520 nm upon the addition of anion CN^- (change in colour from light yellow to orange).[26] This chromogenic response was selective for CN^-, whereas addition of F^-, Cl^-, Br^-, I^-, ClO_4^-, $H_2PO_2^-$, HSO_4^-, AcO^- and NO_3^- induced negligible changes in the UV-Vis profile of **21**. The changes in the visible spectra were ascribed to the formation of 1:1 complexes between **21** and anion CN^-. ^{1}H-NMR titrations suggest that anion CN^- interacts with **21** through the formation of multiple hydrogen bonds with phenolic hydroxyls and amine protons.

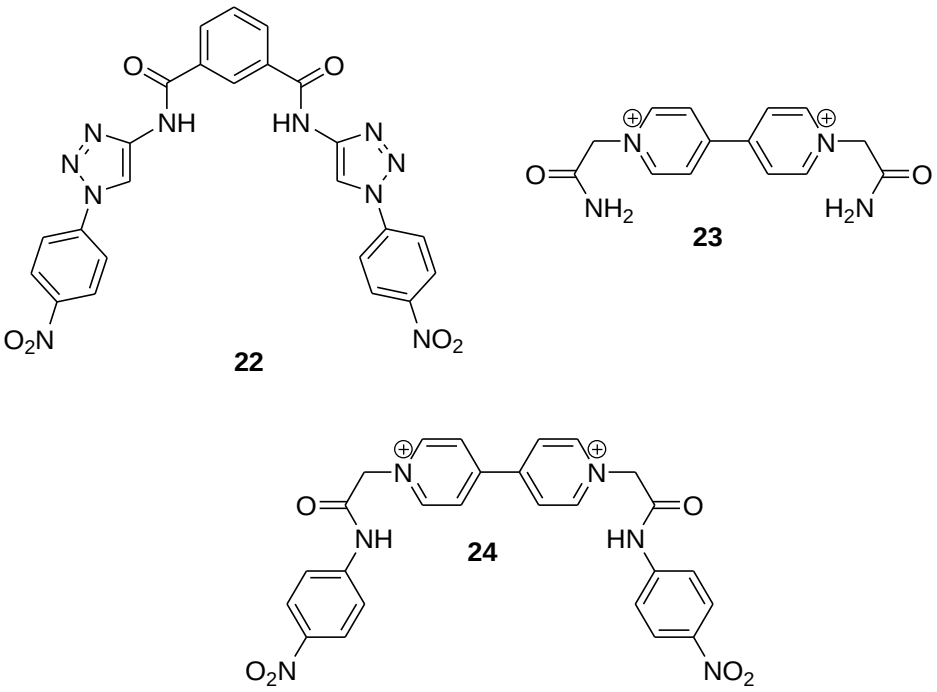

Fig. 10 Structures of receptors **22**, **23** and **24**.

Chromogenic probe **22** (see Fig. 10) used amides and 1,2,3-triazole rings as binding sites for halides.[27] $CHCl_3$:DMSO 98:2 v/v solutions of **22** showed a yellow colour that changed to orange upon the addition of anion F^-. Other halides tested (Cl^-, Br^- and I^-) induced negligible colour variations. This selective chromogenic response was due to the perfect fit of anion F^- with the coordinating cavity of **22** and the F^- interaction with the receptor through hydrogen bonds with amide N-H, the C-H of the triazole rings and the C-H of the 1,3-disusbstituted benzene ring.

Viologen-based probes **23** and **24** were tested to anions in DMSO (see Fig. 10).[28] These chemosensors presented absorption bands at 273 and 317 nm for **23** and **24,** respectively. Addition of anions Cl^-, Br^- and HSO_4^- induced negligible changes in the absorptions of both receptors, whereas basic anions such as F^-, AcO^- and $H_2PO_4^-$ induced the appearance of a new red-shifted band at 430 nm for **23** and in the 450-600 nm interval for **24**. The charge transfer interactions of basic anions with the positively charged viologen moieties of both receptors were responsible for the new bands generated upon binding.

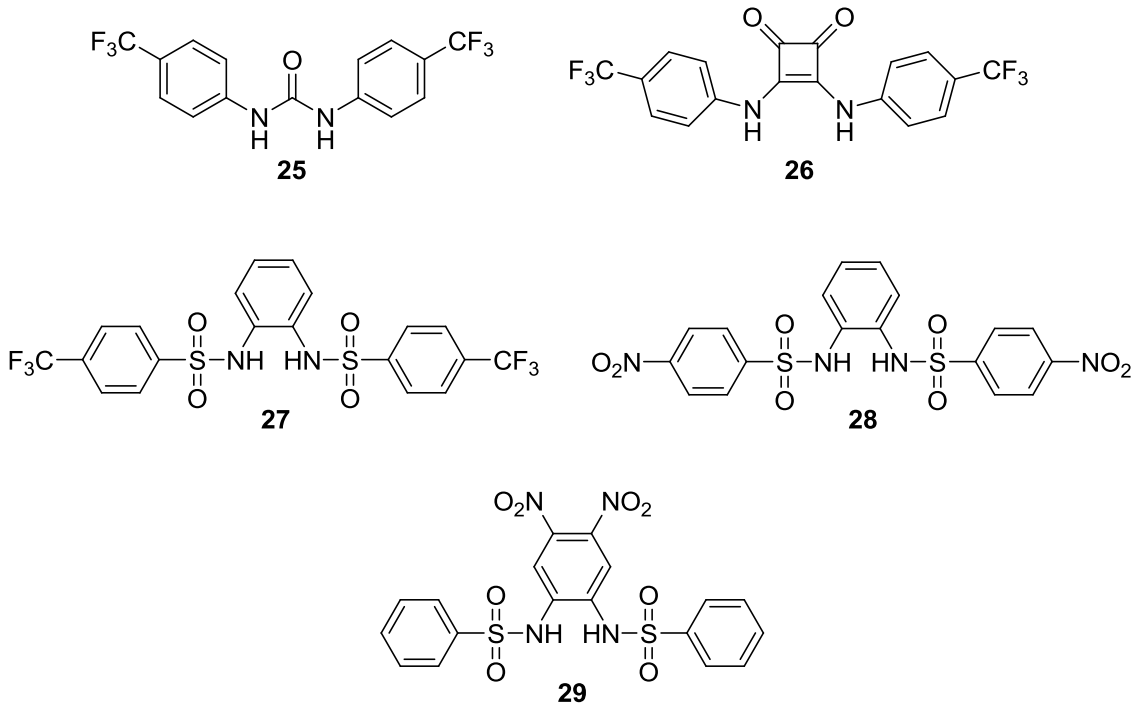

Fig. 11 Structures of receptors **25**, **26**, **27**, **28** and **29**.

The receptors containing different hydrogen-bond donor moieties, **25**-**29** depicted in Fig. 11, were tested in CH_3CN in the presence of selected anions.[29] The charge transfer bands of **25** and **26** (centred at 263 and 330 nm, respectively) underwent slight bathochromic shifts upon the addition of increasing quantities of anions Cl^-, Br^-, AcO^-, HSO_4^- and $H_2PO_4^-$, which are indicative of the formation of 1:1 hydrogen bonding complexes. In the case of sulphonamide receptors **27**-**29**, addition of Cl^-, Br^- and HSO_4^- also induced slight bathochromic shifts of the UV bands, indicative of the formation of 1:1 adducts. However, addition of anions AcO^- and $H_2PO_4^-$ to the CH_3CN solutions of **27**-**29** induced the appearance of new absorption bands in the visible zone ascribed to a deprotonation of the receptors. Additionally, quantitative studies of anion binding with receptors **25**-**29** by isothermal titration calorimetry were carried out.

2.1.2.- Containing N-heterocycles

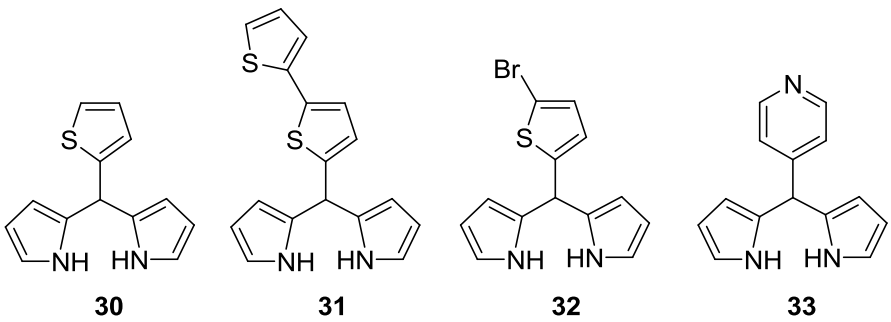

Fig. 12 Structures of receptors **30**-**33**.

Dipyrrolemethane compounds **30-33** (see Fig. 12) were able to selectively detect F^- in CH_3CN via dramatic colour changes from colourless to yellow-red in the case of compounds **30** and **33,** and from light yellow to deep red for **31** and **32**.[30] Neither the addition of Br^-, Cl^-, NO_3^-, HSO_4^-, SO_4^{2-}, AcO^- and $H_2PO_4^-$ nor the addition of protic solvents, such as H_2O, CH_3OH or CH_3CH_2OH, produced significant change in colour. Titration of the **30-33** CH_3CN solutions with F^- resulted in new absorption bands emerging at 490 nm for compound **30** and at 487 nm for compound **33**. For **31** and **32,** absorptions were observed at 510 nm and 501 nm, respectively, upon the addition of F^-. The bathochromic shifts were attributed to the formation of hydrogen-bonding complexes between the pyrrole-NH protons and anion F^-, as confirmed by the ^{1}H-NMR titrations in CD_3CN.

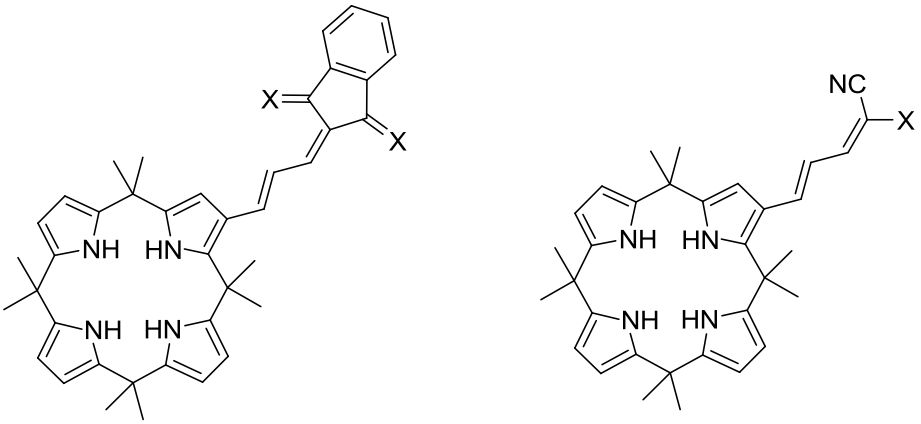

34: X = $C(CN)_2$
35: X = O

36: X = CN
37: X = CO_2Et

Fig. 13 Structures of receptors **34**-**37**.

Calix[4]pyrrole-based derivatives **34-37** (Fig. 13) were described to display colour modulations in the presence of certain basic anions.[31] Addition of F^- and AcO^- to **35** resulted in a change in colour from orange to pinkish, whereas a bleaching of the initial orange solution was observed in the presence of Cl^-. The calculated affinity constants for **35**, in DMSO using a 1:1 binding model, were established in this order: $F^- > AcO^- > H_2PO_4^-$. The addition of F^- and AcO^- to **34** resulted in changes from blue to purple, whereas minor changes were generally noted for compounds **36** and **37**. The addition of Br^-, NO_3^- and NO_2^- caused no variations in colour. ^{1}H-NMR anion-binding studies carried out with probe **35** and F^- indicated that calixpyrrole NH protons were involved in hydrogen-bonding interactions with F^-. The authors ruled out the presence of possible deprotonation processes.

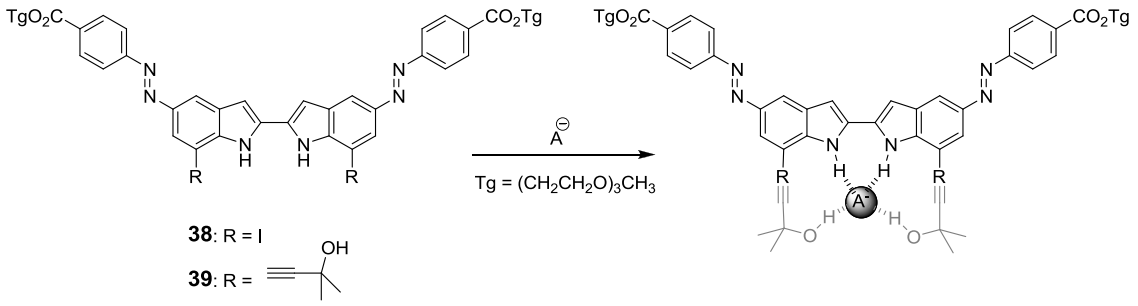

Fig. 14 Proposed binding mechanism of receptors **38** and **39** with several anions (F^-, AcO^- and $H_2PO_4^-$).

Probes **38** and **39** were tested in the presence of F^-, Cl^-, Br^-, I^-, N_3^-, AcO^-, $H_2PO_4^-$, NO_3^-, HSO_4^-, CN^- and OH^- in DMSO:CH_3CN 1:9 v/v mixtures.[32] Anions F^-, AcO^- and $H_2PO_4^-$ with **38** and **39** displayed noticeable colour changes from pale yellow to orange or reddish orange due to the formation of hydrogen bonding complexes between the indole NHs and certain anions (see Fig. 14). For instance for **38,** an increase in absorption at 480 nm was observed upon the addition of F^-, AcO^- and $H_2PO_4^-$. Moreover, the fact that **39** showed a much higher affinity for anions than **38,** by up to 2 orders of magnitude, suggests that the two additional OH groups in **39** were also involved in hydrogen-bonding interactions with the anions. Furthermore upon the addition of CN^- and OH^- to **38** and **39,** a new strong band at 480 nm appeared, which was attributed to the deprotonation of the indole groups.

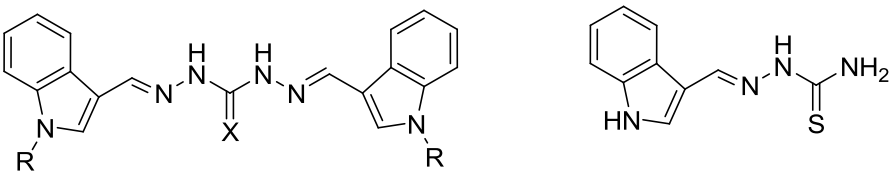

40: X = S; R = H
41: X = O; R = H
42: X = S; R = -CH_2-Ph
43: X = O; R = -CH_2-Ph

44

Fig. 15 Structures of receptors **40**-**44**.

Visible and near-infrared (NIR) sensing of F^- were studied using the indole-conjugated urea/thiourea ligands **40-44** (see Fig. 15).[33] In the presence of F^-, receptors **40** and **41** in CH_3CN:DMF 9.6:0.4 v/v showed selective colour modulations, whereas the other anions tested (i.e., Cl^-, Br^-, I^-, AcO^-, NO_3^-, $H_2PO_4^-$) induced no changes. In particular, addition of 4 equiv. of F^-, to **40** resulted in the the absorption at 342 nm disappearing and in a new band appearing at 442 nm due to H-bonded F^- complex formation. With the increased F^- concentration, **40** started to deprotonate and formed the corresponding conjugate base, showing the simultaneous generation of new peaks at 358, 522, 572 and 936 nm. Such a massive shift (a 594 nm red-shift from 343 nm to 936 nm) was attributed to the high conjugation and planarity of **40,** which favour the maximum distribution of the negative charge of the deprotonated receptor. Receptor **41** showed a similar NIR signature for F^- despite displaying a relatively weaker binding affinity if compared with **40**. **40** also exhibited a slight yellow colouration in the presence of AcO^-. With indole NH-alkylated analogues **42** and **43** or in the case of

monothiocarbonohydrazone **44,** neither visible colour changes nor NIR signals were observed with F^-.

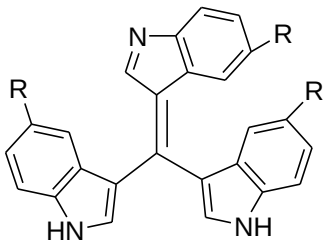

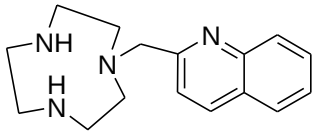

48

45: R=H, **46:** R=OCH_3 **47:** R=NO_2

Fig. 16 Structures of receptors **45**-**48**.

Tris(indolyl)methene receptors **45–47** (see Fig. 16) were designed as colorimetric chemosensors for the detection of F^-, AcO^- and $H_2PO_4^-$.[34] Solutions of **45-47** in CH_3CN and DMSO were prepared. Upon the addition of increasing amounts of F^- to the **45** solutions, the absorption at 457 nm decreased and a new absorption band at 513 nm was observed concomitantly with a colour change from yellow to light pink. When adding excess F^- to **45,** the band at 513 nm gradually decreased and a new blue-shift band at 477 nm evolved, while the solution colour turned from light pink to orange. The spectra and colour changes induced by F^- proved reversible with the addition of protic solvents (CH_3CH_2OH or H_2O). The changes in colour noted upon the addition of F^- to **45** were attributed to two consecutive deprotonation processes. On the other hand, addition of AcO^- to the **45** solutions led to a decrease in the absorption band at 437 nm along with a moderate red-shift, while a shoulder band at 513 nm appeared with no obvious colour change. The addition of excess $H_2PO_4^-$ to **45** caused a red-shift with a new absorption band at 471 nm. A similar response and selective binding towards F^-, AcO^- and $H_2PO_4^-$ over the other anions tested were shown by receptors **46** and **47**. Receptor **47** and **46** displayed the highest and the lowest binding affinity of all the receptors, respectively. No significant spectral and colour changes were found, even in large excess, with the other anions (i.e. Cl^-, Br^-, I^-, ClO_4^- and HSO_4^-) evaluated.

The Cu^{2+}-complex of **48** (Fig. 16) was able to sense CN^- selectively in CH_3CN and H_2O solutions.[35] In H_2O, a colour change of the **48-Cu^{2+}** complex from cyan to dark blue was selectively observed in the presence of CN^-. Moreover in CH_3CN, the formation of two **CN^--48-Cu^{2+}** complexes with different stoichiometries was evident to the naked eye with colour changes from cyan to dark blue (formation of 1:1 complexes) and from dark blue to pink (formation of 2:1 complexes). In CH_3CN, the addition of I^- also caused a colour modulation from cyan to green. No appreciable colour variations were observed in the presence of the other anions (F^-, Cl^-, Br^-, ACO^-, BzO^-, $H_2PO_4^-$, HSO_4^-, HCO_3^-, NO_3^-, N_3^-, and SCN^-) in either CH_3CN or H_2O. Changes in colour were attributed to the coordination of CN^- to the metal centre, which strongly affected the d-d band in **48-Cu^{2+}**. No demetallation processes were observed.

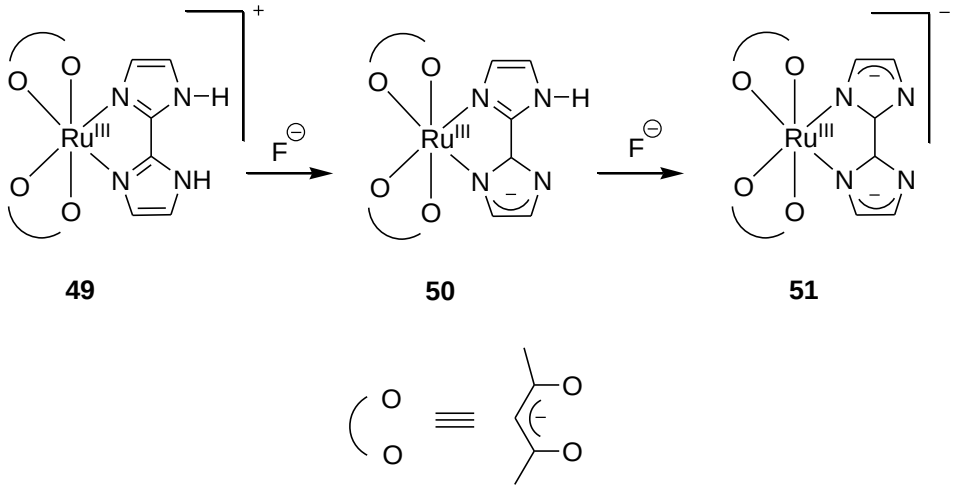

Fig. 17 Proposed binding mechanism of receptors **49-51** with the anion F^-.

Paramagnetic coloured ruthenium-biimidazole complexes **49** and **50** were studied as anion receptors in CH_3CN (see Fig. 17).[36] The spectrophotometric titrations of **49** with F^-, Cl^-, Br^-, I^-, HSO_4^-, AcO^-, $H_2PO_4^-$ in CH_3CN revealed negligible interactions with anions Cl^-, Br^-, I^-, HSO_4^- and $H_2PO_4^-$. Moreover, interactions of biimidazole ligand **49** with $H_2PO_4^-$, AcO^- and F^- were observed. By way of example, the addition of $H_2PO_4^-$ in excess to **49** caused a blue shift of the ligand-to-metal charge transfer (LMCT) band from 516 to 500 nm and a change in colour from pink to red-brown. These changes were ascribed to the formation of a 1:1 stoichiometry complex through hydrogen bonding interactions. Similar spectral behaviour and a colour change were observed for **49** upon the addition of small quantities of AcO^-. In relation to this, the initial addition yielded hydrogen-bonded complexes, whereas a monodeprotonation process (that gives **50**) was produced when increasing anion concentration. Finally, unlike AcO^- and $H_2PO_4^-$, the gradual addition of excess F^- to solutions of **49** shifted the LMCT band from 516 to 500 nm (formation of **50**) and then to 478 nm, which was attributed to the formation of the doubly deprotonated **51**.

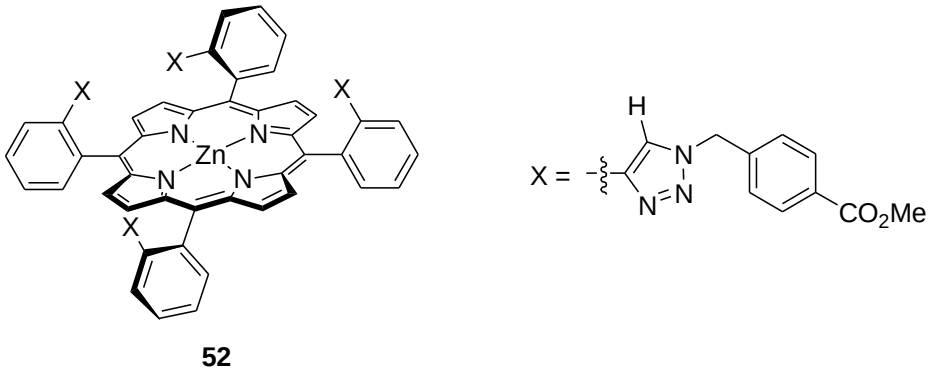

52

Fig. 18 Structure of receptor **52**.

The formation of 1:1 host-guest complexes of porphyrin-based host **52** (Fig. 18) with halides was investigated in CH_2Cl_2.[37] The UV-Vis absorption spectrum showed that both the Soret and Q band absorptions of **52** underwent a strong red shift (to 750, 830 and 990 nm) upon the addition of Cl^-, Br^- and I^-, respectively. Compound **52** exhibited surprisingly strong affinities for halides in this order: $Cl^- > Br^- > I^-$. **52** still showed strong binding affinities for halides when the

experiments were carried out in polar solvents, such as DMSO and acetone. The authors explained the strong binding affinity of halides with **52** by the presence of the cooperative effects of the axial coordination with the Zn^{2+} centre and C-H···X hydrogen-bonding interactions.

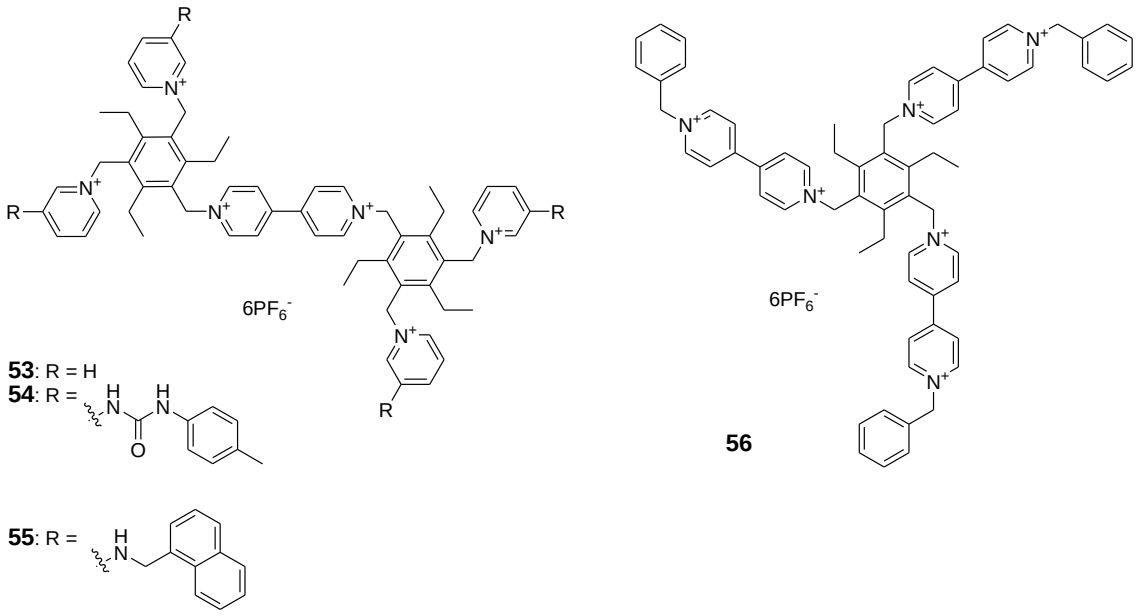

Fig. 19 Chemical structures of the tri- and tetrapodal viologen-derived receptors **53-56**.

The tri- and tetrapodal viologen-derived hosts **53-56** (see Fig. 19 for structures) displayed colorimetric sensing properties to the carboxylate anions in CH_3CN.[38] Anaerobic UV-Vis titrations were performed on compounds **53**-**56** in CH_3CN with AcO^-, succinate and malonate. Interestingly upon the addition of AcO^- to hosts **53**, **55** and **56**, an immediate colour change from colourless to purple was observed. In the case of **53,** pyridinium CH···O hydrogen-bonding interactions occurred. For **56,** a three-up conformation was noted in which AcO^- was bound by three charge-assisted hydrogen bonds. However with host **54**, significant colouration did not appear (AcO^- firstly bound to the urea groups away from viologen) until more than two equiv. of AcO^- were added (as more PF_6^- ions were displaced, AcO^- was able to bind closer to the viologen). Succinate caused significant colour changes for all the compounds similar to AcO^-. Malonate, however, only caused significant colouration with compounds **54** (charge-assisted pyridinium CH···O interactions), **54** and **55**. No significant colour change was noted for compound **56** until a large amount of equivalents was reached (approx. 20 equiv.) due to the unfavourable conformation of the complex formed upon anion binding. All the compounds were also shown to bind halides strongly without causing colour changes.

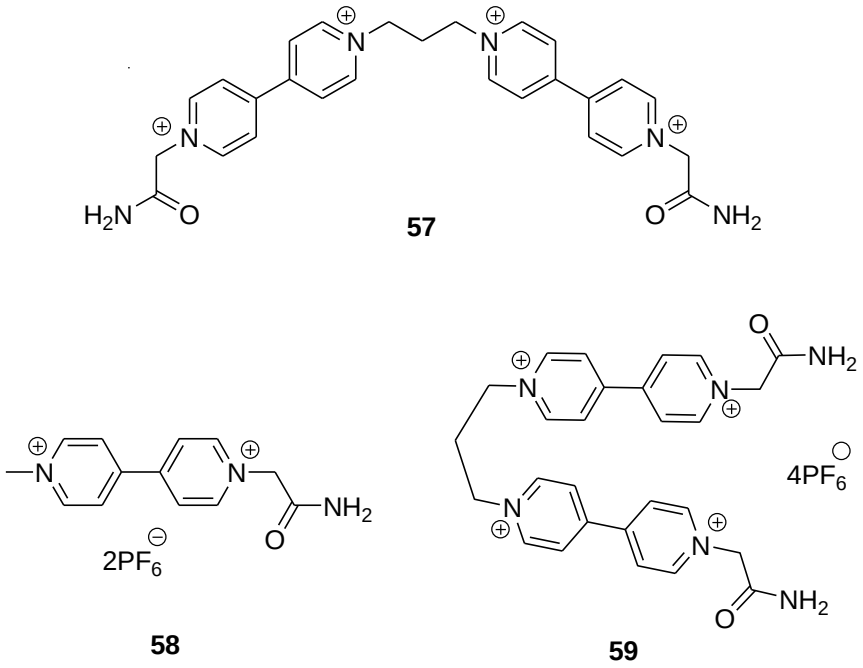

Fig. 20 Structures of the viologen-based receptors **57**-**59**.

Three viologen-based receptors **57**, **58** and **59** (see Fig. 20) were synthesized and their ability to form donor-acceptor complexes with halides was assessed in DMSO by absorption spectroscopy.[39] In agreement with its large electron density and high polarizability, only I^- was able to produce a relatively intense colour change, which is associated with a broad CT absorption band at 430 nm in the presence of **57**. Addition of Br^- did not yield clear additional bands, rather an overall increase in absorption below 450 nm, while no evidence for the formation of CT complexes was found when Cl^- was present. The ability of I^- to form complex [**57**·DMSO·$(I)_4$] was further confirmed by solid-state studies. The addition of 0.2 molar equiv. of F^- to a DMF solution of **58** or **59** induced drastic colour changes from colourless to intense blue or violet, respectively. By means of spectro-electrochemical experiments, these signals were attributed to the reduction-triggered formation of a π-dimer from viologen-based cation radicals.

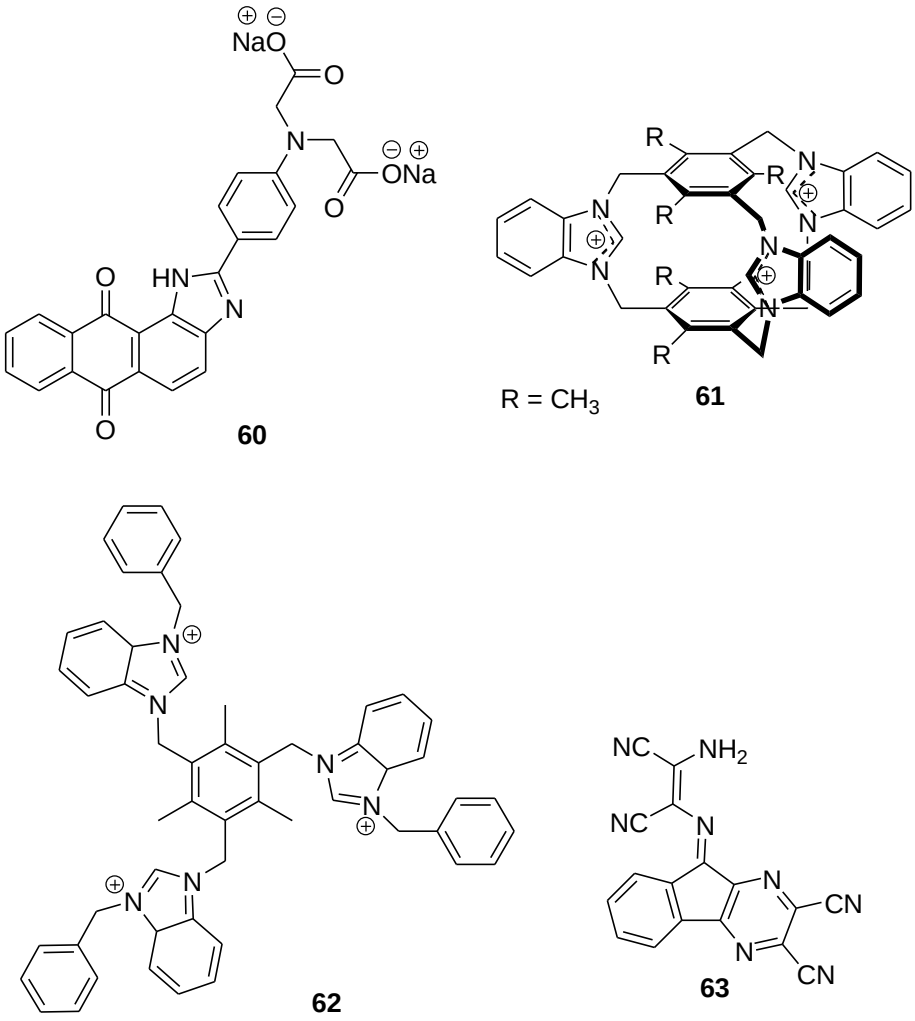

Fig. 21 Chemical structures of receptors **60-63**.

Receptor **60** (see Fig. 21), based on anthraimidazoleidone, acted as a colorimetric probe for F^- and CN^- in CH_3CN via significant red shifts of 120 nm and 81 nm, respectively, of the absorption band of **60,** which resulted in colour changes from light yellow to dark blue (for F^-) and to red (for CN^-).[40] The 1:1 interaction of F^- and CN^- with benzimidazole NH (deprotonation of the most labile proton in **60**) led to an accumulation of a negative charge density at the donor site, which enhanced the intramolecular charge transfer. Only very slight changes in colour to orange were observed upon the addition of AcO^-, $H_2PO_4^-$ or HSO_4^-, while no noticeable changes were seen with the addition of Cl^-, Br^-, I^-, NO_3^- or ClO_4^-. Interestingly, **60** was able to detect F^- even in the presence of CN^- in the organic medium, whereas **60** displayed a selective colour modulation of CN^- in H_2O.

Spectrophotometric experiments in CH_3CN provided evidence (a blue shift of the bands in the 270-285 nm range) for the encapsulation of F^- by trisbenzimidazolium cyclophane receptor **61** (Fig. 21).[41] The parent more flexible tripodal derivative **62** also included F^- in CH_3CN to give a stable complex in which the anion interacted with the three coplanar hydrogens from the imidazolium C-H fragments, as most likely occurred in the corresponding cage complex. In both cases (for **61** and **62**), absorbance increased continuously at 240 nm and a broad defined band,

centred at 300 nm, was formed and developed upon the addition of F^-. This type of coordination was restricted to F^- because larger anions, such as Br^- and NO_3^-, cannot be accommodated in a coplanar fashion in a triangle. Cage **61** was a totally specific receptor for F^- and put the principle of size exclusion into practice. Yet whereas the cage complex $[\mathbf{61}\cdots F]^{2+}$ was stable in the presence of excess F^-, the tripodal complex $[\mathbf{62}\cdots F]^{2+}$, on the addition of further F^-, decomposed due to the deprotonation of an imidazolium C-H fragment and the formation of very stable $[HF_2]^-$ species.

Ninhydrin-based receptor **63** formed a 1:1 complex with Hg^{2+}, which was used as colorimetric probe for the AcO^- and F^- anions (see Fig. 21).[42] The **63-Hg^{2+}** complex in CH_3CH_2OH:H_2O 1:1 v/v mixtures displayed an absorption band at 545 nm (purple colour). Addition of AcO^- and F^- induced a bathocromic shift of 45 nm of the band (change in colour from purple to blue), which was attributed to the formation of ternary **63-Hg^{2+}**-anion complexes. None of the other anions tested (i.e., $H_2PO_4^-$, BzO^-, Cl^-, Br^-, I^- and HCO_2^-) was able to induce colour modulations.

2.1.3.- Containing aromatic alcohols

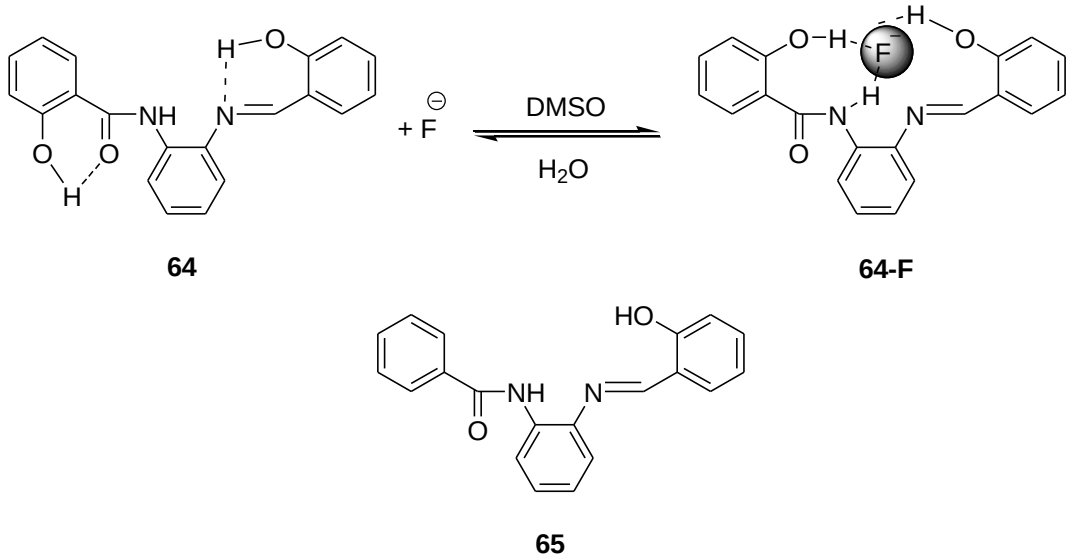

64 **64-F** **65**

Fig. 22 Binding mode of receptor **64** with F^- and structures of receptors **64-65**.

Discrimination of F^-, AcO^- and $H_2PO_4^-$ was achieved by utilising **64** and **65** (see Fig. 22).[43] Compound **64** was able to selectively recognise F^- and AcO^- in DMSO through the formation of 1:1 hydrogen bonding complexes concomitantly with a detectable colour change from colourless to pale yellow. Moreover, **64** displayed only a moderate binding affinity to $H_2PO_4^-$, causing moderate spectral changes, while the addition of other anions, Cl^-, Br^-, I^-, HSO_4^- and NO_3^-, did not trigger noticeable spectral modulations in **64**. For compound **65**, which lacked a salicyloyl OH group compared to **64**, only F^- induced a noticeable colour change from colourless to bright yellow. Both spectral changes and ^{1}H-NMR studies suggest hydrogen-bonding interactions between **65** and F^-, thus deprotonation is rejected.

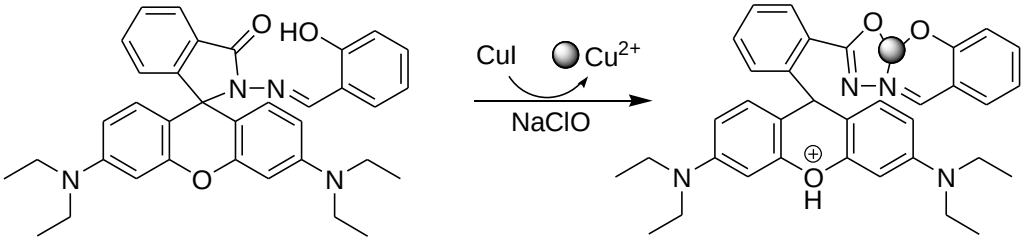

66 **66-Cu**

Fig. 23 Binding mode of receptor **66** with Cu^{2+}.

Rhodamine-based colourimetric probe **66** was reported to be selective to ClO^- with a remarkable limit of detection as low as 8.1 x 10^{-7} mol L^{-1} in aqueous solution.[44] Compound **66,** which predominantly exists in the spirolactam form, formed a colourless solution in H_2O:CH_3CN 1:1 v/v (Tris buffer, pH 7). When adding increasing amounts of ClO^- to the solutions of **66** in the presence of Cu^+, the spectrum changed dramatically; i.e., a new absorption band appeared at 555 nm, increased gradually (with an enhancement as high as 198-fold at 30 min) and showed a colour change from colourless to magenta, suggesting the formation of the Cu^{2+}-induced ring opening of the spirolactam form (see Fig. 23). When probe **66** was treated with various anions, such as CO_3^-, SO_4^{2-}, ClO_4^-, ClO_3^-, NO_2^-, Ac^- and $P_2O_7^{4-}$, virtually no changes were observed. Probe **66** was also able to respond to H_2O_2. **66** was sensitive to ClO^-, even in real tap water samples.

2.1.4.- Miscellaneous

This section contains various examples of chemosensors whose signalling subunits do not contain nitroaromatic derivatives, nitrogen-containing heterocyles or aromatic alcohols. Some of them used metal complexes as binding sites. Interestingly if compared with the above examples, which mostly displayed a sensing behaviour in organic solvents, most of the examples using metal complexes were able to sense anions in aqueous environments or in mixed aqueous solutions.

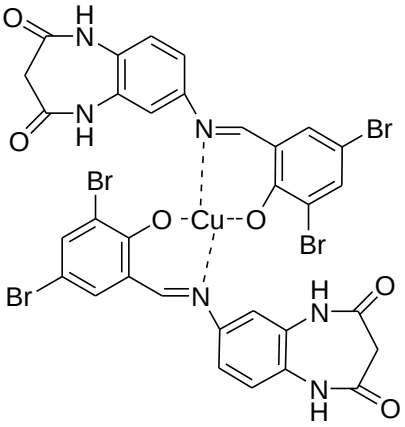

67

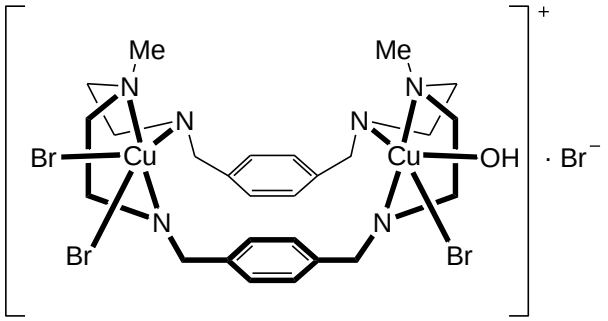

68

Fig. 24 Structures of receptors **67** and **68**.

The UV-Vis spectral changes of complex **67** (Fig. 24) in the presence of AMP, ADP and ATP in DMSO:H_2O 9:1 v/v were investigated.[45] Addition of AMP resulted in the shift of the former bands of **67** at 325 nm to 413 nm. ATP also induced similar spectral changes, whereas the presence of ADP resulted in a new absorption band at 420 nm. The sensing mechanism was attributed to the interaction of **67** with ribonucleotides (forming 1:1 complexes) via both the coordinative interactions of the phosphate groups with the Cu^{2+} centre and π-π stacking forces between the adenine groups in nucleotides with the 7-membered amide cycles. The binding ability of the nucleotides with **67** was in the order of AMP > ADP > ATP, and AMP was successfully discriminated from ADP, ATP.

Macrocycle-based dinuclear Cu^{2+}-complex **68** (Fig. 24) proved an ideal receptor for I^- versus other halides.[46] The titration of **68** in CH_3CN:H_2O 3:1 v/v solutions with F^- and Cl^- resulted in a 29-nm and a 13-nm blue shift of the absorption band at 296 nm (a visual colour change from blue to light blue), whereas the addition of Br^- did not induce any colour modulation. In contrast, the response of **68** to I^- was quite different, showing a remarkable enhancement of the absorption maximum (only 3-nm blue shifted) resulting in a colour change from blue to green. In all cases, 1:1 complexes were formed with stability constants following the order of $I^- > Cl^- > F^- > Br^-$. Selectivity roughly correlated with the size of the halides. The authors attribute these spectral changes to the replacement of the groups linked to Cu by the added anion.

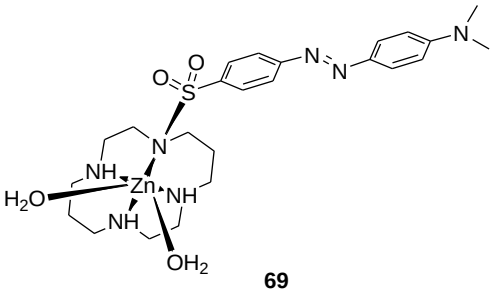

69

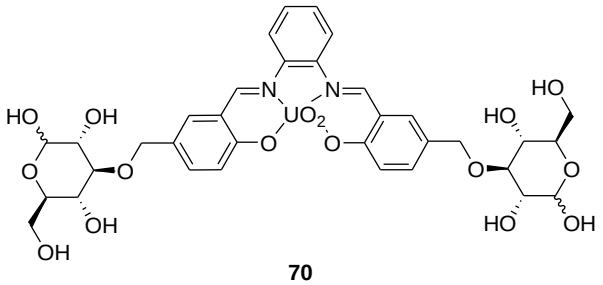

70

Fig. 25 Structures of receptors **69** and **70**.

Two chromogenic complexes, Zn^{2+} Cyclam-based **69** (see Fig. 25) and its [2]pseudorotaxane derivative with α-cyclodextrin (**α-CD-69**), were successfully used to recognise and detectf ATP produced *in situ* during different metabolic processes in living organisms in pure aqueous HEPES buffered (pH 7.2) solutions.[47,48] A visually detectable 40-nm red shift in the absorption band of **70** was achieved upon binding to ATP. Only a 9-nm shift was observed for CTP, while the changes for ADP were even less significant. Other anions (i.e., AMP, $P_2O_7^{4-}$, $H_2PO_4^-$, SO_4^{2-}, AcO^-, I^-, Br^-, Cl^-, F^-, CN^-, SCN^-, NO_3^- and NO_2^-) failed to induce any detectable colour change. When carrying out the spectrophotometric titrations of **69** with ATP, CTP and ADP, the highest affinity seen was to ATP. The authors also used the α-CD inclusion complex of **69**, (**α-CD-69**) to dissolve a larger amount of **69** in aqueous solution to then observe a more intense colour change upon the binding to ATP. Finally, **69** and **α-CD-69** were used for ATP detection in living *S. cerevisiae* cells under physiological conditions.

The new water-soluble uranyl-salophen complex **70** (see Fig. 25), incorporating two glucose units, was reported to display good affinity to F^- and HPO_4^{2-} and to exhibit a strong association for nucleotide polyanions ADP^{3-} and ATP^{4-} in H_2O.[49] The addition of increasing amounts of F^- to **70** caused absorbance changes in the 280-450 nm range due to the formation of 1:1 complexes, where the Lewis acid-base interaction was strong enough to overcome the extremely high hydration enthalpy of the anion. Moreover, the authors attribute the affinity between **70** and HPO_4^{2-} in H_2O to the formation of a hydrogen-bonding intracomplex between the hydroxyl group of the anion and one of the uranyl apical oxygens acting as hydrogen bond acceptors. In addition, the possibility of **70** to bind the biologically relevant anions $P_2O_7^{4-}$, AMP^{2-}, ADP^{3-} and ATP^{4-} in H_2O under physiological pH conditions was investigated to conclude that the association with polyphosphates was stronger than that with the monophosphate derivative.

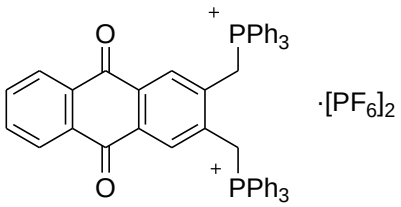

71 $(PF_6)_2$

Fig. 26 Structure of receptor **71**.

Receptor **71,** with an anthraquinone skeleton, was found to act as a selective extractor and a colorimetric sensor of F^- in aqueous solution (Fig. 26).[50] Studies into the electronic spectra for **71** in CH_3CN in the absence and the presence of F^-, Cl^-, Br^-, I^-, HSO_4^-, NO_2^-, NO_3^-, N_3^-, CH_3COO^-, ClO_4^-, IO_4^- and $H_2PO_4^-$ demonstrated that two new absorption bands appeared at 439 and 606 nm only in the presence of F^- or $H_2PO_4^-$, and that the extent of the changes for $H_2PO_4^-$ were much lower. This resulted in a significant colour change to deep blue and pale blue for F^- and $H_2PO_4^-$, respectively. The formation of 1:2 ligand-to-anion complexes was determined and computational studies confirmed that **71** can accommodate two F^- or $H_2PO_4^-$ via interaction with the active methylene hydrogens. The ^1H and ^{31}P-NMR results validated the formation of the H- adducts between -$[CH_2]$- and anions F^- and $H_2PO_4^-$. Furthermore and as a remarkable feature, the authors successfully used **71** for the real-time quantitative extraction and colorimetric detection of F^- (at concentrations as low as 0.06 ppm) in H_2O, where other competing ions were present in excess.

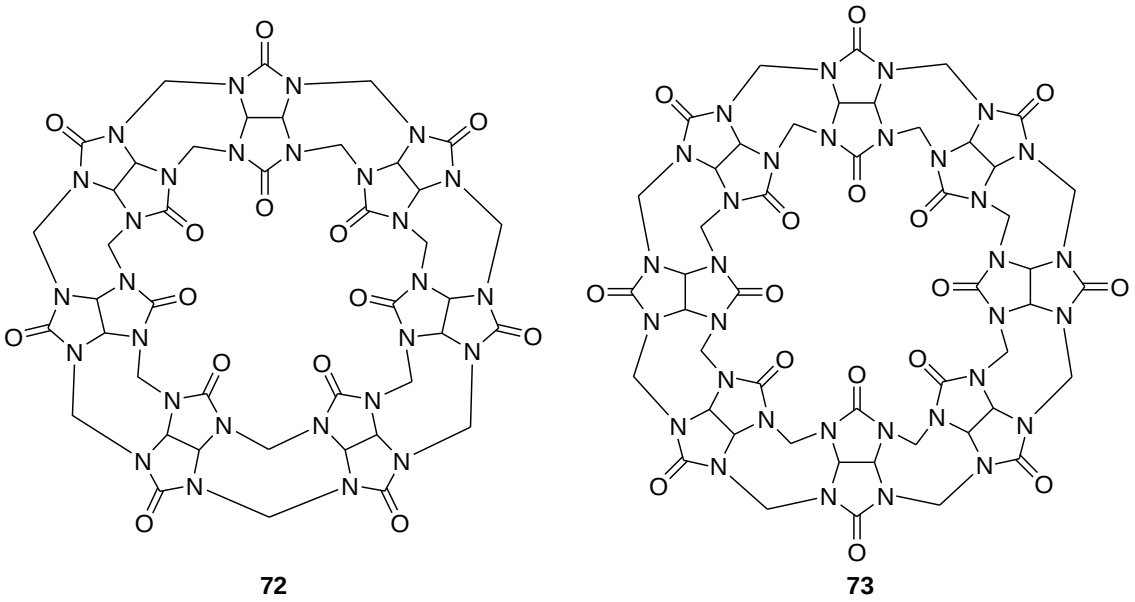

Fig. 27 Structures of receptors **72** and **73**.

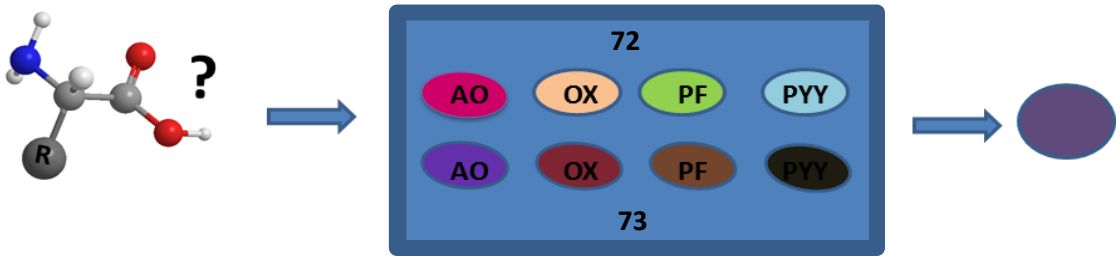

Fig. 28 Schematic representation of a sensing array for α-amino acids using **72** and **73**.

A chromogenic tongue, based on tricyclic basic dyes and cucurbiturils (**72** and **73** in Fig. 27), allowed the detection and discrimination of α-amino acids from their related amines and acids without the need of enzyme activation by simply analysing the sensing array image (see Fig. 28).[51] The array contained organic capsules **72** and **73** and four simple tricyclic fluorescent dyes: proflavine (**PF**), oxonine (**OX**), pyronine Y (**PYY**) and acridine orange (**AO**). These were selected because amino acids can form strong hydrogen bond interactions with them through amine and carboxylate groups. The different changes in colour were ascribed to the formation of ternary complexes organic capsule-dye-amino acid.

A colorimetric sensor array based on supramolecular host-guest complexation interactions using also organic capsules **72** and **73** (see Fig.) and six common fluorescent cationic dyes (**MB**, **TH**, **OX**, **PYY**, **AO** and **PF**) for the sensitive detection of the drug γ-hydroxybutyric acid (GHB) in H_2O-acetone was investigated.[52] Acetone was used as a co-solvent to decrease the dielectric constant, to preserve the solubility of the host-guest complexes and to enhance the ion-pair association between positive host-guest complexes and negative GHB. Multiwell plates were prepared with capsules **72** and **73**, the six fluorescent dyes, GHB and different volumes of acetone as co-solvents. The accuracy of the quantitative determination of GHB concentration

was based on the differences in the responses of the mixtures at different concentrations. The combination of several dyes covers a wide range of concentrations that are not normally covered by a single dye. For instance, the **PF** dye was more useful to distinguish diluted concentrations of GHB, whereas the **PYY** dye proved more helpful to quantify concentrated solutions. The ensemble was seen to be able to discriminate GHB from a series of related compounds with similar structures, such as γ-butyric lactone (GBL), 1,4-butanediol, propionic acid and butyric acid. The discrimination between GHB and GBL was particularly simple and reliable using the sensor array. Once again, changes in colour were ascribed to the formation of ternary CB-dye-GHB complexes.

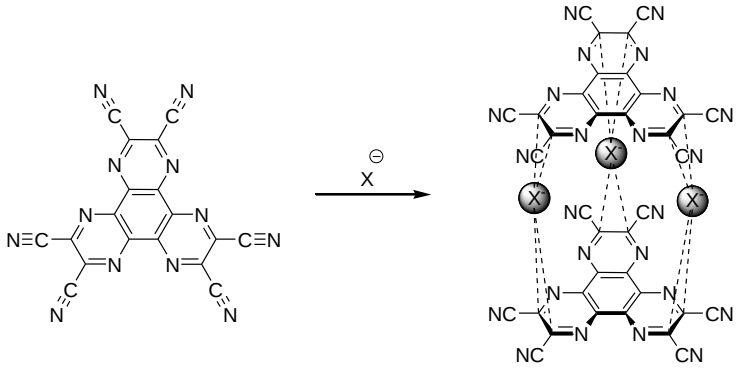

Fig. 27 Binding mode of receptor **74** with halide anions (X^-).

Neutral π electron-deficient 1,4,5,8,9,12-hexaazatriphenylene-hexacarbonitrile entity **74**, exhibited multisite anion halide charge transfer interactions in both solution and the solid-state.[53] Addition of I^-, Br^- and Cl^- to a yellow solution of **74** in THF induced the spontaneous appearance of new intense absorption bands, which progressively grew with increasing concentrations of the anions at 630, 419 or 408 nm. These bands corresponded to a transition from the HOMO of the electron donors (from anions) to the low-lying LUMO of acceptor **74**. Transition energies were directly related to the HOMO→LUMO energy gap of the **[X^-, 74]** complexes and they increased linearly with the oxidation potential of the donor in the order of $Cl^- > Br^- > I^-$, which establishes the unequivocal CT nature of the associations. A 2:3 [**74**]:[X^-] molar ratio of the CT complexes in THF and CH_3NO_2 solutions was found. In solution, the spontaneous formation of **75** (see Fig. 27), with the peripheral η^2- η^2-positioning of the anions and the unambiguous CT nature of the associations with **74** were also fully supported by ES-MS observations in addition to UV-Vis, ^{13}C and halogen NMR studies.

2.2.- Displacement assay approach

Displacement assays have been widely employed in the design of chromogenic probes for anions. In this approach, a selected receptor forms a complex with a dye and upon the addition of a target anion displacement occurs; i.e., the anion binds to the receptor and delivers the dye to the solution. The different optical properties between the free dye and the complexed dye leads to the detection of the corresponding anion. One interesting feature of this approach is that most designed ensembles display sensing features in water or organic-aqueous mixed solutions, which result in the design of realistic sensing systems. The dyes used

in the development of these chromogenic displacement assays for anion sensing are depicted in Fig. 28. Some other dyes, which were also used in some other parts of this review, are also shown in this figure.

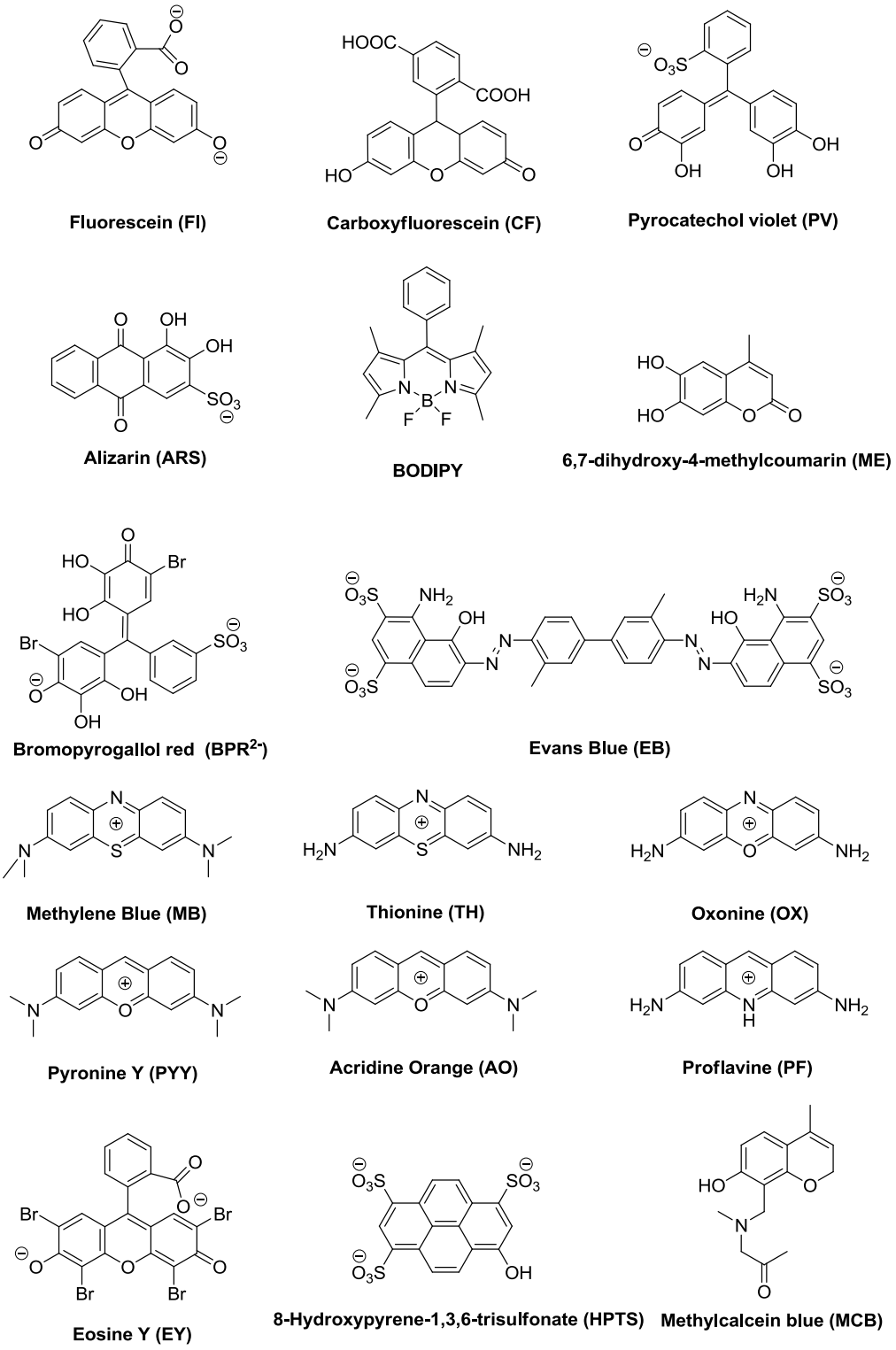

Fig. 28 Dyes employed for the chromo-fluorogenic sensing of anions.

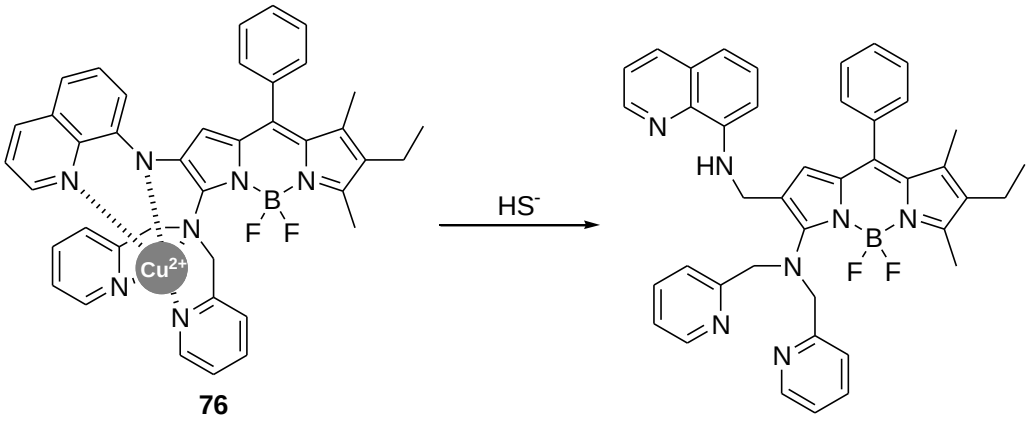

Fig. 29 Proposed signalling mechanism of HS^- using complex **76**.

The boron-dipyrromethene-Cu^{2+} complex **76** was used for the colorimetric recognition of HS^- in aqueous media.[54] The H_2O:DMSO 95:5 v/v (HEPES buffer, pH 7.4) solutions of **76** presented an absorption band at 520 nm which was responsible for the orange colour observed. Addition of anion HS^- induced a progressive decrease in the absorption band at 520 nm with a concomitant increase of a new absorption at 569 nm (colour modulation from orange to pink). This new band was ascribed to the boron-dipyrromethene dye released to the solution after the formation of HS^--Cu^{2+} complexes (see Fig. 29). Addition of F^-, Cl^-, Br^-, I^-, HCO_3^-, $H_2PO_4^-$, SO_4^{2-}, SO_3^{2-}, N_3^-, SCN^-, CN^-, NO_2^- and NO_3^- induced negligible changes.

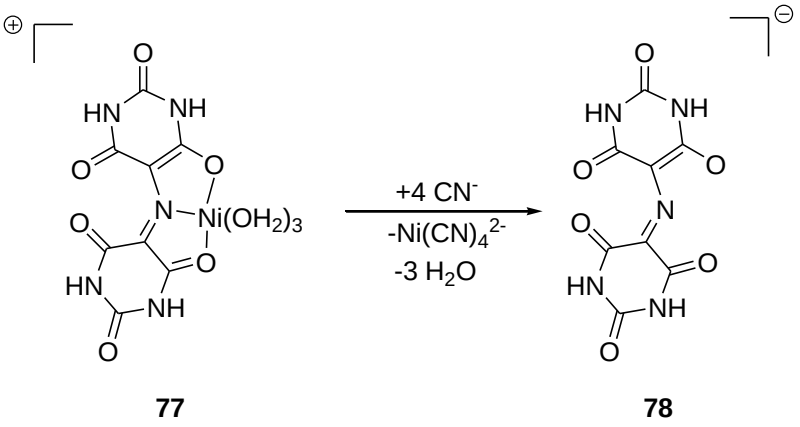

Fig. 30 Proposed signalling mechanism of CN^- using complex **77**.

A two-step "naked-eye" screening using metal-based chemosensors for biologically important anions such as CN^-, PO_4^{3-} and oxalate was developed.[55] The authors started from 12 possible probes by combining five commercially available metal indicators (Murexide, Eriochrom black T, Pyrocatechol, Alizarin and Zircon) and equimolar amounts of Fe^{2+}, Fe^{3+}, Co^{2+}, Ni^{2+} or Zn^{2+}. The array was screened against different anions, including CN^-, F^-, SCN^-, Cl^-, $H_2PO_4^-$ and OCN^-. Colour changes were observed in some cases due to an anion-induced decomplexation of the indicator (Fig. 30). The authors selected three systems with the most pronounced colour changes: i.e., Murexide/Ni^{2+} or Co^{2+} and Zircon/Zn^{2+}. The Murexide/Ni^{2+} complex **77** was the most sensitive for CN^- with a limit of detection as low as 7.7 µM (decomplexation of **77** yielded **78**). However, HPO_4^{2-} (> 3 mM) and oxalate (0.5 mM) also induced decomplexation. The Zircon/Zn^{2+} system, despite being less sensitive to CN^- (LOD of 65 µM), was not affected by

these anions. Moreover, the Murexide/Ni^{2+} (**77**) and Zircon/Zn^{2+} systems were successfully used for the detection of endogenous CN^- in pickled bamboo shoots and in crushed flax seeds. A second array consisted in 36 combinations of the above-mentioned metal indicators and metal ions (Ce^{4+}, Zr^{4+}, Mg^{2+} and Ca^{2+}). After screening procedures and selectivity studies, the two Calcon/Ca^{2+} and Eriochrom black T/Mg^{2+} (for both, colour changed from violet to blue) systems were selected as suitable probes for the optical detection of micromolar PO_4^{3-} and millimolar oxalate, respectively.

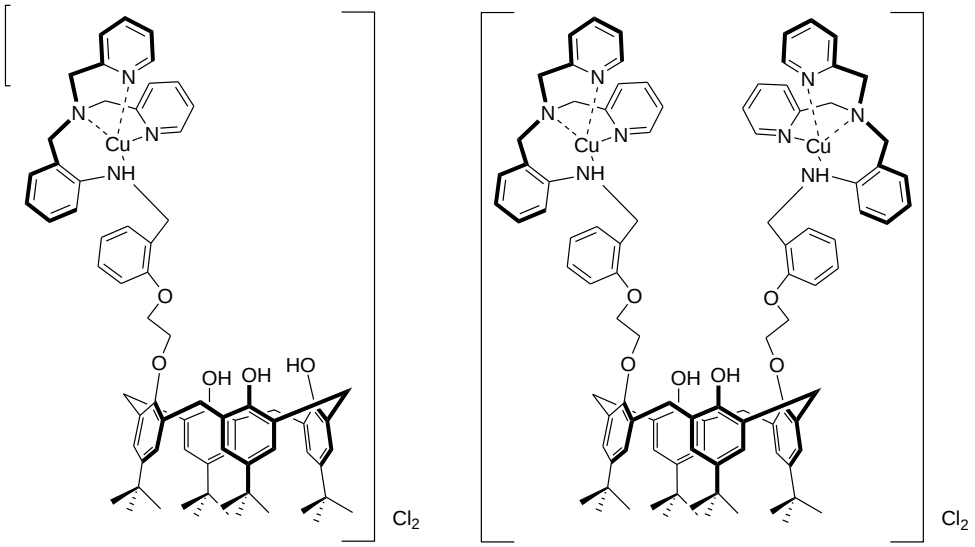

Fig. 31 Chemical structures of tripodal amine calix[4]arene-based Cu^{2+} complexes **79** and **80**.

Tripodal amine calix[4]arene-based Cu^{2+} complexes **79** and **80** (see Fig. 31) were chosen as indicator displacement receptors for $P_2O_7^{4-}$.[56] Pyrocatechol violet (**PV**) was chosen as the competitive indicator. The yellow solution (λ_{max} = 430 nm) of **PV** in CH_3CN:H_2O 1:0.25 v/v solution buffered with HEPES at pH 6.4 changed to green (λ_{max} = 670 nm) upon the addition of **80** due to the formation of the corresponding 1:1 **80**:**PV** complex. When adding anions $H_2PO_4^-$, AcO^-, $P_2O_7^{4-}$, BzO^-, I^-, Br^-, Cl^- and F^- to the ensemble **80-PV**, only $P_2O_7^{4-}$ was able to turn colour from green to yellow. Moreover, both ADP and ATP were also able to displace **PV** from the cleft of **80**, whereas AMP was not. Besides, the unobserved changes found with the analogous **79-PV** complex in the presence of anions support the requirement of the cooperative action of two Cu^{2+} ions for the selective sensing of $P_2O_7^{4-}$.

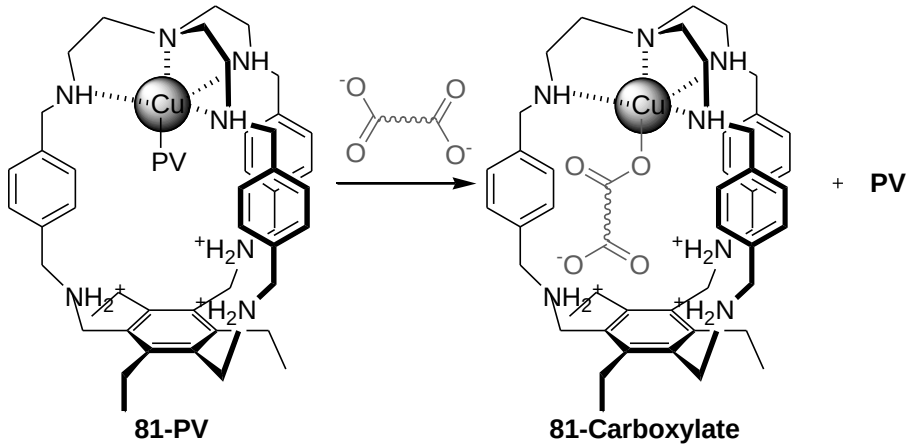

Fig. 32 Schematic representation of the indicator-displacement assay of **81-PV** with the oxalate anion.

By introducing indicator **PV** (yellow) to the Cu^{2+} polyaza macrobicyclic receptor **81**, selectivity for oxalate was proved by indicator-displacement assays in aqueous solution (Fig. 32).[57] Among the several dicarboxylates tested (malonate, succinate, fumarate, maleate), oxalate was the only one able to displace the indicator from receptor **81-PV** to yield a change in colour from blue to green.

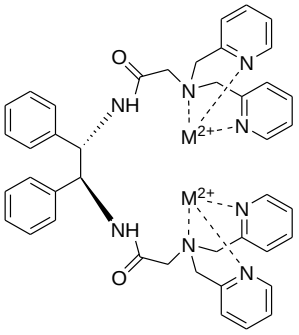

82: M = Zn
83: M = Cu

Fig. 33 Structures of complexes **82** and **83**.

By adding 1 equiv. of pyrocatechol violet (**PV**) indicator to the bright yellow complexes **82** and **83** (see Fig. 33) in aqueous buffered HEPES solutions at pH 7.4, complexes **82-PV** and **83-PV** were formed and resulted in dark blue colour solutions.[58] Upon the addition of $P_2O_7^{4-}$ to **82-PV,** colour changes from dark blue to bright yellow were observed due to displacement of **PV** and the formation of the corresponding 1:1 **82**-$P_2O_7^{4-}$ complex. Weaker but homologous responses were obtained with other anions (with binding constants in the order of $P_2O_7^{4-}$ >> ATP > PO_4^{3-} > ADP > AMP). Titration of **83-PV** with $P_2O_7^{4-}$ gradually resulted in the same optical changes. Furthermore **83-PV** hardly showed a response in the presence of PO_4^{3-}, ATP, ADP, AMP or AcO^-. The selective recognition ability displayed to $P_2O_7^{4-}$ can be ascribed to the appropriate size of the $P_2O_7^{4-}$ anion and to the complementary structure between the receptors and $P_2O_7^{4-}$ with each phosphoryl oxygen atom binding to one metal centre.

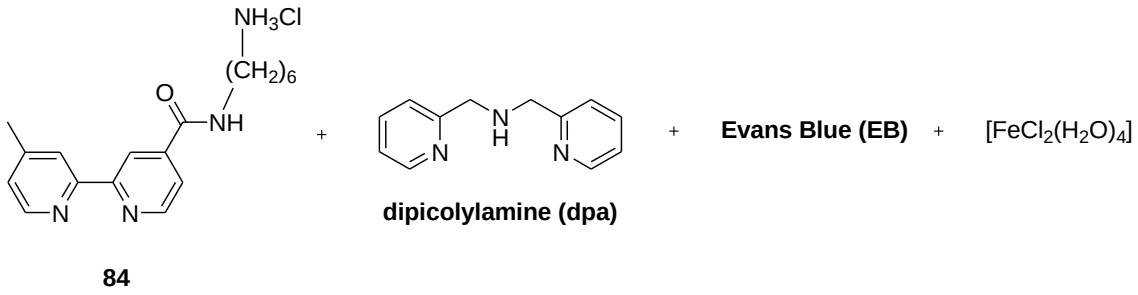

Fig. 34 Reactants to obtain a dynamic mixture of homo- and heteroleptic iron complexes.

A dynamic mixture of homo- and heteroleptic iron complexes with affinity for negatively-charged polysulphated sugars was obtained by mixing $[FeCl_2(H_2O)_4]$ with **dpa**, **84** and **EB** (see Fig. 34) in buffered aqueous solution (MOPS, pH 7).[59] To evaluate the sensing behaviour of the mixture aliquots of stock solutions of low molecular-weight heparin (LMWH), unfractionated heparin (UFH), dextrane sulphate, chondroitin sulphate A, chondroitin sulphate B/dermatan sulphate, and heparin sulphate were added to the ensemble. Samples were analysed by UV-Vis spectroscopy after an equilibration time of 90 min and by focusing on six different wavelengths: 431, 545, 585, 612, 632 and 669 nm. LMWH, UFH and dextrane sulphate caused a re-equilibrium, plus a strong interaction with the assay mixture, therefore showing a decrease at the 431 nm peak (the concentration of the $[Fe(dpa)_2]^{2+}$ complex decreased) and an increase at the other bands (negatively-charged analytes stabilise the formation of the Fe-complexes containing ligands **84** and **EB**). However, dextrane sulphate displayed a distinct change at 545 nm, but relatively slight changes at 612, 632 and 669 nm. Chondroitin sulphate A, dermatan sulphate and heparin sulphate gave an overall lower response due to their reduced charge density. From linear discriminant analysis, a characteristic response was obtained for each glycosaminoglycan. Different glycosaminoglycans appeared in well separated clusters and the authors suggest that the dynamic mixture could be used to identify the respective glycosaminoglycans. Finally, the sensing ensemble was successfully used to differentiate mixtures of UFH and heparin sulphate with high precision.

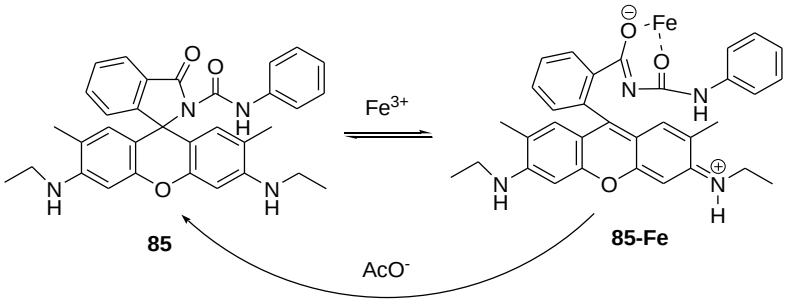

Fig. 35 Representation of the method to detect AcO^- ions with **85**.

A new selective and sensitive method to detect AcO^- ions in H_2O:CH_3CN 1:1 v/v based on a Fe^{3+} complex with a rhodamine 6G phenylurea derivative (**85**) was reported (see Fig. 35).[60] Addition of Fe^{3+} to solutions of the dye resulted in a colour change from colourless to pink due to the appearance of a new band at 530 nm. In addition, a fluorescence band at 556 nm was also observed (fluorescence quantum yield of 0.86). The stoichiometry of complex **85-Fe^{3+}** was

determined to be 1:1. Other metals such as Ba^{2+}, Ce^{3+}, Na^{+}, K^{+}, Hg^{2+}, Cu^{2+}, Co^{2+}, Pb^{2+}, Al^{3+}, Ag^{+}, Mg^{2+}, Ni^{2+}, Cd^{2+}, Fe^{2+} and Zn^{2+} created no obvious colour or fluorescent changes in **85**. When AcO^{-} was added to complex **85-Fe^{3+}**, a switch-off of absorbance and fluorescence was observed, and the colourless appearance of **85** was restored. A limit of detection for AcO^{-} of 1.8 x 10^{-7} mol L^{-1} was found, whereas other anions such as F^{-}, Cl^{-}, Br^{-}, I^{-}, HSO_4^{-}, $H_2PO_4^{-}$, NO_3^{-}, CO_3^{2-} did not produce any change in the absorbance and fluorescence spectra.

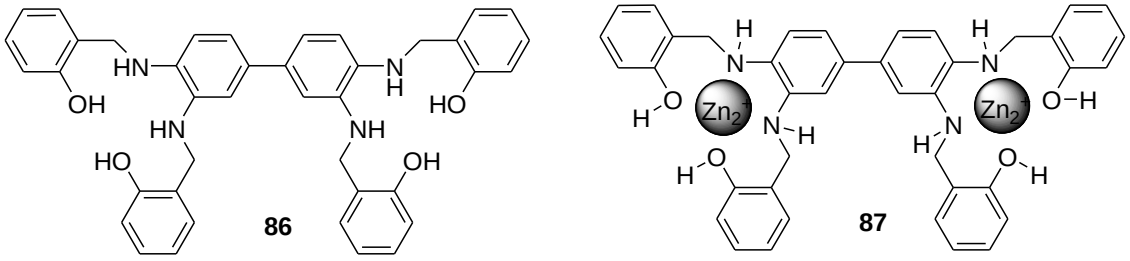

Fig. 36 Structures of receptors **86** and **87**.

Dinuclear Zn^{2+} complex **87** was able to detect ATP in DMSO:H_2O 1:9 v/v via a simple indicator displacement assay using fluoresceine (**Fl**) as an exchanged ligand.[61] Probe **86** contains sp^3 nitrogen and oxygen donor ligands capable of complexing Zn^{2+}, yielding **87** (see Fig. 36). The UV-Vis spectrum of fluoresceine in DMSO-H_2O 1:9 v/v revealed two bands of equal absorbance (at ca. 450 and 480 nm), which showed a displacement to a higher wavelength along with an enhanced absorbance upon binding with dinuclear complex **87**. This **87-Fl** ensemble was tested as a signalling system for the potential recognition of biomolecules adenine, thymine, guanine, cytosine, AMP, ADP and ATP. When anion ATP was present, a displacement of fluoresceine was observed. A limit of detection for ATP of 0.1 x 10^{-6} mol L^{-1} was determined. ADP caused minor interference in the analysis of the samples containing low ATP levels, whereas ADP, thymine, guanine and cytosine did not cause any interference in the ATP analysis.

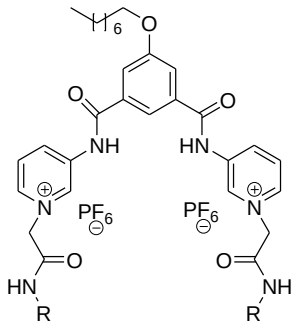

88. R = Propyl
89. R = Pyrene

Fig. 37 Structures of receptors **88** and **89**.

Pyridinium-based symmetrical diamides **88** and **89** (Fig. 37) in CH_3CN:H_2O 4:1 v/v solution (Tris buffer, pH 6.3) proved capable of detecting, to the naked-eye, citrate through an indicator-displacement assay.[62] This was achieved using fluoresceine (**Fl**) as a dye. Upon the addition of **88** to an **Fl** aqueous solution, the absorbance and emission of the dye significantly reduced and the resulting solution became colourless. Upon the addition of citrate, a displacement of dye **Fl** occurred, and both absorbance and fluorescence were restored. Sensing studies using the **88-**

Fl ensemble were performed in the presence of citrate, pimelate, tartrate, malate, adipate, glutarate, succinate, malonate, N-Ts glutamate, F^-, Cl^-, Br^-, I^-, $H_2PO_4^-$ and AcO^-, and a selective response to citrate was noted. Virtually the same results, and selective response for citrate, were obtained with sensing ensemble **89-Fl**. Moreover, it was possible to use receptor **89** alone as a fluorescent probe for anions because it includes a pyrene fluorophore in their structure. In particular, CH_3CN:H_2O 4:1 v/v solutions of receptor **89** presented the typical pyrene monomer emission in the 350-450 nm interval upon excitation at 340 nm. Then the response of **89** in the presence of citrate, pimelate, tartrate, malate, adipate, glutarate, succinate, malonate, N-Ts glutamate, F^-, Cl^-, Br^-, I^-, $H_2PO_4^-$ and AcO^- was studied. Of all the anions tested, citrate induced a significant emission enhancement, whereas pimelate and $H_2PO_4^-$ induced moderate enhancements.

2.3.- Chemodosimeter approach

Although this approach proved minimal some years ago, today is a well-established procedure for the design of anion probes. In this paradigm, specific anion-induced reactions occur which commonly involve the rupture and formation of several covalent bonds. This generally results in major chemical changes in the probe and in remarkable spectroscopic modulations. The key issue in this paradigm consists in finding rather quick selective anion-induced reactions occurring preferably in water or mixed organic-aqueous solutions. Apart from the examples for anion signalling, this section also includes the probes designed for the detection of thiol-containing amino acids. As we can see below, in most cases, chemodosimeters take advantage of the nucleophilic attack of target species to electron-deficient functional groups, which leads to a re-organisation of electron density in the whole molecule and to colour modulation. In this section, pure anion-induced deprotonation reactions have also been included.

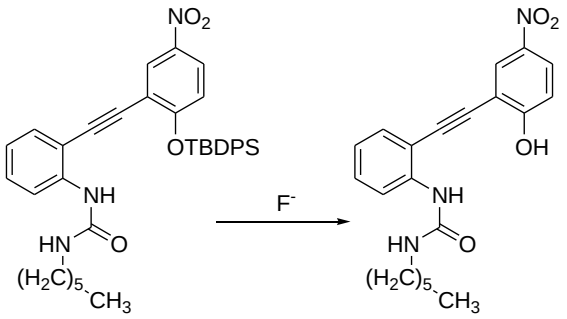

90 **91**

Fig. 38 Reaction of receptor **90** with anion F^- that yielded **91**.

Atta and co-workers synthesised a new diphenylacetilene derivative functionalised with an Si-O bond (**90**) for the selective detection of anion F^- in aqueous media.[63] CH_3CN:H_2O 9:1 v/v solutions of **90,** buffered at pH 7.0, showed an intense absorption band at 275 nm with a pronounced shoulder at 320 nm. The chromogenic behaviour of **90** was tested in the presence of F^-, Cl^-, Br^-, I^-, AcO^-, $H_2PO_4^-$, HSO_4^-, BzO^-, AcO^-, N_3^- and CN^- yet only a with significant chromogenic change was observed when adding F^-. In particular, addition of F^- induced the growth of a new red shifted absorption band at 420 nm with a change in colour from

colourless to yellow. When using this chemodosimeter, a limit of detection of 64 μM was estimated. The chromogenic response mechanism arises from an F^--induced hydrolysis of the Si-O bond that yielded compound **91** (see Fig. 38). The presence in compound **91** of a phenolic –OH and the urea moiety allowed the formation of hydrogen-bonding interactions with F^-, which are responsible for the colour changes observed.

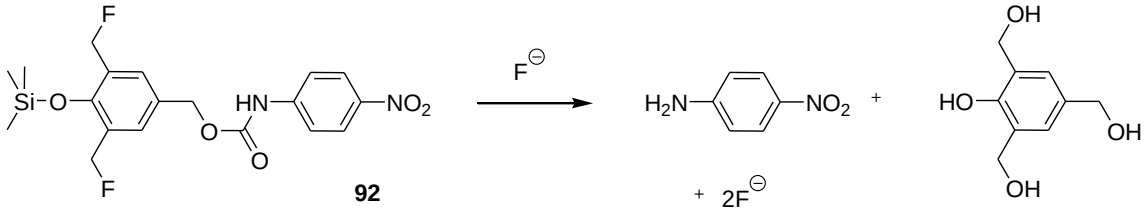

Fig. 39 Reaction of receptor **92** with anion F^-.

This work demonstrates a new example of an exponential signal amplification strategy for the direct detection of F^-.[64] Amplification occurred through the reaction of F^- with probe **92** and the initiation of a dendritic chain reaction (DCR). The DCR probe contained a silyl ether group, which was cleaved by F^- giving a phenolate, which disassembled to release a dye reporter that absorbed at 400 nm and two additional F^- (Fig. 39). These two F^- atoms were able to activate two more molecules of probe **92** and to generate the self-inductive disassembly and exponential amplification of the signal. Studies were performed in CH_3CN:DMSO 1:1 v/v with 5% H_2O. Probe **92** displayed an immediate response with 1 equiv. of F^-. When the number of equiv. lowered (0.004 equiv.), the amplification signal was observed after 10 h. Probe **92** was tested in the presence of other anions (Cl^-, Br^-, I^-, AcO^-), but no colour changes were observed.

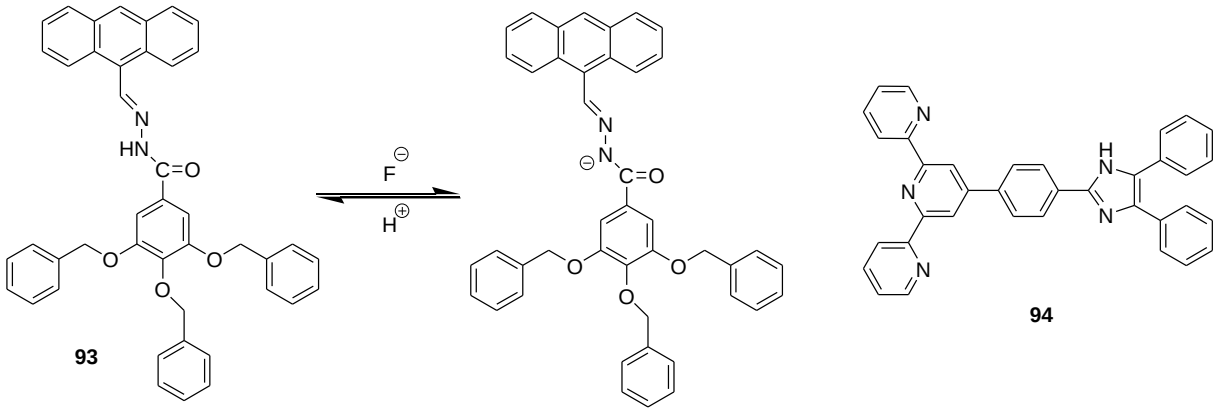

Fig. 40 Reversible **r**eaction of receptor **93** with anion F^- and the structure of **94**.

Low Molecular-Weight Gel (LMWG) **93,** based on poly(arylether) dendrons with an anthracene chromophore attached through an acylhydrazone linkage, was used for the efficient detection of F^- (Fig. 40).[65] Compound **93** was able to form a gel in $CHCl_3$:CH_3OH 1:1 v/v mixtures. Upon the addition of small quantities of anion F^- (0.1 equiv.) to this gel, changes in colour from deep yellow to bright red were observed. Recognition took place through a reversible gel-sol transition due to the deprotonation of NH groups upon the addition of F^- anions. The other anions tested (Cl^-, Br^-, I^-, ClO_4^-, AcO^-, $H_2PO_4^-$ and HSO_4^-) induced negligible colour changes.

Absorption studies of terpyridyl-imidazole-based bifunctional receptor **94** (Fig. 40) in DMF:CH_3CN 1:9 v/v solutions revealed F^- binding and sensing properties.[66] Upon the addition of several anions (F^-, Cl^-, Br^-, I^-, AcO^-, $H_2PO_4^-$, OH^- and ClO_4^-), dramatic colour changes of receptor **94** were observed in only the presence of F^- and OH^-. Anion-sensing studies indicate that the deprotonation of the imidazole N-H proton of receptor **94** occurred with the development of a bright yellow colour (the absorption band at 341 nm was red-shifted to 420 nm) in the presence of excess F^- . The authors also demonstrated that the free receptor was a suitable solvatochromic probe.

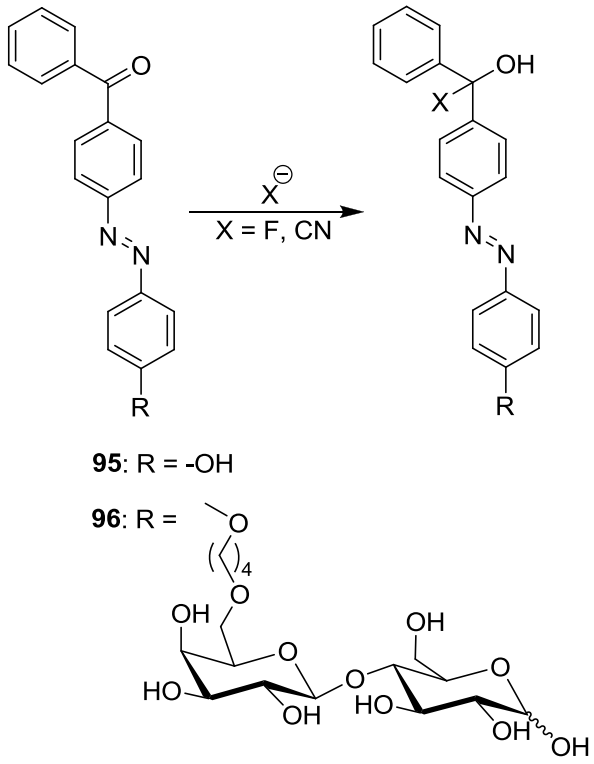

Fig. 41 Proposed signalling mechanism of CN- or F- using **95** and **96**.

Solutions of **95** in DMSO reacted with CN^- or F^- inducing distinct spectra changes (i.e., the intensity of the band at 356 nm diminished and a new band at 455 nm appeared).[67] Solutions changed from colourless to yellow, while other anions such as Cl^-, AcO^-, $H_2PO_4^-$ and SCN^- did not induce any colour modification, even when in excess. In H_2O, glycoconjugated dye **96** showed better selectivity to CN^- if compared to **95**. A limit of detection of 2.0 x 10^{-5} M to CN^- was estimated using **96** in pure H_2O. Changes in colour were ascribed to the formation of the corresponding cyanohydrin and fluorohydrin derivatibes via the nucleophilic attack of CN^- and F^- anions to the carbonyl group in **95** and **96** (as shown in Fig. 41).

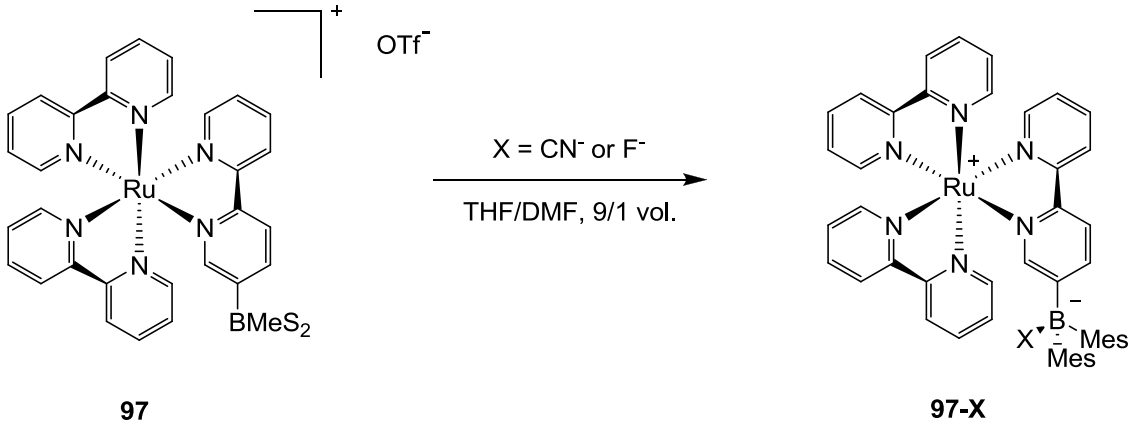

97 **97-X**

Fig. 42 Proposed signalling mechanism of CN^- or F^- using **97**.

A cationic cyclometalated Ru^{2+} complex **97,** decorated by a peripheral Lewis acidic boryl moiety, proved to be a suitable chromogenic chemosensor for F^- or CN^- anions.[68] Addition of these anions to solutions of **97** in CH_3COCH_3 resulted in a colour change from deep purple to nearly black. Additional studies in $CHCl_3$:DMF 9:1 v/v showed that **97** displayed a higher affinity for CN^- than for F^-. The UV-Vis spectral changes in the presence of either F^- or CN^- were similar and included a decrease in the absorption band at 335 nm (assigned to the triarylborane chromophore absorbance) and a 30 nm bathochromic shift (from 550 to 580 nm) of the metal-to-ligand charge transfer band in **97**. This shift was attributed to the increased donor ability of the boron-substituted phenylpyridine ligand upon CN^- and F^- binding to the boron centre (see Fig. 42). Addition of other anions, including Cl^-, Br^-, I^-, or NO_3^-, resulted in no colour changes.

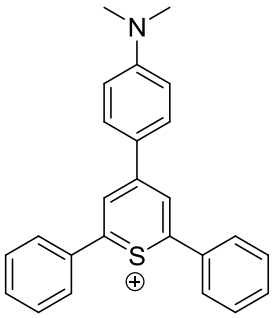

98

Fig. 43 Structure of receptor **98**.

The response of receptor **98** (Fig. 43) in the presence of certain anions in CH_3CN was studied.[69] Solutions of **98** showed a charge transfer band at 585 nm which remained unchanged upon the addition of Cl^-, Br^-, I^-, NO_3^-, $H_2PO_4^-$, HSO_4^-, AcO^-, BzO^- and NCS^-. However, addition of CN^- induced the complete bleaching of the solution due to a nucleophilic addition reaction on the C2 and C4 carbon atoms in the thiopyrylium ring. The modification and use of **98** for the colourimetric recognition of CN^- in aqueous solutions has also been previously published.[70]

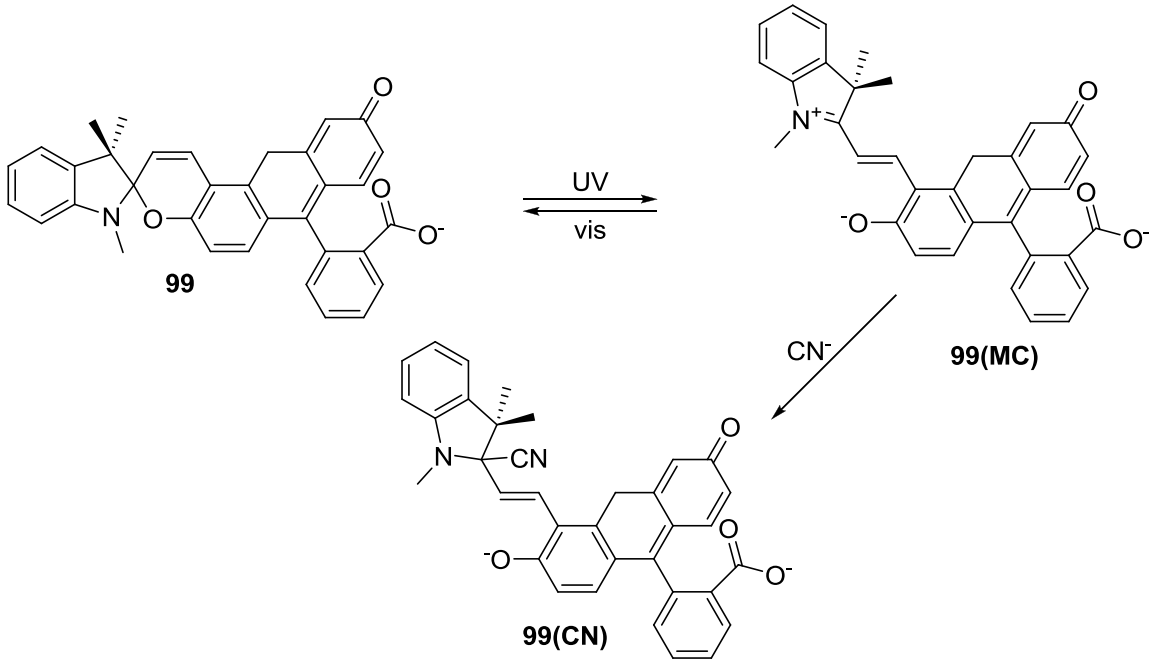

Fig. 44 Proposed signalling mechanism of CN^- using **99**.

Sumiya and co-workers prepared a new fluoresceine-spiropyran-conjugated derivative (**99**) for the selective detection of anion CN^- in aqueous media (see Fig. 44).[71] Solutions of **99** in $CH_3CN:H_2O$ 1:1 v/v, buffered at pH 9.3 and irradiated at 254 nm, yielded merocyanine **99(MC)** which presented two absorption bands at 467 and 568 nm. Addition of anion CN^- reduced both absorptions, and also increased the new band centred at 512 nm. The changes in colour were ascribed to the CN^- addition to the charged spirocarbon of **99(MC)** which leads to the formation of **99(CN)**. A limit of detection for CN^- of 5.0 μM was determined. Addition of other anions, i.e., F^-, Cl^-, Br^-, I^-, AcO^-, $H_2PO_4^-$, HSO_4^-, ClO_4^-, NO_3^- and SCN^-, induced negligible changes in the absorption bands of **99(MC)**.

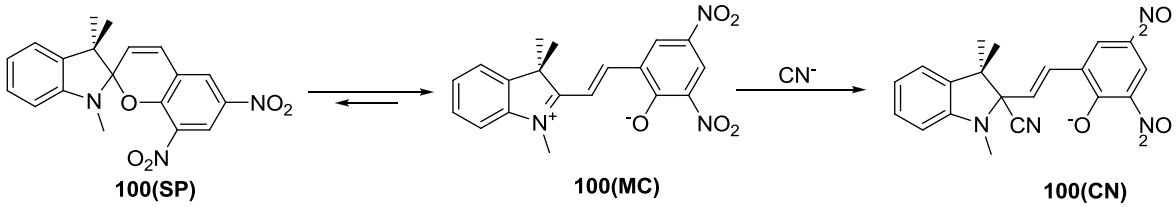

Fig. 45 Proposed signalling mechanism of CN^- using **100**.

A similar probe for CN^- was developed by Shirashi and co-workers using the merocyanine **100(MC)** isomer (see Fig. 45), obtained from the corresponding spirobenzopyran **100(SP)**.[72] In this case, **100(MC)** was obtained without irradiation, but by simply dissolving **100(SP)** in aqueous media under dark conditions. In this environment, anion CN^- was able to give nucleophilic addition to the spirocarbon of **100(MC)** with subsequent UV-vis spectral changes. In particular, when $CH_3CN:H_2O$ 98:2 v/v solutions of **100(MC)** (buffered at pH 9.3) were treated with increasing amounts of CN^-, the band at 523 nm gradually decreased, while a new band at 400 nm formed. The sensing mechanism was confirmed by NMR studies. Moreover the

authors treated the probe under the same conditions with other anions (F^-, Cl^-, Br^-, AcO^-, $H_2PO_4^-$, HSO_4^-, ClO_4^-, NO_3^-, SCN^-, N_3^- and SO_3^{2-}), but none was able to induce appreciable spectral changes. A limit of detection for CN^- of 0.8 μM was determined.

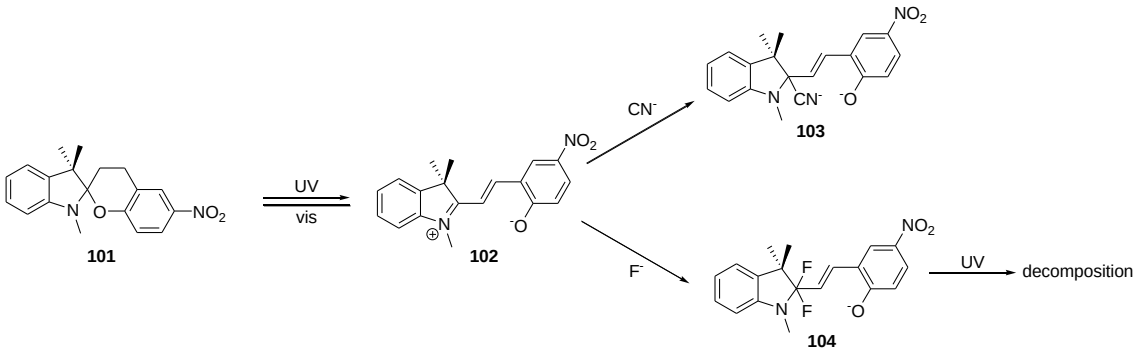

Fig. 46 Proposed signalling mechanism of CN^- and F^- using **101**.

Similarly, spirobenzopyran **101,** in its merocyanine form **102,** was used for the chromogenic sensing of anions CN^- and F^- (see Fig. 46).[73] CH_3CN:H_2O 1:1 v/v solutions of **102,** buffered at pH 9.3, showed two absorption bands at 340 and 520 nm. Addition of anion CN^- induced a marked reduction in the absorbance of these bands, together with the appearance of a new absorption at 421 nm. Addition of F^-, Cl^-, Br^-, I^-, AcO^-, $H_2PO_4^-$, HSO_4^-, ClO_4^-, NO_3^- and SCN^- induced negligible changes in the bands of receptor **102**. As in the above cases, colour changes were ascribed to the addition of CN^- to **102,** which led to the formation of **103**. In CH_3CN solution, F^- was also able to induce the same spectral modifications observed with CN^-. In this case, the addition of F^- to **102** yielded compound **104,** which decomposed upon UV irradiation.

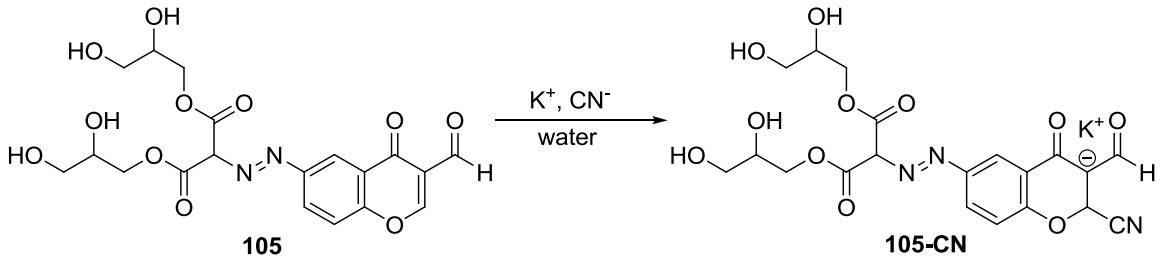

Fig. 47 Proposed signalling mechanism of CN^- using **105**.

The chromenyl-azo dye (**105**) was reported to behave as a selective probe for CN^-.[74] Water solutions of **105** presented an absorption band at 380 nm. Of all the anions tested (BrO_3^-, Cl^-, ClO_4^-, SCN^-, oxalate, IO_3^-, NO_2^-, NO_3^-, PO_4^{3-}, SO_3^{2-}, SO_4^{2-}, $S_2O_8^{2-}$, F^- and CN^-), only CN^- induced the disappearance of this absorption, along with the subsequent growth of a new band at 490 nm (colour change from light orange to pink). The observed spectral changes were induced by the nucleophilic addition of CN^- to the α,β–unsatured aldehyde of the chromenyl moiety of **105,** which yielded **105-CN** (see Fig. 47).

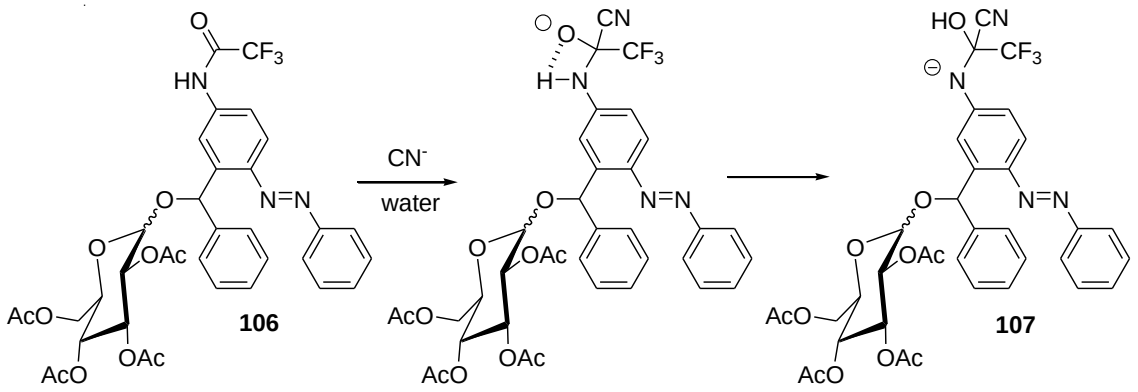

Fig. 48 Proposed signalling mechanism of CN^- using **106**.

Chemodosimeter **106,** based on trifluoroacetamide benzhydrol, allowed the naked eye detection of CN^- in aqueous media.[75] The UV-visible spectrum of **106,** in pure water at pH 7.0, showed a band at 361 nm which decreased upon the addition of increasing quantities in CN^- with concomitant grow of a new absorption at 447 nm. Selectivity of **106** towards CN^- was assessed and the authors found that the addition of F^-, Cl^-, Br^-, I^-, AcO^-, $H_2PO_4^-$, HSO_4^-, N_3^-, CO_3^- and S^{2-} induced negligible changes in the UV-visible spectrum. A limit of detection of 0.33 μM for CN^- was determined. Changes in absorption were ascribed to a reaction of adding CN^- to the trifluroacetamide moiety, which led to the formation of compound **107** (Fig. 48).

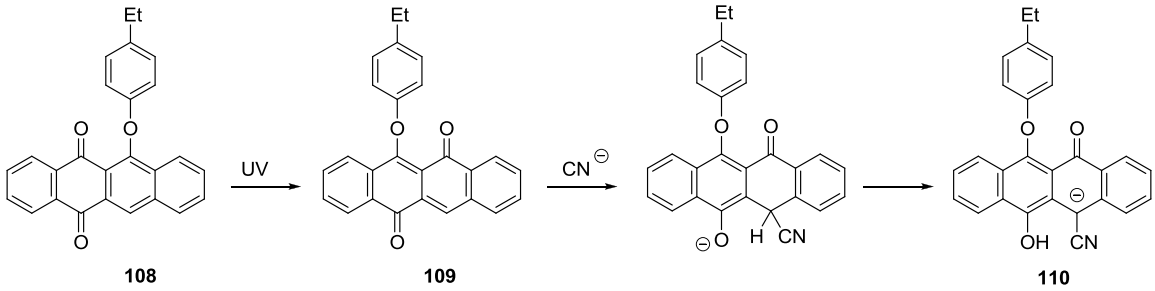

Fig. 49 Proposed signalling mechanism of CN^- using **108-109**.

Photoisomerisation of phenoxyquinone **108** upon UV irradiation produced **109,** which was used for the chromogenic sensing of CN^- (see Fig. 49).[76] In particular, CH_3CN solutions of **108** showed an absorption band at 400 nm. Irradiation with UV light (365 nm) induced the appearance of a broad absorption in the 400-550 nm interval, which was ascribed to the formation of quinone **109**. Adding anion CN^- to CH_3CN solutions of **109** resulted in a colour change from yellow to pale brown due to the generation of broad absorption bands in the 630-940 nm range. These spectral changes allowed the authors to determine a limit of detection for CN^- in CH_3CN of 5.26 μM. Addition of F^-, Cl^-, Br^-, I^-, NO_3^- and AcO^- induced negligible changes in **109**. The chromogenic changes observed were attributed to a nucleophilic addition of CN^- in **109,** yielding an intermediate product, which upon tautomerisation, gave **110**.

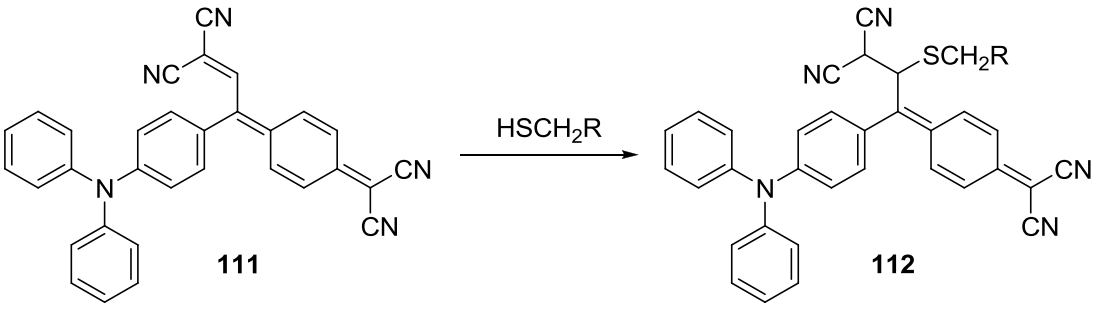

Fig. 50 Proposed signalling mechanism of Cys using **111**.

Tang and co-workers prepared receptor **111** and studied its chromogenic behaviour upon the addition of amino acids.[77] $CH_3CN:H_2O$ 1:1 v/v solutions of **111,** buffered at pH 7.4, gave two absorption bands at 426 and 710 nm. Addition of Cys induced the disappearance of both absorptions with the enhancement of a new band at 300 nm (change in colour from yellow-green to colourless). The same colour changes were observed upon the addition of GSH and Hcy, whereas other amino acids tested (i.e., Ala, Arg, Asp, Glu, Gly, Leu, *i*-Leu, Lys, Met, Ser, Thr, Trp, Tyr and Val) induced no response. The chromogenic response mechanism arose from a nucleophilic addition of Cys to the dicyanovinyl moiety of **111,** yielding **112** (see Fig. 50).

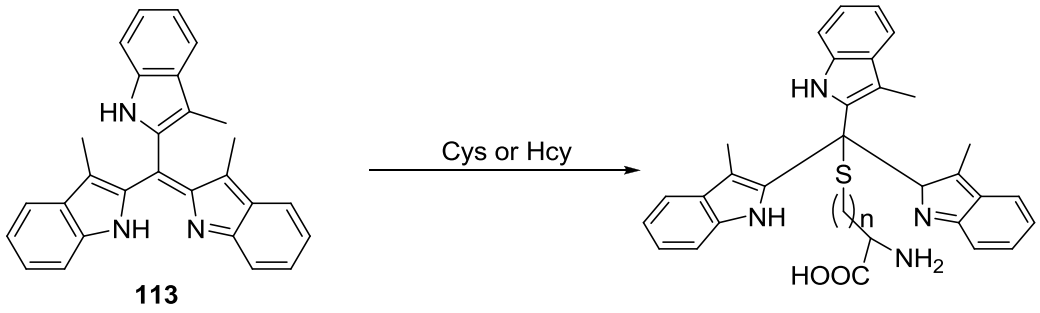

Fig. 51 Reaction between **113** and Cys or Hcy.

Tris(3-methylindol-2-yl)methane (**113**) was used for the chromogenic recognition of thiol-containing amino acids (Fig. 51).[78] For this purpose, $CH_3CN:H_2O$ 1:1 v/v solutions of **113,** buffered at pH 7.0, were tested in the presence of target amino acids (i.e., Gly, Ala, Val, Leu, Ile, Pro, Phe, Tyr, Trp, Ser, Thr, Met, Asp, Glu, Lys, Arg, Cys, Hcy, His and GSH). The solutions of **113** displayed an intense purple colour due to a broad absorption band in the 400-700 nm interval, assignable to an ICT process of the conjugated trisindoylmethane skeleton. Addition of Cys and Hcy markedly decreased the absorption band, with a clear colour change from violet to colourless. The authors proposed that the observed bleaching upon Cys and Hcy addition was the result of a nucleophilic attack of the thiol group of both amino acids to the electron-rich double bond of **113**. Limits of detection of 2.0×10^{-5} mol L^{-1} and 1.4×10^{-5} mol L^{-1} for Cys and Hcy were respectively determined.

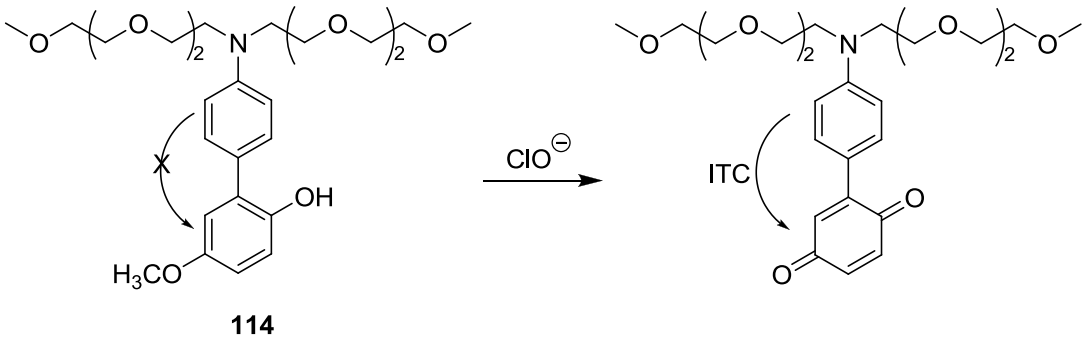

Fig. 52 Proposed signalling mechanism of ClO^- using **114**.

A new highly selective naked-eye probe for the detection of ClO^- in aqueous solutions in the pH range of 5-9 using *p*-methoxyphenol-substituted aniline derivative **114** was described.[79] After adding different amounts of ClO^- in PBS to **114,** the colourless solution (**114** absorbed strongly at around 310 nm) became blue (a new band at 572 nm appeared). This new absorption was attributed to the oxidation of the *p*-methoxyphenol unit to the corresponding benzoquinone-substituted aniline (see Fig. 52). The limit of detection for ClO^- was estimated at 1.74 µM. In the presence of other reactive oxygen species (ROS) and reactive nitrogen species (RNS), including H_2O_2, $^1O_2$, O_2^-, $ROO^\cdot$, $NO^\cdot$ and $^\cdot OH$, the absorption spectrum of **114** remained almost unaltered. Furthermore the presence of other anions (i.e., F^-, Cl^-, Br^-, I^-, ClO_3^-, ClO_4^-, CO_3^{2-}, SO_4^{2-}, PO_4^{3-}, $H_2PO_4^-$ and OH^-) and cations (i.e., Fe^{2+}, Fe^{3+}, Cu^{2+} and Zn^{2+}) did not interfere with the naked-eye detection of ClO^-.

2.4.- Nanomaterials and polymers

This section involves the use of functionalised pre-organised nanoscopic solid structures or polymers in anion-sensing protocols. In most cases, the combination of these supports with molecular or supramolecular concepts result in new sensing protocols that are difficult to obtain when using simple molecular-based systems like those shown above. Yet despite these examples (*vide infra*), the use of nanomaterials or polymeric supports for anion signalling is still scarce.

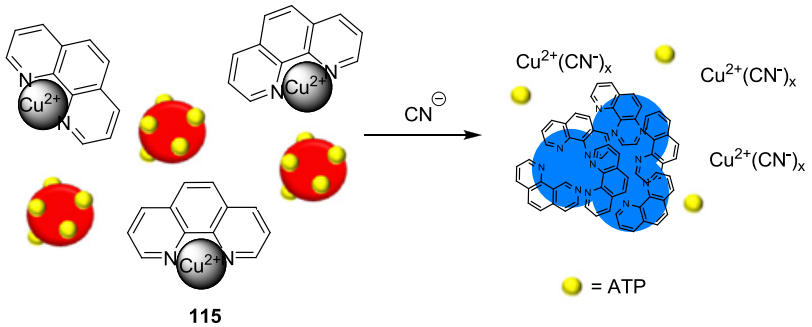

Fig. 53 Proposed signalling mechanism of CN^- using **115** in combination with AuNPs

The colorimetric sensing ensemble **115** for the detection of CN^- anions in aqueous solution combines ATP-stabilised AuNPs (sAuNPs) as a reporter and a Cu^{2+}-phenanthroline complex as

the receptor unit.[80] In the presence of Cu^{2+}-phenanthroline, both TEM observation and surface plasmon resonance (SPR) band at 520 nm confirmed the initial dispersion of the AuNPs. Upon the addition of CN^- the sAuNPs aggregated, resulting in a SPR red shift from 520 to 680 nm. The sensing mechanism involved Cu^{2+}-phenanthroline complex conversion to free phenanthroline when exposed to CN^- which caused the ATP-stabilized AuNPs to aggregate resulting in a visible red to blue colour change (see Fig. 53). High selectivity for CN^- was found as no significant change in the absorbance of the ensemble **115** was observed upon addition of F^-, Cl^-, Br^-, ClO_4^-, SO_4^{2-}, HCO_3^-, AcO^-, HPO_4^{2-}, NO_3^-, N_3^- or $P_2O_7^{4-}$. The detection limit for CN^- in neutral aqueous solutions was estimated to be 1.4×10^{-5} mol L^{-1}.

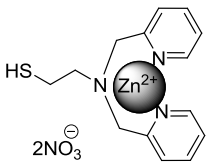

116

Fig. 54 Structure of complex **116**.

The Zn^{2+}-dipicolylamine complex **116** (Fig. 54) attached to gold nanoparticles **116-AuNPs** was described to detect bis-phosphorylated peptides (BPPs).[81] The detection ability of the **116-AuNPs** colloid was studied by adding BPP Y**p**SPT**p**SPS (C-terminal domain of the RNA polymerase II large subunit) at different concentrations. When the concentration reached 1.21 x 10^{-4} mol L^{-1}, the colour of the system changed from the original wine red to purple, indicating the aggregation of **116-AuNPs**. As the concentration of the peptide increased, the colour gradually became blue, the intensity of the absorption peak at 521 nm gradually decreased, and a new peak at 680 nm appeared. Two other BPPs models (i.e., GG**p**SGG**p**SG and GG**p**SG**p**SGG) were tested, both inducing a colour change to purple in the **116-AuNPs** colloid aqueous solution, although **116-AuNPs** displayed a higher affinity to Y**p**SPT**p**SPS.

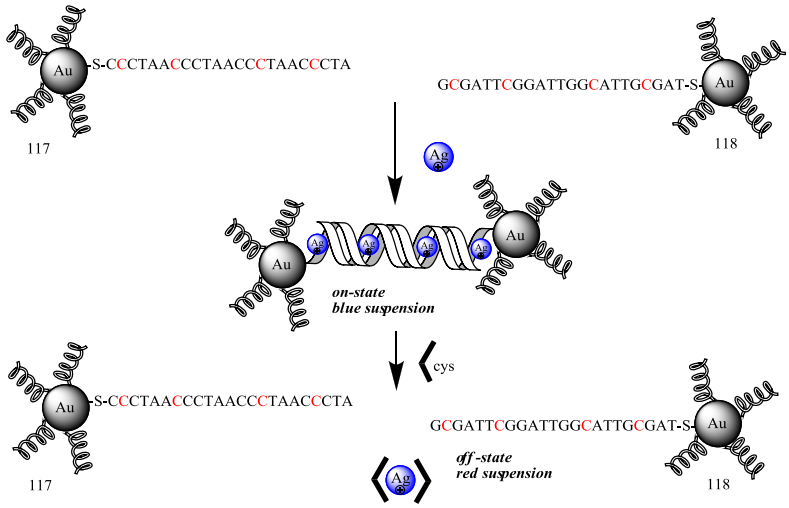

Fig. 55 Schematic representation of the signalling mechanism of silver and Cys using AuNP functionalised with oligonucleotide sequences (**117** and **118**).

DNA-functionalised gold nanoparticles were able to act as on-off probes for silver ions and Cys (see Fig. 55).[82] The basic design consists in two types of AuNP functionalised with different oligonucleotide sequences (**117** and **118**). The DNA single strands employed in both nanoparticles were complementary, except for four nucleotide sites, where a cytosine nucleotide was employed. When these NPs were suspended in PBS buffer (pH 7), no aggregation was observed due to the non C-C mismatched strands, and suspension presented a red colour. However, the presence of Ag^{+} produced an aggregation of the NPs, and the colour of the suspension changed to blue. The interconnexion of duplex DNA was produced due to the thiophilicity of Ag^{+} for the non C-C mismatched strands. This aggregation phenomenon activated the light-scattering signal. On the other hand, when Cys was introduced into the system, the formation of the Cys–Ag^{+}–Cys chelates led to the dispersion of aggregates, inducing a turn-off of the light-scattering signal. No changes were observed when employing K^{+}, Li^{+}, Zn^{2+}, Ca^{2+}, Mn^{2+}, Cu^{2+}, Pb^{2+}, Ni^{2+}, Ba^{2+}, Co^{2+}, Fe^{2+}, Fe^{3+}, Mg^{2+}, and Cr^{3+}. Meanwhile, disaggregation was found to be selective for Cys. By using this approach, a limit of detection of 50 x 10^{-9} mol L^{-1} and 5 x 10^{-9} mol L^{-1} was found,for Ag^{+} ion and Cys, respectively.

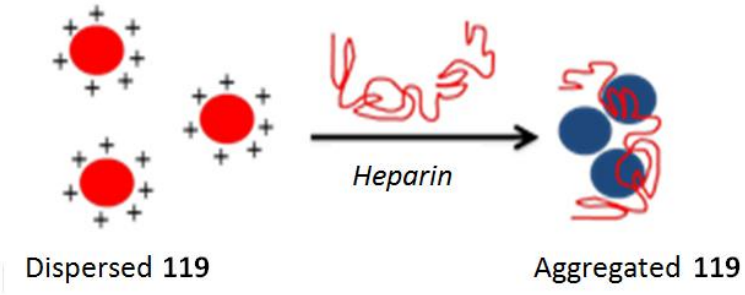

Fig. 56 Schematic representation of the signalling mechanism of heparin using positively-charged AuNPs **119**.

A simple, sensitive method for the visual detection of heparin using positively-charged cysteamine-stabilised **119** gold nanoparticles was reported.[83] In the presence of heparin, an electrostratic attraction between the positively-charged **119** and polyanionic heparin induced the aggregation of **119,** which resulted in a colour change from red to blue (see Fig. 56). Both the ξ-potential and UV measurements confirmed the principle of the assay. Particularly, in the presence of heparin, cysteamine-capped **119** displayed a decrease in the band at 520 nm and an increase in the absorption at 670 nm. A limit of detection for heparin in H_2O of 0.03 μg mL^{-1} was found. Finally, selectivity studies showed that the presence of physiological levels of Na^{+}, K^{+}, Mg^{2+}, Ca^{2+}, Cl^{-}, CO_3^{2-}, PO_4^{3-}, glucose, lactic acid, bovine serum albumin, Cys, cationic biopolymers such chitosan, polylysine, protamine, hyaluronic acid and DNA did not interfere with heparin detection. Finally, in order to apply the method to real samples, recovery experiments were carried out with spiked human serum samples.

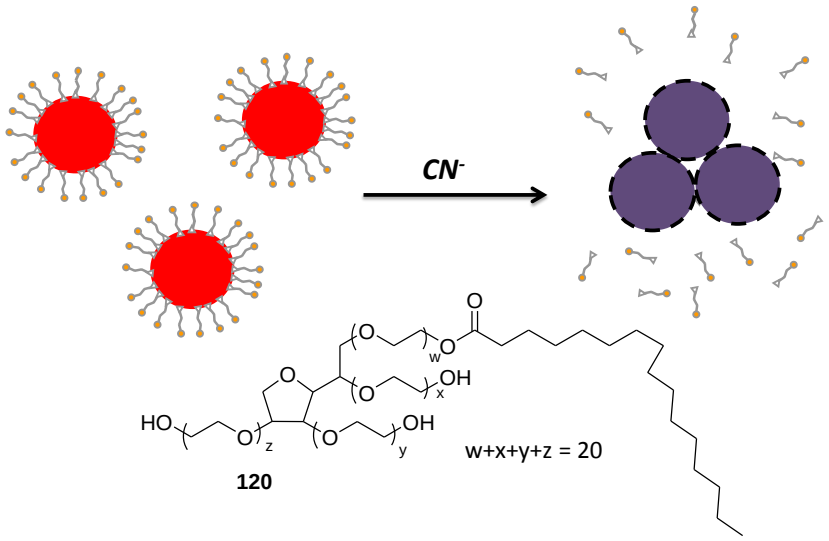

Fig. 57. Schematic representation of the signalling mechanism of CN^- using **120-AuNPs**.

Polysorbate 40 (**120**) stabilised gold nanoparticles (**120-AuNPs**) were used as a simple method for the selective and sensitive detection of CN^- and endogenous biological CN^- (See Fig. 57).[84] **120**, a neutral surfactant, stabilizsd citrate-capped **AuNPS** against high ionic strength conditions, such as solutions containing 5x PBS buffer (pH 7.4). The addition of CN^- to **120-AuNPs** produced both the formation of AuCN(s) on the surface of **AuNPs** and the $Au(CN)_2^-$ complex in aqueous solution. As a result, **120** molecules were detached from **AuNPs** and an aggregation of **AuNPs** was produced. This effect significantly decreased the SPR peak at 520 nm and formed a new SPR absorbance in the long-wavelength region (colour change from red to violet). The TEM images also confirmed the CN^--induced aggregation in **120-AuNPs**, whereas surface-assisted laser desorption/ionization time-of-flight mass spectrometry (SALDI-TOF-MS) was used to detect the existence of AuCN(s) on the **AuNPs** surface. Other anions and metal cations exhibited negligible effects on **120-AuNPs**. A limit of detection of 5.0×10^{-7} mol L^{-1} for CN^- was determined. Moreover, the authors also demonstrated that CN^- generated by the hydrolysis of linamarin induced a change in the extinction spectrum of **AuNPs** due to aggregation. A linear calibration was obtained by plotting the ratio between the absorbances at 650 and 520 nm against the concentrations of linamarin, and a limit of detection of 1×10^{-6} mol L^{-1} was calculated. The authors concluded the work with the detection of CN^- in tap H_2O and linamarin in cassava roots.

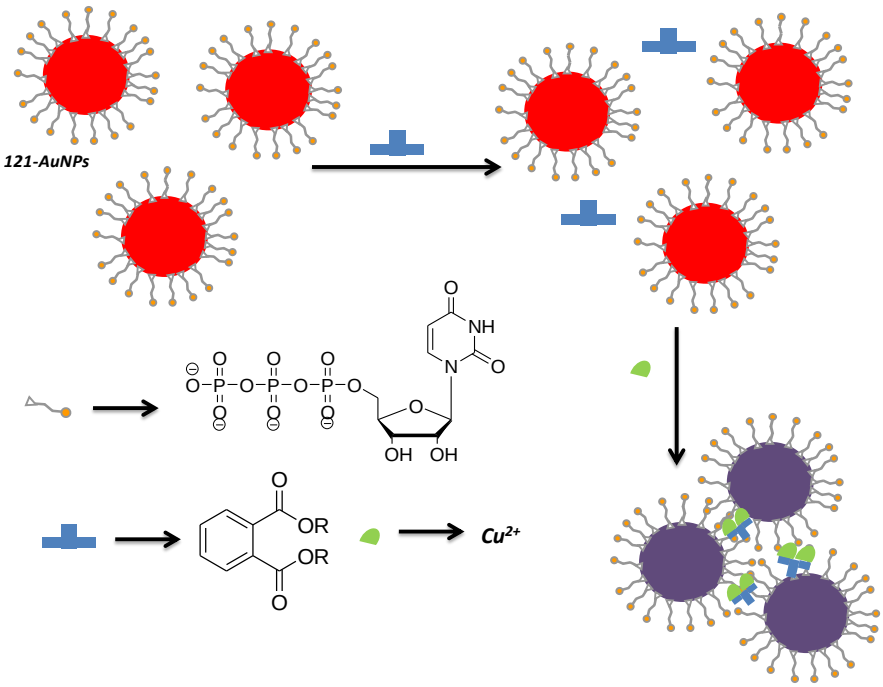

Fig. 58 Schematic representation of the signalling mechanism of Cu^{2+} using **121-AuNPs**.

The determination of phthalates in aqueous solution employing uridine-50-triphosphate (UTP)-modified gold nanoparticles (**121-AuNPs**) as a colour indicator and Cu^{2+} as a cross-linker was reported (Fig. 58).[85] Phthalates induced the aggregation of **121-AuNPs** in the presence of Cu^{2+} resulting in a colour change from red to purple due to a shift of the plasmon absorption from 520 nm to 600-650 nm. The specificity of Cu^{2+} , acting as a cross-linker for the detection of phthalates, was examined in the presence of certain competing metal ions, including K^{+}, Ba^{2+}, Na^{+}, Mn^{2+}, Zn^{2+}, Fe^{3+}, Mg^{2+}, Ca^{2+}, yet only Cu^{2+} produced a appreciable change. The system's sensitivity was tested by employing several amounts of di(2-ethyl-hexyl)phthalate (DEHP) and a limit of detection of 0.5 mg L^{-1} was found. Other phthalates including dimethyl phthalate (DMP) and di(*n*-octhyl phthalate) (DNOP), and some other species including ethyl benzoate, phthalate acid, sodium oxalate and sodium citrate, were challenged to the **121-AuNPs** probes in the presence of Cu^{2+} , but only the phthalates such as DMP, DNOP and DEHP displayed optical changes.

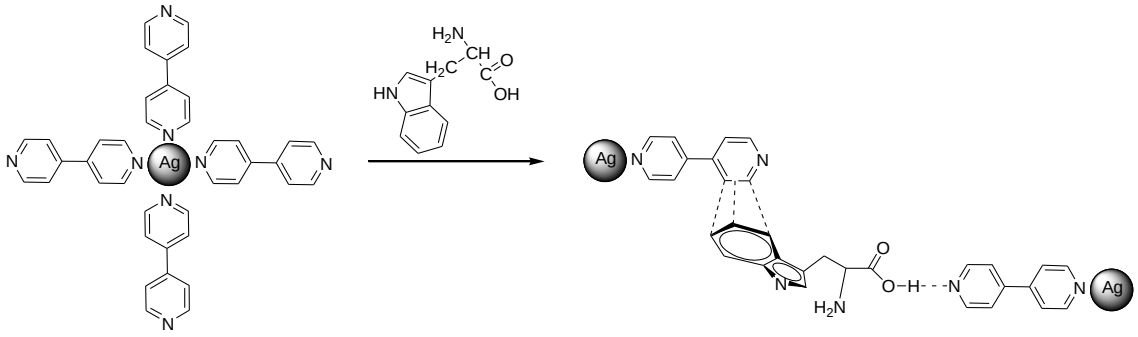

122 **122---Trp---122**

Fig. 59 Schematic representation of the signalling mechanism of Trp using 4,4-bipyridine-functionalised AgNPs (**122**).

Water-soluble 4,4-bipyridine-functionalised silver nanoparticles (**122**) were prepared and used as selective colorimetric probes for Trp.[86] Having set the pH stability of **122** in the interval of 4.0-11.0, the molecular recognition ability of the nanoparticles in the presence of amino acids was examined. After 15 min, the solution of **122** containing Trp changed from yellow to red, while other amino acids (i.e., Leu, Thr, Val, Phe, Pro, Ser, Pyr, Cys) induced no changes. For the solution containing Trp, a remarkable absorption appeared at 556 nm due to nanoparticle aggregation. A limit of detection for Trp of 2 x 10^{-5} mol L^{-1} was found. The authors suggested that aggregation was due to the interaction of Trp with the pyridine ring of 4,4-bipyridine via both π-π forces and hydrogen-bonding interactions between the carboxyl acid of Trp and pyridine (see Fig. 59). Although some aromatic compounds containing carboxyl acid group, such as indole-acetic acid, indole-butanoic acid and 1-naphthlcetic acid, turned the solutions of **122** red, it was proved that neither Tyr nor Phe caused any interference due to a weaker π-π stacking interaction with **122**.

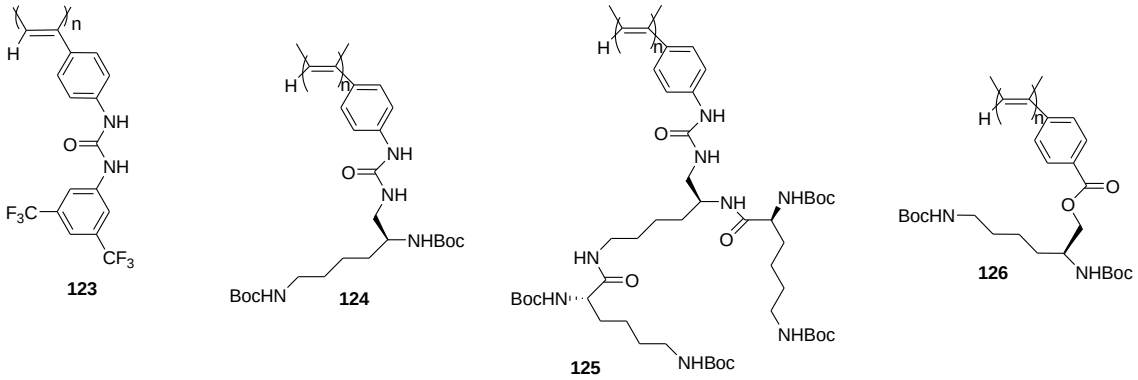

Fig. 60 Chemical structures of polymers **123-126**.

Polymer **123** (see Fig. 60), containing electron-withdrawing $–CF_3$ groups in poly(phenylacetylene) with [bis(trifluoromethyl)phenyl]urea pendants as anion-sensing system, was studied.[87] Upon the addition of BzO^-, AcO^-, Cl^-, Br^-, F^-, NO_3^-, N_3^- and HSO_4^- the yellow THF solution of **123** immediately turned to a different reddish colour depending on the anion used, although ClO_4^- produced no changes. Particularly, the ^{1}H-NMR titration studies of **123** with AcO^- showed the establishment of hydrogen-bonding interactions. Absorption titration experiments demonstrated the existence of a cooperative binding. The partially formed urea/ AcO^- complex units in the polymer chain was proposed to induce a change in the whole main chain conformation, and proved more suitable for further AcO^- binding. Similar positive allosteric binding was observed for BzO^-, Cl^- and F^-, although almost no cooperativity was found for Br^-, NO_3^-, N_3^- and HSO_4^-.

Poly(phenylacetylene) bearing second generation (G2) lysine dendrons (**125**) were used as a novel anion receptor with colorimetric detection ability (Fig. 60).[88] **125** presented no absorption bands in the visible range, whereas the presence of AcO^-, Cl^- and F^- induced a colour change to red due to the development of an absorbance at 512 nm in THF. On the other hand, the **125** circular dichroism (CD) spectra in the presence of AcO^- and Cl^- showed an intense split-type Cotton effect in the 340 to 630 nm range, but exhibited a weak negative Cotton effect at 500 nm in the presence of F^-, indicating that the F^- recognition by **125**

produced a different helical conformation than those driven by AcO^- and Cl^-. Other anions (i.e., Br^-, NO_3^-, N_3^- and ClO_4^-) apparently caused no remarkable changes in either CD or absorption spectra, although slightly pale yellow solutions were obtained for NO_3^- and N_3^-. The authors compared these results with those obtained when using (**124**) and the urea-deficient poly-(phenylacetylene) **126**. Various analyses including ^{1}H-NMR, light scattering, and viscosity measurements concluded that the conjugation of the bulky G2 dendrons in the vicinity of the urea receptors played a crucial role in the strict size specificity sensing ability of **125**.

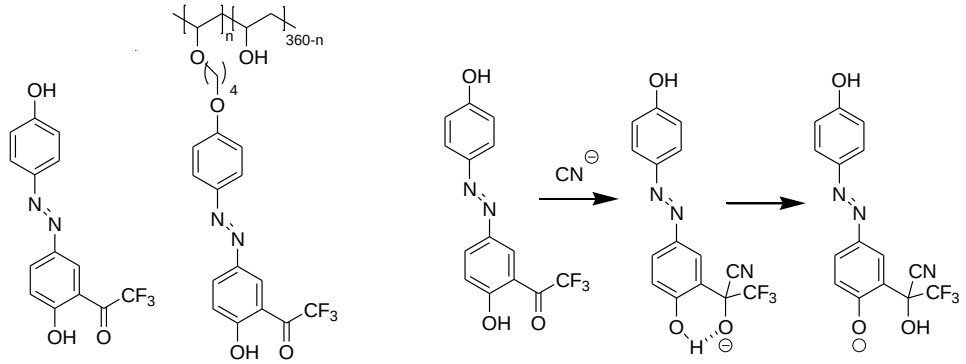

127 **128**

Fig. 61 Structures of receptors **127** and **128**, and the reaction of the former with CN^-.

New poly(vinyl alcohol) (**128**) derivative containing pendant functionalities was used for the detection of CN^- in pure H_2O with a limit of detection as low as 1 x 10^{-5} mol L^{-1} (see Fig. 61).[89] Molecular-based receptor **127** in DMSO displayed absorption at 415 nm, and the addition of F^-, AcO^- and CN^- resulted in a shift of the band to 495 nm, while other anions such as ClO_4^-, Cl^-, I^-, SCN^-, $H_2PO_4^-$, HSO_4^- did not induce any colour modulation, even when in excess. Additionally, the authors found that addition of 1% of H_2O completely avoided the reaction of **127** with AcO^-, whereas the presence of 5% of H_2O in DMSO solutions of **127** was selective to CN^-. Moreover, the anion-sensing properties of polymer **128** were studied using H_2O as a solvent at 40°C. Only the addition of CN^- led to a change in colour of **128**. The chromogenic response of **127** (and **128**) was due to an additional reaction in which CN^- reacted with the trifluoroacetyl group.

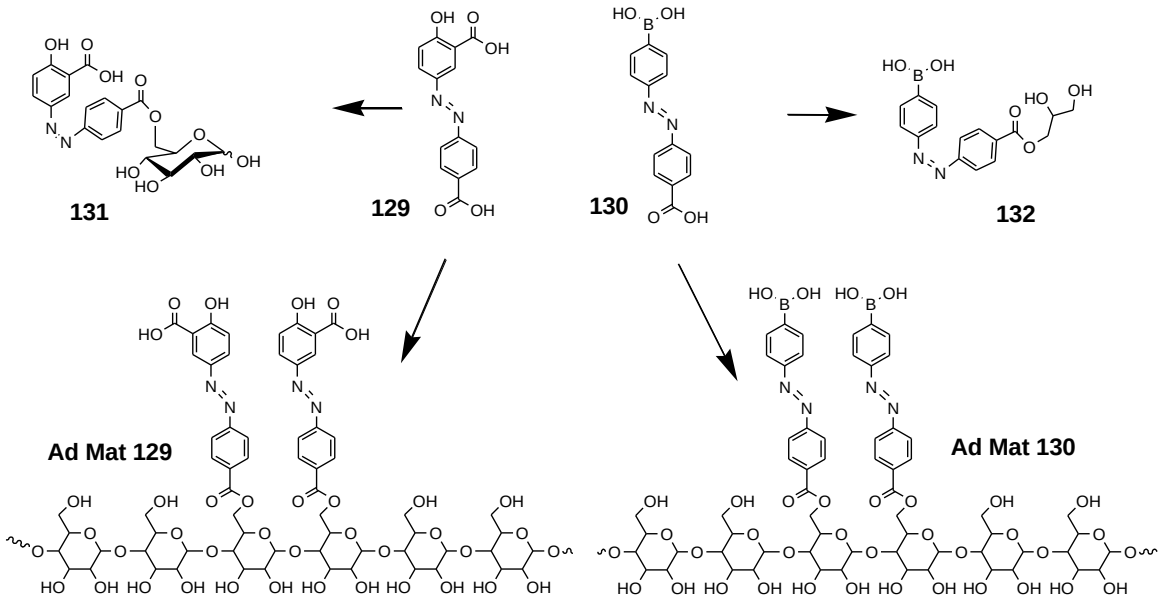

Fig. 62 Chemical structures of receptors **129–132** and materials **Ad Mat-129** and **Ad Mat-130**.

Two new azo dyes, **131** and **132** (Fig. 62), were used to detect CN^- in aqueous solutions.[90] H_2O solutions of **131** and **132** were able to induce a colour change in the presence of CN^- from colourless to yellow for **131** (shift from 357 nm to 432 nm) and from green-yellow to colourless for **132** (shift from 412 nm to 351 nm), whereas no changes were observed in the presence of other anions, such as AcO^-, HSO_4^-, ClO_3^-, ClO_4^-, Cl^-, Br^-, $H_2PO_4^-$, $S_2O_3^-$, F^-, NO_3^-,I^-, NO_2^-, SO_3^{2-}, S^{2-}, $C_2O_4^{2-}$, SO_4^{2-}, N_3^-, SCN^-, $CO_3^{2-}$and HCO_3^-. The high selectivity of anion CN^- was due to the strong nucleophilicity of this anion in H_2O. A limit of detection of 0.39 x 10^{-5} mol L^{-1} and 0.37 x 10^{-5} mol L^{-1} was found respectively for dyes **131** and **132**. In order to incorporate these groups into nano-structured natural cellulose fibres, dyes **129** and **130** were treated with $SOCl_2$ to afford the corresponding acyl chlorides, which reacted with the hydroxyl groups of cellulose to produce the corresponding materials **Ad Mat-129** and **Ad Mat-130** (Fig. 63). These materials were able to detect, via colour modulations, selectively CN^- with a limit of detection of 1.1 x 10^{-8} mol L^{-1} and 7.5 - 7 x 10^{-8} mol L^{-1}, respectively.

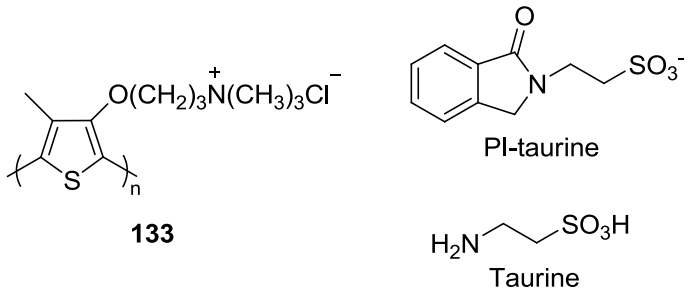

Fig. 63 Structures of **133**, Pl-taurine and taurine

The colourimetric sensing of taurine (2-aminoethanesulfonic acid) with probe poly(3-(4-methyl-3'-thienyloxy)propyltrimethylammonium) (**133**) was examined based on the strong interaction between quaternary ammonium groups in **133** and sulfonate groups in Pl-taurine which inducing aggregation of **133** (Fig. 63).[91] Taurine, having no aromatic moiety, interacted

weakly with **133** in borate buffer and scarcely induced any spectral change. However, once taurine was converted into the corresponding sulfonate-containing PI-taurine by reaction with *o*-phthalaldehyde (OPA) and then added to solutions of **133**, the colour changed from yellow to red-pink. This colour modulation was characteristic of the aggregation of **133** chains. Titrations of **133** with increasing amounts of PI-taurine in borate buffer (at pH 9) displayed a linear relationship between A_{541}/A_{407} and PI-taurine making this approach applicable to ratiometric detection. The specificity of probe **133** towards taurine (upon transformation to PI-taurine) was confirmed; addition of OPA and sulphur-containing amino acids (Met, Cys, Hcy and Cyt) to solutions of **133** induced no colour modulations.

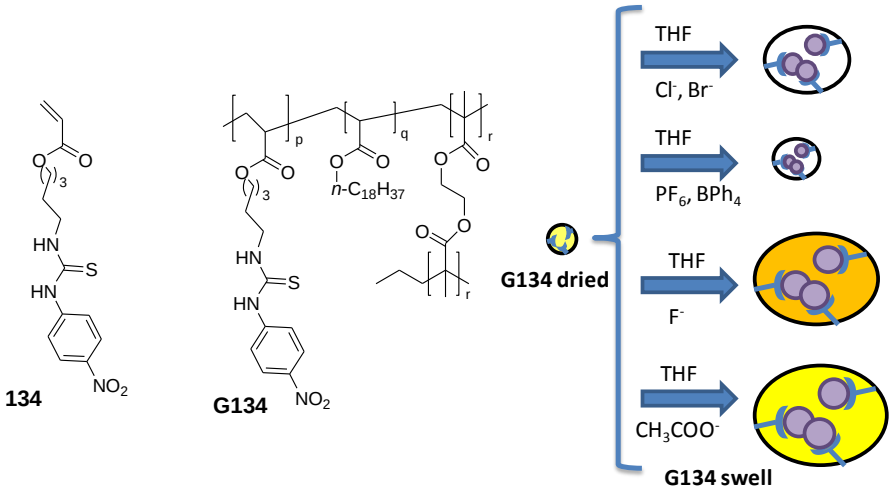

Fig. 64 Chemical structures of polymer **134** and polymer **G134** and a schematic representation of their interaction with anions Cl^-, Br^-, PF_6^-, BPh_4^-, F^- and CH_3COO^- in THF.

Material **G134** consisted in a polymer gel that was able to change size and colour in the swelling state in the presence of anion F^- or anion AcO^- in THF (see Fig. 64).[92] The polymer gel of poly(octadecyl acrylate) contained thiourea monomer **134** and was prepared by radical copolymeriyation gelation from octadecyl acrylate (**ODA**), thiourea monomer **134** and ethylene glycol dimethacrylate (**EGDMA**) as a cross-linker at a ratio of 95:5:1. When the authors introduced **G134** into a solution of various TBA salts in THF (F^-, Cl^-, Br^-, CH_3COO^-, PF_6^- and BPh_4^-) for 48 h and removed the gels from the solution, the slightly yellow dried gel **G134** turned to red and yellow-green in the presence of F^- and AcO^-, whereas other salts did not induce any colour modulation. On the other hand, it was found that the swelling degrees (the quotient between the difference of wet gel weight and dried gel weight) of the gels in the presence of anions F^- and AcO^- increased to about 40, whereas this value was ca. 20 for Cl^- and Br^-. Other more hydrophobic anions, such as PF_6^- and BPh_4^-, induced lower swelling degree values.

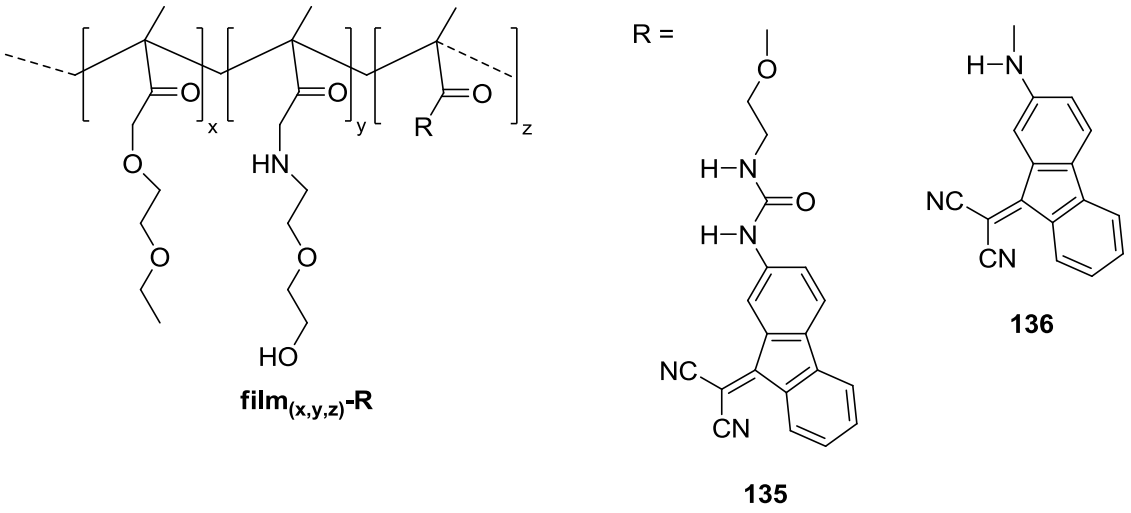

Fig. 65 Chemical structures of polymers methacrylamide (**film-135**) and methacrylic (**film-136**).

Water-insoluble organic groups **135** and **136,** containing a chemodosimeter unit (the dicyanovinyl gtoup) for CN^- anion sensing, were chemically incorporated into the lateral chain of methacrylamide (**film-135**) and methacrylic (**film-136**) polymers to give different dense membranes (Fig. 65).[93] The hydrophilic character of the designed solid material depended on the molar composition ratio (x, y, z) of the monomer used to prepare films. The colour of the different films varied from brownish, reddish to light violet. Upon soaking in aqueous solutions of CN^-, films turned colourless in less than 72 seconds. Bleaching was ascribed to a Michael reaction of anion CN^- to the dicyanovinyl moiety. An interesting response in terms of response time and colour variation was obtained with **film$_{(50,50,2)}$-135,** giving rise to a limit of detection for CN^- of ca. 260 ppb. Moreover, **film$_{(50,50,0.2)}$-136** permitted to detect CN^- at a concentration as low as 13 ppb.

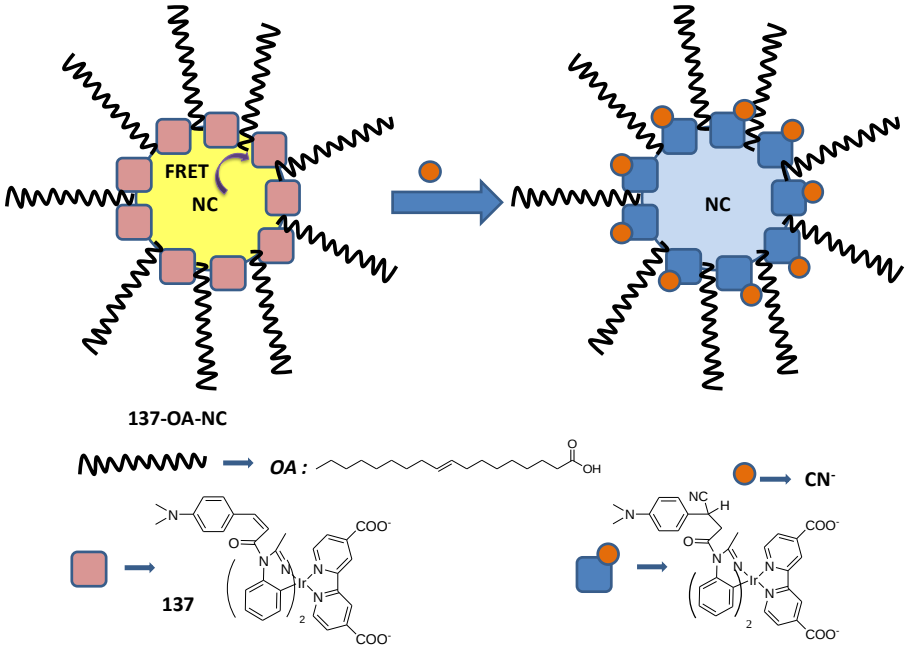

Fig. 66 Chemical structure of **137** and schematic representation of the **137-OA-NC** sensory material.

The authors designed a sensory material (**137-OA-NC**) based on nanocrystals ($NaYF_4$:20% Yb, 1.6% Er, 0.4% Tm, **NC**) functionalised with oleic acid (**OA**) and coated with a chromophoric Ir^{3+} complex (**137**) for the detection of anion CN^- and the bioimaging CN^- in living cells (see Fig. 66).[94] Nanocrystals, with visible upconversion luminescence imaging (UCL), were used as a energy donor (possess UCL emission at 800 nm as an internal standard), whereas CN^--responsive and chromophoric iridium complex **137** was chosen as an energy acceptor. Furthermore, in order to obtain a hydrophobic surrounding for **137**, **NC** were coated with oleic acid (**OA**). In the absence of CN^-, **137** shows absorbance at 505 nm, whereas UCL intensity at 540 and 800 nm was weak (due to a fluorescence resonance energy transfer (FRET) process). However, addition of CN^- caused the bleaching of the absorbance peak at 505 nm, and a colour change from pink to colourless was induced, with a 0.95 x 10^{-6} mol L^{-1} limit of detection. This limit of detection was lower than that offered by **137** (1.73 x 10^{-6} mol L^{-1}). On the other hand, emission of the **137-OA-NC** at 514-560 nm was enhanced, with a new UCL emission appearing at 475 nm upon the addition of CN^-. Finally, the authors improved the limit of detection to 0.18 x 10^{-6} mol L^{-1} by using the UCL emission at 800 nm as an internal standard and the I_{540}/I_{800} ratio as signal. Selectivity for CN^- was studied with other competing species, such as NO_3^-, ClO_4^-, F^-, Cl^-, Br^-, I^-, AcO^- and SO_4^{2-}, but no significant colour changes were observed. Finally, the authors employed the **137-OA-NC** nanocrystals for the bioimaging of CN^- in living cells.

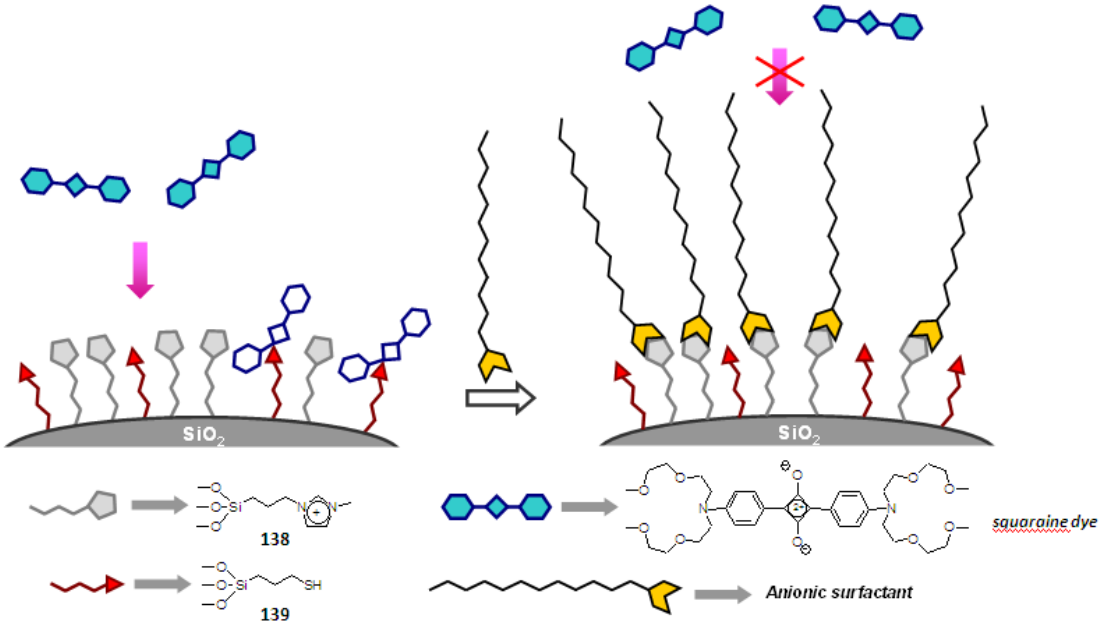

Fig. 67 Schematic representation of hybrid silica nanoparticles functionalised with thiol derivative **139** (signalling system) and imidazolium groups **138** (binding site) for the sensing of anionic surfactants using a squaraine dye as the reported unit.

Silica nanoparticles functionalised with the imidazolium (**138**) and thiol (**139**) groups were used for the chromogenic recognition of anionic surfactants.[95] A squaraine dye (absorption band at 643 nm) was used as a signalling reporter as it was able to react with thiol moieties (**139**) with the subsequent solution bleaching. H_2O:CH_3CN 9:1 (v/v) suspensions of the hybrid material were capable to bleaching the squaraine due to the free accessibility of the dye to the functionalised nanoparticle surface. However in the presence of lauryl sulphate, the reaction

of thiols (**139**) and squaraine was highly inhibited (the suspension remained blue) owing to the coordination of the anionic surfactant with the charged imidazolium (**138**) groups (through (C-H)$^{+}$···anion hydrogen-bonding interactions), which inhibited the reaction between squaraine and thiols (see Fig. 67). Other anionic surfactants, such as dodecylbenzene sulphonate, tetradecyl sulphate and dodecyl phosphate, were also able to inhibit the squaraine-thiol reaction with the subsequent chromogenic response. Long-chain carboxylates, decyl sulphate, octyl sulphate, hexyl sulphate, and cationic and neutral surfactants, were unable to inhibit the squaraine-thiol reaction with the subsequent bleaching of suspensions.

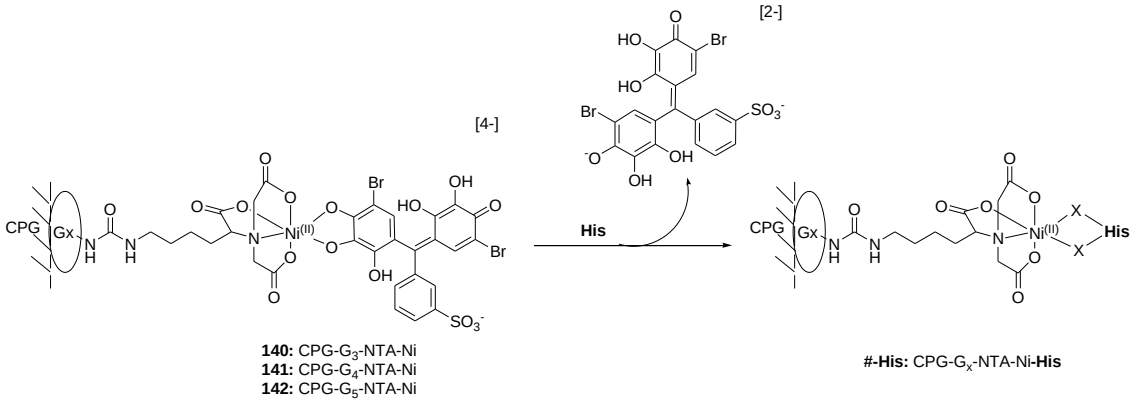

Fig. 68 Schematic representation of the signalling mechanism of His using **140-142**.

Systems **140**, **141** and **142** consist in PAMAM dendrimers (generations three, four and five; G3, G4 and G5, respectively), monolayers covalently anchored on controlled pore glass (CPG) and modified with Ni^{2+}-*N*,*N*-bis(carboxymethyl)-L-lysine (Ni^{2+}-NTA), took up the indicator dye **BPR**$^{2-}$ from solutions at pH 7.1 and functioned as a sensitive indicator displacement assay for His (Fig. 68).[96] Initially in the presence of **BPR.** the glass surface was blue, which justifies the deprotonation and coordination of the dye to the metal ion centres. When His was added, displacement occurred and **BPR** was released back into the solutions. Addition of small quantities of His clearly led to a dye release from systems **141** and **142**, while the same amount of dye released from **140** required larger His concentrations. Among other ligands, His showed the largest **BPR** displacement (43% of the surface-bound dye) compared to the 12% dye displacement observed when using Cys and 8% for Asp. Lys, Pro, Ser, Thr, Tyr and Val were the only other amino acids able to give a noticeable response (less than 5% dye displacement).

3.- Fluorogenic anion chemosensors and reagents

The use of fluorescent signalling subunits to design probes for anions has been extensively employed using well-known signal transduction procedures.[97] However, this review does not aim to detail the fluorescence signalling mechanisms in the examples shown below. As for chromogenic systems, most fluorogenic probes contained binding and signalling units. When both subunits were not electronically connected, only emission changes were observed,

whereas usually both changes in colour and emission were found if they were electronically connected.

3.1.- Binding site-signalling subunit approach

3.1.1.- Containing polycyclic aromatic hydrocarbons

Polycyclic aromatic hydrocarbons have been extensively used in the development of fluorescent chemosensors for anions. The popularity of these units is related with their well-known photo-physical properties and the large number of commercially available derivatives. Moreover polycyclic aromatic hydrocarbons are known to also act as binding groups via π-interactions.

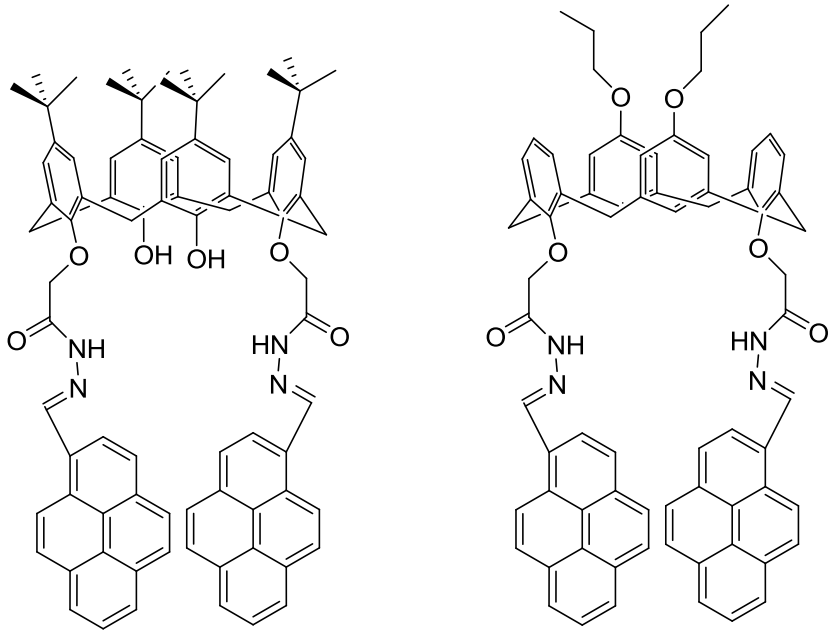

143 **144**

Fig. 69 Chemical structures of receptors **143** and **144**.

The binding behaviour of calix[4]arene-based molecular sensors **143** and **144** (functionalised with pyrene as a fluorogenic unit) was investigated in CH_3CN:$CHCl_3$ 9:1 v/v (Fig. 69).[98] Both receptors showed a broad absorption band in the 325-410 nm range ascribed to the pyrene fluorophore. In the presence of anions F^-, Cl^-, Br^-, I^-, $H_2PO_4^-$, ClO_4^-, NO_3^-, BF_4^-, AcO^-, and HSO_4^-, only F^- was able to induce a change in colour from colourless to yellow due to the appearance of a new absorption at 430 nm. Colour changes were ascribed to an ICT transition generated upon the deprotonation of the –OH (**143**) and –NH- (**144**) groups. Furthermore CH_3CN:$CHCl_3$ 9:1 v/v solutions of both receptors showed two fluorescence bands (excitation at 365 nm) in both the 400-450 nm (pyrene monomer) and 450-600 nm (pyrene excimer) ranges. Once again, of all the anions tested, only F^- was able to induce the quenching of both monomer and excimer emissions.

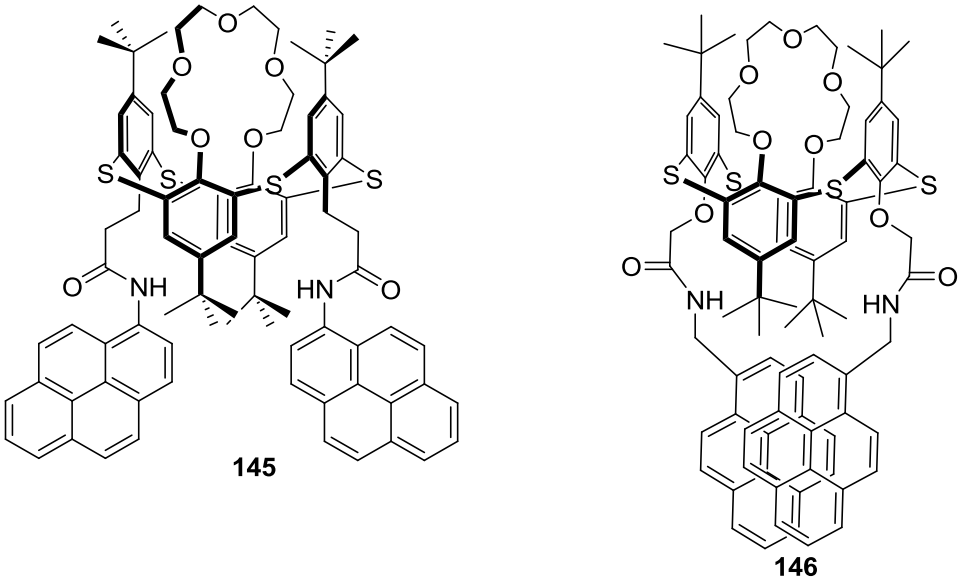

Fig. 70 Chemical structures of receptors **145** and **146**.

A new pyrene-appended probe based on a thiacalix[4]arene in a 1,3-*alternate* conformation (**145**) was prepared and tested as a fluorogenic receptor for anions (see Fig. 70).[99] THF solutions of **145** showed a strong pyrene monomer emission at 386 nm upon excitation at 344 nm. Addition of anion F^- induced the quenching of the emission band together with a slight increase in the excimer band (centred at 475 nm). Addition of other anions (i.e., Cl^-, Br^-, I^-, CN^-, AcO^-, HSO_4^-, $H_2PO_4^-$ and NO_3^-) induced negligible modifications in the emission profiles. Such changes upon the addition of anion F^- were ascribed to a PET process that was active upon the formation of the 1:1 (**145**-F^-) complex in which the anion coordinated with the N-H amides through hydrogen-bonding interactions. Receptor **145** was also used in a displacement assay for the fluorimetric recognition of anion F^-. In particular, addition of Fe^{3+} to CH_3CH_2OH solutions of **145** induced the quenching of the pyrene monomer emission due to the formation of the **145**-Fe^{3+} complex. The subsequent addition of anion F^- induced the recovery of the pyrene fluorescence due to the release of free **145**.

A thiacalix[4]arene-based chemosensor **146** (Fig. 70) was prepared for sensing Ag^+, Fe^{3+}, and Cys.[100] A solution of receptor **146** in CH_3CH_2OH:H_2O 90:10 v/v showed a weak monomer and a strong excimer pyrene emission at 377 and 470 nm, respectively (λ_{ex}= 344 nm). Upon the addition of increasing amounts of Ag^+ to solutions of **146**, a ratiometric response was noted with significant monomer enhancement and excimer quenching. The addition of increasing amounts of Fe^{3+} ions to **146** led to significant quenching in the monomer and excimer emissions. Formation of 1:1 complexes of **146** with Ag^+ and Fe^{3+} were found based on Job´s plot studies. Furthermore, the behaviour of the *in situ*-prepared ferric and silver complexes of **146** towards different amino acids was studied and a selective response to Cys was found. In particular when increasing amounts of Cys were added to the **146-Fe^{3+}** complex, a complete revival of fluorescence emission was observed (due to a Fe^{3+} displacement). On the other hand when Cys was added to the solution of the **146-Ag^+** complex, a significant quenching in the monomer emission was seen, but with only a slight revival of the excimer emission (Cys was unable to completely remove Ag^+ from the complex).

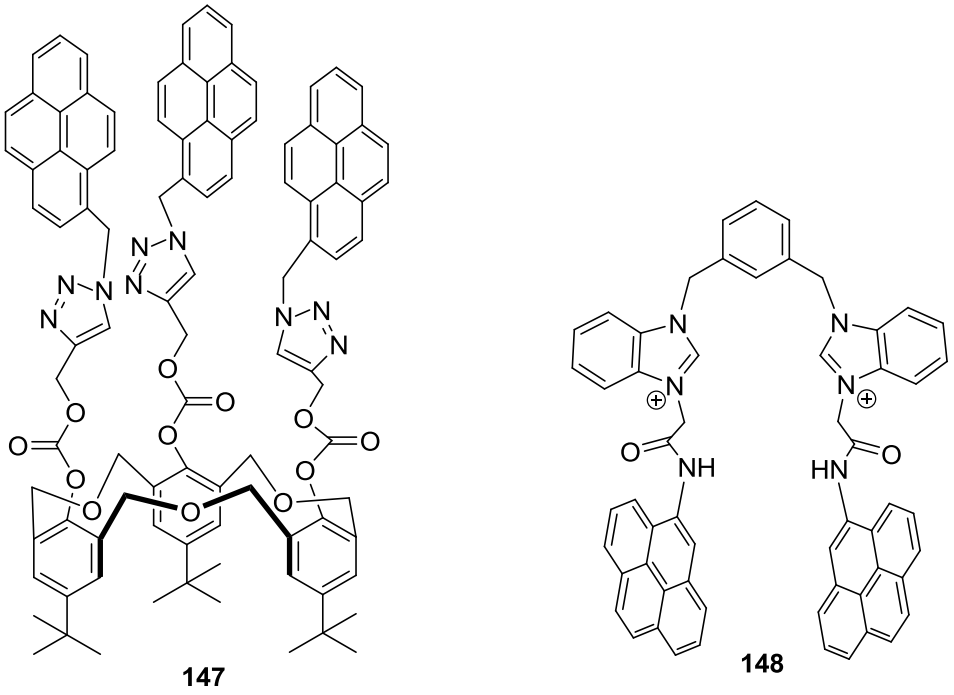

Fig. 71 Chemical structures of receptors **147** and **148**.

The pyrene-linked triazole-modified homooxacalix[3]arene (**147**) receptor was used as a ratiometric fluorescent probe for the Zn^{2+} and $H_2PO_4^-$ ions (Fig. 71).[101] Upon excitation at 343 nm of CH_3CN:CH_2Cl_2 1000:1 v/v solutions of **147,** monomer and excimer emissions were observed at 396 and 485 nm, respectively. The fluorescence intensity of the excimer of **147** gradually decreased and was accompanied by an enhancement of the monomer emission with the addition of increasing amounts of Zn^{2+}. Moreover, a solution of **147-Zn^{2+}** ([**147**]/[Zn^{2+}] 1:50) in CH_3CN:CH_2Cl_2:H_2O 1000:1:5 v/v/v) was prepared, and a 67% enhancement of excimer fluorescence intensity and reduced monomer emission were observed upon the addition of $H_2PO_4^-$. NMR spectroscopic studies suggested that the Zn^{2+} ion in the **147-Zn^{2+}** complex was located in the negative cavity formed by the nitrogen-rich triazole ligand and the carbonyl group. Upon the addition of anion $H_2PO_4^-$, only the nitrogen atoms of three triazole groups of **147** were involved in the binding with Zn^{2+}, probably due to the coordination of $H_2PO_4^-$ to the metal centre.

Benzimidazolium-based receptor **148** (see Fig. 71) was used for the fluorescent recognition and sensing of $H_2PO_4^-$, F^-, PO_4^{3-} and AMP using different solvents and pHs.[102] CH_3CN solutions of **148** showed a dual emission profile with pyrene monomer bands in the 380-405 nm interval and the excimer fluorescence centred at 482 nm. Upon the addition of different anions (i.e., F^-, Cl^-, Br^-, I^-, ClO_4^-, $H_2PO_4^-$ and HSO_4^-), only F^- and $H_2PO_4^-$ were able to induce significant changes in the fluorescence behaviour of **148**. F^- induced the quenching of both monomer and excimer emissions, whereas $H_2PO_4^-$ was able to not only quench the monomer, but to also enhance excimer fluorescence. This different behaviour was ascribed to the fact that anion $H_2PO_4^-$ formed 1:1 hydrogen-bonding complexes with **148**, whereas F^- induced the deprotonation of the receptor. The selectivity trend changed when CH_3CN:H_2O 4:1 v/v solutions of receptor **148,** buffered at pH 6.5, were used. In this case, both the monomer and excimer emission bands were gradually quenched. but only upon the addition of anion PO_4^{3-}, whereas AMP, ADP, ATP,

$H_2PO_4^-$, HPO_4^{2-} and $P_2O_7^{4-}$ induced negligible changes. With increased water content (CH_3CN:H_2O 1:1 v/v buffered at pH 7.3), only the addition of AMP induced monomer/excimer emission quenching. The quenching observed with PO_4^{3-} and AMP was ascribed to the formation of 1:1 hydrogen-bonding complexes that pushed both pyrene subunits in **148** apart.

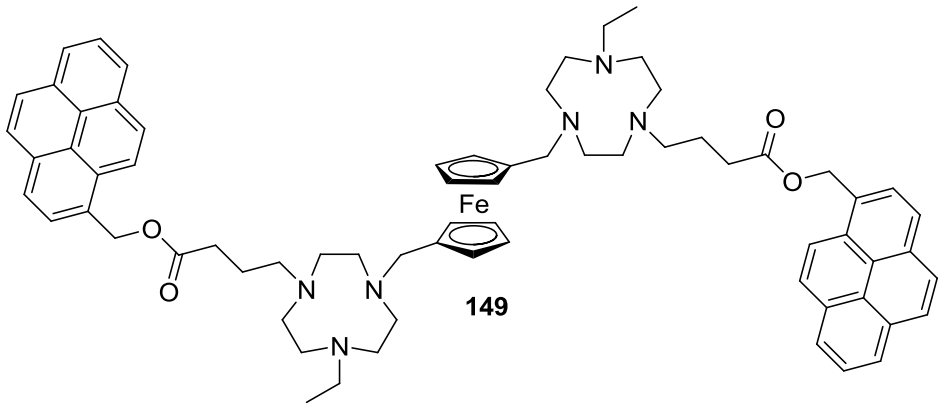

149

Fig. 72 Chemical structure of receptor **149**.

CH_3CN:H_2O 1:9 v/v solutions, buffered at pH 7.4, of the **149-(Zn^{2+})$_2$** complex showed two emission bands at 375 (from the monomer) and 475 nm (from the excimer) upon excitation at 350 nm (see Fig. 72).[103] The excimer emission in the complex was weak due to the *trans*-like configuration of the pyrene groups in relation to the central ferrocene bridging unit. Addition of anion $P_2O_7^{4-}$ induced a 6-fold enhancement in the excimer emission due to the formation of a 1:1 adduct, which induced a change in conformation that located both pyrenes into close proximity. Addition of ATP and ADP also induced an enhancement of the excimer emission at 475 nm, but with less intensity than that obtained for $P_2O_7^{4-}$. Moreover, the addition of AMP, F^-, AcO^- and HPO_4^- induced negligible changes in the emission profile.

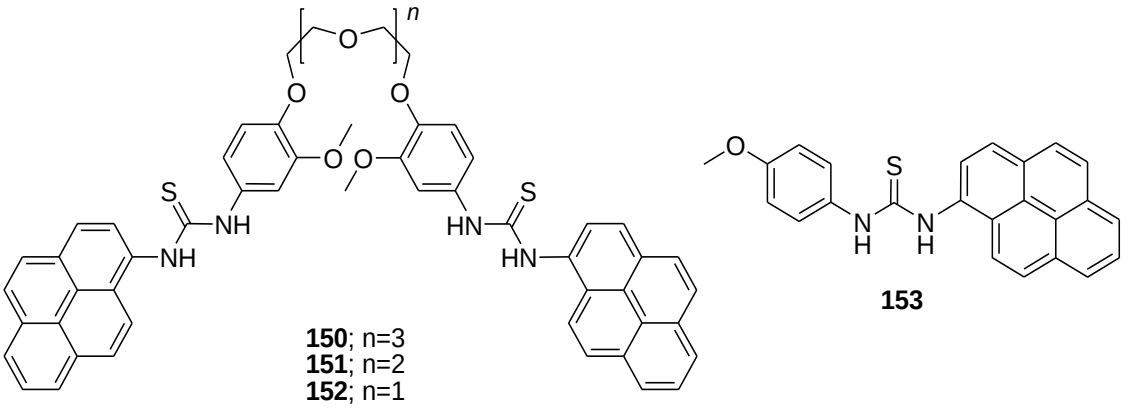

150; n=3
151; n=2
152; n=1

153

Fig. 73 Chemical structures of receptors **150-153**.

The new bispyrenyl thioureas linked by polyethylene glycol (PEG) chains, **150-152**, and the methoxy benzene pyrene thiourea, **153**, were used as fluorescent chemosensors for F^- (Fig. 73).[104] Upon excitation at 347 nm, the $CHCl_3$ solutions of **150** showed the typical pyrene monomer emission bands in the 390-410 nm range with the absence of excimer fluorescence. Of all the anions tested (OH^-, AcO^-, BzO^-,$H_2PO_4^-$, F^-, Br^-, Cl^-, and I^-), only the addition of F^- induced the appearance of a strong excimer band at 500 nm together with the minor

quenching of the monomer emission. The formation of 1:1 or 2:2 **150**-F^- species, through hydrogen-bonding interactions with the thiourea moieties, induced the appearance of the excimer emission because the two pyrene fluorophores in the final complexes were located in close spatial proximity. The fluorescence behavior of **151**-**153** was the same and only the addition of anion F^- induced the appearance of the excimer red-shifted emission band (of less intensity for **153** when compared with that obtained with **151** and **152**).

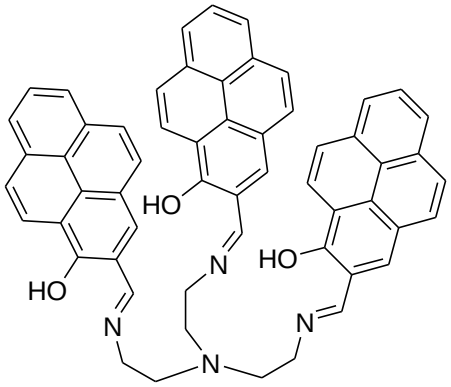

154

Fig. 76 Chemical structure of receptor **154**.

Tris(2-((ethylimino)methyl)pyren-1-ol)amine **154** was synthesized and used as fluorescent sensor for HVO_4^{2-} anion (Fig. 76).[105] DMSO solutions of receptor **154** showed the characteristic pyrene monomer emission bands centered at 390, 410 and 437 nm (excitation at 335 nm). Addition of increasing quantities of HVO_4^{2-} anion induced the immediate and progressive quenching of the monomer emission while a new peak at 513 nm appeared (maximum 30-fold enhancement upon addition of 7 equivalents of HVO_4^{2-} anion) adscribed to the pyrene excimer. Receptor **154** and HVO_4^{2-} anion formed 1:1 stoichimetry complex in which the pyrene fluorophores are in close proximity with the subsequent excimer emission appearance. After the addition of 7 equivalents of HVO_4^{2-} and with the progression of time, the excimer emission band centered at 513 nm was quenched while a peak at 564 nm appeared. ^{51}V NMR studies indicated that this new emission at 564 nm was due to the formation of a 1:1 complexex between **154** and $V_4O_{12}^{4-}$ (formed by the hydrolysis of HVO_4^{2-}).

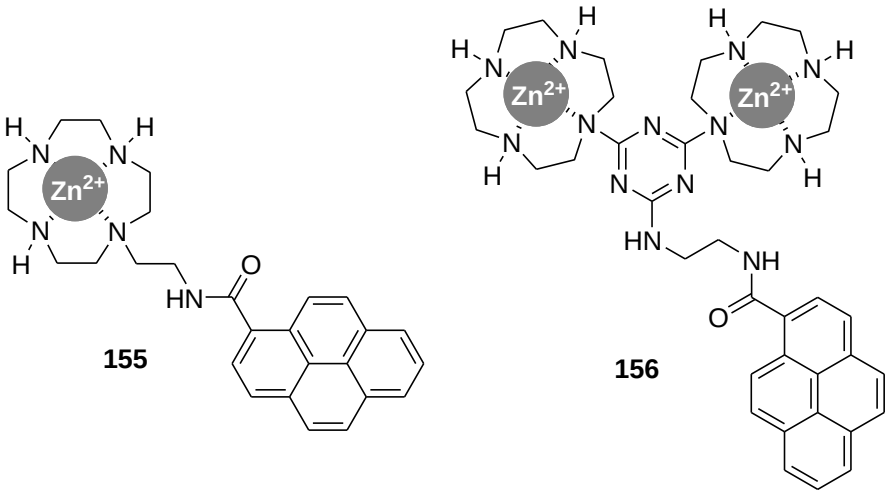

Fig. 77 Chemical structures of receptors **155** and **156**.

Zinc(II)-cyclen complexes **155** and **156** (see Fig. 77) were used as fluorescent probes for nucleotides.[106] Aqueous solutions of complex **155** (buffered at pH 7.4) presented an intense monomer emission centred at 400 nm upon excitation at 360 nm. Addition of $P_2O_7^{4-}$, TTP, UDP and UTP induced a marked decrease of the monomer band with the subsequent appearance and growth of the pyrene excimer at 500 nm (20-fold enhancement). The formation of 2:1 receptor-anion adducts induced a spatial proximity between two pyrenes from two receptor molecules, which accounted for the excimer emission growth. Addition of fructose-1,6-diphosphate induced a 5-fold enhancement in the excimer emission, whereas HPO_4^-, AMP, ATP, CMP, CDP, GMP, GDP, GTP, IMP, IDP, ITP and UMP induced negligible changes in the emission profile of **155**. For **156,** under the same conditions, anions UDP, UTP, IDP and ITP induced the enhancement of the pyrene excimer emission.

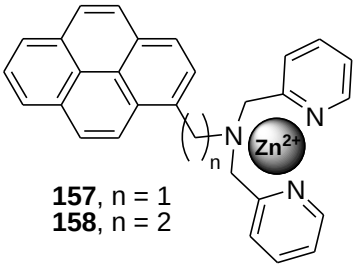

Fig. 78 Chemical structures of probes **157** and **158**.

HEPES solution of receptor **157** (upon excitation at 345 nm) showed the structured pyrene emission bands in the 370-450 nm interval (see Fig. 78).[107] Addition of 0.5 equivalents of CTP, GTP, TTP and UTP induced small quenching of the monomer emission together with the appearance of a red shifted pyrene excimer emission at 475 nm. Addition of more than 0.5 equivalents induced the quenching of the excimer fluorescence. The initial appearance of the excimer band was ascribed to the formation of 2:1 receptor-nucleotide complexes that located the two pyrene fluorophores in close spatial proximity, whereas the further quenching observed (upon addition of more than 0.5 equivalents) was ascribed to the disruption of the 2:1 aducts and the formation of 1:1 complexes. Addition of $P_2O_7^{4-}$ and AMP induced negligible changes in the emission profile of **157**. However, the response observed in the presence of ATP

and ADP was very different. Addition of ATP and ADP (0.5 and 2 equivalents) only induced enhancement of the monomer emission without the appearance of any excimer band. The authors proposed, based in ^{1}H NMR measurements, that the adenine heterocycle was located in-between both pyrene fluorophores in the 2:1 receptor-nucleotide complexes disabling the appearance of the excimer emission. The same emission response, namely the appearance of the excimer band and the subsequent quenching, was observed upon addition of CTP, GTP, TTP and UTP to HEPES solutions of **158**, whereas in the presence of $P_2O_7^{4-}$ and AMP negligible changes were found. Besides, receptor **158** was able to distinguish between ATP and ADP because the former anion induced the appearance of the excimer band when 0.5 equivalents were added (due to the formation of 2:1 receptor-nucleotide complexes in which the adenine base is outside the pyrene dimer), whereas the later only induced an enhancement of the monomer emission.

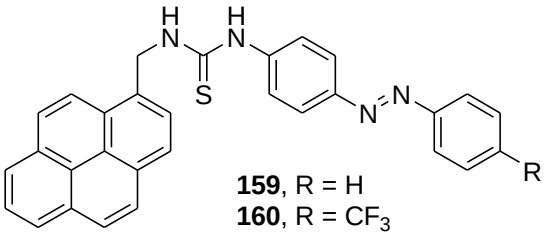

159, R = H
160, R = CF_3

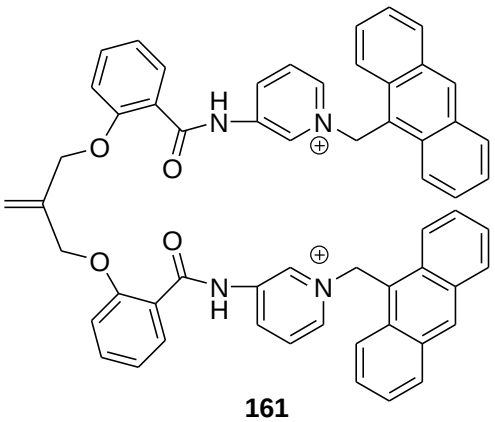

161

Fig. 79 Chemical structures of receptors **159-161**.

Pyrene-containing receptors **159** and **160** (Fig 79) were synthesised and their fluorescent behaviour in the presence of anions was studied.[108] In particular, CH_3CN:DMSO:H_2O 85:10:5 v/v/v solutions of **159** proved practically non-fluorescent upon excitation at 344 nm. However, addition of anion $P_2O_7^{4-}$ induced the appearance of a broad emission band at 410 nm (a 10-fold intensity enhancement), whereas the other anions tested (i.e., F^-, Cl^-, Br^-, I^-, NO_3^-, CN^-, SCN^-, AcO^-, $H_2PO_4^-$, HPO_4^{2-}, PO_4^{3-} and ATP) induced negligible changes. The authors attributed the emission variations to the formation of hydrogen-bonding 1:1 complexes between **159** and anion $P_2O_7^{4-}$. Virtually the same emission changes wereobserved with CH_3CN:DMSO:H_2O 85:10:5 v/v/v solutions of **160** upon the addition of anion $P_2O_7^{4-}$. In the case of **160,** addition of anions $P_2O_7^{4-}$ and F^- also induced colour changes from yellow to orange due to a partial deprotonation of the receptor.

CH_3CN solutions of receptor **161** (Fig. 79) showed the typical broad emission band in the 400-550 nm range of the anthracene monomer upon excitation at 350 nm.[109] The emission behaviour of receptor **161** was tested in the presence of anions F^-, Cl^-, Br^-, I^-, $H_2PO_4^-$, HSO_4^- and AcO^-. Only $H_2PO_4^-$ was able to induce emission enhancements due to the formation of 1:2 (**161**-anion) complexes through hydrogen-bonding interactions (with amide N-H) and electrostatic forces (with the charged pyridinium ring). Nearly the same response, namely intensity

enhancement in the presence of $H_2PO_4^-$, was observed when changing CH_3CN to a less polar solvent such as $CHCl_3$.

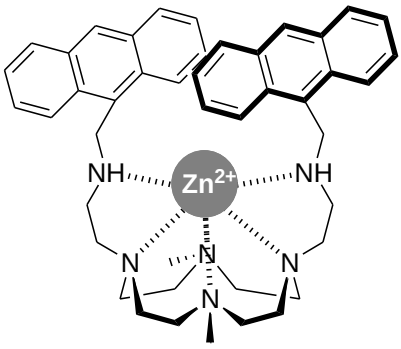

162

Fig. 80 Chemical structure of receptor **162**.

Aqueous solutions of complex **162** (HEPES, pH 7.4) showed an intense broad excimer emission at 520 nm (excitation at 370 nm) due to the spatial proximity of both anthracene fluorophores (see Fig. 80).[110] Addition of ATP induced the reduction of the excimer emission with the simultaneous growth of anthracene monomer fluorescence in the 380-450 nm interval (13.7-fold enhancement). This enhancement was ascribed to the coordination of ATP with the metal centre and with the secondary amines by pushing away both anthracene fluorophores and reducing the π-π interactions. Practically the same behaviour, but with small enhancement factors, was observed upon the addition of ADP and $P_2O_7^{4-}$, whereas no obvious emission changes were found in the presence of anions AMP, HPO_4^{2-} and ACO^-.

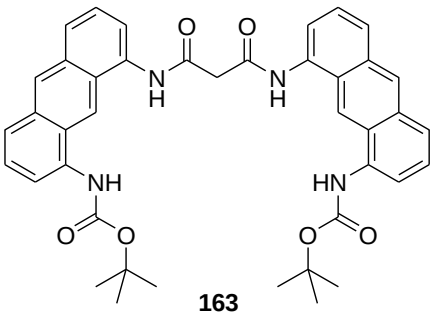

163

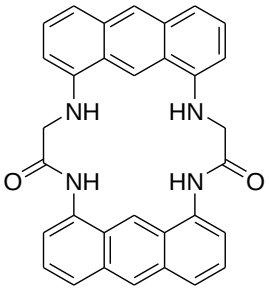

164

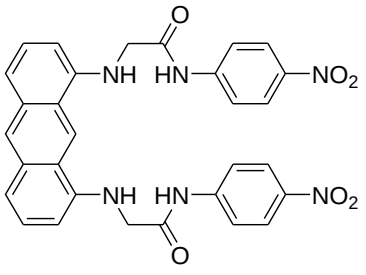

165

Fig. 81 Chemical structures of receptors **163-165**.

An acetate selective anion receptor (**163**), based on two anthracene units with a malonamide spacer, was described (see Fig. 81).[111] Solution of receptor **163** in DMSO displayed strong fluorescence at 445 nm (λ_{ex} = 387 nm), which gradually decreased upon the addition of increasing amounts of anion AcO^-, possibly due to a photo-induced electron transfer (PET) process. The stoichiometry between receptor **163** and AcO^- was determined to be 1:1 by Job´s plot analyses and ^{1}H-NMR data. Compound **163** showed good selectivity for AcO^- and no changes were noted in the presence of other anions (i.e., I^-, Br^-, Cl^-, HSO_4^-, $H_2PO_4^-$, BzO^- and

NO_3^-). A similar response to that found for AcO^- was observed with valine and phenylalanine. Major changes also took place with proline.

The new macrocyclic anion receptor **164** (Fig. 81), containing amide and amine groups and two anthracenyl fluorescent subunits, was developed as a probe for anions.[112] Solutions of **164** in DMSO displayed strong fluorescence at 484 nm (λ_{ex} = 392 nm). Upon the addition of increasing amounts of $H_2PO_4^-$, the emission intensity decreased. The formation of 1:1 species was determined by Job´s Plot analysis and ^{1}H-NMR titrations. The fluorescence quenching effect was most likely due to a PET process between the anthracene moiety and the electro-rich bounded anion. A similar behaviour was observed when other anions were added, be it to a lesser extent, and selectivity was displayed as: $H_2PO_4^- > AcO^- > F^- > C_6H_5CO_2^- > Cl^- > Br^- > I^-$.

Receptor **165** contained two N-H amides and two N-H amines proved to be a suitable chromo-fluororenic probe for basic anions in DMSO (see Fig. 81).[113] **165** showed an intense absorption at 331 nm with a shoulder at ca. 440 nm. Addition of F^- and $HP_2O_7^{3-}$ induced a red shift of the band at 331 nm to 446 nm with a colour change from colourless to yellow. The observed red shift was ascribed to a deprotonation of one of the N-H amide moieties. Addition of AcO^- and $H_2PO_4^-$ induced small red shifts in the band at 331 nm, which is indicative of the formation of 1:1 hydrogen-bonding complexes. Addition of these anions also induced an increase in emission intensity at 440 nm upon excitation at 331 nm. Other anions tested (i.e., ClO_4^-, NO_3^-, HSO_4^- and BzO^-) induced negligible changes, indicating a very weak interaction.

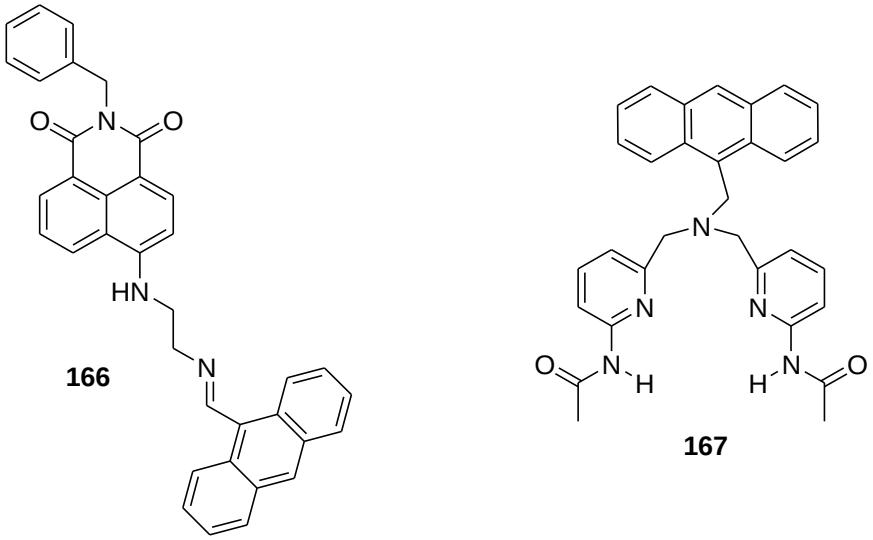

Fig. 82 Chemical structures of receptors **166** and **167**.

An efficient naphthalimide-based fluorescent dyad probe for F^- and Hg^{2+} was used for mimicking the OR, XNOR and INHIBIT logic functions.[114] Solution of **166** (see Fig. 82) in DMSO displayed a band at 448 nm, which disappeared upon the addition of F^-, while two new bands at 538 and 342 nm appeared. A colour change from light green to red was observed. Job's plot analyses revealed the formation of 1:1 complexes. DMSO solutions of **166** showed a strong emission band centred at 535 nm (naphthalimide fluorophore) upon excitation at 378 nm (anthracene fluorophore) due to an efficient FRET process. Addition of anion F^- induced a

quenching of the emission band centred at 535 nm, whereas, an emission band in the 417-437 nm interval concomitantly appeared. These emission changes were ascribed to a suppression of the FRET process upon F^- binding. No considerable changes in either the absorption or the emission of **166** were observed upon the addition of other evaluated anions (Br^-, Cl^-, I^- and SCN^-), although a weak interaction with anion AcO^- was observed.

The anthracene-containing di(6-acetylamino-2-picolyl)amine, **167**, was used as a probe for the recognition of carboxylates (Fig. 82).[115] In particular, $CHCl_3$:DMSO 98:2 v/v solutions of **167** showed the typical broad band of anthracene fluorophore in the 390-440 nm interval when exited at 369 nm. Addition of citrate, malate, fumarate, maleate and succinate induced a moderate quenching of the emission. The greatest quenching efficiency was obtained with the fumarate anion. The formation of 1:1 complexes was responsible for the emission quenching observed

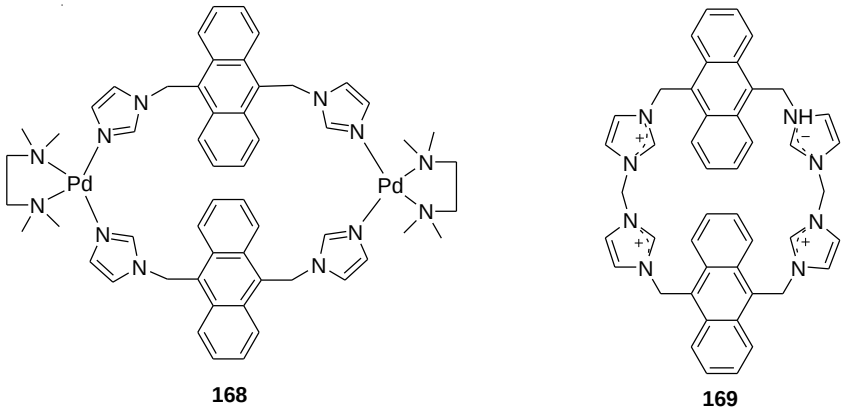

168 **169**

Fig. 83 Chemical structures of receptors **168** and **169**.

Water soluble palladium complex **168** (Fig. 83) was prepared and its fluorescent response to anions was tested.[116] H_2O:CH_3CN 2:1 v/v solutions of **168** showed the typical anthracene emission in the 390-450 nm range upon excitation at 370 nm. Addition of F^- and NO_3^- induced an enhancement in the emission intensity due to the formation of 1:1 **168**-anion complexes. However, when changing to only H_2O, addition of F^-, NO_3^-, $H_2PO_4^-$ and SO_4^{2-} induced negligible changes in the emission profile, whereas HSO_4^- induced significant enhancement. The authors ascribed the enhancement in emission intensity to a proton transfer process from anion HSO_4^- to receptor **168**.

Imidazolium-based cyclophane **169** for the fluorogenic detection of GTP and I^- in H_2O was described (see Fig. 83).[117] In particular, the aqueous solutions of **169,** buffered at pH 7.4, showed the typical monomer (centred at 427 nm) and excimer (centred at 525 nm) anthracene emission bands when excited at 367 nm. The behaviour of aqueous solutions of receptor **169** was tested in the presence of anions $P_2O_7^{4-}$, ATP, CTP, TTP, UTP, GTP, F^-, Cl^-, I-, HSO_4^- and NO_3^-. All the tested anions induced different degrees of quenching of both monomer and excimer emission bands, but the most remarkable results were obtained with GTP and I^-. The Job´s plot analyses of the titration profiles indicated the formation of 1:1 host-guest complexes between **169** and I^- with a limit of detection of 8 $x10^{-5}$ mol L^{-1}. Quenching was ascribed to a heavy atom

effect. In the case of GTP, this anion formed 2:1 host-guest complexes with **169** through hydrogen-bonding and electrostatic interactions. As a result of complex formation, both anthracene fluorophores were pushed apart with the subsequent quenching of the excimer emission. Finally, a limit of detection of 4.8 x10^{-7}mol L^{-1} for GTP was estimated.

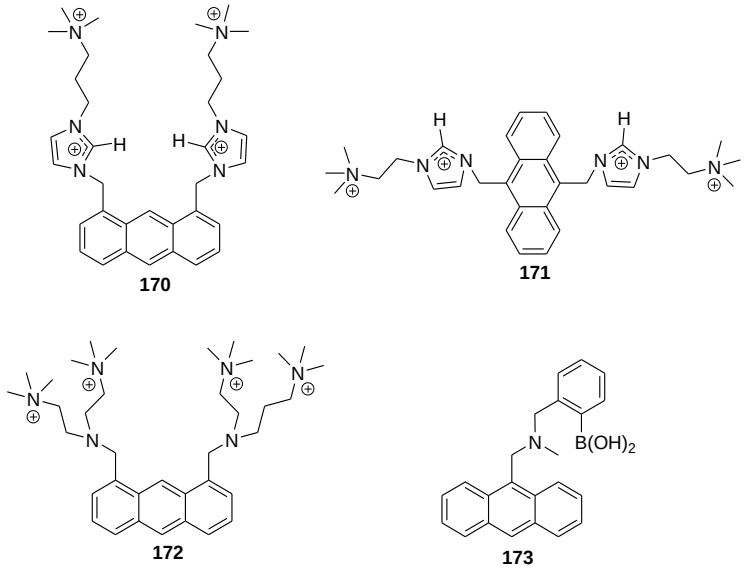

Fig. 84 Chemical structures of receptors **170**-**173**.

Anthracene derivatives **170**-**173** (see Fig. 84) were prepared for the recognition of triphosphate nucleotides.[118] Aqueous solutions of the four receptors showed the typical anthracene emission bands in the 380-450 nm range upon excitation at 373 (for **170**) and 367 nm (for **171**-**173**). The anthracene fluorophore was expected to interact with the nucleobases, whereas the imidazolium and quaternary ammonium groups could interact via hydrogen-bonding and electrostatic forces with the phosphate moieties. In particular, addition of GTP to aqueous solutions of compound **170** in HEPES (pH 7.4) brought about a large fluorescent quenching effect, while ATP, CTP, TTP and UTP were unable to induce any noticeable change. When changing to **171**, addition of TTP, CTP and UTP to solutions of compound **171** in HEPES (pH 7.4) induced slight enhancements of fluorescent, while ADP, AMP, ATP and GTP displayed fluorescence quenching (the most remarkable was noted for GTP). For **172** (CHES at pH 9.0), slight fluorescence enhancement with $P_2O_7^{4-}$, ATP and CTP was observed, while significant quenching was caused by adding GTP. Finally, aqueous solutions of **173** showed considerable fluorescence enhancement with AMP, ADP, and ATP, as well as fluorescent quenching with GTP.

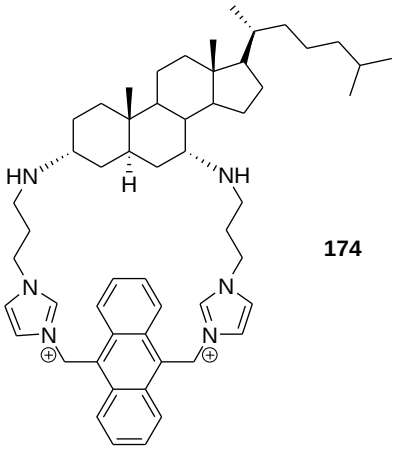

174

Fig. 85 Chemical structure of receptor **174**.

Imidazolium-functionalized cholestane-based receptor **174** behaved as a probe for $H_2PO_4^-$(see Fig. 85).[119] CH_3CN solutions of **174** showed the typical anthracene emission in the 390-470 nm interval upon excitation at 374 nm. Addition of F^-, Cl^-, Br^-, I^-, AcO^- and HSO_4^- induced a slight quenching of the emission intensity whereas in the presence of $H_2PO_4^-$ and $HP_2O_7^{3-}$ a significant reduction of the fluorescence (of 95 and 90% respectively) was respectively obtained. Both anions formed 1:1 complexes through hydrogen-bonding and electrostatic interactions, which were responsible for the quenching observed (PET process from the bonded anion to the exited fluorophore). When changing to CH_3CN:H_2O 9:1 v/v solutions (buffered at pH 7.4), addition of F^-, Cl^-, Br^-, I^-, AcO^- and $H_2PO_4^-$ brought about negligible changes, whereas HSO_4^- and $HP_2O_7^{3-}$ induced moderate emission enhancements. The authors ascribed the enhancement to an inhibition of the PET process due to the protonation of the secondary amines in the aqueous environment.

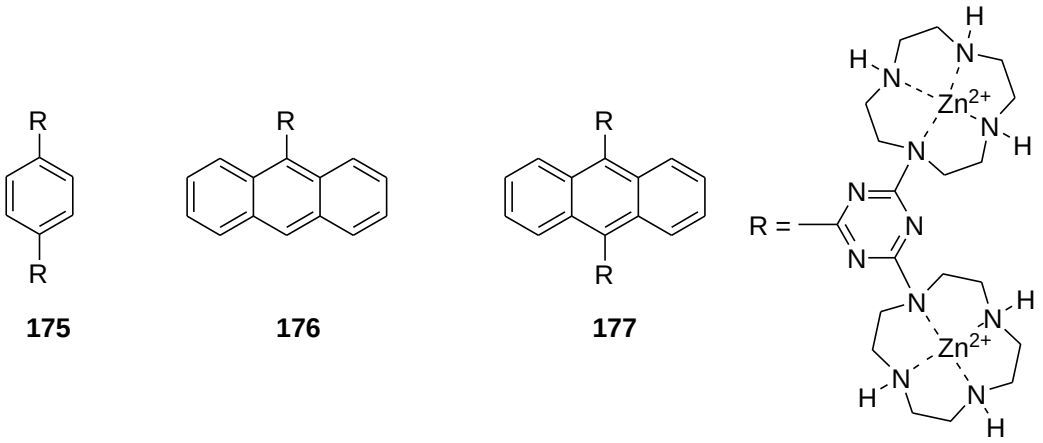

175 **176** **177**

Fig. 86 Chemical structures of the bis-zinc(II)–bis-cyclen complexes **175-177**.

Rigid luminescent bis-zinc(II)–bis-cyclen (**175-177**) complexes for the detection of anion $P_2O_7^{4-}$ were reported (see Fig. 86).[120] H_2O solutions (buffered at pH 7.4) of receptor **175** showed an emission band at 385 nm (excitation at 290 nm), which was completely quenched upon the addition of increasing quantities of anion $P_2O_7^{4-}$. Job's plot analyses indicated the formation of 1:2 **175**-anion complexes, in which both planar benzene-triazine moieties yielded π–π stacking interactions, accounting for the quenching observed. Aqueous solutions of **176** showed a

broad emission band at 455 nm upon excitation at 364 nm, with enhanced in intensity (3.4-fold) when anion $P_2O_7^{4-}$ was added. The same behaviour was observed for **177**, namely enhancement in the emission band (5.5-fold) at 456 nm (excitation at 372 nm). In this case, the only difference between **176** and **177** arose from the stoichiometry of the complex formed (2:2 and 1:2 receptor-anion for **176** and **177** respectively). Receptors **176** and **177** in solution were weakly emissive due to the fact that Zn(II) cation coordinated softly with the nitrogen atom that was directly linked with the triazine moiety in the cyclen macrocycle. This enabled a PET process from the poorly coordinated lone electron pair to the photo-excited anthracene fluorophore. Coordination of anion $P_2O_7^{4-}$ with Zn(II) induced a complete interaction of the nitrogen atom of the cyclen macrocycle with the metal centre, thus inhibiting the PET process and, consequently, the emission was enhanced. Finally regarding selectivity, addition of phenylphosphate or O-phospho-l-serine induced negligible changes in the emission profiles of the three receptors.

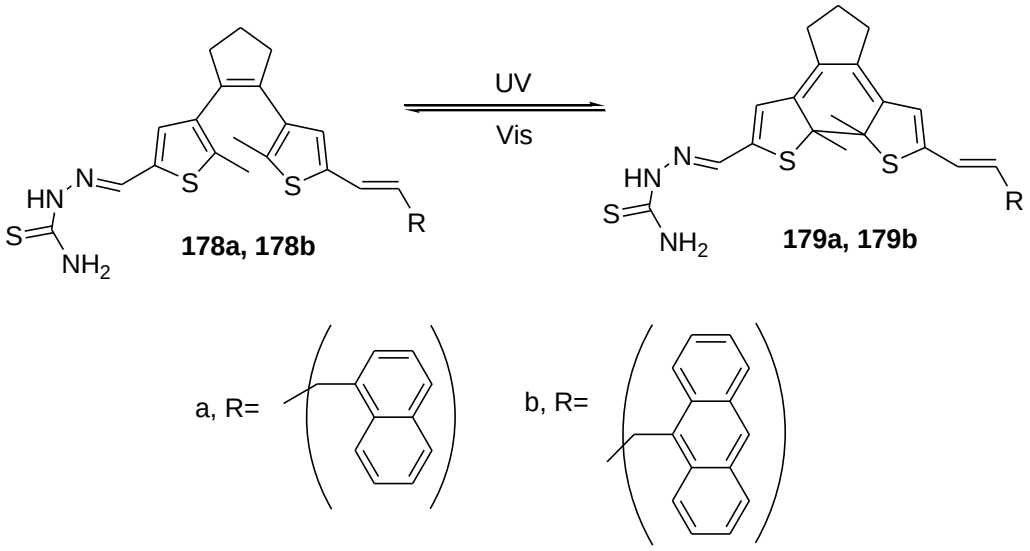

Fig. 87 Chemical structures of receptors **178(a-b)** and **179(a-b)**.

Receptors **178a** and **178b**, containing a dithienylcyclopentene unit, were used for the chromo-fluorogenic sensing of anion F^- (see Fig. 87).[121] CH_3CN solutions of receptor **178a** showed an absorption at 350 nm, which underwent a minor hypochromic effect together with the appearance of a broad shoulder at ca. 400 upon the addition of anion F^-. As regards fluorescence, CH_3CN solutions of **178a** showed an intense emission band at 450 nm (excitation at 350 nm), which was quenched upon the addition of F^-. Addition of other anions (i.e., Cl^-, Br^-, I^-, NO_3^-, HSO_4^-, $H_2PO_4^-$, AcO^- and ClO_4^-) induced negligible changes in the absorption and emission bands of **178a**. The authors ascribed the changes to an F^--induced deprotonation of the thioamide moiety, although the moderate bathochromic shift of the observed absorption band suggested a two-step mechanism in which: (i) the anion coordinated with receptors through hydrogen bonds and, then; (ii) a proton transfer took place at a high F^- concentration. Practically the same changes and selectivity trend were obtained with receptor **178b** and only anion F^- induced a bathochromic shift of the visible band (from 348 to 389 nm) and a quenching of the emission band (at 510 nm upon excitation at 348 nm). The visible bands of

cyclised forms **179a** and **179b** also underwent bathochromic shifts selectively in the presence of F^- anions (from 583 to 601 nm for **179a** and from 570 to 598 for **179b**).

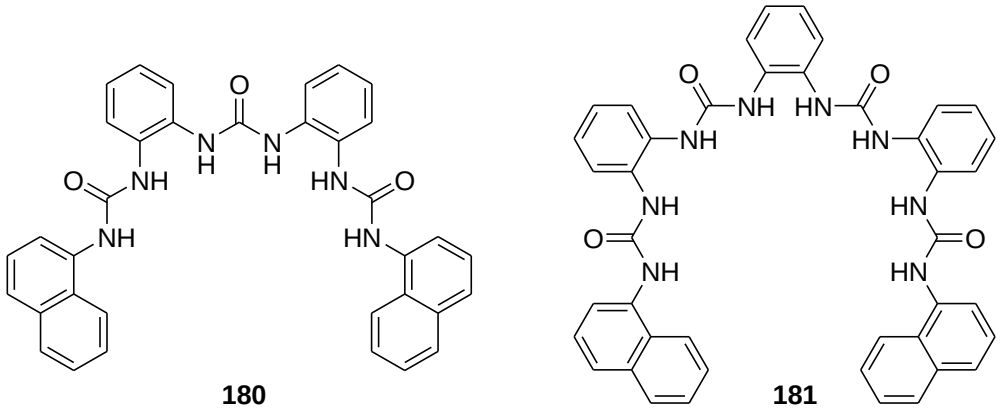

Fig. 88 Chemical structures of naphthyl derivatives **180** and **181**.

Naphthyl derivatives **180** and **181** bearing three and four urea groups (see Fig. 88) were used as fluorescent chemosensors for anions.[122] DMSO:H_2O 90:10 v/v solutions of both receptors displayed an intense emission band at 370 nm, which was quenched upon the addition of anion SO_4^{2-}. Addition of $H_2PO_4^-$ and AcO^- induced moderate quenching, whereas the emission profile remained unchanged in the presence of Cl^-, Br^-, ClO_4^- and NO_3^-. The authors suggested that the selectivity to anion SO_4^{2-} was due to its perfect fit into the binding cavity of both receptors. SO_4^{2-} formed 1:1 complexes with **180** and **181** via hydrogen-bonding interactions.

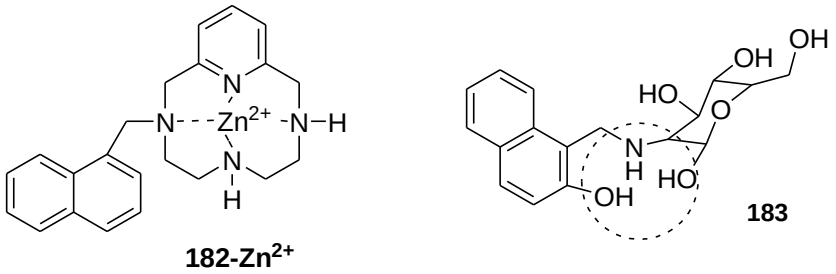

Fig. 89 Chemical structures of the Zn(II) complexes of **182** and **183**.

A Zn^{2+} specific turn-on fluorescent probe for the ratiometric sensing of $P_2O_7^{4-}$ in both water and blood serum was reported.[123] Solution of the **182-Zn^{2+}** (see Fig. 89) complex in water (HEPES buffer at pH 7.4) showed two main absorption bands at 223 nm and 275 nm and a fluorescence emission in the 310-380 nm range. Upon the addition of increasing amounts of $P_2O_7^{4-}$, a new emission band at 415 nm appeared, which was attributed to excimer formation due to the creation of 2:1 complexes. No significant fluorescence variations were observed with other anions (F^-, Cl^-, Br^-, I^-, AcO^-, PO_3^{3-}, PO_4^{3-}). Addition of ATP, ADP, and AMP only quenched the monomer emission of the **182-Zn^{2+}** complex. The authors used **182-Zn^{2+}** to monitor $P_2O_7^{4-}$ hydrolysis in blood serum.

A Zn-sensing glucose-based naphthyl-imino conjugate, used as a probe for inorganic and organic phosphates, including DNA, was reported.[124] Addition of Zn^{2+} to CH_3OH solutions of **183**

(Fig. 89) resulted in an emission intensity enhancement. Similar results were obtained in H_2O:CH_3CH_2OH 1:4 v/v mixtures. A limit of detection of 2.4 mmol L^{-1} for Zn^{2+} was observed. Titrations between the *in situ*-generated **183-Zn^{2+}** complex and 16 different anions were also carried out, and only the phosphate-based species quenched the fluorescence of the complex. Fluorescence quenching followed the order of: DNA > H_2PO_4 > ATP > NaH_2PO_4 > ADP ~ Na_2HPO_4 > AMP.

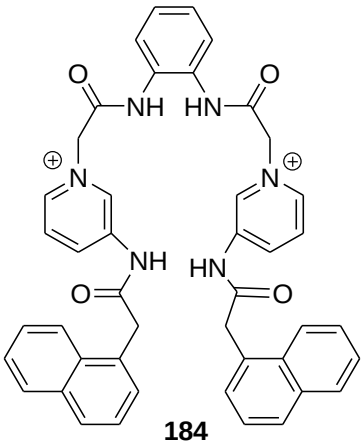

184

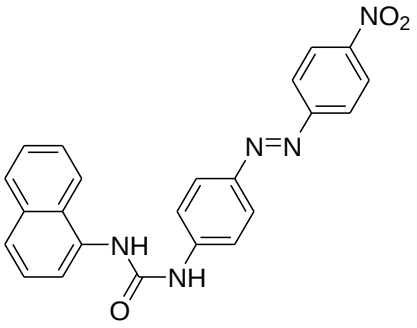

185

Fig. 90 Chemical structures of receptors **184** and **185**.

Ortho-phenylenediamine-based cleft **184** (Fig. 90) was reported to behave as a probe for $H_2PO_4^-$ and ATP.[125] Solution of **184** in CH_3CN showed a weak and broad naphthyl monomer emission band at 350 nm upon excitation at 290 nm. Addition of F^-, Cl^-, Br^-, I^-, NO_3^-, AcO^-, ClO_4^-, HSO_4^- and $H_2PO_4^-$ to **184** solutions showed that only $H_2PO_4^-$ caused a small perturbation in the monomer emission at 350 nm and a gradual increase of a new broad emission at 456 nm. However, further additions of $H_2PO_4^-$ lowered emission intensity. 1:1 complexes were formed between **184** and $H_2PO_4^-$. Besides, the solutions of **184** in CH_3CN:H_2O 1:1 v/v at pH 6.5 were used to investigate the interaction with ATP, ADP, AMP, $H_2PO_4^-$, HPO_4^{2-} PO_4^{3-} and $P_2O_7^-$. In all cases, changes in absorbance and in monomer emission were negligible. However, addition of ATP and ADP induced the appearance of a new broad emission at 380 nm (of less intensity with ADP than with ATP). Benesi-Hildebrand plots for the interaction of ATP and ADP with **184** were carried out and the formation of 1:1 complexes was confirmed.

Receptor **185,** containing a urea-binding site and two signalling subunits (i.e., a naphthalene fluorophore and an azo dye), was developed as a probe for certain basic anions (see Fig. 90).[126] CH_3CN:DMSO 90:10 v/v solutions of **185** showed absorption bands at 260 and 401 nm. Addition of F^- and $P_2O_7^{4-}$ induced the appearance of red-shifted absorptions at 599 and 617 nm, respectively. These new bands were ascribed to a deprotonation of **185** induced by basic anions F^- and $P_2O_7^{4-}$. The other anions tested (i.e., Cl^-, Br^-, I^-, HSO_4^-, $H_2PO_4^-$, AcO^- and NO_3^-) induced negligible colour changes. Moreover, CH_3CN:DMSO 90:10 v/v solutions of receptor **185** showed typical naphthalene emission bands centred at 370 nm,upon excitation at 260 nm. Addition of the anions used in the UV-Vis studies induced different degrees of quenching due to a PET process from the bonded anion/deprotonated receptor to the excited fluoropohore.

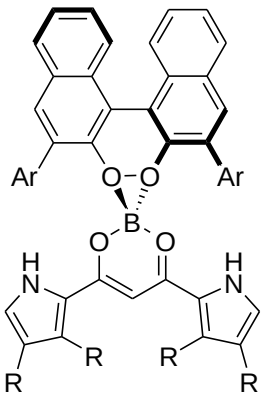

186a: R = H, Ar = H
186b: R = H, Ar = Ph
187a: R = Et, Ar = H
187b: R = Et, Ar = Ph
188a: R = Ph, Ar = H
188b: R = Ph, Ar = Ph

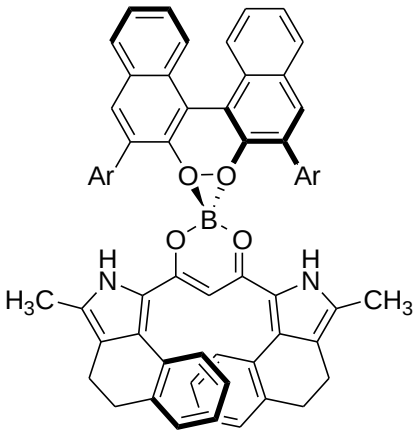

189a: Ar = H
189b: Ar = Ph

Fig. 91 Chemical structures of π-conjugated receptors **186-189**.

186a-189b receptors (see Fig. 91 for their structures) showed intense absorption bands in the 430-520 nm range and were fluorescent with emissions in the 440-560 nm range (in CH_2Cl_2 solution).[127] Addition of anions Cl^- and AcO^- induced changes in colour in all the tested receptors and also enhancements in the quantum yields. For example, the quantum yield of receptor **189a** increased from 0.28 to 0.40 upon the addition of Cl^-, whereas it increased from 0.51 to 0.72 with the same anion for receptor **189b**. These changes in colour and in emission were ascribed to the formation of hydrogen-bonding complexes involving the pyrrolic N-H groups. CPL (circularly polarized luminescence) spectral changes were observed only for **189b** upon the complexation with Cl^- and AcO^-. No other anions were tested.

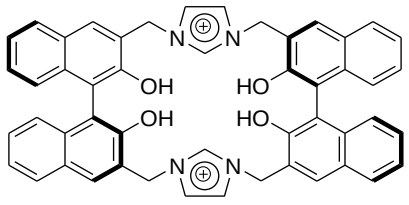

190

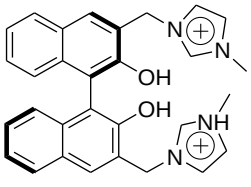

(R)-**191**

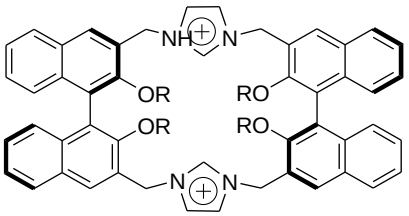

(R)-**192**: R = CH_2OCH_3
(R)-**193**: R = H
(R)-**194**: R = CH_3

Fig. 92 Chemical structures of imidazolium receptors **190-194**.

Imidazolium-functionalised BINOL cyclophane **190** (Fig. 92) presented a pre-organised rigid cavity that was able to encompass certain anions.[128] CH_3CN:DMSO 9:1 v/v solutions of **190** showed a dual emission consisting in a structured band centred at 370 nm (BINOL monomer emission) and a broad less intense band centred at 465 nm (BINOL excimer emission) upon excitation at 290 nm. Addition of anion F^- induced a significant decrease of the monomer emission, whereas the excimer emission increased and underwent a 20-nm bathochormic shift. The same emission changes were mainly obtained upon the addition of anion AcO^- to solutions of receptor **190**, whereas the presence of Cl^-, Br^-, I^-, HSO_4^- and $H_2PO_4^-$ induced

negligible optical modulations. Changes in emission were ascribed to the formation of 1:1 complexes in which F^- interacted with **190** through electrostatic and hydrogen-bonding forces (O-H···F^- with the hydroxyl moieties and C-H···F^- with the imidazolium cations). Receptor **190** was also able to discriminate *t*-Boc-L-Phe from *t*-Boc-D-Phe by fluorescence.

A family of 1,1'-binaphtyl-based imidazolium chemosensors for the highly selective recognition of tryptophan in aqueous solutions was prepared (see Fig. 92).[129] In particular, aqueous solutions of *(R)*-**191**, *(R)*-**192**-*(R)*-**194,** buffered at pH 7.4, presented intense broad emission bands in the 400-500 nm interval upon excitation at ca. 340 nm. The emission behaviour of these receptors was tested in the presence of selected amino acids (i.e., Trp, Tyr, Phe, His, Pro, Gly, Glu, Ala, Val, Cys and Ser). The best response was obtained with Trp and receptor *(R)*-**191**; when this amino acid was added, which induced a remarkable enhancement of the emission intensity at 422 nm. The other amino acids tested induced negligible changes in the emission profile of *(R)*-**191**. Receptors *(R)*-**192** and *(R)*-**194** presented similar behaviour and, of all the amino acids tested, only Trp was able to induce a moderate enhancement (of less magnitude than that obtained with *(R)*-**191**) in the emission band. Receptor (*R)*-**193** presented moderate fluorescence enhancement upon the addition of Trp, whereas Tyr displayed fluorescence quenching. The changes in the emission intensity of these receptors were ascribed to the formation of 1:1 complexes through hydrogen-bonding and electrostatic interactions. Finally, the authors investigated the possibility of employing one of these sensors to discriminate between the two enantiomers of Trp. (*R*)-**192** displayed a remarkable ability (K_D/K_L= 6.2) to discriminate between L and D-Trp.

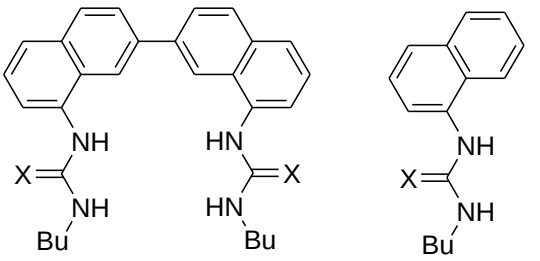

195; X=S
196; X=O

197; X=S
198; X=O

Fig. 93 Chemical structures of receptors **195-198**.

A family of 2,2'-binaphthalene derivatives bearing two thiourea and urea groups at the 8- and 8'-positions (**195**, **196**, **197** and **198**) was prepared and its anion recognition properties were reported (see Fig. 93).[130] Addition of AcO^-, F^- and $H_2PO_4^-$ to CH_3CN solutions of **195** resulted in a decreased absorbance at 316 nm, while a new band at around 360 nm developed. Cl^- showed minor spectral changes, while the addition of Br^-, I^-, HSO_4^-, and NO_3^- virtually resulted in no spectral variations. Job's plots were carried out and showed the formation of 1:1 complexes between **195** and anions AcO^-, F^-, Cl^- and $H_2PO_4^-$. A similar behaviour was observed with **196**, **197** and **198** in the presence of AcO^-, F^-, Cl^- and $H_2PO_4^-$. Moreover, the association constants of receptors **195** and **196** were one or two orders of magnitude greater than the corresponding monothiourea and urea receptors **197** and **198**. Selectivity trends of association of anions were calculated as $F^- > AcO^- > H_2PO_4^- > Cl^- >> HSO_4^- \approx NO_3^- \approx Br^- \approx I^-$ for **195**, $F^- > AcO^- \approx Cl^- > H_2PO_4^- > Br^-$

> HSO_4^- > I^- ≈ NO_3^- for **196**, F^- > AcO^- > $H_2PO_4^-$ > Cl^- >> HSO_4^- ≈ NO_3^- ≈ Br^- ≈ I^- for **197,** and as AcO^- > F^- > $H_2PO_4^-$ > Cl^- >> HSO_4^- ≈ NO_3^- ≈ Br^- ≈ I^- for **198**. Receptor **196** showed remarkable Cl^- selectivity, presumably owing to the suitable orientation of the binding groups for effective hydrogen-bonding formation. The emission behaviour of receptors **195** and **196** was also tested. In particular, addition of anions F^-, AcO^- and $H_2PO_4^-$ to CH_3CN solutions of both receptors induced a remarkable quenching of the emission bands (centred at 475 and 433 nm for **195** and **196**, respectively).

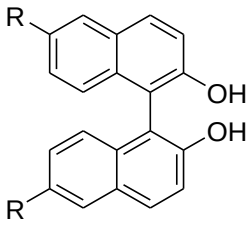

199; R = $Ph_2NC_6H_4$

Fig. 94 Chemical structure of receptor **199**.

The use of 6,6´-bis(triphenylamine) substituted BINOL (**199**) as a probe for selective F^- detection was reported (see Fig. 94).[131] Solution of **199** in CH_2Cl_2 exhibited an absorption band at 340 nm and a shoulder at 300 nm. Upon the addition of increasing amounts of anion F^-, a new red-shift band at 400 nm was grown due to the formation of 1:2 receptor-anion complexes. The addition of OH^-, AcO^-, OTs^- and $H_2PO_4^-$ also caused similar spectral changes, but in this case, 1:1 complexes were formed. Furthermore, the emission intensity of solutions of **199** in dried CH_2Cl_2 was gradually quenched during titration with F^-. Additionally, the induced fluorescence quenching ability of OH^-, OAc^-, $H_2PO_4^-$, and OTs^- was relatively weak in comparison to F^-. Minor changes in absorption and emission were observed in the presence of other anions (Cl^-, Br^-, I^-, and HSO_4^-). The order of the apparent quenching (i.e., F^- > OAc^- > $H_2PO_4^-$ > OH^- > OTs^- > HSO_4^- > Cl^- > Br^- ≈ I^-) was in parallel to the order of the intrinsic basicity of the anions. The formation of complexes with **199** induced the opening of non-radiative decay channels, which accounted for the quenching observed.

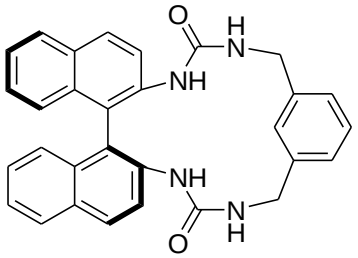

200

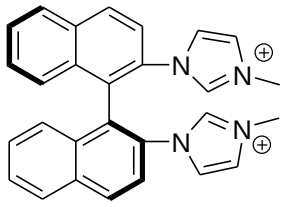

201

Fig. 95 Chemical structures of probes **200** and **201**.

The chiral binaphthyl derivatives **200** and **201** were used for the fluorescent recognition of (*S*)-2-phenylbutylate over (*R*)-2-phenylbutylate (see Fig. 95).[132] Solutions of both receptors (CH_3CN for **200** and CH_3CN-DMSO 8:2 v/v for **201**) showed the typical binaphthyl emission band centered at ca. 360 nm upon excitation at 320 nm. Addition of (*S*)-2-phenylbutylate to solutions of both receptors induced a progressive quenching of the emission band due to a PET

process active when the anion coordinates to **200** (through the formation of hydrogen bonds with the urea binding sites) and **201** (also through the formation of hydrogen bonds with the imidazolium cations). However, addition of (*R*)-2-phenylbutylate induced a less intense emission quenching that allowed chiral discrimination.

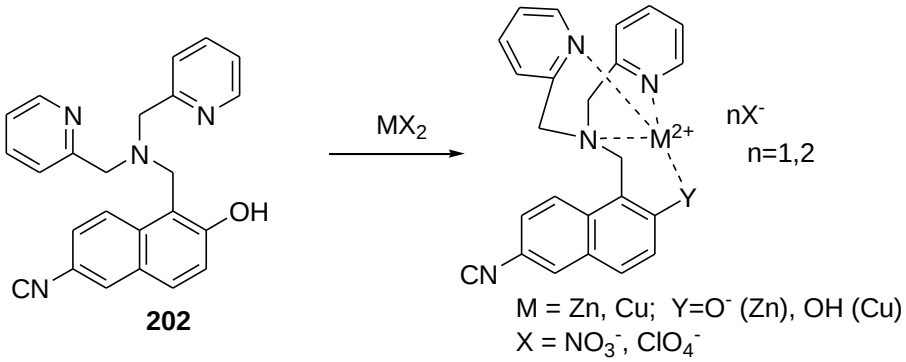

202

Fig. 96 Chemical structure of **202** and binding mode of **202** with Zn(II) and Cu(II).

The mononuclear **202-Zn^{2+}** and **202-Cu^{2+}** (see Fig. 96) complexes of a hydroxynaphthalene-containing dipicolylamine derivative displayed sensing behaviour for $P_2O_7^{4-}$.[133] Solution of the **202-Zn^{2+}** complex in HEPES (pH 7.4) resulted in a fluorescence enhancement (17-fold) at 435nm (λ_{ex}= 310 nm) upon the addition of $P_2O_7^{4-}$. Addition of other anions in excess (i.e., ATP, ADP, PO_4^{3-}, AcO^-, HPO_4^{2-}, HSO_4^-, F^- and Cl^-) resulted in no significant emission changes. Solutions of **202-Cu^{2+}** also showed a turn-on fluorescence response (24-fold) in the presence of $P_2O_7^{4-}$, which was selective over other anions tested (i.e., ATP, ADP, PO_4^{3-}, HPO_4^{2-},AcO^-, Cl^-, F^-, I^-, Br^-, N_3^-, NO_2^-, NO_3^-, HSO_4^-, and ClO_4^-). The emission enhancement upon the addition of $P_2O_7^{4-}$ was ascribed to a rupture of the M(II)···$O_{phenolate}$ bond upon the coordination of $P_2O_7^{4-}$ with the metal centre.

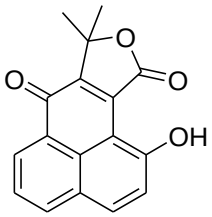

203

Fig. 97 Chemical structure of phenalenone receptor **203**.

Phenalenone derivative **203** (Fig. 97) was used as fluorescent chemosensor for anion F^-.[134] Addition of F^- to THF solutions of **203** led to a reduced intensity of the absorptions at 432 nm and 454 nm and to increased absorbances at 502 nm and 536 nm. At the same time, no obvious changes were found in the fluorescence band of **203** at 478 nm, but a new emission appeared at 550 nm. No significant changes in the emission spectra were noted when other anions were evaluated (i.e., AcO^-, Cl^-, Br^-, HPO_4^{2-} and $H_2PO_4^-$). The enhanced emission intensity at 550 nm was ascribed to a photoinduced charge transfer process which became active upon F^- addition. The authors did not clarify if anion F^- coordinated with **203** or induced phenol deprotonation.

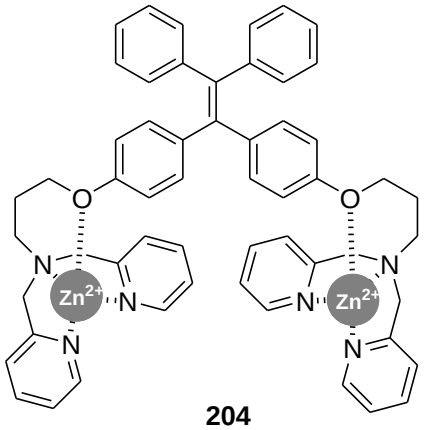

204

Fig. 98 Chemical structure of dinuclear Zn^{2+} complex **204**.

Dinuclear Zn^{2+} complex **204**, based on a tetraphenylethylene moiety, was used for the fluorimetric sensing of anion $P_2O_7^{4-}$ (see Fig. 98).[135] H_2O:DMSO 10:1 v/v solutions of **204** showed a very weak emission band at 472 nm upon excitation at 320 nm. Addition of increasing quantities of anion $P_2O_7^{4-}$ induced an emission enhancement at 472 nm. This enhancement was attributed to the formation of 1:1 complexes of **204** with $P_2O_7^{4-}$, which induced a marked restriction of the intramolecular rotation of the phenyl rings, resulting in enhanced fluorescence. Addition of other anions such as F^-, Cl^-, Br^-, I^-, $H_2PO_4^-$, HCO_3^-, N_3^-, NO_3^-, AcO^- and SO_4^- induced negligible changes. Moreover, the presence of ATP and AMP also induced emission enhancements, but of lesser intensity than that obtained for $P_2O_7^{4-}$.

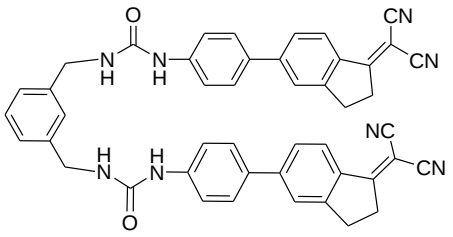

205

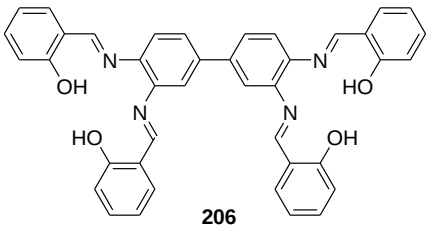

206

Fig. 99 Chemical structures of receptors **205** and **206**.

Fluorescent probe **205** (Fig. 99) was used for sensing certain amino acids.[136] DMSO solutions of receptor **205** presented an intense emission at 557 nm (excitation at 390 nm), which was partially quenched upon the addition of increasing quantities of Gln, Lys, Asn and Arg (basic amino acids), but remained unaltered with the other amino acids tested (i.e., Leu, Met, Ser, Thr, Cys, Pro, Phe, Tyr, Trp, His, Asp and Glu). Besides, addition of ω-amino acids, such as GABA, 5-aminovaleric acid, 6-aminohexanoic acid and 7-aminoheptanoic acids, to DMSO solutions of **205** induced different degrees of quenching of the emission band at 557 nm, depending on the distance between the terminal ammonium cation and the carboxylate moiety.

Tetrapodal receptor **206**, containing mixed hydrogen bond donor and hydrogen bond acceptor motifs as recognition sites, was reported to be a suitable chemosensor for AMP (see Fig. 99).[137] Solutions of **206** in $CH_3CN:H_2O$ 95:5 v/v displayed two absorption bands at 365 and 400 nm and an emission band at 460 nm (excitation at 365). When certain anions (i.e., F^-, Cl^-, Br^-, I^-, NO_3^-, HSO_4^-, AcO^-, $H_2PO_4^-$, AMP, ADP, ATP and adenine) were added, only AMP caused increased emission intensity with a simultaneous blue shift. Receptor **206** formed 1:1 complexes with AMP, which induced an increase in the rigidity of the receptor with the subsequent emission enhancement.

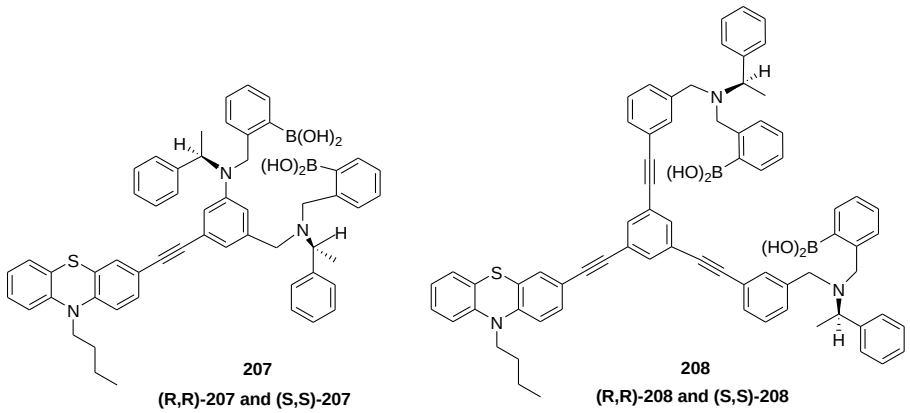

Fig. 100 Chemical structures of chiral boronic acid-containing probes **207** and **208**.

Chiral boronic acid-containing probes **207** and **208** (Fig. 100) were used for the selective recognition of isomers of tartrate.[138] Addition of D-tartrate induced a significant quenching of the emission band of the *(R,R)*-**207** receptor (in $CH_3OH:H_2O$ 3:1 v/v), whereas L-tartrate also induced a significant quenching, but of less intensity, proving enantioselective recognition. The reverse trend was observed upon the addition of D- and L-tartrate to *(S,S)*-**207.** In this case, a higher degree of quenching was observed when adding the L enantiomer. Addition of D- and L-mandelates induced moderate quenching, but no enantioselectivity was observed. $CH_3OH:H_2O$ 3:1 v/v solutions of receptors *(S,S)*-**208** and *(R,R)*-**208,** buffered at pH 5.5, showed strong emission bands at 492 nm upon excitation at 380 nm. With both receptors, the quenching of the emission intensity was observed upon the addition of D- and L-tartrate and D- and L-mandelate (which was greater for the former), but with no significant enantioselectivity. Receptor **207** formed 1:1 complexes with the carboxylates tested, whereas **208** formed 1:1 and 1:2 host-guest complexes in a consecutive fashion.

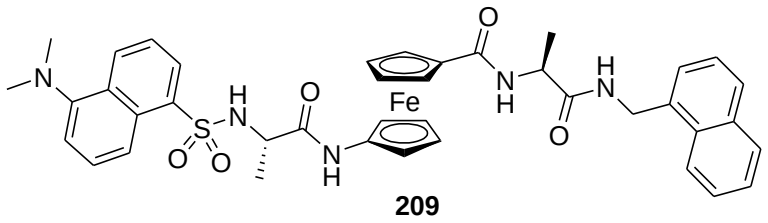

Fig. 101 Chemical structure of receptor **209**.

Receptor **209** contained two fluorophores (dansyl and naphthyl moieties) and amide groups as binding sites (see Fig. 101).[139] When CH_2Cl_2 solutions of receptor **209** were irradiated at 284 nm (excitation at the naphthalene fluorophore), a dual emission was observed with bands at

335 nm (emission of naphthalene fluorophore) and at 505 nm (emission of dansyl fluorophore) due to a FRET process from the naphthalene to the dansyl fluorophore. However, both emission bands were weak given the existence of a quenching process from the ferrocene to the fluorophores. All the tested anions (i.e., F^-, Cl^-, Br^-, HSO_4^-, NO_3^- and $H_2PO_4^-$) induced enhancement in both emission bands, of which the most important was obtained with $H_2PO_4^-$. The observed emission enhancements were ascribed to changes in the FRET process upon anion binding. The response of oxidised receptor **209**$^+$ was similar, namely different degrees of emission enhancement upon anion binding, but with less selectivity.

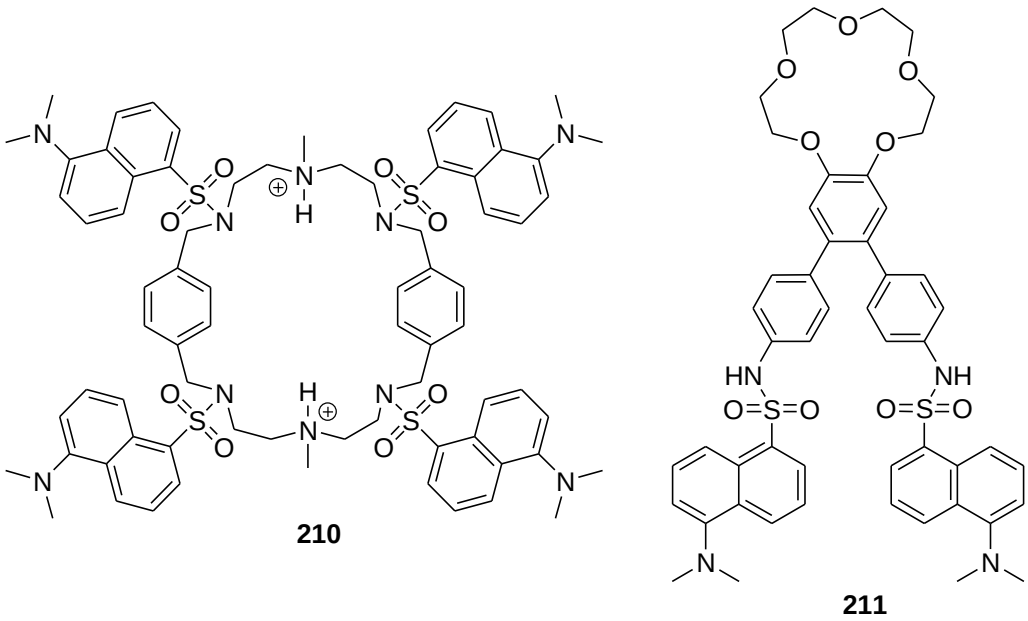

Fig. 102 Chemical structures of receptors **210** and **211**.

DMSO solutions of macrocycle **210** (Fig. 102) containing four dansyl fluorophores presented an intense emission band at 530 nm (excitation at 350 nm) which was quenched, to some extent, upon the addition of Cl^-, I^-, NO_3^-, HSO_4^- and $H_2PO_4^-$.[140] Moreover when adding F^- and Br^-, slight changes in emission intensity were found. The binding trend observed for the formation of 1:1 complexes (via N-H···A$^-$ and C-H···A$^-$ hydrogen-bonding interactios) was $H_2PO_4^- > HSO_4^- > Cl^- > NO_3^- > I^- > F^- > Br^-$. The observed quenching was attributed to a PET process from the lone pair of the unprotonated nitrogens, facilitated by the formation of the corresponding anion complexes, which increased these linking atoms' charge density.

The terphenyl-based **211-Hg^{2+}** probe for the detection of AcO^- ions was reported.[141] Solution of **211** (see Fig. 102 for their structure) in THF showed absorption bands at 220, 255 and 298 nm and emission at 500 nm. Addition of increasing amounts of Hg^{2+} resulted in an increase in the absorption bands at 220 nm and 255 nm, while the fluorescence intensity at 500 nm (λ_{ex} = 340nm) was completely quenched. The sensing behaviour of **211** towards different anions (i.e., F^-, Cl^-, Br^-, I^-, HSO_4^-, $H_2PO_4^-$, CH_3COO^-,NO_3^-, N_3^-, SO_4^{2-}, SO_3^{2-}, $Cr_2O_7^{2-}$) was tested and only addition of the F^- and AcO^- ions caused the significant fluorescence quenching of the emission at 500 nm. These changes were due to deprotonation. The sensing ability of the **211-Hg^{2+}** complex in THF was also studied. When AcO^- was added, a 60-fold enhancement in the emission band at

500 nm was noted. F^- also displayed emission enhancement, but to a lesser extent. Addition of other anions (i.e., Cl^-, Br^-, I^-, HSO_4^-, $H_2PO_4^-$, NO_3^-, N_3^-, SO_4^{2-}, SO_3^{2-}, $Cr_2O_7^{2-}$) did not induce any apparent emission change. A limit of detection for AcO^- of 100 x 10^{-9} mol L^{-1} was calculated. Finally, the authors performed assays for acetate sensing in a plasma-like aqueous solution (PLAS: 0.1 M Cl, 2 mM HPO_4^{2-}, 0.1M Na^+, 4 mM K^+, pH 7.4) and also PLAS containing bovine serum albumin (PLAS and 46 g l^{-1} BSA, pH 7.4).

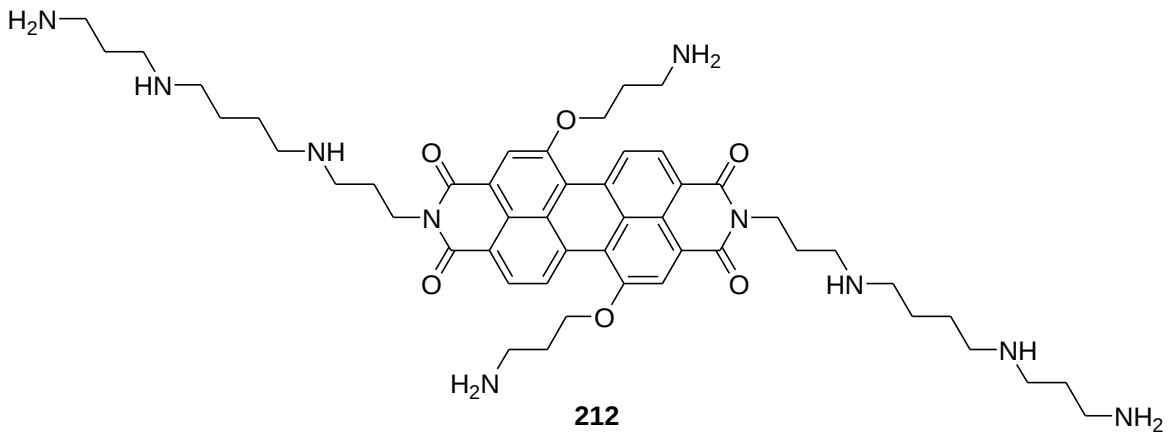

212

Fig. 103 Chemical structure of receptor **212**.

Perylene diimide **212** (Fig. 103) was used for the fluorescent detection of heparin in plasma.[142] In particular, water solutions buffered at pH 7.0 of **212** presented a strong emission band centred at 615 nm upon excitation at 485 nm. The intensity of the emission band decreased gradually upon the addition of heparin due to an aggregation process of **212** mediated by the negatively charged polysaccharide. Receptor **212** was used for the detection of heparin in clinical samples with fine results.

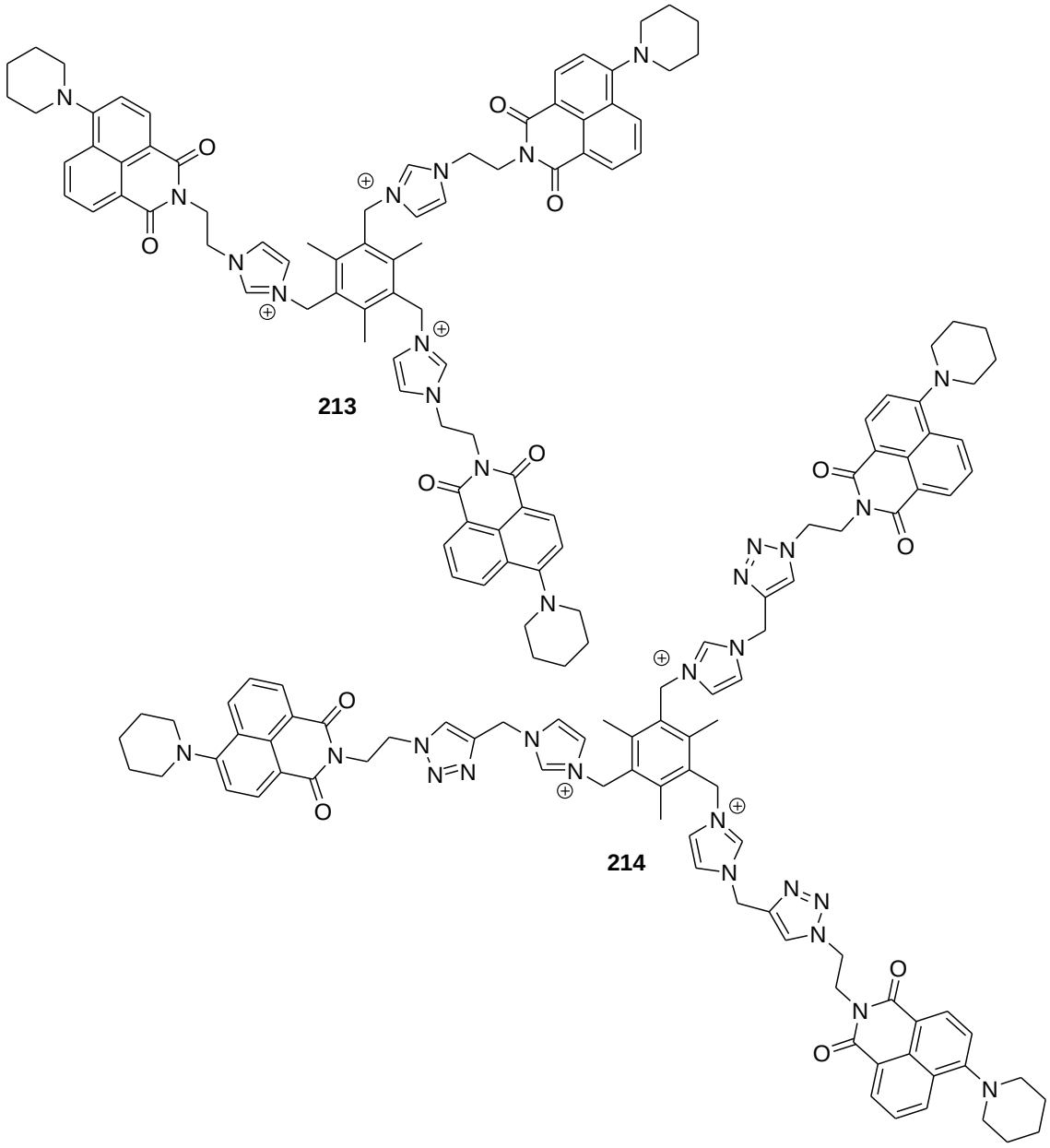

Fig. 104 Chemical structures of podands **213** and **214**.

Podands **213** and **214** (Fig. 104) were prepared by Duan and co-workers, who studied their emission behaviour in the presence of certain nucleotides.[143] Acetonitrile solutions of **213** showed a strong green emission at 548 nm (excitation at 465 nm), which was assigned to the 1,8-naphthalimide fluorophore. Of all the nucleotides added (i.e., ADP, GDP, GTP, ATP, UTP, UDP, CTP and CDP), only ADP was able to induce an emission enhancement. ADP forms 1:3 (host-guest) complexes with receptor **213** via the coordination of the nucleotide with the imidazolium subunit in the receptor through electrostatic and hydrogen-bonding interactions. This coordination induced a reduction of the electron charge density at the imidazolium, which diminished the "push-pull" nature of the ICT excited state of free **213**. Acetonitrile solutions of receptor **214** also showed an intense emission at 550 nm upon excitation at 395 nm. In this case, addition of triphosphates ATP, GTP and UTP induced emission enhancements (more marked in the presence of ATP), whereas addition of CTP, GDP, ADP, AMP, GMP, CDP, CMP,

UDP and UMP brought about negligible changes. Receptor **214** formed 1:2 (host-guest) complexes with ATP, GTP and UTP. Both receptors were successfully applied to the cell imaging of the corresponding nucleotide.

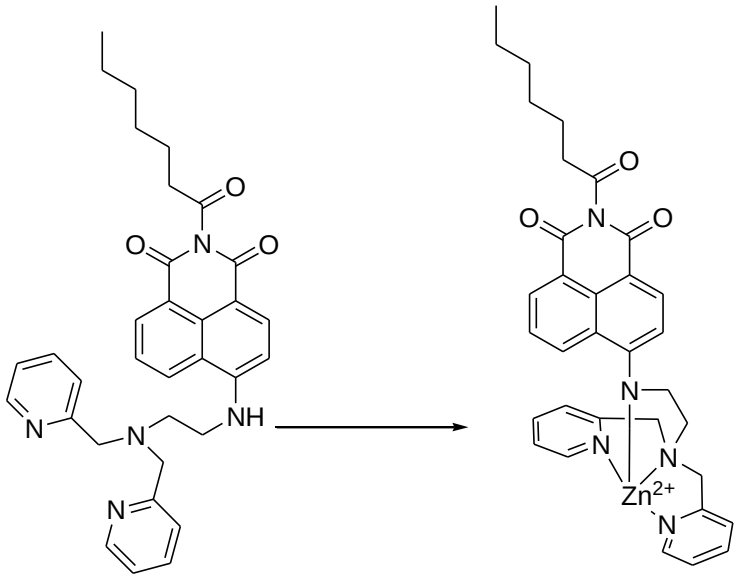

215 **216**

Fig. 105 Chemical structure of receptor **215** and its Zn(II) complex **216**.

Moro and co-workers presented a new water-soluble selective probe for ATP and ADP[144] Aqueous solutions of receptor **215** (see Fig. 105), buffered at pH 7.4, showed an absorption band at 450 nm, which underwent a hypsochromic shift (9 nm) and a hypochromic effect upon the addition of the Zn^{2+} cation. Moreover, the emission band of **215** (centred at 535 nm upon excitation at 450 nm) was enhanced, due to the suppression of a PET process from the lone electron pair of the tertiary amine to the fluorophore, upon complexation with the Zn^{2+} cation. These spectroscopic changes were ascribed to the formation of complex **216**. The variations in the emission band of complex **216** were studied in the presence of anions ATP, ADP, citrate, PPi, GTP, NO_3^- and PO_4^{3-}. The most remarkable results were obtained when adding ATP and ADP, which induced increased emission intensity of the 535 band and allowed the detection of these anions at the micromolar level. The authors suggested that the binding of ATP and ADP with Zn^{2+}-dipicolylamine diminished the strength of the $Zn^{2+}\cdots$N-H interaction, resulting in significantly increased emission intensity.

3.1.2.- Containing aromatic heterocycles

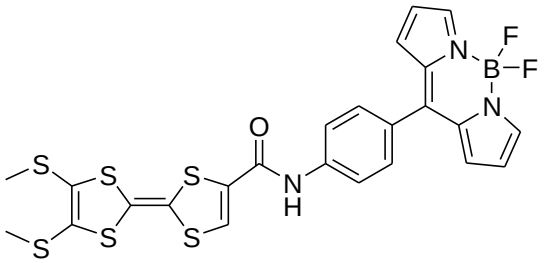

217

Fig. 106 Chemical structure of receptor **217**.

Zuo and co-workers synthesised the tetrathiafulvalene containing a BODIPY group dye **217** as a chromogenic and fluorogenic probe for anions (see Fig. 106).[145] DMSO:H_2O 95:5 v/v solutions of **217** presented an intense absorption band at 502 nm due to the BODIPY chromophore. Addition of increasing quantities of anion F^- induced a change in colour from orange to amaranth due to the formation of a new absorption band centred at 580 nm. Addition of other anions, such as $H_2PO_4^-$, BF_4^-, AcO^-, ClO_4^-, HSO_4^-, NO_3^-, Cl^-, Br^- and I^-, induced negligible changes. The same F^- selective response was observed when fluorescence titrations were carried out. In particular upon excitation at 450 nm, solutions of **217** showed an intense emission at 527 nm, which was gradually and selectively quenched upon the addition of increasing quantities of anion F^-. The interaction of F^- with the amide N-H moiety of **217**, through hydrogen-bonding interactions, yielded 1:1 complexes. The quenching of the emission intensity was tentatively ascribed to a PET process that became active upon anion coordination.

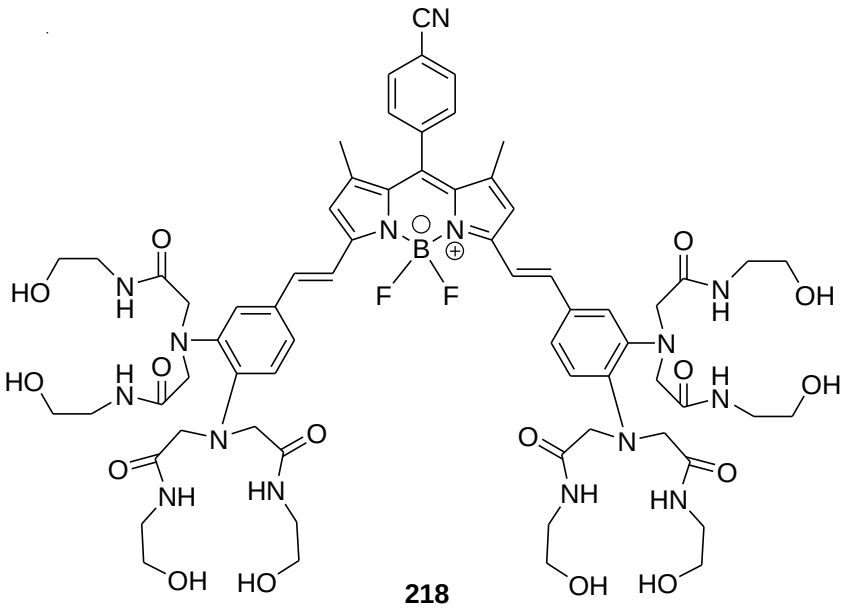

218

Fig. 107 Chemical structure of receptor **218**.

A new fluorescent probe (**218**, Fig. 107), based on a functionalised BODIPY fluorophore for the selective sensing of Cd^{2+} and $P_2O_7^{4-}$, was described.[146] Solutions of **218** in DMSO:H_2O 10:90 v/v (TRIS, pH 7.5, containing Na_3PO_4) displayed two absorption bands at 665 and 614 nm. Addition of increasing amounts of Cd^{2+} to **218** solutions exhibited two blue-shifted bands at 627 and 580 nm, whereas the band at 665 nm gradually decreased. The fluorescence intensity at 638 nm increased significantly. 1:4 ligand-to-metal complexes were formed. Upon the addition of increasing amounts of $P_2O_7^{4-}$ to the **218-Cd^{2+}** system in CH_3CN:H_2O 1:199 v/v, diminished absorbance intensity and a small red shift were observed, while fluorescence intensity 637 nm decreased. No significant variation in fluorescence intensity was observed in the presence of other anions (i.e., F^-, Cl^-, Br^-, I^-, HPO^{4-}, HSO_4^-, NO_3^-, HCO_3^-, $CF_3SO_3^-$, AcO^-, SO_4^{2-}, ATP and ADP), which were also evaluated with **218-Cd^{2+}**.

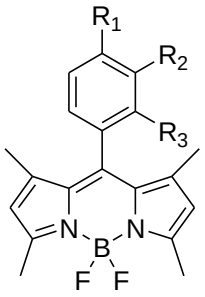

219 $R_1 = OCH_3$, $R_2 = OCH_3$, $R_3 = H$
220 $R_1 = OH$, $R_2 = OCH_3$, $R_3 = H$
221 $R_1 = OH$, $R_2 = OH$, $R_3 = H$
222 $R_1 = OH$, $R_2 = H$, $R_3 = H$
223 $R_1 = H$, $R_2 = OH$, $R_3 = H$
224 $R_1 = OH$, $R_2 = t\text{-}Bu$, $R_3 = H$
225 $R_1 = H$, $R_2 = t\text{-}Bu$, $R_3 = OH$
226 $R_1 = H$, $R_2 = H$, $R_3 = OH$
227 $R_1 = H$, $R_2 = CH_3$, $R_3 = OH$

Fig. 108 Chemical structures of BODIPYs **219-227**.

BODIPYs **219–224** (see Fig. 108) showed almost the same absorption maxima at 496 nm and a fluorescence band at 515 nm, while the presence of ortho-OH groups made both the absorption and emission bands undergo a slight red shift (λ_{abs} = 499 nm, λ_{em} = 520 nm)[147] for BODIPYs **225–227.** BODIPYs **222–227** were highly fluorescent, whereas BODIPYs **219–221** displayed low fluorescence**.** Upon the addition of increasing amounts of F^-, a similar response was observed in BODIPYs **220-227**, with significant fluorescence quenching. BODIPYs **220**, **222–227** formed 1:1 complexes with F^-, while BODIPYs **221** gave 1:2 ligand-to-anion species. The order of affinity of BODIPYs **220-227** by F^- in CH_3CN was found to be: **222** > **226** > **223** > **224** > **220** > **227** > **225.** No significant changes were observed with BODIPYs **219,** even with excess anion F^-. Significant selectivity to F^- was shown by BODIPYs **220–227** when other anions (i.e., Cl^-, Br^-, I^-, ClO_4^-, HSO_4^-, NO_3^-, $H_2PO_4^-$, and AcO^-) were evaluated. In particular, BODIPY **225** showed the highest selectivity to F^- with no significant interference from other anions and with a visible colour change from bright yellow to brownish yellow. Besides, BODIPY **227** also displayed a very slight quenching with $H_2PO_4^-$, whereas BODIPYs **220, 222-224** and **226** showed a significant fluorescence quenching with AcO^- and $H_2PO_4^-$. The fluorescence of BODIPY **221** was affected by the addition of AcO^-, $H_2PO_4^-$ and Cl^-. Changes in fluorescence upon the addition of anions were attributed by the formation of O–H···anion hydrogen-bonding interactions with dependence on the electronic effect exerted by the ancillary substituent in the meso-phenyl moiety and the phenolic OH position.

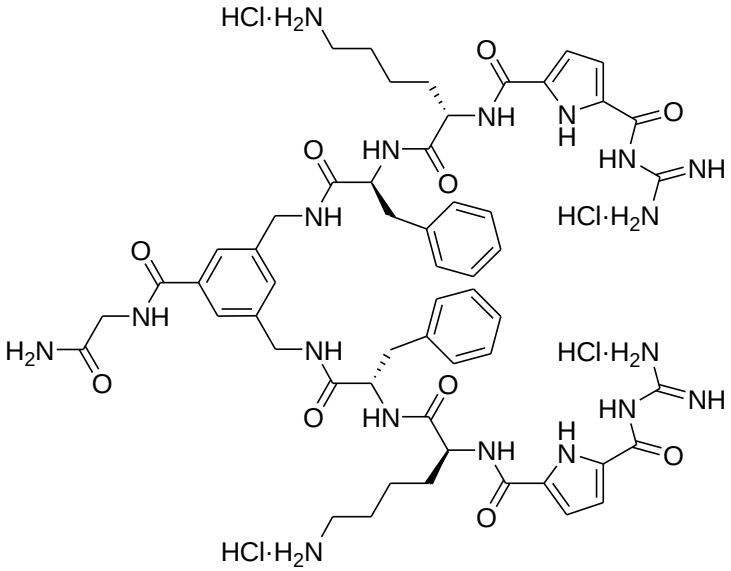

228

Fig. 109 Chemical structure of guanidinium-based tweezer receptor **228**.

Guanidinium-based tweezer receptor **228** (Fig. 109) was able to bind phosphates and nucleotides in buffered water at pH 7.[148] Aqueous solution of **228** presented an absorption at 300 nm. The intensity of this band gradually reduced upon the addition of selected anions (AMP, ADP, ATP, cAMP, UMP, GMP, CMP, PO_4^{3-} and $P_2O_7^{4-}$). Furthermore, the aqueous solutions of **228** presented an intense emission at 355 nm (due to the pyrrole moiety) that also was quenched to some extent with the addition of these anions. **228** formed well-defined 1:1 complexes, and the overall sequence of the binding constants was UMP > GMP ≈ AMP > cAMP ≈ CMP > ADP > ATP ≈ $P_2O_7^{4-}$ ≈ PO_4^{3-}. The host-guest interaction was based on non-covalent electrostatic, hydrophobic and/or π-π-stacking. π-π-stacking forces helped to differentiate nucleotides from PO_4^{3-} or $P_2O_7^{4-}$. Furthermore, these specific interactions helped explain the unusual binding selectivity of **228** for the less-charged AMP when compared with the higher-charged ADP and ATP in water.

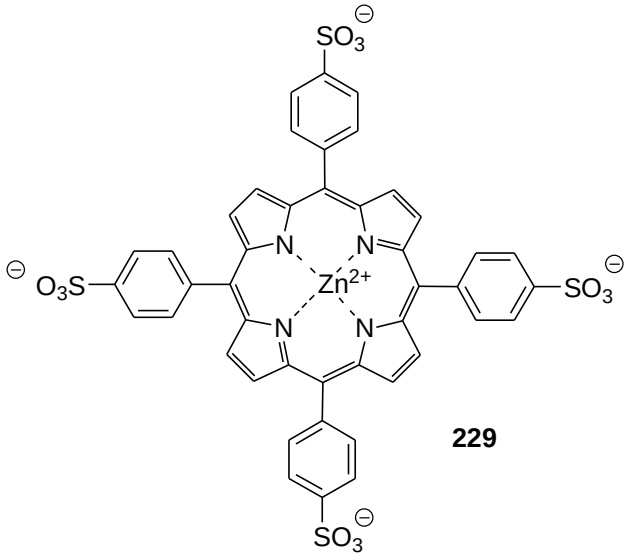

229

Fig. 110 Chemical structure of receptor **229**.

Aqueous solutions of **229** (see Fig. 110) presented absorption bands centred at 425, 560 and 595 nm, which were gradually enhanced upon the addition of anion I^-.[149] Moreover, aqueous solutions of **229**, when excited at 400 nm, showed two emissions at 607 and 659 nm. Addition of anion I^- induced a moderate quenching of both bands. No studies with other halides or oxygen containing anions were carried out.

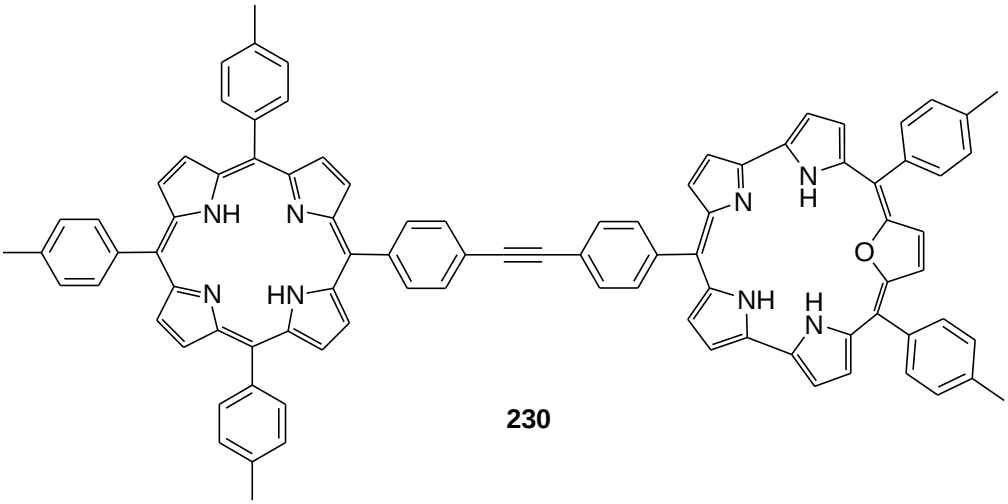

230

Fig. 111 Chemical structure of receptor **230**.

Porphyrin-expanded heteroporphyrin dyad **230** (see Fig. 111) as a fluorescent probe for anions was reported.[150] Addition of trifluoroacetic acid to toluene solution of **230** resulted in no changes in the absorption bands of the porphyrin subunit, while the absorptions of the smaragdyrin groups group (at 452, 637, and 703 nm) underwent red shifts and appeared at 457, 669, and 735 nm. Additionally, the fluorescence of the porphyrin subunit remained almost the same, but the strong fluorescence from the smaragdyrin group was completely quenched. Addition of increasing amounts of several anions (i.e., F^-, Br^-, I^-, SO_4^- and HPO_4^{2-}) to the protonated dyad **230-H$^+$** in toluene resulted in a gradual enhancement of the intensity of the porphyrin emission band at 650 nm (λ_{ex} = 410 nm), suggesting that anions were bonded at the protonated smaragdyrin sub-unit site in dyad **230-H$^+$**.

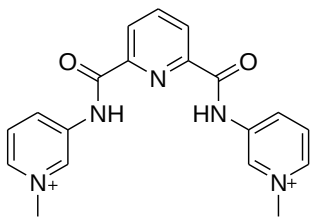

231

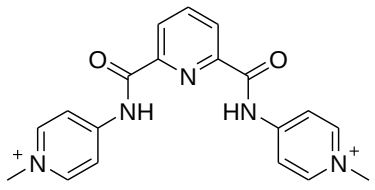

232

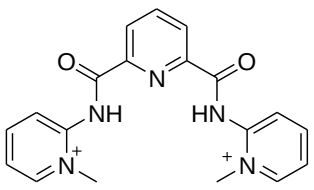

233

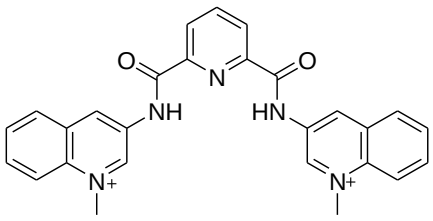

234

Fig. 112 Chemical structures of receptors **231-234**.

CH_3CN solutions of receptors **231**, **232** and **233** (presented in Fig. 112) showed a broad absorption band at ca. 280 nm which was red-shifted (ca. 20 nm) upon the addition of anions Cl^-, Br^-, I^-, $H_2PO_4^-$ and NO_3^-.[151] In contrast, addition of basic F^- and AcO^- anions induced the appearance of a new absorption at ca. 350 nm. The small red shifts observed upon addition of Cl^-, Br^-, I^-, $H_2PO_4^-$ and NO_3^- were ascribed to the formation of 1:1 complexes via hydrogen bonding interactions (involving the N-H and C-H pyridinium groups), whereas the absorption at 350 nm was generated by N-H amide deprotonation induced by basic F^- and AcO^- anions. Additionally, the authors tested the fluoresecence behaviour of receptor **234** in the presence of anions. CH_3CN solutions of this receptor showed an absorption band centred at 300 which, upon excitation, yielded a broad emission at 400 nm. All the anions tested induced several degrees of emission quenching besides NO_3^-, which induced moderate enhancement. 1:1 binding isotherms were fitted for all the anions, except for $H_2PO_4^-$ which formed 1:2 ligand-to-anion complexes. Moreover, a preliminary test showed strong quenching by nucleotides.

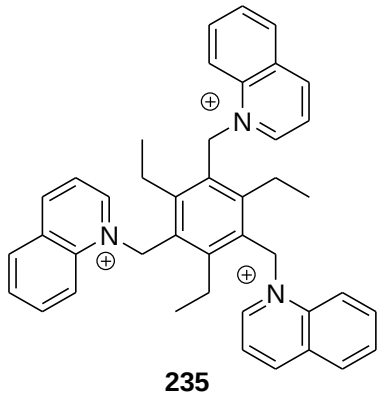

235

Fig. 113 Chemical structure of receptor **235**.

Quinolinium preorganised tripodal receptor **235** (Fig. 113) was prepared and used as a fluorescent probe for anions.[152] This work is an extension of a similar study carried out with receptors containing quinolinium heterocycles in a 1,3,5-trimethylbenzene scaffold.[153] CH_3CN solutions of **235** showed an emission band centred at 408 nm (excitation at 317 nm), typical of the quinolinium fluorophore, which was quenched upon the addition of Cl^-, Br^-, I^-, NO_3^- and AcO^-. Of all the anions tested, the more significant quenching was observed upon the addition of anion AcO^-. A charge transfer process, from the coordinated anion to the fluorophore, was the dominant mechanism of the observed quenching.

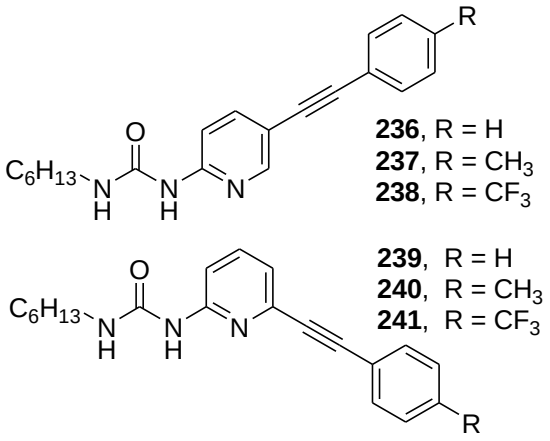

Fig. 114 Chemical structures of receptors **236-241**.

Fluorescent pyrid-2-yl ureas **236**-**241** (see Fig. 114 for structures) were prepared and their fluorogenic behaviour in the presence of carboxylic acids was tested.[154] CH_3CN solutions of **236**-**241** exhibited broad emission bands in the 350-370 nm interval upon excitation at ca. 310 nm. Receptors **236** and **237** underwent red shifts of the emission bands of 49 and 64 nm upon the addition of trichloroacetic and trifluoroacetic acid, respectively, whereas a 10-nm red shift was seen for **238**. The same red shifts, but less pronounced ones, were observed when adding trichloroacetic and trifluoroacetic acid to **239**-**241**. The new bands were ascribed to a protonation of the pyridine and to the subsequent coordination of the generated anion with the urea subunits of the receptors. Addition of other acids (acetic and dicloroacetic) induced negligible changes in the emission profiles of the receptors.

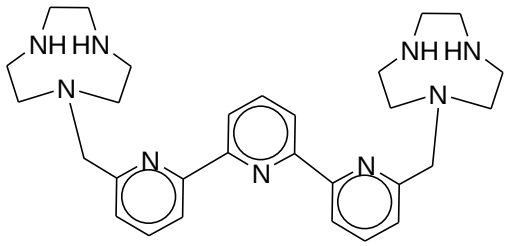

242

Fig. 115 Chemical structure of receptor **242**.

Terpyridine-based receptor **242** (Fig. 115), containing two [9]aneN_3 units, was used as a selective probe for $P_2O_7^{4-}$ over PO_4^{3-} and $P_3O_{10}^{5-}$ in an aqueous solution at pH 7, thanks to the conformational change of its structure induced by the Zn^{2+} coordination to the polypyridyl moiety.[155] The authors demonstrated that the addition of an excess PO_4^{3-}, $P_2O_7^{4-}$ or $P_3O_{10}^{5-}$ did not affect the **242** spectrum. Adding increasing amounts of Zn^{2+} to the aqueous solutions of **242** resulted in a decrease of the absorption band at 295, the appearance a new band at 315 nm and an additional remarkable enhancement on the fluorescence emission at 355 nm. Performing titrations experiments of the **242-Zn^{2+}** complex with PO_4^{3-}, $P_2O_7^{4-}$ and $P_3O_{10}^{5-}$, a marked tendency to bind $P_2O_7^{4-}$ over $P_3O_{10}^{5-}$ and $P_2O_7^{4-}$ was found. This coordination of $P_2O_7^{4-}$ was concomitant with the quenching of fluorescence.

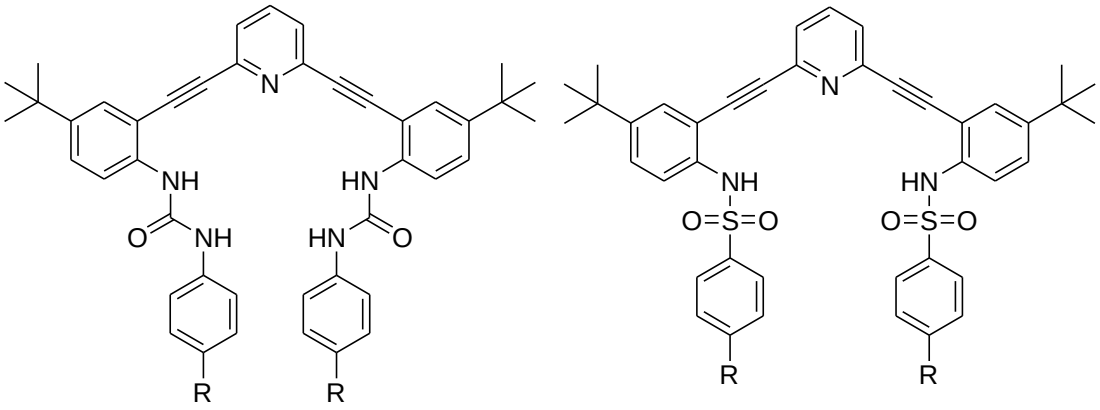

243a; R=OMe
243b; R=NO_2

244a; R=OMe
244b; R=NO_2

Fig. 116 Chemical structures of receptors **243a,b** and **244a,b**.

With the protonation with HCl of $CHCl_3$ solutions of **243a,b** and **244a,b** (see Fig. 116), a change in colour from colourless to yellow was observed.[156] Besides, electron-rich receptors **243a** and **244a** were fluorescent in the neutral state and their emission was quenched when protonated, whereas electron-poor receptors **243b** and **244b** were weakly-fluorescent and their emission increased, with a concomitant red shift noted when protonated. The authors suggested that these changes in fluorescence from the free-base to the protonated receptors could be used to sense the Cl^- ion and can be used in molecular logic systems.

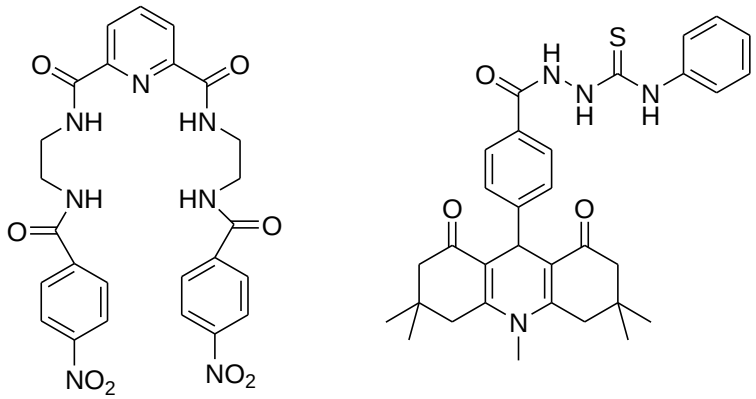

245 **246**

Fig. 117 Chemical structures of receptors **245** and **246**.

Addition of anion I^- to THF:H_2O 4:1 v/v solutions of receptor **245** (see Fig. 117) resulted in an enhancement of the absorption band at 250 nm and in the appearance of a new peak centred at 365 nm (change in colour from colourless to yellow).[157] Upon excitation at 280 nm, receptor **245** showed an emission at 310 nm, which was quenched upon the addition of anion I^-. No significant fluorescence or absorbance changes were observed in the presence of other anions (i.e., F^-, Cl^-, Br^-, HCO_3^-, NO_3^-, CO_3^{2-} and SO_4^{2-}) and no interference from them was observed

while performing the detection of I^-. The red shift in the absorption and emission maxima was attributed to the formation of an ICT complex between **245** and anion I^-, whereas the fluorescence quenching of **245** was explained by the "heavy atom" effect. High selectivity was explained by bearing in mind that the flexible binding site in **245** was more compatible to I^- than to other anions.

N-benzamidobisthiourea receptor **246** (see Fig. 117) was used as a ratiometric fluorescent sensor for anion F^-.[158] CH_3CN solutions of **246** exhibited a broad emission band at 480 nm (upon excitation at 404 nm). Addition of small quantities of F^- induced the initial quenching of the emission band at 480 nm, whereas addition of further F^- induced the emergence of a new emission at 600 nm. The authors assigned the first quenching to the formation of hydrogen-bonding complexes between **246** and F^-, and the second emission to a F^--induced deprotonation of the receptor. Addition of AcO^- and $H_2PO_4^-$ induced only the quenching of the emission at 480 nm, whereas Cl^-, Br^-, I^-, HSO_4^- and ClO_4^- induced negligible changes in the emission profile.

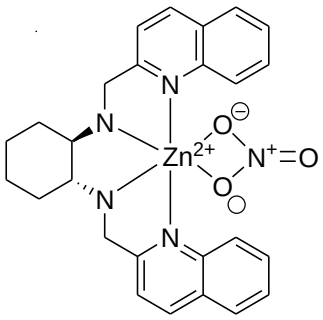

247

Fig. 118 Chemical structure of receptor **247**.

Quinoline-based Zn^{2+} complex **247** (see Fig. 118) was prepared and used as a fluorescent chemosensor for $P_2O_7^{4-}$ under physiological conditions.[159] Solution of **247** in HEPES (pH 7.4) displayed an emission band at 376 nm when excited at 315 nm. Addition of anion $P_2O_7^{4-}$ induced strong fluorescence quenching, whereas only a slight decrease in intensity was observed with ATP. No significant change in the fluorescence intensity of **247** was detected upon the addition of the other anions in excess investigated (i.e., F^-, Cl^-, Br^-, $HCOO^-$, AcO^-, ClO_4^-, SO_4^{2-}, PO_4^{3-}, and AMP). $P_2O_7^{4-}$ formed 1:2 anion-receptor complexes with **247**.

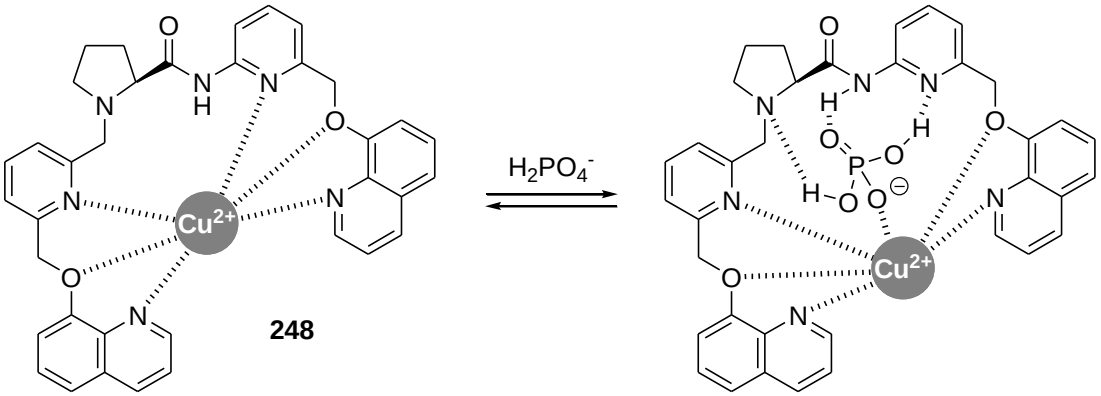

Fig. 119 Schematic representation of the binding mode between receptor **248** and $H_2PO_4^-$.

CH_3CN solutions of complex **248** (Fig. 119), containing two quinoline fluorophores and a binding cavity able to accommodate anions, presented a weak emission band at 398 nm upon excitation at 285 nm due to an effective PET process involving the Cu^{2+} cation and the quinoline fluorophore.[160] Of all the anions tested (i.e., F^-, Cl^-, Br^-, I^-, AcO^-, BzO^-, HSO_4^-, $H_2PO_4^-$, isophthalate, $(COO)_2^{2-}$ and L-(+)-mandelate), only the addition of $H_2PO_4^-$ induced an increase in the emission intensity. The selectivity observed was due to the presence of a coordination cavity in **248,** which perfectly fitted the size and shape of $H_2PO_4^-$. The anion coordinated with **248** through the formation of hydrogen bonds and electrostatic interactions. The emission enhancement observed upon coordination with $H_2PO_4^-$ was ascribed to an increase in the rigidity of the formed complex. Nonetheless, a restriction of the PET process, which was active in the receptor alone, upon coordination cannot be ruled out.

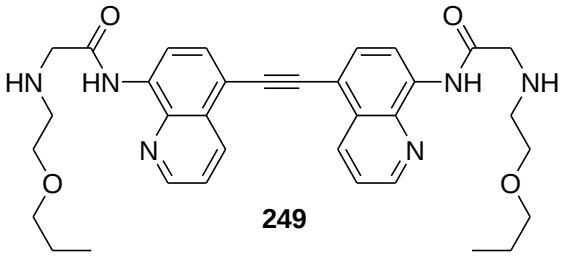

Fig. 120 Chemical structure of receptor **249**.

A ratiometric fluorescent probe for oxalate, based on alkyne-conjugated carboxamidoquinolines **249** (see Fig. 120), in aqueous solution and in living cells was reported.[161] Solutions of **249** in CH_3CH_2OH:H_2O 1:9 v/v at pH 7.02 showed a significant emission decrease at 470 nm and an emission increase at 512 nm upon the addition of Zn^{2+}. Job's plot studies confirmed the formation of the 1:2 **249-$(Zn^{2+})_2$** complex. When adding increasing amounts of oxalate, a significant 80% decrease in the emission intensity and a 20-nm blue shift were observed. Besides, coordination studies suggested the formation of 1:2 complexes between **249-$(Zn^{2+})_2$** and oxalate. ^{1}H-NMR studies also provided evidence for the interaction between the **249-$(Zn^{2+})_2$** complex and oxalate. When **249-$(Zn^{2+})_2$** was titrated with mono- and dicarboxylates (i.e., formate, AcO^-, propionate, butanoate, malonate, succinate, adipate, sebacate, *o*-phthalate and *p*-phthalate) and phosphate anions (i.e., PO_4^{3-}, HPO_4^{2-}, $H_2PO_4^-$), only a decrease in the emission intensity of about 20% was noted. Oxalate

concentrations down to 3.0 x 10^{-6} mol L^{-1} were detected using the probe. Finally, the **249-$(Zn^{2+})_2$** complex was also used for imaging oxalate in living cells (HeLa cells).

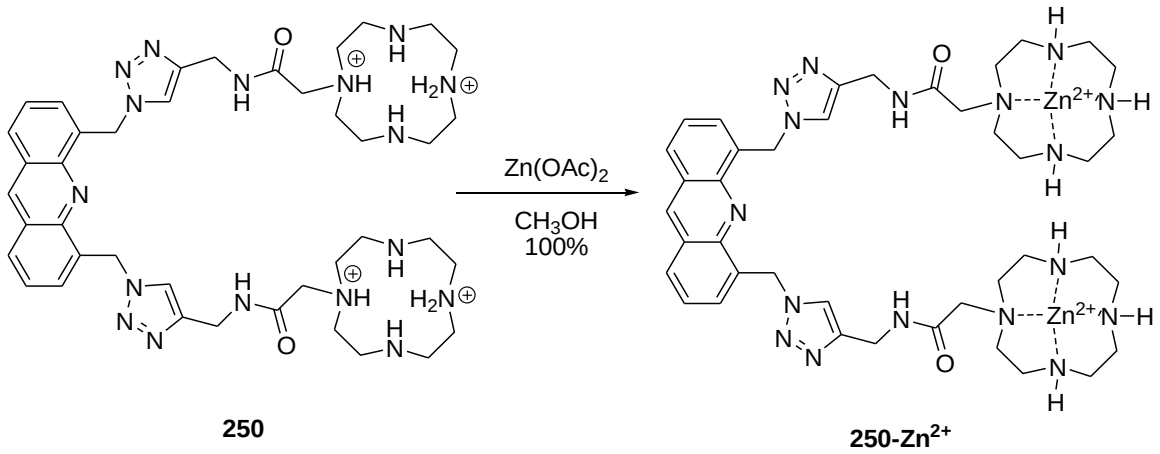

250 **250-Zn^{2+}**

Fig. 121 Chemical structure and binding mode of receptor **250** with Zn^{2+}.

Bis-cyclen tweezer receptors **250** and the corresponding Zn^{2+} complex **250-Zn^{2+}** (see Fig. 121) as probes for inositol 1,4,5-trisphosphate ($InsP_3$) were reported.[162] Solution of **250** in CH_3OH:H_2O 1:1 v/v (buffered at pH 7.4) displayed an absorption band at 355 nm and an emission band at 440 nm (λ_{ex} = 355 nm). When increasing amounts of $InsP_3$ were added to **250** solutions, a slight decrease (10-15%) in the emission signal was seen. Upon the addition of several related phosphorylated derivatives (i.e., D-fructose 1,6-bisphosphate trisodium [**a**], cyanoethyl phosphate barium [**b**], and dihydrogen phosphate [**c**]) over **250**, a binding affinity in the order of $InsP_3$>**a**>**b**>**c** was determined. When similar titration binding experiments were performed with **250-Zn^{2+}** and the same series of phosphorylated guests ($InsP_3$, **a**, **b** and **c**), (now also including sodium pyrophosphate (**d**)) emission decrease changes were observed (20-25%), but with slightly lower binding affinities than those found for **250**. In this case, the order of binding affinity was **b** > **$InsP_3$** > **a** > **d** > **c**. The authors also found that phosphorylated guests containing several phosphate units (i.e., **$InsP_3$**, **a**, and **d**) produced greater changes in fluorescence than those analytes containing a single phosphate group (**b** and **c**).

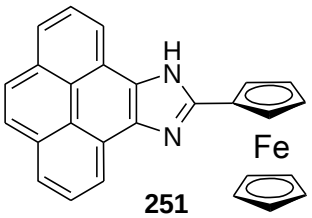

251

Fig. 122 Chemical structure of ferrocene-imidazopyrene receptor **251**.

Ferrocene-imidazopyrene dyad **251** (Fig. 122) was synthesised as a redox and optical molecular probe for ion pairs.[163] Titrations of the solution of **251** in CH_3CN with several anions (i.e., F^-, Cl^-, Br^-, AcO^-, NO_3^-, HSO_4^-, $H_2PO_4^-$, and $HP_2O_7^{3-}$) revealed that only $H_2PO_4^-$ and AcO^- induced detectable changes in the emission bands at 382 and 402 nm. 1:1 receptor-anion complexes were formed. Moreover, the authors carried out titrations with cations in the presence of

anions and found that when 0.5 equiv. of cations were added to a solution containing the preformed complex **[251-3H_2PO_4]$^-$**, a red-shifted broad emission band at 422 nm appeared, whose intensity was higher for Pb^{2+} (λ_{422} /λ_{402} =2.02) and Hg^{2+} (λ_{422} /λ_{402} =1.89) than for Zn^{2+} (λ_{422} /λ_{402} =0.89). When similar titrations were done on the preformed **[251-AcO]$^-$** complex, changes were much less pronounced. The same results were obtained by changing the addition sequence: i.e., addition of $H_2PO_4^-$ to a solution of the preformed **251_2-M^{2+}** complex (M: Zn, Hg, Pb).

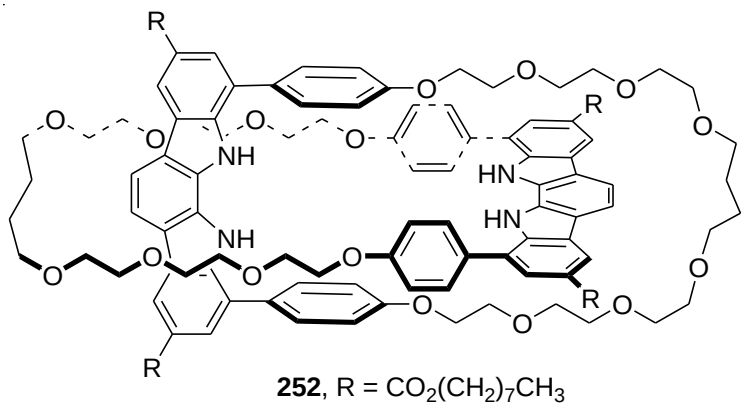

Fig. 123 Chemical structure of catenand **252**.

Catenand **252**, bearing two indolocarbazole fluorophores, presented a preorganised cavity with four N-H protons (see Fig. 123).[164] H_2O:CH_3COCH_3 1:99 v/v solutions of **252** showed a broad emission at 404 nm upon excitation at 350 nm due to the indolocarbazole fluorophore. The intensity of the emission band was gradually enhanced upon the addition of selected anions (i.e., Cl^-, Br^-, I^-, AcO^-, $H_2PO_4^-$, N_3^-, HSO_4^- and NO_3^-) due to the formation of 1:1 complexes in which anions were encapsulated in the cavity forming hydrogen-bonding interactions with the convergent indole NHs. The magnitude of the stability constants calculated for the 1:1 complexes was in the order $Cl^- > AcO^- > N_3^- > H_2PO_4^- > Br^- > HSO_4^- > I^- \approx NO_3^-$.

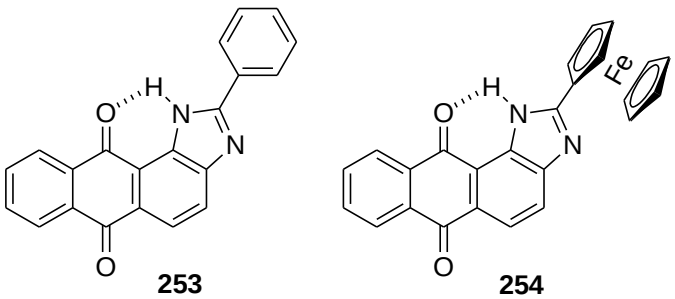

Fig. 124 Chemical structures of imidazole-based receptors **253** and **254**.

Imidazole-based receptors **253** and **254** (Fig. 124) were used for the chromo-fluorogenic sensing of anion CN^-.[165] Regarding the chromogenic response, the CH_3CN:water (HEPES buffer) 1:1 v/v solutions of receptor **253** showed an intense absorption at 393 nm (related to an antraquinone/imidazole $\pi \rightarrow \pi^*$ transition) which was red-shifted to 474 nm upon the addition

of anion CN^-, producing a colour change from yellow to orange. This change was due to the coordination of CN^- with the imidazole N-H through hydrogen-bonding interactions. None of the other anions tested (i.e., F^-, Cl^-, Br^-, I^-, SCN^-, AcO^-, $H_2PO_4^-$, PPi, HSO_4^-, NO_2^- and NO_3^-) induced changes in the UV-visible spectrum of **253**. Virtually the same selective chromogenic response was obtained with **254,** which presented two absorption bands at 390 and 530 nm (ferrocene-based metal-to-ligand charge transfer and intraligand $\pi \rightarrow \pi^*$ transitions). Addition of CN^- induced a decrease in the band at 390 nm, together with an increase in absorbance at around 552 nm (change in colour from red to blue). Besides, receptor **253** was fluorescent with maxima at 510 nm upon excitation at 427 nm. Addition of anion CN^- induced the quenching of the 510 nm band and the appearance of a new emission at 602 nm. These changes were selective for anion CN^- and allowed its ratiometric sensing with a limit of detection of 0.06 ppm.

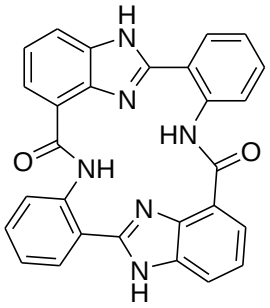

255

Fig. 125 Chemical structure of receptor **255**.

Cyclo[2]benzimidazole (**255**, see Fig. 125) was used as a fluorogenic chemosensor for F^-.[166] DMSO:H_2O 99.9-0.1 v/v solutions of **255** presented an absorption band at 309 nm and a very weak emission at 467 nm (excitation at 309 nm). The weak emission observed for **255** was ascribed to an excited state intramolecular proton transfer (ESIPT) process, which was active in the free receptor. Of all the anions tested (i.e., NO_3^-, F^-, Cl^-, Br^-, I^-, SCN^-, HSO_4^-, *p*-toluensulphonate, PF_6^-, BF_4^- and BPh_4^-), only F^- induced changes in the UV-visible and fluorescence profiles. In particular, F^- induced a marked decrease in the absorbance at 309 nm with the concomitant appearance of a new band centred at 340 nm. Besides, the addition of F^- induced the appearance of a new emission band centred at 412 nm (60-fold enhancement) when excited at 322 nm. The spectroscopic changes observed upon the addition of F^- were ascribed to the formation of a 1:1 stoichiometry complex between the anion and the central four nitrogen atoms of the receptor. This coordination effectively blocked the ESIPT process that was active in the receptor alone, and consequently, emission was enhanced.

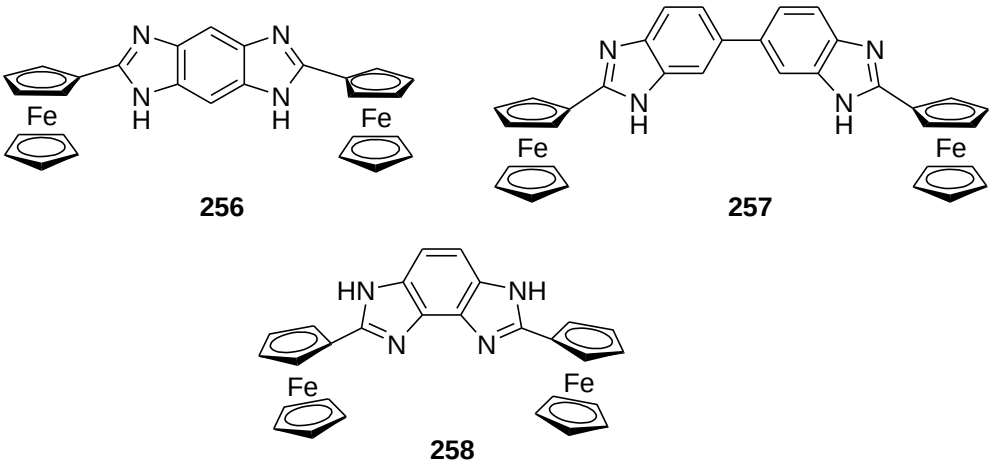

Fig. 126 Chemical structures of ferrocene imidazole receptors **256-258**.

Ferrocene-fused imidazole dyads **256** and **257** (see Fig. 126) were used for the fluorogenic recognition of anions AcO^-, $H_2PO_4^-$ and $HP_2O_7^{3-}$.[167] DMSO solutions of **256** showed a weak emission band at 428 nm which underwent suffered a small red shift (13 nm) together with a 71-fold enhancement in intensity upon the addition of anion AcO^-. No other anion tested (i.e., F^-, Cl^-, Br^-, I^-, HSO_4^-, $H_2PO_4^-$, $HP_2O_7^{3-}$, BzO^-, $(COO)_2^{2-}$, $CH_2(COO)_2^{2-}$ and NO_3^-) was able to induce any change in the emission profiles. The enhanced emission intensity was ascribed to the formation of 1:1 complexes between the receptor anion and AcO^-, which involved hydrogen-bonding interactions with the NH moieties in the imidazole rings. Moreover, DMSO solutions of receptor **257** showed enhanced emission (at 430 nm) only in the presence of $H_2PO_4^-$ (46-fold) and $HP_2O_7^{3-}$ (4-fold).

Bisferrocene-benzobisimidazole triad **258** (Fig. 126) acted as a multichannel ditopic receptor for the selective sensing of HSO_4^-.[168] CH_3CH_2OH solutions of **258** presented an absorption band at 304 nm. Of all the anions tested (i.e., F^-, Cl^-, Br^-, AcO^-, HSO_4^-, NO_3^-, $H_2PO_4^-$, and $HP_2O_7^{3-}$), addition of F^-, AcO^-, HSO_4^-, $H_2PO_4^-$, and $HP_2O_7^{3-}$ induced slight decreases in the absorption band intensity. This lack of selectivity changed when fluorescence measurements were taken. CH_3CH_2OH solutions of **258** were weakly fluorescent with an emission at 405 nm (excitation at 322 nm). Of all the anions tested, only HSO_4^- was able to induce a red shift of the emission band from 405 to 418 nm, together with marked enhancement in intensity. Upon the addition of anion HSO_4^-, a proton transfer process occurred that yielded the protonated receptor and anion SO_4^{2-}. Formation of 1:1 complex between **258**·H^+ and SO_4^{2-} through hydrogen-bonding interactions with the N-H moieties of the protonated receptor accounted for the emission changes observed.

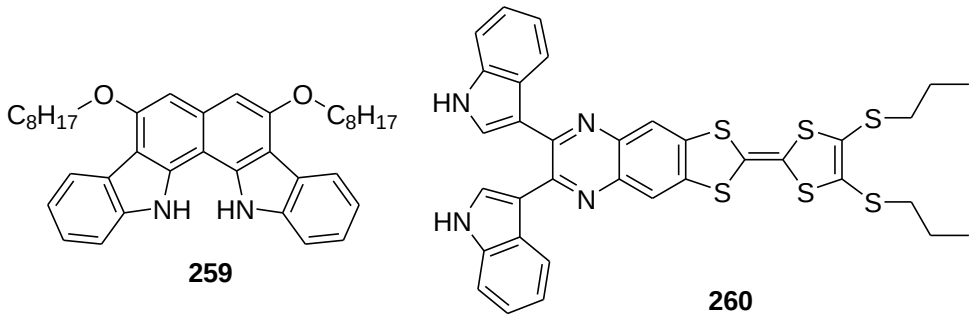

Fig. 127 Chemical structures of receptors **259** and **260**.

Carbazolo[1,2-*a*]carbazole receptor **259** (see Fig. 127) was prepared and used as a fluorogenic chemosensor for carboxylates.[169] In particular, DMF solutions of **259** exhibited a broad emission in the 370-440 nm interval, which was quenched upon the addition of anion BzO^-. All the other anions tested (i.e., AcO^-, $H_2PO_4^-$, Cl^-, Br^-, NO_3^- and HSO_4^-) were unable to induce changes in the emission profile of **259**. The changes in emission noted when BzO^- was added were ascribed to static quenching, which was active upon the formation of a 1:1 complex through hydrogen-bonding interactions of the anion with the N-H moieties of the receptor.

Receptor **260** (see also Fig. 127) was able to fluorogenically sense anion $H_2PO_4^-$ in CH_2Cl_2.[170] Solutions of **260** in CH_2Cl_2 showed an intense emission band at 620 nm (excitation at 468 nm), which was assigned to the quinoxaline fluorophore. Addition of $H_2PO_4^-$ induced a significant quenching of fluorescence due to the formation of a 1: 1 complex in which the anion bound with the N-H moieties of the indoloquinoxaline receptor. Addition of F^- induced slight emission intensity quenching, whereas Cl^-, BzO^-, or HSO_4^- were unable to induce any noticeable change.

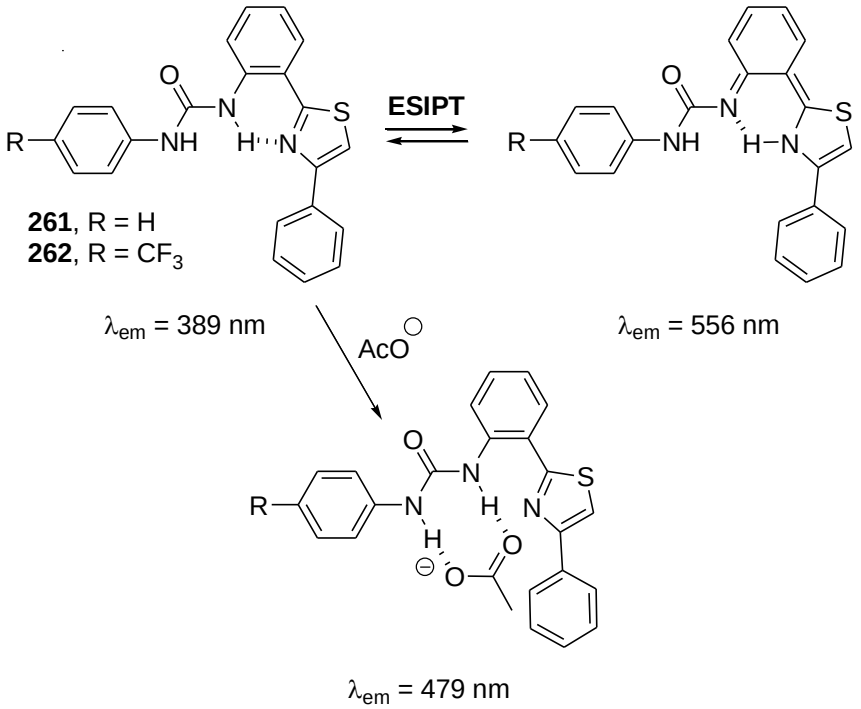

Fig. 128 Chemical structures of thiazole-based receptors **261** and **262** and the coordination mode with AcO^-

Thiazole-based chemosensors **261** and **262** (Fig. 128) were used for the fluorogenic sensing of anion AcO^- in CH_3CN.[171] Solutions of receptor **261** showed a dual emission profile with two bands at 389 (normal emission) and 556 nm (tautomer emission) due to an active excited-state intramolecular proton transfer (ESIPT) process. Addition of AcO^- induced the appearance of a new emission band centred at 479 nm ascribed to the formation of 1:1 hydrogen-bonding complexes between **261** and the anion with the subsequent quenching of tautomer fluorescence. Of all the anions tested, only F^- induced some minor changes in the emission profile, whereas Cl^-, Br^-, I^-, $H_2PO_4^-$, NO_3^-, ClO_4^- and HSO_4^- induced negligible changes. Practically the same selective response to AcO^- was obtained with probe **262**.

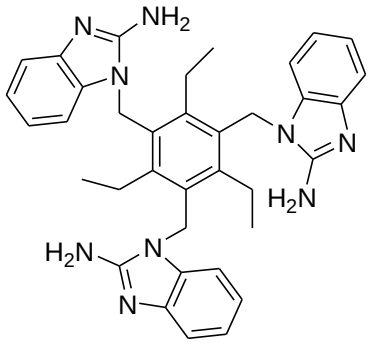

263

Fig. 129 Chemical structure of benzimidazole-based receptor **263**.

A new benzimidazole-based receptor (**263**, Fig. 129) was developed as fluorescent chemosensor for I^-.[172] Upon the addition of I^- to solutions of **263** in CH_3CN:H_2O 99:1, v/v (HEPES, pH 7.91), a concomitant increase in absorbance with a small shift (from 250 nm to 248 nm) was observed. Moreover, **263** displayed two emission bands at 318 nm and 408 nm (excitation at 258 nm), which were quenched upon the addition of I^-. The formation of 1:1 complexes and a limit of detection for I^- of 7.45 x 10^{-6} mol L^{-1} were determined. No significant variation in the fluorescence intensity was seen in the presence of the other anions (F^-, Cl^-, Br^-, HPO_4^-, HSO_4^-, NO_3^-, ClO_4^-, CN^-, and CH_3COO^-) evaluated.

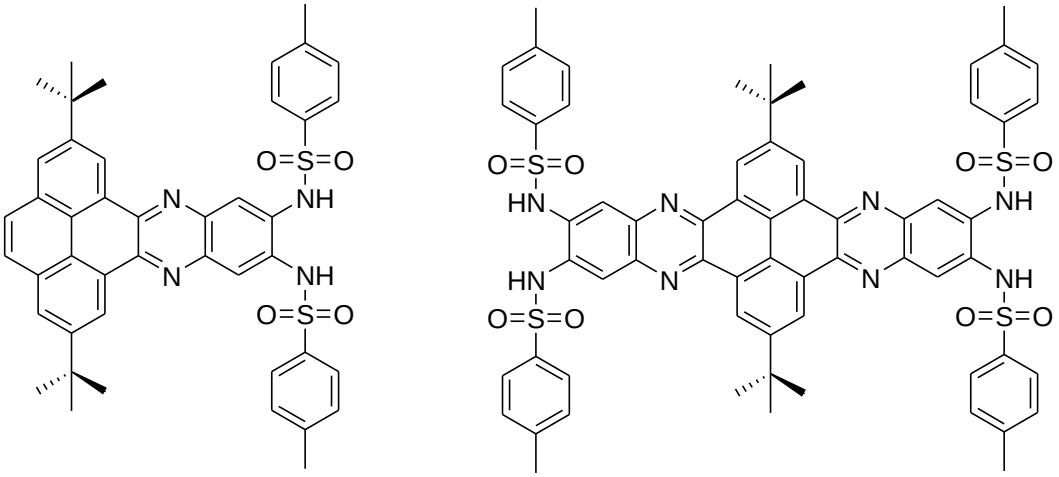

264 **265**

Fig. 130 Chemical structures of quinoxalinophenanthrophenazine-based receptors **264** and **265**.

Quinoxalinophenanthrophenazine-based receptors **264** and **265** (see Fig. 130) were used as chromogenic and fluorogenic probes for anions.[173] In particular, CH_2Cl_2:CH_3CN 1:1 v/v solutions of **264** and **265** showed intense absorption bands at 450 and 433 nm, respectively. Addition of F^-, CN^-, AcO^- and BzO^- to solutions of both receptors induced bathochromic shifts of ca. 30 nm, which were ascribed to the formation of 1:1 (for **264**) and 2:1 (for **265**) anion-receptor complexes, in which the anion bound to the sulphonamide fragment through hydrogen-bonding interactions. All the other anions tested (i.e., Cl^-, Br^-, I^-, NO_3^- and ClO_4^-) induced negligible changes. The same anion selectivity was observed using fluorescence measurements. CH_2Cl_2:CH_3CN 1:1 v/v solutions of receptor **264** presented an intense emission band at 500 nm (excitation at 350 nm). Addition of anions F^-, CN^-, AcO^- and BzO^- induced emission quenching together with the appearance of a new band at 550 nm. Regarding **265**, excitation at 350 nm resulted in an emission at 450 nm, which was quenched and progressively substituted for a new fluorescence at 550 nm upon the addition of anions F^-, CN^-, AcO^- and BzO^-. Changes in the absorption and emission bands were ascribed to alterations in the electronic density of the chromophore upon anion binding.

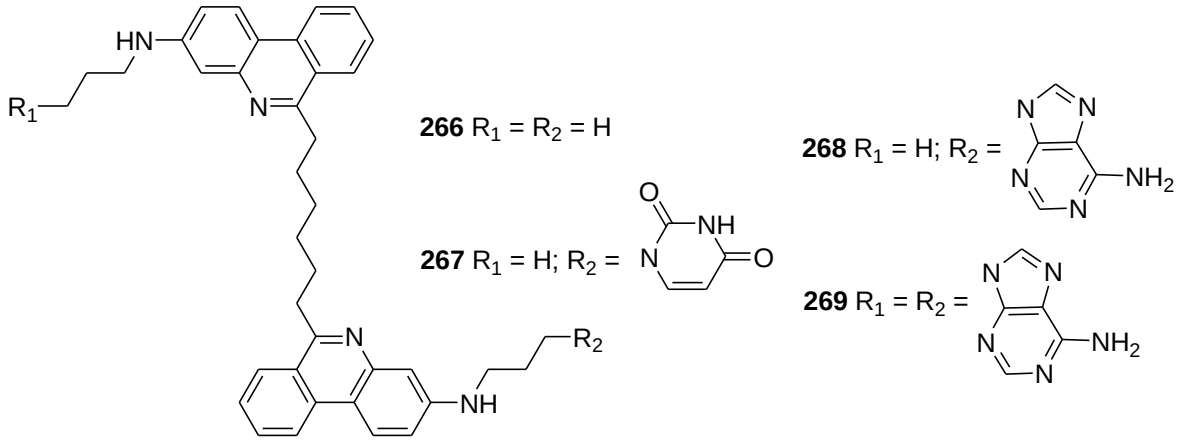

Fig. 131 Chemical structures of bis-phenanthridinium derivatives receptors **266** and **269**.

The interaction of bis-phenanthridinium derivatives **266**-**269** (Fig. 131) with certain nucleotides was studied in an aqueous environment.[174] Solutions of **266**-**269** at pH 5.0 showed broad emission bands in the 540-570 nm range upon excitation at 270 nm. This emission band for all four receptors was quenched, to some extent, upon the addition of UMP, AMP, GMP and CMP. Hydrogen-bonding interactions between **266**-**269** and the nucleotides yielded 1:1 complexes, which allowed the phenanthridinium fluorophore and the bases to establish π-stacking interactions that were responsible for the quenching observed. Receptor **268** gave the most selective response and a higher affinity to UMP.

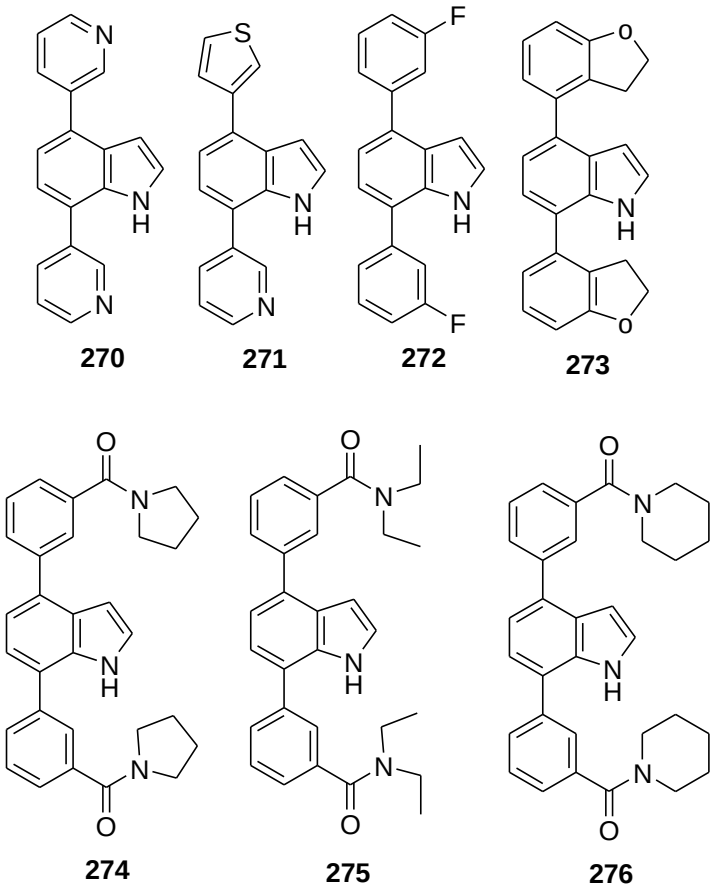

Fig. 132 Chemical structures of bis-phenanthridinium derivatives **270**-**276**.

A family of 4,7-Diaryl indole-based fluorescent probes for I^- was reported.[175] Solutions of **270-276** (see Fig. 132) in THF showed an absorption maximum in the 315-328 nm range. When receptors **270-276** were excited at their absorption maximum, emissions in the 396-409 nm range were observed. When adding increasing amounts of I^- to solutions of **270-276**, a blue shift in the absorption spectrum and a decrease in fluorescence intensity were observed. In all cases, 1:1 receptor-anion complexes were formed. Fluorescence quenching was explained by a heavy atom effect. No significant changes in either absorption or emission were observed with the addition of excess F^-, Cl^- and Br^- anions.

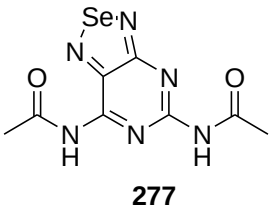

Fig. 133 Chemical structure of receptor **277**.

Goswami and co-workers prepared selenediazole-fused diacetamidopyrimidine **277** (Fig. 133) utilised as a selective fluorescent probe for aliphatic monocarboxylates.[176] In particular, CH_3CN solutions of **277** showed an emission band at 412 nm when excited at 351 nm. Addition of increasing quantities of AcO^-, pivalate, phenyl acetate and adamantane-1-carboxylate induced

the shift of the emission band to 459 nm, along with significantly enhanced intensity. The fluorescence of **277** remained unchanged upon the addition of BzO^-, Cl^-, Br^- and I^-, whereas the addition of F^- induced the same changes to those observed with AcO^-, but with less emission enhancement. In addition, a chromogenic response was observed; CH_3CN solutions of **277** presented an intense absorption band centred at 351 nm and addition of AcO^-, pivalate and phenyl acetate induced a change in colour from colourless to pale yellow due to the gradual decrease of absorbance at 351 nm with the simultaneous formation of a new band at 385 nm.

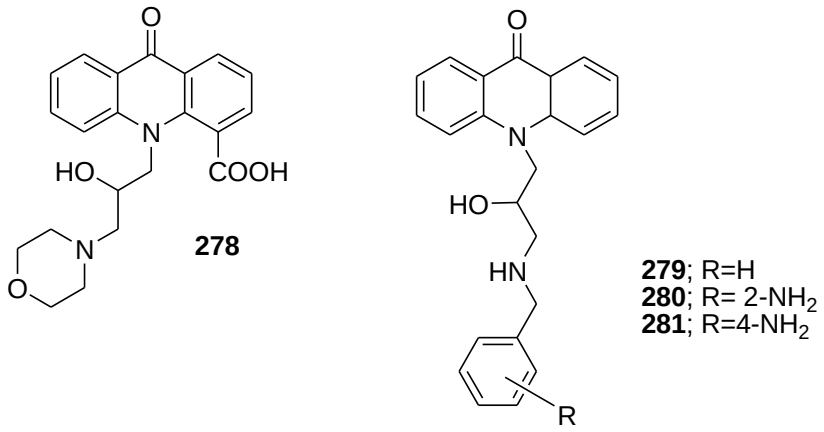

Fig. 134 Chemical structures of receptors **278-281**.

Acridone-based receptor **278** (see Fig. 134) was used for the fluorimetric detection of anion F^- .[177] THF solutions of **278** showed two emissions at 432 and 556 nm upon excitation at 253 nm. Of all the anions tested (i.e., F^-, Cl^-, Br^-, I^-, NO_3^-, AcO^-, $H_2PO_4^-$ and HSO_4^-), only F^- induced the quenching of the emission band at 432 nm. Emission quenching was ascribed to the activation of a PET process upon F^- binding with receptor **278**. This anion formed 1:1 complexes through simultaneous hydrogen-bonding interactions with the hydroxyl and carboxylic acid moieties in **278**. These interactions developed partial negative charges in the oxygen atoms of the hydroxyl and carboxylic acid groups, which were responsible for the PET deactivation path. This receptor could also be used as a colorimetric sensor for F^-; the initial colourless THF solutions of **278** turned yellow when this anion was added.

Acridones with an appropriate substituent at N-10 (structures **279-281** in Fig. 134) were prepared as fluorogenic probes for ATP and were used for monitoring metabolic processes.[178] **279** in HEPES solutions (pH 7.2) exhibited absorption bands at 253, 387 and 405 nm. With the addition of ATP, the absorbance at 253 significantly lowered. Furthermore, compound **279** showed emission bands at 417 nm and 440 nm when excited at 253 nm. Addition of ATP produced fluorescence quenching of 97.5% due to the formation of 1:1 **279**-ATP complexes. Similar changes in the absorption and fluorescence spectra for **280** and **281** were observed. It was found that binding constants of **279–281** for ATP were significantly high. By adding adenosine, AMP, ADP, GDP, IDP, CDP, UDP, GTP, ITP, CTP, and UTP separately to solutions of **279–281,** no change in their fluorescence spectra was noted. Finally, **279-281** were tested for *in vitro* real-time monitoring in response to the generation and consumption of ATP in two enzymatic reactions with fine results.

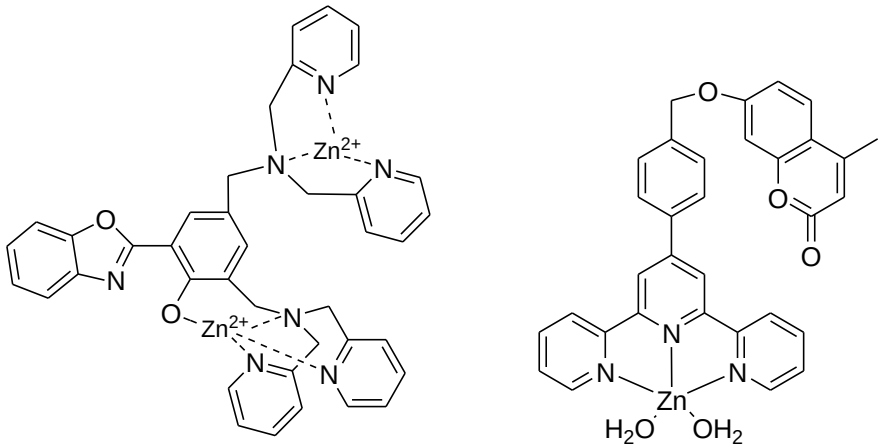

282-$(Zn^{2+})_2$ **283**

Fig. 135 Chemical structures of receptors **282** and **283**.

A binuclear system **282-$(Zn^{2+})_2$** (see Fig. 135) was used as a ratiometric fluorescent sensor to $P_2O_7^{4-}$ in water.[179] Upon the addition of anion $P_2O_7^{4-}$ to **282-$(Zn^{2+})_2$** solutions in HEPES (pH 7.4), the emission band was shifted to longer wavelengths (from 420 to 518 nm) due to the formation of 1:1 complexes. No significant changes were found in the presence of other anions (i.e., HCO_3^-, $H_2PO_4^-$, Cl^-, F^-, AcO^-, ATP, Citrate and HPO_4^{2-}). Furthermore, a molecular modelling optimisation of the geometry, by using AM1 on HyperChem, was carried out to find that the two DPA-Zn^{2+} groups in **282-$(Zn^{2+})_2$** were located at a suitable distance to create a strong binding environment to selectively recognise $P_2O_7^{4-}$ over structurally similar anions. Probe **282-$(Zn^{2+})_2$** was tested in pyrosequencing of DNA and the results were compared with gel electrophoresis. The authors also found that the **282-$(Zn^{2+})_2$** complex could be used as a simple, effective, rapid method to detect the $P_2O_7^{4-}$ released from dNTPs (Deoxynucleotide Triposphates) in PCR.

Zn^{2+}–2,2′:6′,2′′-terpyridine-based complex **283** (see Fig. 135) was used as a probe for $P_2O_7^{4-}$, AMP and ADP.[180] Solution of **283** in H_2O:CH_3CN 1:4 v/v at pH 7.4 showed two absorption bands at 286 and 325 nm, along with a distinct hump at around 347 nm. Upon excitation at 315 nm, two emissions at 381 and 467 nm were also noted. After adding several anions (i.e., F^-, Cl^-, Br^-, I^-, NO_3^-, AcO^-, $C_6H_5COO^-$, SO_4^{2-},HSO_4^-, $H_2PO_4^-$ and $P_2O_7^{4-}$) to the aqueous solution of **283**, only $P_2O_7^{4-}$ caused significant changes in absorbance, as well as a blue shift and an intensity enhancement in the emission spectra. The affinity of **283** to other phosphates (ATP, CTP, ADP and AMP) was tested in H_2O:CH_3CN 2:3 v/v HEPES buffer at pH 7.4. No changes in the absorption bands were found with the addition of ATP and CTP. However in the presence of AMP and ADP,a blue shift and an enhancement of the emission bands were observed. In all cases, 1:1 complexes between the anions ($P_2O_7^{4-}$, AMP and ADP) and the receptor were formed.

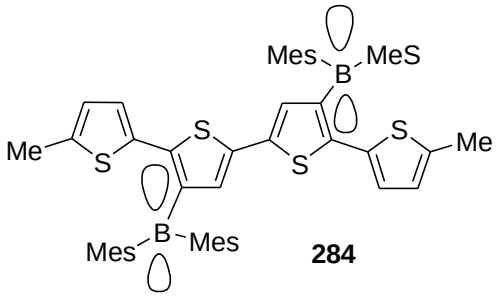

284

Fig. 136 Chemical structure of receptor **284**.

Boron-functionalised quaterthiophene (**284**, Fig. 136) was used as a fluorogenic chemosensor with a turn-on fluorescence response for anions F^- and CN^-.[181] Solutions of **284** in THF were prepared and titrated with F^- or CN^-. A two-step process was observed. During the first step, which occurred with the addition of 0-1 equiv. of anion F^-, the original band at 343 nm gradually decreased, while a new band at 418 nm increased in intensity (colour change from yellow to blue-green). During a second step (with the addition of 1.2–2.2 equiv.) the absorption band shifted back to a slightly lower energy. A similar behaviour was found for CN^-. Exposure to excess N_3^- resulted in less pronounced changes, whereas no significant modifications were observed in the presence of other anions in excess (i.e., Cl^-, Br^-, I^- and SCN^-). When THF solutions of **284** were excited at 343 nm, a very weak emission centred at 560 nm was found. In this case, only the addition of F^- and CN^- anions induced marked enhancement (about 10-fold for both anions) in the emission intensity, together with a blue shift (to 486 and 476 nm for F^- and CN^-, respectively). Intensity enhancement was attributed to a rigidification of the receptor backbone upon anion binding.

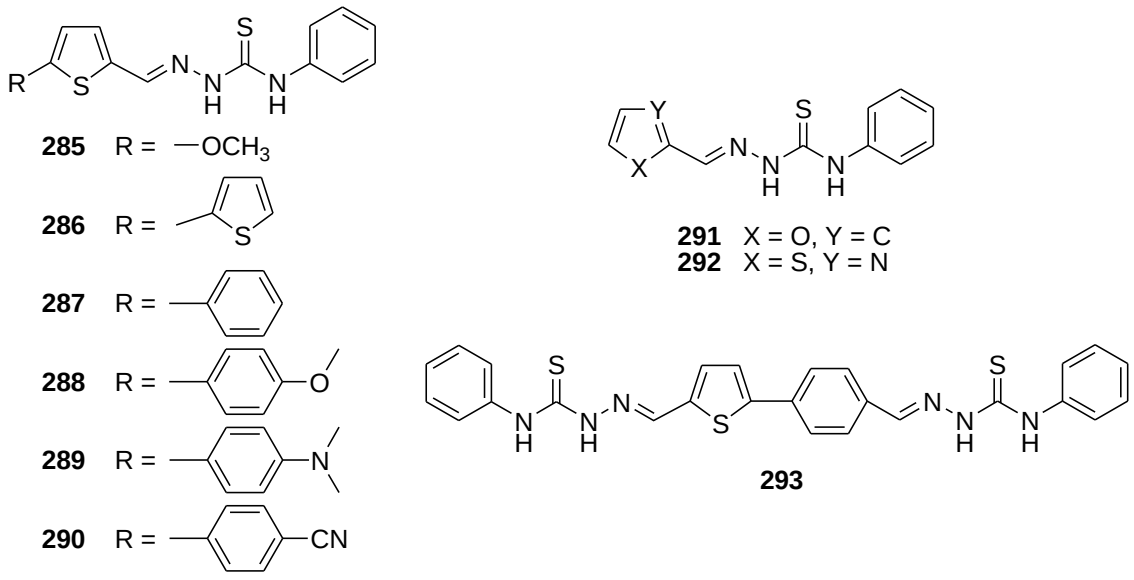

Fig. 137 Chemical structures of receptors **285-293**.

A family of heterocyclic thiosemicarbazones was synthesised and used as probes to detect certain anions.[182] CH_3CN solutions of receptors **285-293** (see Fig. 137) showed intense absorption bands in the 350-410 nm range. Addition of increasing quantities of anion F^- to

solutions of **285-293** induced an intensity decrease and a small bathochromic shift of the absorption bands, together with a simultaneous growth of a new red-shifted absorption in the 376-515 nm range. Similar behavior was noted with receptors **285-293** in the presence of anion CN^-. These changes in the UV-Vis spectra of the receptors upon the addition of anions F^- and CN^- were attributed to the existence of two consecutive equilibria: (i) the formation of hydrogen-bonding complexes during a first step; (ii) a deprotonation of receptors by the anion during a second step. The observed changes clearly related with the basicity of the anions, thus AcO^- induced the appearance of the red-shifted band, butonly with receptors **286**, **287** and **290-293** which contain the more acidic N-H moieties, whereas $H_2PO_4^-$ was able to deprotonate only **290,** whose structure contains a CN electron-withdrawing group. No significant changes in the UV-Vis bands of all the receptors were observed in the presence of any other anions in excess with a less basic character (i.e., Cl^-, Br^-, I^-, HSO_4^-, NO_3^- and SCN^-). Additionally, fluorimetric studies of **285**-**293** in the presence of anions were carried out. The formation of hydrogen-bonding complexes between receptors and anions induced an increase in the emission band (410-530 nm), whereas the deprotonation process led to the appearance of a new red-shifted emission band.

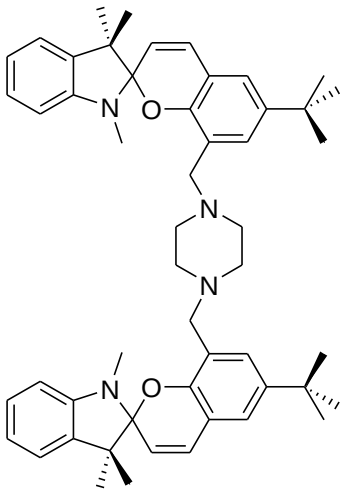

294

Fig. 138 Chemical structure of receptor **294**.

Bis-spiropyran receptor **294** (Fig. 138) was used as a fluorescent probe for glutathione (GSH) in aqueous environments.[183] In particular CH_3CH_2OH:water 2:8 v/v solutions of **294** showed an intense absorption band at 334, which was ascribed to the spiropyran chromophore. This band in **294** remained unchanged despite the addition of Cys and Glu amino acids, whereas addition of GSH induced the appearance of an absorption band at 446 nm (change in colour from colourless to yellow). This new absorption band was ascribed to the merocyanine form of **294**, which was obtained upon the coordination with GSH (through electrostatic and hydrogen-bonding interactions). The same selectivity was observed when using fluorescent measurements. When excited at 446 nm, CH_3CH_2OH:water 2:8 v/v solutions of **294** exhibited a weak emission band at 516 nm. Addition of increasing quantities of GSH induced the quenching of the 516 nm band together with the appearance of a new emission at 643 nm. The authors indicated that this new red-shifted emission was due not only to the increases concentration of the mercoyanine form, but also to GSH binding, which induced

conformational rigidity. Finally, receptor **294** was used for the fluorescent imaging of GSH in living cells.

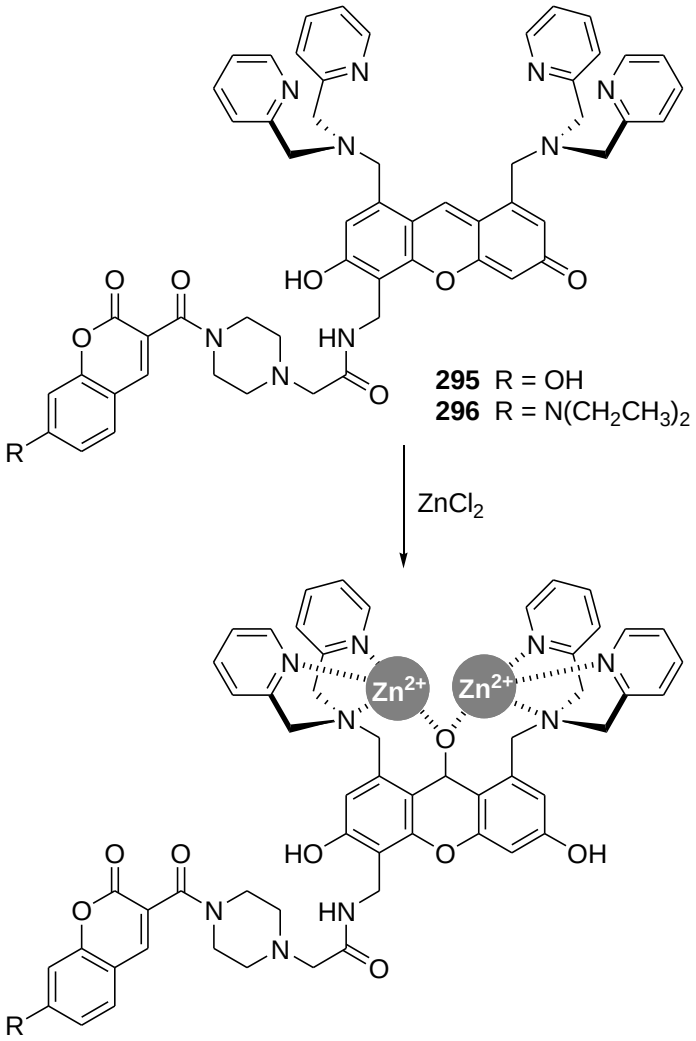

Fig. 139 Chemical structure and binding mode of receptors **295** and **296** with Zn^{2+}.

Hamachi et al prepared the FRET-based receptors **295** and **296** (see Fig. 139) for the ratiometric fluorescence sensing of nucleoside polyphosphates.[184] Aqueous solutions (HEPES, 10 mM NaCl, 1 mM $MgCl_2$, pH 7.2) of receptor **295** showed two emission bands upon excitation at 341 nm (absorption band of coumarin), centred at 454 (from the coumarin) and 525 nm (from the xanthene). This dual emission was ascribed to a FRET process from the coumarin to the xanthene group due to the effective spectral overlapping of both fluorophores. Addition of $ZnCl_2$ induced a marked increase in emission at 454 nm, together with the almost complete disappearance of fluorescence at 525 nm. This change was attributed to the formation of the **295-$(Zn^{2+})_2$** complex which induced the xanthene ring to adopt a non-conjugated form. FRET was cancelled as a result of a decrease in the spectral overlap between coumarin emission and xanthene absorption. The **295-$(Zn^{2+})_2$** complex was used as a fluorescent ratiometric sensor of nucleoside polyphosphates. In particular, addition of ATP, GTP, CTP, ADP, UDP and $P_2O_7^{4-}$ induced an intense quenching of the emission band centred at 454 nm with the concomitant increase of xanthene emission at 525 nm. These

changes were ascribed to the recovery of the FRET process upon the formation of 1:1 adducts between the nucleotide and the **295-(Zn^{2+})$_2$** complex. On the other hand, addition of AMP, c-GMP, c-AMP, ADP-Glu, UDP-Gal, HPO_4^-, AcO^-, SO_4^{2-}, NO_3^- and HCO_3^- induced negligible changes in the emission profile of the **295-(Zn^{2+})$_2$** complex. Similar results were obtained with receptor **296**. Finally, both complexes were applied for the real-time monitoring of enzyme reactions and for the ratiometric visualisation of nucleoside polyphosphates in living cells.

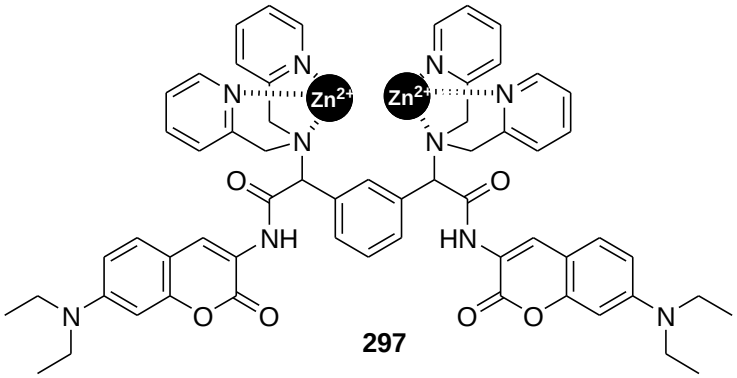

Fig. 140 Chemical structure of the Zn^{2+} complex receptor **297**.

The well-known ability of phosphates to bind with Zn^{2+} complexes was exploited in this example to prepare **297** (see Fig. 140), which acted as a probe for anion $P_2O_7^{4-}$.[185] Aqueous buffered solutions (HEPES, pH 7.4) of **297** presented an intense emission at 511 nm due to the inhibition of a PET process from the lone pair of the tertiary amine N to the coumarin fluorophore upon complexation with the Zn^{2+} cation. Of all the anions tested (i.e., ADP, AMP, cAMP, $P_2O_7^{4-}$, Br^-, Cl^-, ClO_4^-, $H_2PO_4^-$, HCO_3^-, N_3^-, AcO^-, PO_4^{3-} and SO_4^{2-}), only $P_2O_7^{4-}$ was able to quench, to some extent, the emission intensity of aqueous solutions of **297**. Emission quenching was ascribed to a preferential coordination of $P_2O_7^{4-}$ with both the Zn^{2+} cations presented in **297** through the formation of a 1:1 ensemble. This coordination weakened the Zn^{2+} interaction with the lone pair of the tertiary amine restoring the PET process to some degree.

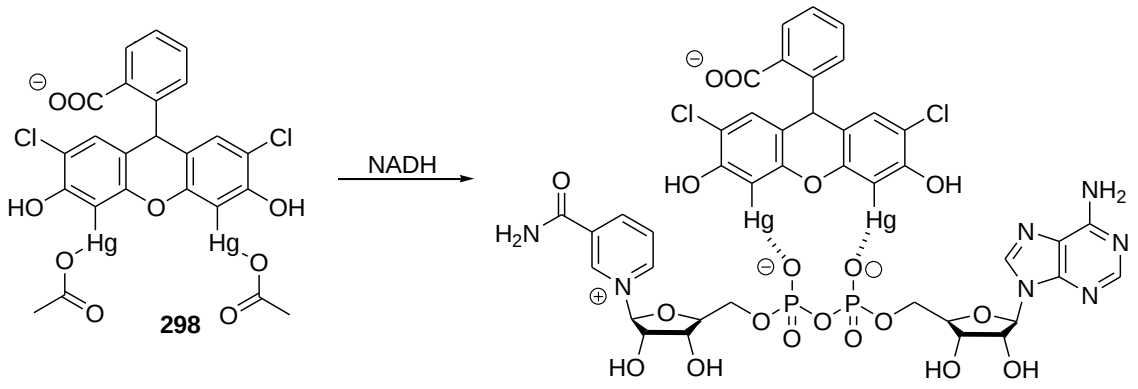

Fig. 141 Chemical structure and binding mode of receptors **298** with NADH.

Fluoresceine derivative **298** (Fig. 141) was used as a fluorogenic chemosensor for NADH, an anion that plays key roles in cellular energy metabolism and dehydrogenase enzymatic

reactions.[186] Aqueous solutions of **298** buffered at pH 7.2 displayed an intense emission band at 524 nm typical of the fluorescein fluorophore. Changes in the emission intensity were studied in the presence of NADH, CO_3^{2-}, SO_4^{2-}, Cl^-, NO_3^-, AcO^-, HSO_4^-, ClO_4^-, ADP, GTP, CTP, TTP, AMP, ATP and NAD^+. Only addition of NADH induced quenching of the emission of **298**. The quenching was a direct consequence of a PET process between the bounded **298** (through metal-anion interactions) and the pyridinium ring of NADH.

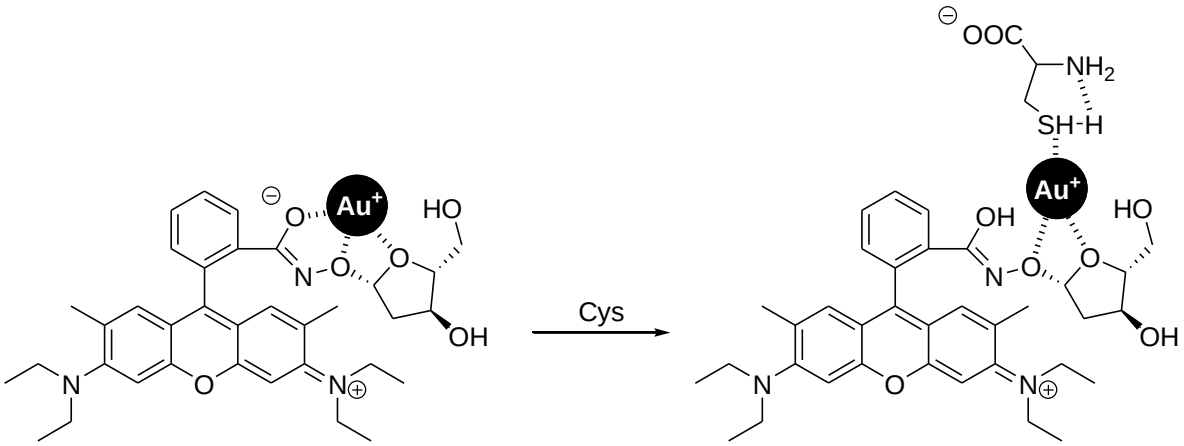

Fig. 142 Chemical structure and binding mode of receptors **299** with Cys.

Complex **299** (see Fig. 142) was used for the fluorimetric sensing of thiol-containing amino acids.[187] H_2O:CH_3OH 99:1 v/v solutions of **299** showed a weak emission band at 560 nm (excitation at 500 nm) whose intensity increased upon the addition of Cys and Hcy. The other amino acids tested (i.e., Asp, Glu, GSH, Iso, Pro, Met, Leu, Try, Gly, Ser, Asn, Phe, Gln, Tyr, Lys, His, Arg, Thr, Ala, Val) induced negligible changes in the emission profile of complex **299**. The increase in the emission intensity was ascribed to the formation of a 1:1 aduct. Furthermore, **299** could also be used for the colourimetric detection of Cys because this was the only amino acid that was able to change the colour of the H_2O:CH_3OH 99:1 v/v solutions of the complex from colourless to red.

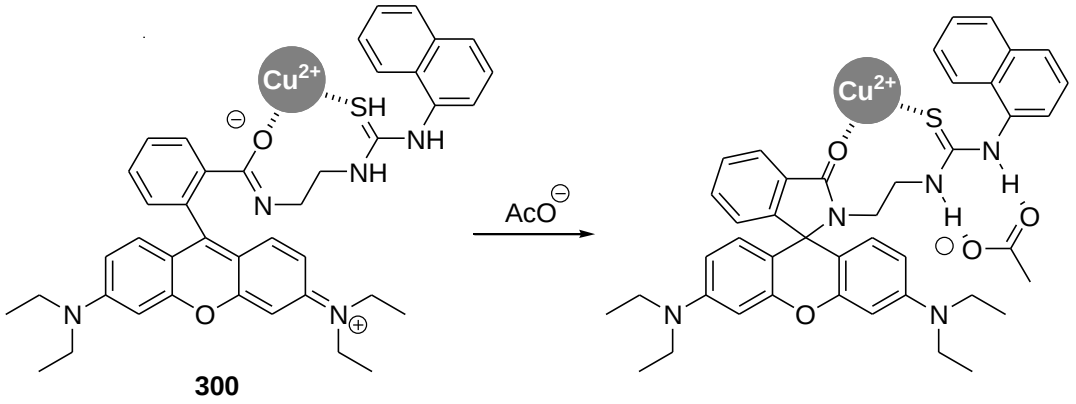

Fig. 143 Chemical structure and binding mode of receptors **300** with AcO^-.

Rhodamine-based complex **300** (Fig. 143) was used as fluorimetric and colourimetric chemosensor for certain anions.[188] **300** showed an intense emission at 584 nm in CH_3CN upon excitation at 300 nm. This emission band was due to a FRET process from energy acceptor naphthalene to the open rhodamine fluorophore. Addition of Cl^-, Br^-, I^-, NO_3^- and ClO_4^- to CH_3CN solutions of **300** induced negligible changes in the emission intensity profiles, whereas the emission intensity was quenched in the presence of AcO^-, BzO^-, F^- and $H_2PO_4^-$. Quenching efficiency followed the order of $AcO^- > F^- > PhO^- > H_2PO_4^-$. Emission intensity quenching was ascribed to a cyclisation of the rhodamine fluorophore upon coordination through hydrogen-bonding interactions of anions AcO^-, BzO^-, F^- and $H_2PO_4^-$ with the thiourea moiety.

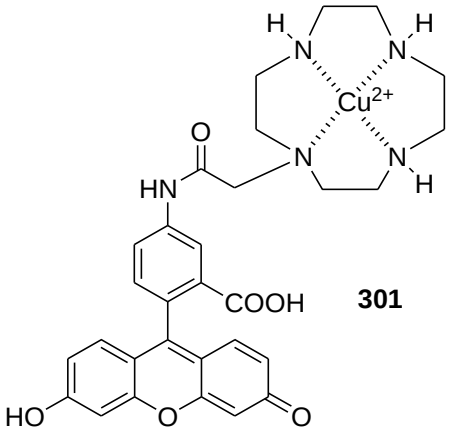

301

Fig. 144 Chemical structure of azamacrocyclic-Cu^{2+} complex **301**.

A novel fluorescence probe for H_2S based on an azamacrocyclic-Cu^{2+} complex (**301**, see Fig. 144) was described.[189] **301** solutions in HEPES at pH 7.4 showed an absorption band at 491 nm and an emission at 516 nm. When adding H_2S to **301** solutions, a considerable, immediate 50-fold enhancement in emission intensity was observed, whereas almost no fluorescence changes were seen with the addition of GSH, even when in excess. **301** also showed high selectivity for H_2S to other thiols (i.e., L-Cys, DL-Hcy, 2-ME, DTT), inorganic sulphur-containing compounds (i.e., SCN^-, SO_3^{2-}, and $NS_2O_3^{2-}$) and reducing agents (sodium ascorbate). Besides, **301** did not show any fluorescence enhancement in the presence of reactive-oxygen or nitrogen species (i.e., H_2O_2, ·OH, $ONOO^-$, ^-OCl, O_2^-, $^1O_2$ and ·NO). Only when Angeli's salt (NO^- donor) was added was small fluorescence enhancement noted. Probe **301** was highly hydrophilic, and consequently, is membrane-impermeable. In order to enhance its permeability for testing the signalling behavior in cells, the diacetylated derivative **301-DA** was prepared. HeLa cells were incubated with **301-DA** and, upon the addition of Na_2S, substantial intracellular fluorescence enhancement was seen. The CCK-8 (Cell Counting Kit-8) assay results revealed that **301-DA** exhibits no cytotoxicity at high concentrations.

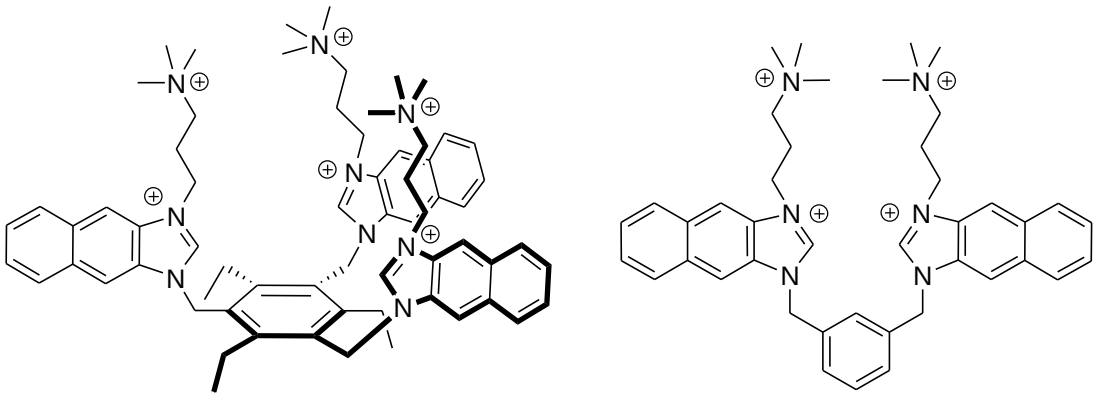

302 **303**

Fig. 145 Chemical structures of receptors **302** and **303**.

Receptors **302** and **303** are composed by naphthoimidazolium groups as both signaling subunits and binding sites due to its ability to form $(C\text{-}H)^{+}\cdots A^{-}$ hydrogen bonds (see Fig. 145).[190] HEPES solutions of tripodal receptor **302**, buffered at pH 7.4, presented a broad emission band centered at 450 nm (upon excitation at 326 nm) that remained unchanged upon addition of AcO^{-}, $H_2PO_4^{-}$, CN^{-}, F^{-}, Cl^{-}, I^{-}, NO_3^{-}, $P_2O_7^{4-}$, AMP and ADP. However, addition of UTP, CTP, TTP and ATP induced moderate enhancements whereas in the presence of GTP an emission quenching was observed. The response of receptor **303** is more selective because, of all the anions tested, only addition of ATP induced a 2-fold enhacement of the emission band at 460 nm (excitation alos at 326 nm) whereas GTP also induced a moderate quenching. Both receptors formed 1:1 stoichiometry complexes with the nucleotides tested, through the formation of hydrogen bonding and electrostatic interactions.

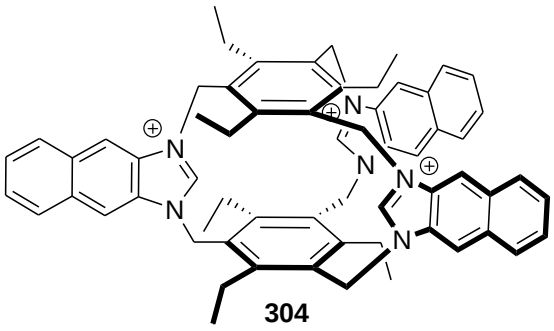

304

Fig. 146 Structure of cyclophane receptor **304**.

Acetonitrile solutions of cyclophane **304** (see Fig. 146), bearing three naphthoimidazolium moieties, showed a broad emission at 474 nm (excitation at 326 nm).[191] Addition of HSO_4^{-}, Cl^{-}, Br^{-}, I^{-}, $H_2PO_4^{-}$, AcO^{-} and CN^{-} induced quenching of the emission band at 474 nm, whereas only addition of F^{-} induced the appearance of a blue shifted fluorescence centered at 385. This result indicated the possible use of receptor **304** for the ratiometric fluorescent sensing of fluoride. The new emission band was ascribed to the formation of a 1:1 inclusion complex in which the F^{-} anion in encompassed into the cavity of receptor **304** by means of a combination of anion-π interactions and $(C\text{-}H)^{+}\cdots F^{-}$ hydrogen bonds. The formation of this inclusion complex was assessed by ^{1}H NMR, ^{19}F NMR and isothermal titration calorimetry (ITC) studies.

3.1.3.- Containing Ln, Ir, Pt and Ru complexes

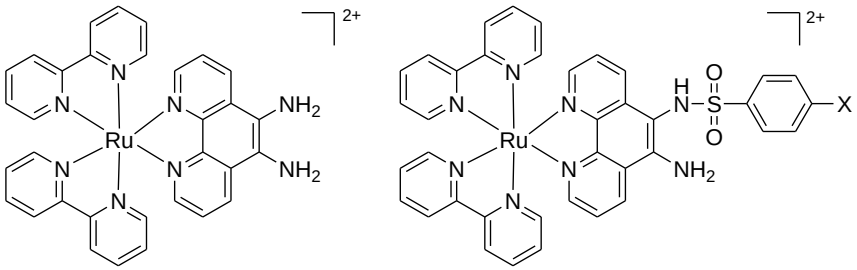

305

306: X = H
307: X = CH_3
308: X = NO_2

Fig. 147 Chemical structures of receptors **305-308**.

Chakraborty and coworkers designed different receptors (**305-308**, see Fig. 147), incorporating Ru^{2+}-polypyridine moieties as fluorogenic unit and functionalised with 1,10-phenatroline containing amino and benzenesulphonamide groups as binding sites for anion recognition.[192] The absorption spectra of **305-308** in CH_3CN exhibited a band in the 440-453 nm range, which was assigned to a metal-to-ligand charge transfer (MLCT) transition. These receptors also exhibited a higher energy band at 286 nm, which was attributed to a ligand centred charge transfer (CT) involving $\pi-\pi^*$ transitions. The luminescence spectra of **305-308** in CH_3CN exhibited an emission in the 603-609 nm range (excitation at the 440-453 nm absorption bands). The emission of **306**-**308** was substantially quenched (65-80%) upon the addition of F^-, AcO^- and $H_2PO_4^-$, whereas the other anions tested showed no significant changes. The emission intensity of receptor **305** was quenched by F^-, AcO^-, $H_2PO_4^-$, and also by I^- and HSO_4^- (35-45%). Emission intensity quenching indicated a strong interaction between the anions and the fluoroionophore. The strong to moderate bases F^-, AcO^- and $H_2PO_4^-$ were hydrogen-binding acceptors and they formed complexes with the NH and NH_2 groups through $N\cdots F^-/O^-$ interactions. The strong basicity of these anions enhanced the electron density of NH and NH_2, which subsequently propagated to the metal bound to 1,10-phenantroline, causing increased intramolecular quenching of emission intensity.

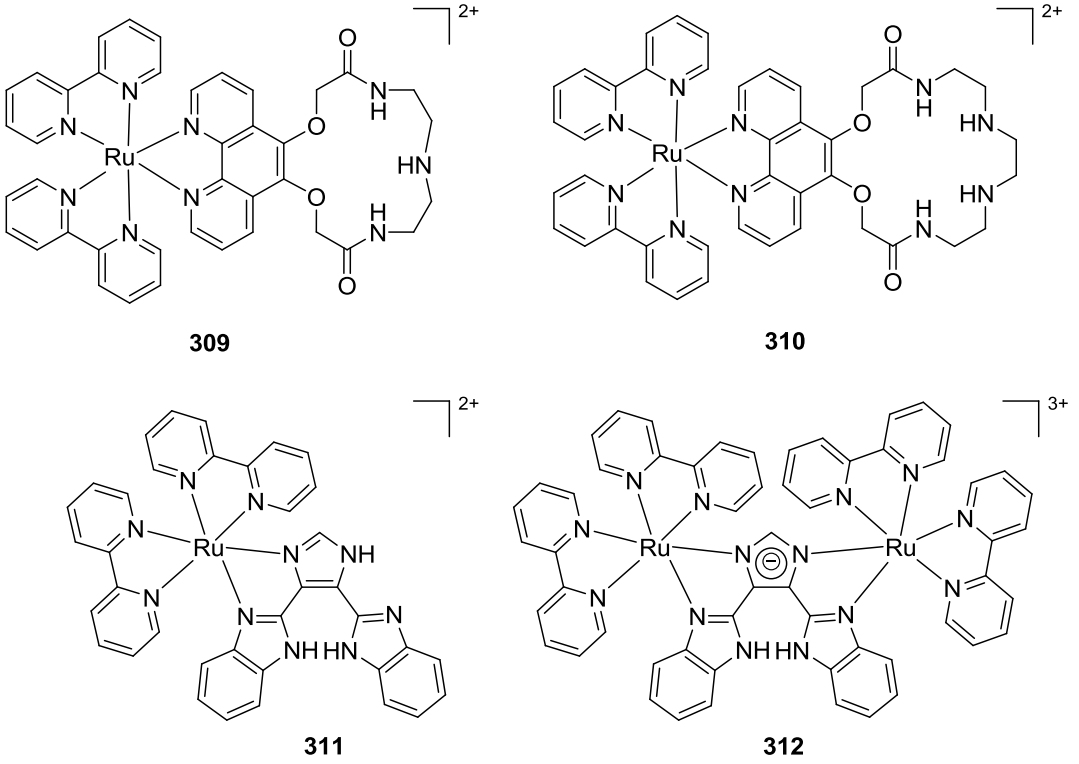

Fig. 148 Chemical structures of receptors with Ru^{2+}-polypyridine moieties **309**-**312**.

S. Patra et al. reported the synthesis of two luminescent metalloreceptores (**309** and **310**, see Fig. 148) characterised by having macrocycles with different dimensions with amide and amine hydrogen donor groups as active binding sites.[193] CH_3CN solutions of **309** and **310** presented absorption bands at 450 and 452 nm, respectively. By excitation in the absorption maxima, luminescence bands at 604 (for **309**) and 603 nm (for **310**) were obtained. The luminescence response of both receptors was studied in the presence of selected anions (i.e., F^-, Cl^-, Br^-, I^-, $H_2PO_4^-$, ClO_4^-, NO_3^-, BF_4^-, AcO^- and HSO_4^-). For receptor **309,** a substantial quenching of luminescence (76%) was observed upon the addition of F^-. Interestingly, the same probe displayed significant enhancement in emission intensity (52%) when treated with anion $H_2PO_4^-$, whereas other anions did not induce any appreciable change. For complex **310,** the authors reported that $H_2PO_4^-$ and F^- induced a significant quenching of luminiscence (32% and 66%, respectively). With **309** and **310,** the different dimensions of the binding site were seen to modulate receptor selectivity. In fact, the smaller **309** was able to interact with only F^-, whereas the bigger binding site of **310** allowed interactions with F^- and $H_2PO_4^-$. The formation of complexes between **309** and **310** and $H_2PO_4^-$ and F^- was also confirmed by ^{1}H-NMR studies.

Saha et al. described the synthesis and the selective binding properties to different anions of receptors **311** and **312**, consisting of a central bis(benzimidazol-2-yl)imidazole moiety complexed with one and two $[Ru(bipy)_2]^{2+}$ fluorophores, respectively (see Fig. 148).[194] CH_3CN solutions of receptors **311** and **312** showed broad MLTCT absorption bands at 475 and 488 nm, respectively. Addition of anions F^- and AcO^- to the solutions of both receptors induced moderate red shifts of the visible bands from 475 to 535 nm and from 488 to 503 nm for **311** and **312,** respectively (changes in colour from yellow-orange to magenta). When anion $H_2PO_4^-$

was added, only the absorption band of **311** underwent a 30 nm bathochromic shift. The other anions tested (i.e., Cl^-, Br^-, I^-, NO_3^- and ClO_4^-) were unable to induce changes in the visible bands of both receptors. The changes in colour observed with F^-, AcO^- and $H_2PO_4^-$ were ascribed to a two-tep coordination process. During the first step, at lower anion concentration, 1:1 anion-receptor complexes were formed via hydrogen bonding interactions with the N-H fragments of the benzimidazole moieties. In a second step, in the presence of an excess of anion, a deprotonation of the N-H group of the benzimidazole took place. Both complexes were luminescent and, upon excitation in their MLCT absorption maxima, emission bands at 660 and 685 nm were observed for **311** and **312**. Addition of anions F^- and AcO^- induced a total quenching of luminescence, whereas moderate quenching was found for $H_2PO_4^-$. The other anions tested induced negligible changes in the emission profiles of both receptors.

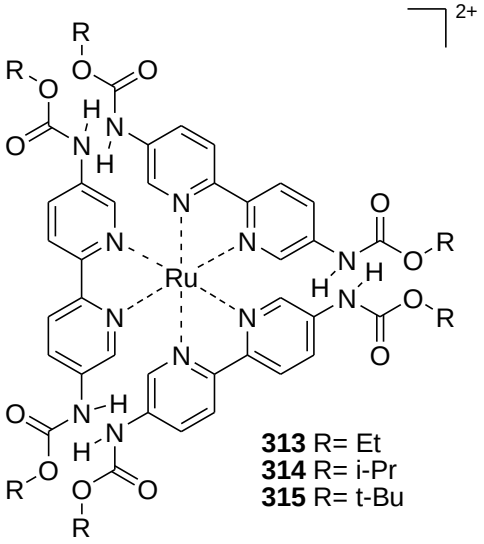

Fig. 149 Chemical structures of receptors **313-315**.

Three Ruthenium complexes containing 5,5´-dicarbamate-2,2´-bipyridine ligands (**313**, **314** and **315**, see Fig. 149) were used as probes for SO_4^{2-}.[195] CH_3CN solutions of receptor **313** showed an intense emission band at 571 nm upon excitation at 374 nm. Addition of NO_3^-, ClO_4^-, Cl^-, Br^- and I^- anions induced negligible changes in emission intensity, whereas F^-, AcO^- and HSO_4^- induced moderate fluorescence quenching. However, the most remarkable quenching (80%) was achieved upon SO_4^{2-} addition. Quenching was ascribed to the formation of complexes between anions and **313** (1:1 with anions HSO_4^- and SO_4^{2-} and 1:2 host-guest species with F^- and AcO^-). The same quenching effects with anions F^-, AcO^-, SO_4^{2-} and HSO_4^- were found for receptors **314** and **315**.

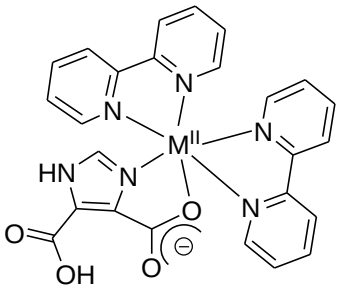

316; M = Ru
317; M = Os

Fig. 150 Chemical structures of receptors **316** and **317**.

Ru^{2+} and Os^{2+} complexes, containing imidazole-4,5-dicarboxylic acid and 2,2´-bipyridine units (**316** and **317** in Fig. 150), displayed colourimetric signalling events in the presence of certain anions.[196] The MLCT peaks at 485 and 440 nm for **316** and at 715 and 505 nm for **317**, remained practically unchanged upon the addition of Cl^-, Br^-,I^-, NO_3^- and ClO_4^- anions in CH_3CN, while the addition of F^-, AcO^- and $H_2PO_4^-$ caused a significant change in colour from yellow to orange due to the red shift of the absorption bands to 525 and 465 nm for **316** and to 765 and 540 nm for **317**. When CH_3CN solutions of receptor **316** were excited at 485 nm, a luminescent band at 690 nm was observed. Of all the anions tested, only the addition of F^-, AcO^- and $H_2PO_4^-$ induced a red shift (to 740 nm) and enhancement in the emission intensity. Binding studies showed that at low concentrations of anions, 1:1 hydrogen bonding complexes were formed, whereas a deprotonation of the N–H proton occured in the presence of anions in excess.

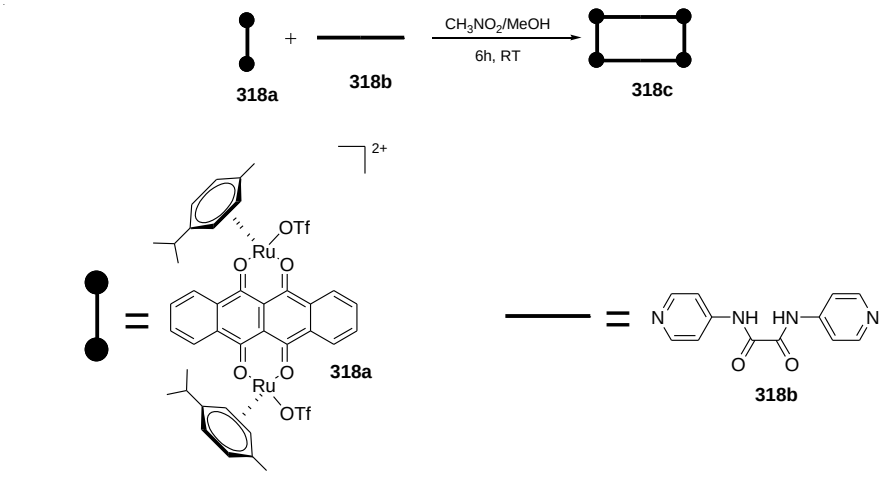

Fig. 151 Structure and preparation of the self-assembled arene-ruthenium-based rectangle **318c**.

Self-assembled arene-ruthenium-based rectangle (**318c**), for the selective sensing of poly-carboxylate anions, was reported (see Fig. 151).[197] CH_3OH solutions of cage **318c** presented weak emission bands at 558 and 524 nm (upon excitation at 377 nm) due to a PET process involving the Ru(II) fluorophore to the amide moieties. The emission behaviour of **318c** was studied upon the addition of anions F^-, Br^-, Cl^-, AcO^-, $C_2O_4^{2-}$ malonate, succinate tartrate and citrate. Of all the anions tested, only the addition of $C_2O_4^{2-}$ (2.5-fold), citrate (3-fold) and tartrate (4.5-fold) was able to induce emission enhancements. The tartrare, citrate and $C_2O_4^{2-}$ anions formed 1:1 complexes through hydrogen-bonding interactions with the N-H amide

moieties in cage **318c**. This coordination inhibited the PET process that was active in the receptor alone and accounted for the emission enhancement observed.

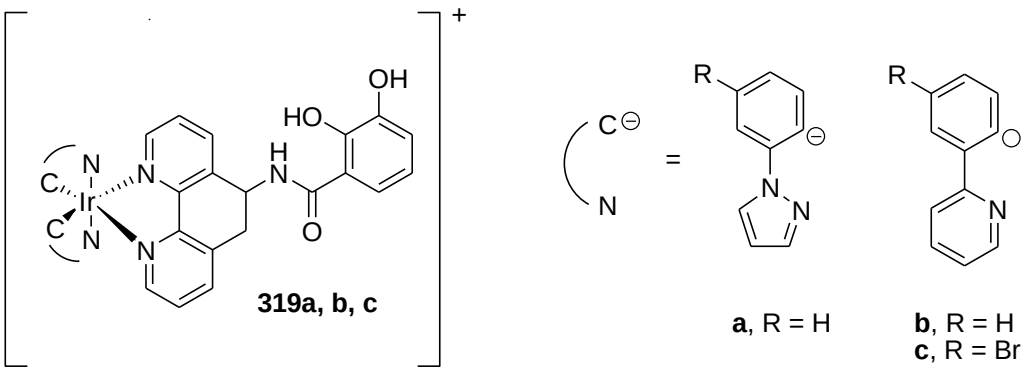

Fig. 152 Chemical structure of iridium complex **319a-c**.

Luminescent iridium complexes [**319a, b, c**]$^{+}$ (see Fig. 152) were reported for the detection of anion MoO_4^{2-}.[198] Solutions of the complexes [**319a, b, c**]$^{+}$ in CH_3CN:H_2O 20:1 v/v, showed emission bands with maxima at 596, 610 and 588 nm upon excitation at 326, 310 and 400 nm, respectively. Addition of MoO_4^{2-} to solutions of [**319a, b, c**]$^{+}$ resulted in diminished emission intensity which was proportional to the concentration of this anion. In all cases, 2:1 receptor-MoO_4^{2-} complexes were formed. This ratio was consistent with the predominant formation of cis-dioxo-Mo(VI)-dicatecholate complexes at these pH values. In spite of these interesting results, the authors did not test the luminescent responses of the complex in the presence of other anions.

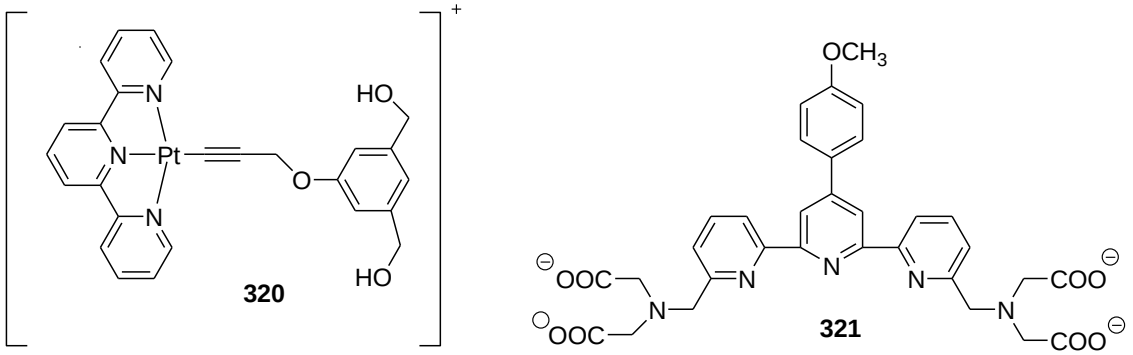

Fig. 153 Chemical structure of receptors **320** and **321**.

NIR-emissive alkynylplatinum(II) terpyridyl complex **320** (see Fig. 153) was used as a turn-on selective probe for heparin.[199] H_2O solutions, buffered at pH 7.4, of complex **320** showed an emission band at 748 nm which increased in intensity upon the addition of unfractioned (UFH) or low molecular-weight heparin (LMWH). This emission enhancement was ascribed to the electrostatic interactions between positively-charged **320** and negatively-charged heparin, which located **320** complex molecules in close proximity via metal-metal and π-π interactions. Consequently, the triplet metal-metal-to-ligand charge transfer (^{3}MMLCT) emission was observed. Addition of chondroitin 4-sulphate (ChS) to the aqueous solutions of **320** also

induced emission enhancement, but of less intensity than that found for heparin (67% when compared with heparin), whereas the fluorescence response to hyaluronic acid (HA) was minimum (17% when compared with heparin). The ability of **320** to detect UFH and LMWH in foetal bovine serum was tested with fine results.

J. Yuan and coworkers synthesised Eu^{3+} and Tb^{3+} water-soluble complexes of **321** (Fig. 153), which were able to selectively react with $ONOO^-$.[200] In particular, H_2O solutions (borate buffer, pH 9.1) of the **321-Tb^{3+}** complex presented typical luminescence bands at 485, 541 (main peak), 581 and 617 nm (excitation at 335 nm), whereas the luminescence bands of **321-Eu^{3+}** complex appeared at 584, 592, 612 (main peak), 646 and 692 nm (excitation at 335 nm). The luminescent response of both complexes with reactive oxygen species (ROS), such as $ONOO^-$, ·OH, ClO^-, $^1O_2$, $O_2^{\cdot-}$, H_2O_2, NO, NO_2^- and NO_3^-, was tested. The results indicated that $ONOO^-$ was able to quench the luminescence of **321-Tb^{3+}** (98%), whereas other ROS tested induced minor (·OH, NO and NO_2^-) or negligible changes in the emission profile. Emission intensity quenching was ascribed by the authors to an electron-transfer process involving the electron-rich $ONOO^-$ and the excited complex. On the other hand, the luminescence of **321-Eu^{3+}** remained unaltered in the presence of anion $ONOO^-$. By bearing this fact in mind, the authors used a mixture of both complexes for the ratiometric detection of $ONOO^-$.

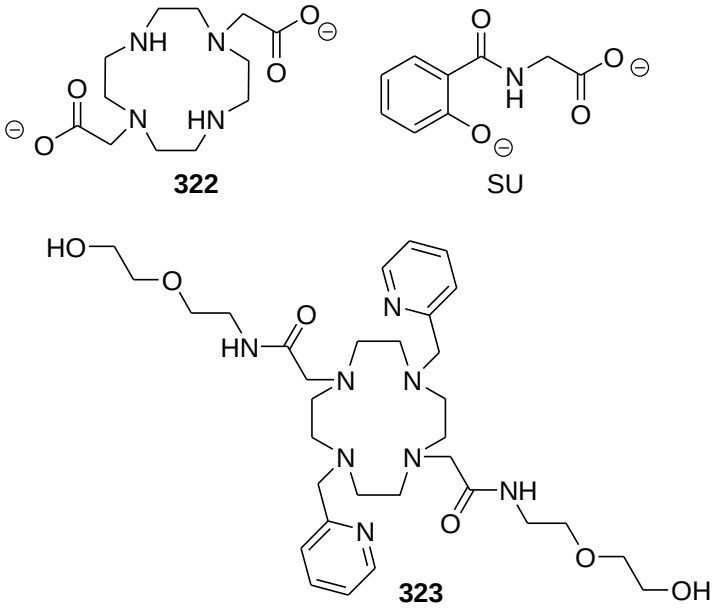

Fig. 154 Chemical structures of receptors **322** and **323**.

The following examples used complexes of lanthanide ions to design anion-sensing probes. In this file, two basic mechanisms have been reported: (i) perturbation, upon anion binding, of the rate of the energy transfer from the antenna to the lanthanide centre; (ii) displacement of water molecules from the coordination sphere of the lanthanide centre by anions. Both cases resulted in changes in the lanthanide complex's emission intensity.[201]

Esplin and co-workers reported the preparation of a probe for salicyluric acid (SU) detection in urine samples based on the complexation of SU with the **322-Tb^{3+}** complex (see Fig. 154).[202] SU

is the principal metabolite of salicylic acid (SA) and its detection in urine offers a variety of applications. Receptor **322** presented high affinity to Tb^{3+} which reduced the vibrational quenching of Tb^{3+} luminescence by excluding the solvent molecules from the lanthanide coordination sphere. Addition of SU to aqueous solutions of **322-Tb^{3+}** (TAPS, buffered at pH 8.4) led to the formation of the highly luminescent ternary complex **322-Tb^{3+}**-SU. In particular, excitation at 316 nm induced the appearance of a broad emission band at 419 nm (the SU chromophore acted as sensitiser of Tb^{3+} through an intramolecular proton transfer from the hydroxyl moiety to the nearby carbonyl group on SU) and the typical sharp emission bands centred at 488, 545, 585 and 651 nm ($^5D_4 \rightarrow {}^7F_n$ transitions of the Tb^{3+} centre). The **322-Tb^{3+}** complex was applied to SU detection in urine samples with fine results and with a limit of detection as low as 9.4 μM.

An Eu^{3+} complex of the cylen-based ligand **323** (Fig. 154) was used for the luminescent sensing of anion F^-.[203] Water solutions of the complex **323-Eu^{3+}**-H_2O, buffered at pH 7.0, showed an intense absorption band at 263 nm (ascribable to a $\pi \rightarrow \pi^*$ transition in the pyridyl rings). Upon excitation at 263 nm, the typical sharp emissions of the Eu^{3+} metal centre at 574, 589, 612, 647 and 692 nm appeared. Addition of anions F^-, Cl^- and Br^- to aqueous solutions of the **323-Eu^{3+}**-H_2O complex induced negligible changes in the UV-Vis bands, whereas the addition of only F^- induced a significant enhancement in the luminescence emissions. This behaviour was ascribed to the substitution of the coordinated H_2O molecule for the more polarisable F^- anion. The observed selectivity could be attributed to the hard nature of the F^- ligand, which resulted in stronger interactions with hard cations such as Eu^{3+}. However, anion size could also play an important role in the observed selectivity. The authors demonstrated that F^- could displace the apical H_2O molecule in the complex with no major perturbation to the coordination sphere, as evidenced by DFT calculations.

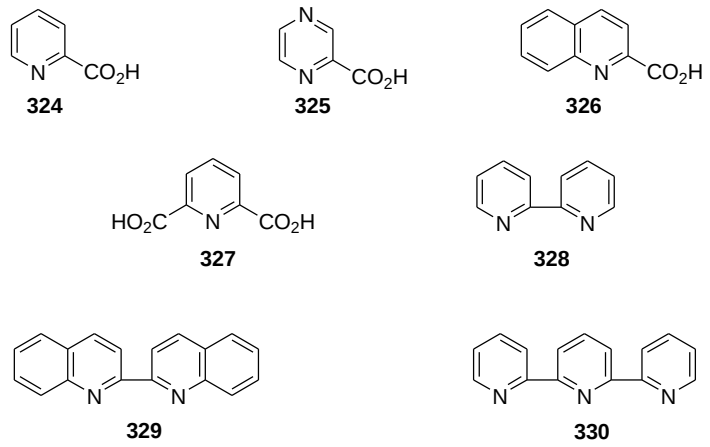

Fig. 155 Chemical structures of receptors **324**-**330**.

S. Shinoda and co-workers prepared receptors **324**-**330** (see Fig. 155) and their corresponding lanthanide complexes (Eu^{3+}, Tb^{3+}, Nd^{3+} and Yb^{3+}) to perform a combinatorial study in order to discriminate among seven different amino acids (Ala, Val, Phe, Gln, Glu, Asp and Lys).[204] For this purpose, the authors monitored the different luminescence changes induced by the interaction between one amino acid and the 28 possible different complexes in CH_3CN:H_2O 99:1 v/v mixtures. As a general trend, addition of amino acids to solutions of the complexes induced different enhancements in the luminescence bands. Among the 196 combinations

tested, **324-Yb^{3+}** gave a selective response with zwitterionic amino acids, whereas **324-Tb^{3+}** responded selectively to Glu.

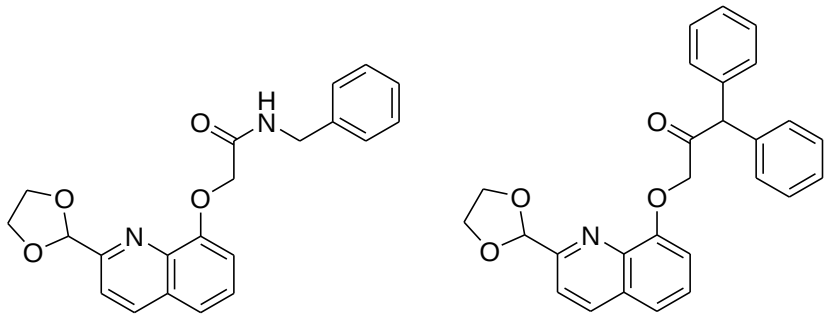

331 **332**

Fig. 156 Chemical structures of receptors **331** and **332**.

Wang and co-workers reported the synthesis of two Eu^{3+} metallic complexes (i.e., **331-Eu^{3+}** and **332-Eu^{3+}**; see Fig. 156) as selective probes for anions NO_3^- and Cl^-.[205] CH_3CN solutions of both complexes presented absorption bands at 317 nm for **331-Eu^{3+}** and at 320 nm for **332-Eu^{3+}**. Upon the excitation at these wavelengths, both complexes displayed the characteristic sensitised luminescence bands at 592 and 617 nm. The luminescence of both complexes in the presence of selected anions (i.e., F^-, Cl^-, Br^-, I^-, ClO_4^-, NO_3^-, AcO^-, HSO_4^- and $H_2PO_4^-$) was tested. Remarkable intensity enhancements were observed, but only upon the addition of Cl^- and NO_3^- which were ascribed to the formation of ternary complexes in which the anions coordinated with the metal centre thus preventing the quenching by the surrounding solvent molecules.

3.1.4.- Miscellaneous

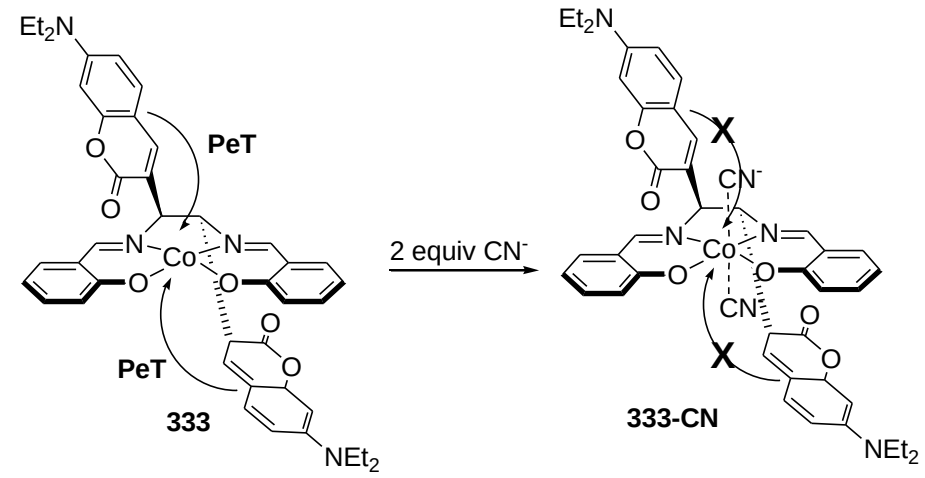

Fig. 157 Proposed binding mechanism of receptors **333** with the CN^- anion.

Co^{2+} salen-based fluorescent sensor **333** (see Fig. 157), bearing coumarine derivatives on 1,2-positions of the ethylenediamine moiety of the salen ligand, was used for the fluorogenic recognition of anion CN^-.[206] CH_3CN solutions of complex **333** were weakly emissive, with a band at 460 nm, due to a PET from the coumarin to the Co^{2+} cation. Upon the ddition of increasing quantities of anion CN^-, the emission band was enhanced. This emission enhancement was

ascribed to a blocking of the PET process upon CN^- binding with the metal centre. Addition of HSO_4^-, N_3^-, F^-, Br^- and $H_2PO_4^-$ induced negligible changes.

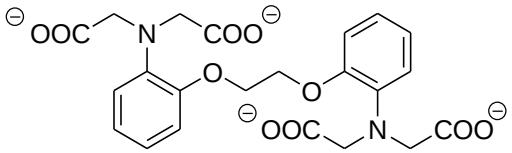

334

Fig. 158 Chemical structure of receptor **334**.

Receptor 1,2-bis(*o*-aminophenoxy)-ethane-*N*,*N*,*N'*,*N'*-tetraacetic acid (**334**) was used in a fluorimetric assay for the selective detection of F^- in H_2O (see Fig. 158).[207] **334** was highly fluorescent in water at pH 7.0 (emission at 370 nm upon excitation at 316 nm). The emission was selectively quenched upon the addition of the Ca^{2+} cation, which led to the formation of the $[Ca(\mathbf{334})]^{2-}$ complex. This sensing ability of **334,** together with the fact that F^- induced the precipitation of Ca^{2+} in the form of CaF_2, was used to develop a fluorescent assay for the recognition of F^-. In particular, the authors precipitated the F^- present in H_2O in the form of CaF_2 upon the addition of the Ca^{2+} cation in excess. Then, Ca^{2+} in excess was detected with receptor **334**. The emission response of **334** directly related with the Ca^{2+} concentration which, in turn, depends on the amount of F^- in the initial solution. By this method, the limit of detection of F^- was 0.30 mM. The system was unresponsive to Cl^-, Br^-, I^-, CN^-, N_3^-, SCN^-, AcO^-, NO_2^-, NO_3^-, ClO_4^-, HCO_3^- and SO_4^{2-}. However, addition of PO_4^{3-} and $P_2O_7^{4-}$ also induced the precipitation of Ca^{2+} and an intense response.

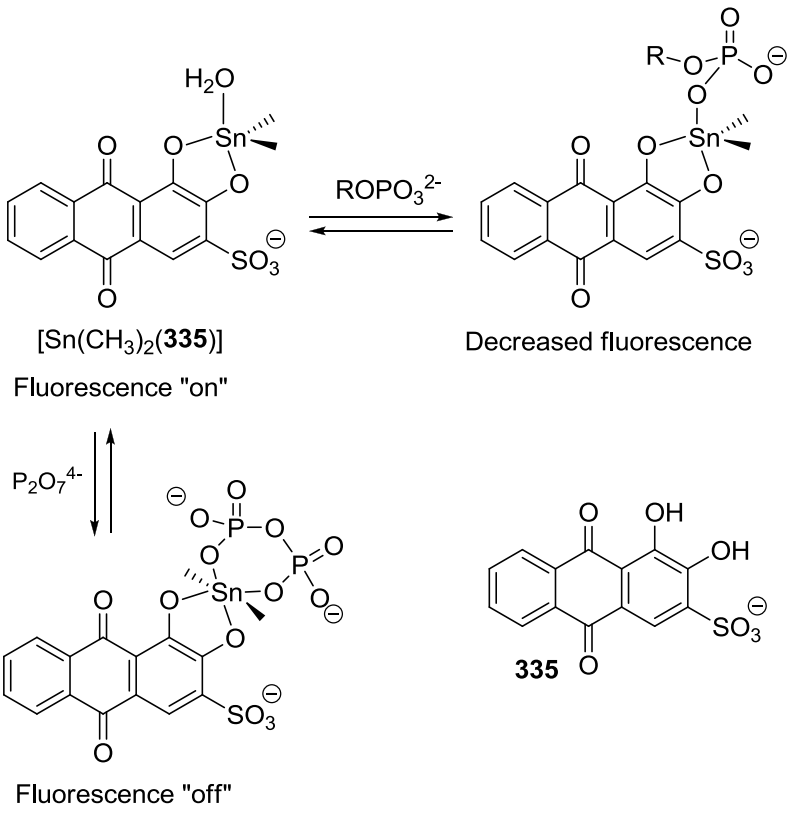

Fig. 159 Signalling mechanism of $P_2O_7^{4-}$ using complex **335**.

Alizarin red (**335**) was used to prepare the metal complex **335**-$Sn(CH_3)_2$, which was used for the selective fluorimetric recognition of $P_2O_7^{4-}$ (see Fig. 159).[208] Aqueous solutions (phosphate buffer at pH 6.7) of **335** showed very weak fluorescence upon excitation at 490 nm. Addition of $(CH_3)_2SnCl_2$ to **335** yielded the highly fluorescent **335**-$Sn(CH_3)_2$ complex (emission band centred at 610 nm upon excitation at 490 nm). Changes in the emission intensity of **335**-$Sn(CH_3)_2$ complex were studied in the presence of selected anions (i.e., AcO^-, F^-, Cl^-, $(CH_3)OPO_4^{2-}$, AMP, glucose-6-phosphate, ADP, ATP and $P_2O_7^{4-}$). Addition of AcO^-, F^- and Cl^- induced negligible modifications in emission intensity, whereas $(CH_3)OPO_4^{2-}$, AMP and glucose-6-phosphate induced reduced emission of ca. 10%. Addition of ADP and ATP induced a moderate 20% and 30% quenching of the emission intensity, respectively. The most selective response was obtained with $P_2O_7^{4-}$, which induced a 90% quenching of the emission intensity. The moderate decreases in the emission intensity observed in the presence of AMP, ADP and ATP were related to the formation of ternary complexes upon the displacement of the H_2O molecule coordinated with the metal centre, whereas the addition of $P_2O_7^{4-}$ induced the formation of a non-emissive hexacoordinated complex.

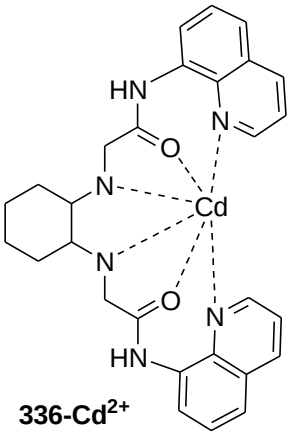

336-Cd^{2+}

Fig. 160 Chemical structures of probe **336-Cd^{2+}**.

The fluorescence probe **336-Cd^{2+}** (see Fig. 160) was used for the detection of polyphosphate anions.[209] Upon the addition of increasing amounts of ATP to solutions of **336-Cd^{2+}** in CH_3OH:H_2O 8:2 v/v, (HEPES at pH 7.4), a ratiometric fluorescence response with emission quenching at 497 nm (λ_{ex} = 316 nm) and the growth of a new band at 397 nm were observed. A Job's plot confirmed the formation of 1:1 complexes. Solutions of the analogous Zn^{2+} complex showed a similar fluorescence spectrum to **336-Cd^{2+}**, but no changes were observed when ATP was added. When the proportion of water increased in the **336-Cd^{2+}** solution, the fluorescence intensity change ratio lowered in the presence of ATP, but the ratiometric change was still discernible, even when CH_3OH:H_2O was adjusted to a ratio of 2:8 v/v. When other anions were tested (i.e., ADP, AMP, $P_2O_7^{4-}$, F^-, Cl^-, Br^-, I^-, HPO_4^{2-},$H_2PO_4^-$, HSO_4^-, NO_3^-, AcO^-), only $P_2O_7^{4-}$ caused a significant change in the emission of the **336-Cd^{2+}** complex, very similarly to that observed for ATP. Moreover, excesses of oxalate or citrate also induced a substantial change in the fluorescence of **336-Cd^{2+}**.

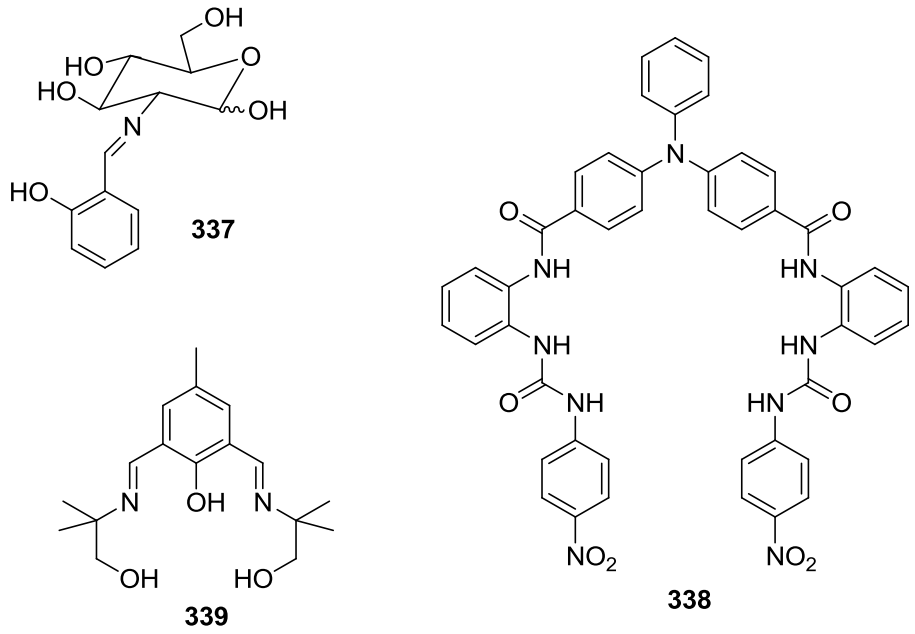

Fig. 161 Chemical structures of receptors **337-339**.

1-(D-Glucopyranosyl-2'-deoxy-2'-iminomethyl)-2-hydroxybenzene (**337**, see Fig. 161) was used as a fluorogenic sensor for aromatic amino acids.[210] The authors found that the emission of aqueous solutions of receptor **337** was highly enhanced (between 5- and 10-fold) upon the addition of Phe, Trp, His and Tyr. None of the other non-aromatic amino acids induced changes in the emission profile of receptor **337**. Aromatic amino acids and receptor **337** formed 1:1 complexes, in which both components interacting through hydrogen-bonding and π-π staking forces.

Receptor **338**, containing a binding cavity with two amide and two urea moieties, was used for the selective recognition of dicarboxylates (Fig. 161).[211] CH_3CN:DMSO 99.6:0.4 v/v solutions of **338** showed an intense emission at 438 nm (excitation at 350 nm) arising from the triphenylamine fluorophore. With the gradual addition of dicarboxylates (i.e., malonate, succinate, glutarate, adipate, pimelate and suberate), the emission intensity was quenched until 1 equiv. was reached (ascribed to an activation of a PET process upon binding). Moreover, upon the addition of more equivs. of dicarboxylates, the emission intensity increased gradually (attributed to subtle changes in receptor conformation). These emission changes were more pronounced upon the addition of glutarate, adipate, pimelate and suberate. A chromogenic response (change in colour from light yellow to red) was observed, but only when malonate was added due to a deprotonation of receptor **338**.

Receptor **339** (see also Fig. 161) formed a dinuclear Cu^{2+} complex, which was utilised for the selective recognition of the azide anion.[212] In particular, aqueous solutions of the dinuclear Cu^{2+} complex presented a weak emission band at 503 nm upon excitation at 440 nm. Addition of Cl^-, Br^-, I^-, F^-, SO_4^{2-}, NO_3^-, HCO_3^- and AcO^- induced negligible changes in the emission profile, whereas minimal quenching was noted in the presence of NCO^-, SCN^-, CN^- and $H_2PO_4^-$. The most remarkable result was a 6-fold enhancement in emission intensity, together with a slight

red shift of 25 nm upon the addition of the N_3^- anion. Emission enhancement was ascribed to a rigidification process, induced by the formation of a 1:4 Cu_2(**339**):N_3^- adduct, which diminished the non-radiative decay of the excited state. This is one of the few fluorogenic sensors described for the toxic and potentially deadly N_3^- anion.

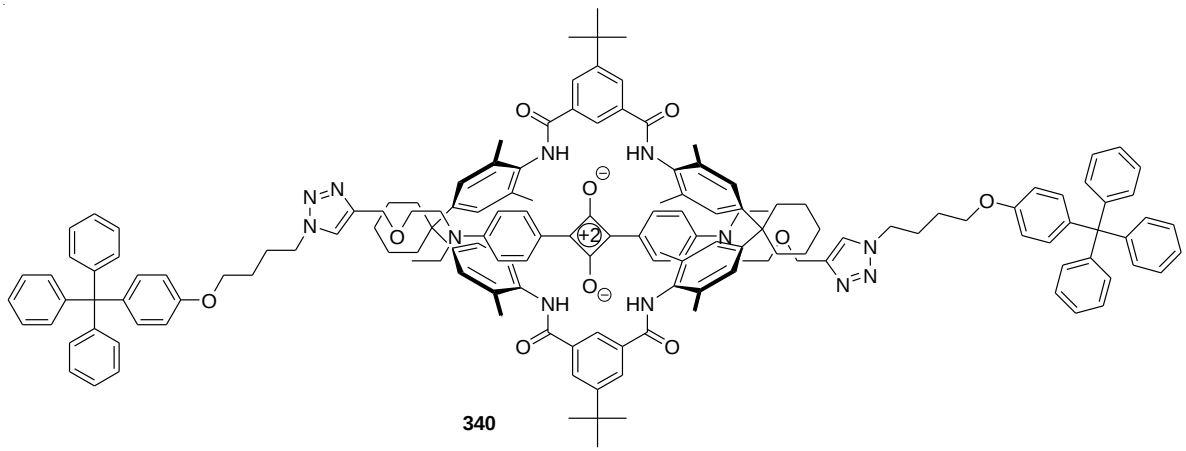

340

Fig. 162 Chemical structure of receptor **340**.

Squaraine-rotaxane **340** (Fig. 162) was used as a fluoro-chromogenic probe for the Cl^- anion.[213] THF solutions of **340** showed a weak squaraine emission at 655 nm due to a quenching process induced by the tetraamide macrocycle that encircled the fluorophore. Addition of the Cl^- anion induced a 3-fold enhancement in emission intensity due to the preferential coordination of the anion with the tetraamide macrocycle, which led to the traslocation of the rotaxane with the subsequent partial inhibition of the quenching observed in the receptor alone. Addition of AcO^-, $H_2PO_4^-$ and I^- induced negligible changes in the emission profile of **340**. Receptor **340** was used to prepare dipsticks by adsorbing it into C18-coated reverse phase silica gel TLC plates. These dipsticks were used for sensing Cl^- in water with fine results.

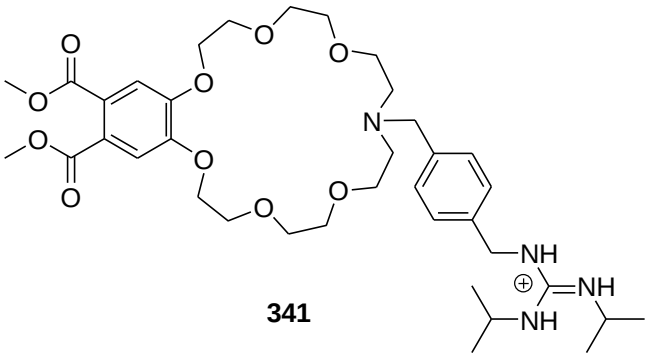

341

Fig. 163 Chemical structure of receptor **341**.

Späth and König prepared a family of ditopic crown ethers containing guanidinium ions for the molecular recognition of amino acids and small peptides through fluorescence changes.[214] The best results in selectivity terms were obtained with receptor **341** (see Fig. 163) and γ-aminobutiric acid (GABA). In particular, CH_3OH:H_2O 9:1 v/v solutions of **341** showed a broad emission band at 390 nm when excited at 300 nm. Addition of increasing quantities of GABA

induced an emission enhancement due to the formation of 1:1 complexes in which the ammonium group of GABA coordinated with the crown ether fragment of the receptor, whereas the carboxylate interacted with the guanidinium moiety.

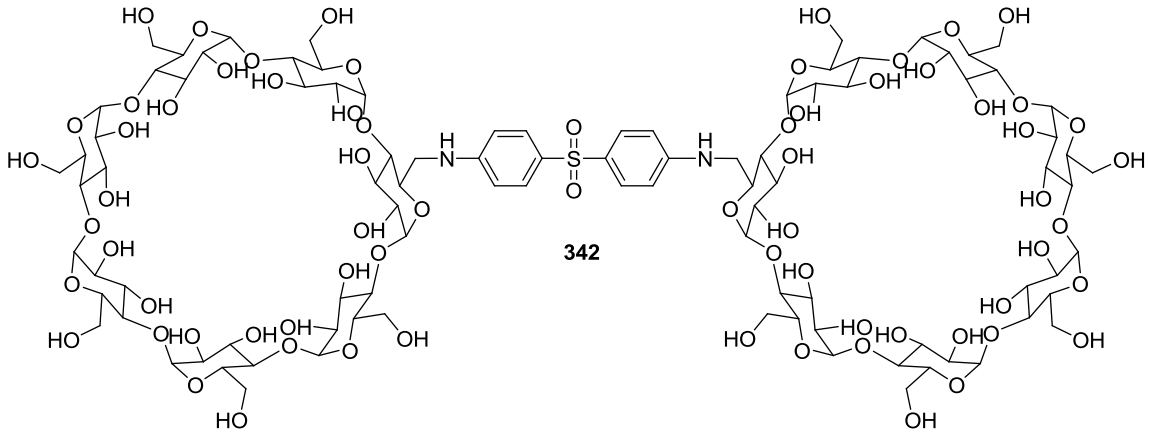

342

Fig. 164 Chemical structure of receptor **342**.

4,4'-sulphonyldianiline-bridged bis(β-cyclodextrin) **342** (Fig. 164) was prepared and used as a fluorescent probe for bile salts.[215] Aqueous solutions of receptor **342** (phosphate buffer pH 7.2) showed an intense emission band at 450 nm upon excitation at 310 nm. Addition of cholate, deoxycholate, glycocholate and taurocholate induced a moderate enhancement of the emission, which was ascribed to the formation of 1:1 inclusion complexes between **342** and the correspondent bile salt.

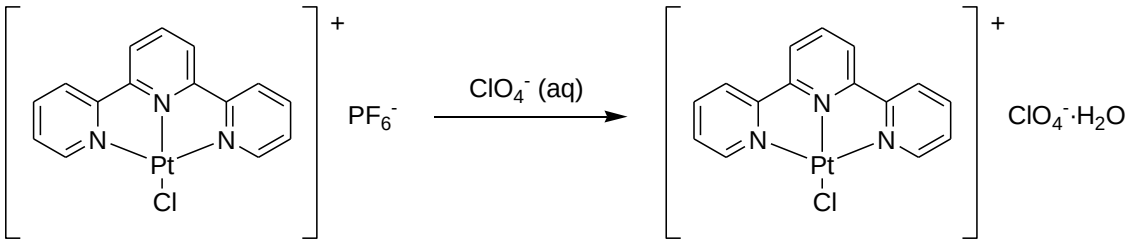

343

Fig. 165 Reaction of receptor **343** with the ClO_4^- anion.

Pt^{2+}salt **343** was used for the selective colorimetric detection and sequestration from aqueous solutions of ClO_4^- via solid-state anion exchange procedures (see Fig. 165).[216] When exposing powder samples of the solid to aqueous solutions of PO_4^{3-}, SO_4^{2-}, HCO_3^-, NO_3^-, I^-, Br^-, Cl^-, F^- and ClO_4^-, **343** underwent a colour change from yellow to red, but only in the presence of ClO_4^-. The same behaviour was seen when compound **343** was casted into HYPAN80 polymer films. In particular, polymer films showed an intense tpy-centred π-π* transition near 340 nm, while the immersion on aqueous solutions of ClO_4^- resulted in the appearance of a new absorption band at 525 nm, attributed to a metal-metal-to-ligand charge-transfer [dσ*(Pt)→π*(tpy)]. After immersing the red ClO_4^- exposed film into 0.5 M NH_4PF_6 for 1 day, the original yellow colour was restored. Salt **343** was also fluorescent and emission changes upon addition of

anions were studied. In line with this, **343** was supported on Vycor porous glass to the tip of an optical fibre and emission spectra recorded while immersed in solutions of common aqueous contaminants (λ_{ex} = 532 nm). Only the addition of ClO_4^- resulted in a strong emission signal at 670 nm with no significant interference from other anions.

3.2.- Displacement assay approach

This approach has also been widely used to develop probes for the fluorogenic detection of anions. Two main approaches are followed: (i) the formation of an ensemble between a certain metal complex and a fluorophore, which is displaced upon the coordination with target anions; (ii) anion-induced displacements of coordinated metals.

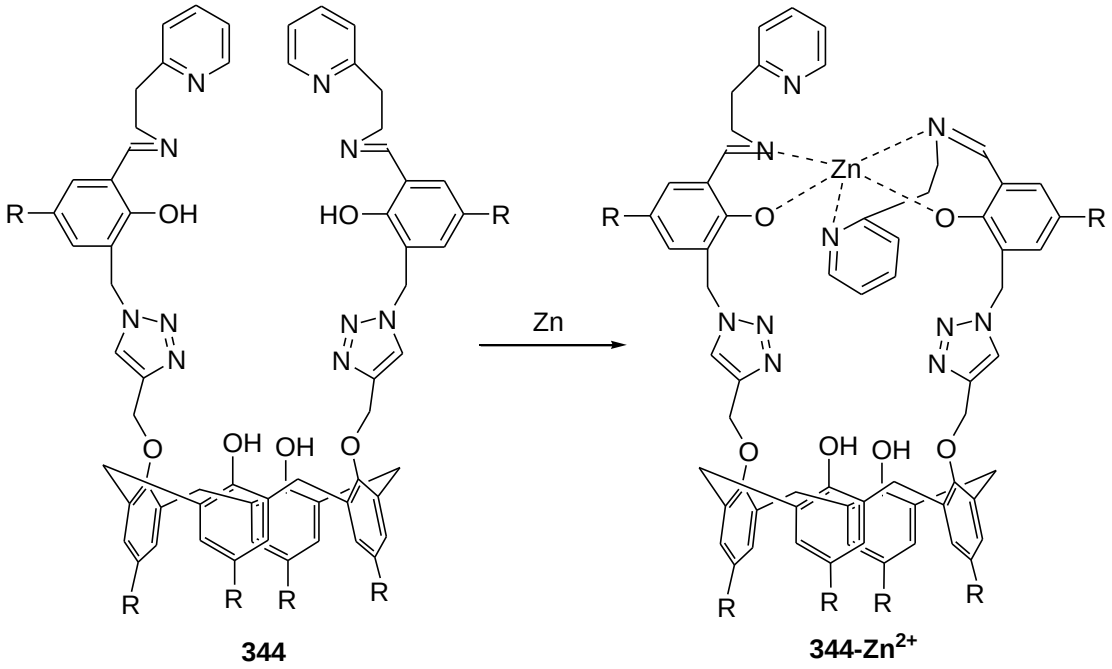

Fig. 166 Binding mode of receptor **344** with Zn^{2+}.

Selective recognition of Cys as free amino acidd and in proteins was achieved using triazole-based calix[4]arene conjugate **344-Zn^{2+}** (Fig. 166).[217] Solution of the **344-Zn^{2+}** complex in H_2O:CH_3OH 1:2 v/v (HEPES at pH 7.4) showed an emission at 454 nm upon excitation at 390. Upon the titration of **344-Zn^{2+}** with Cys, a gradual decrease in fluorescence was observed, together with a decrease in the absorption band at 378 nm and the development of two new absorptions at 325 and 425 nm. These changes were attributed to the displacement of Zn^{2+} from the **344-Zn^{2+}** complex. No significant fluorescence quenching was observed with other biologically relevant molecules containing the SH functionality (i.e., mercaptopropionic acid (MPA), Cyst, Hcy and GSH). No significant absorbance or fluorescence changes upon addition of 19 other naturally-occurring amino acids were observed, except for His. Different control experiments were carried out with imidazole, His-OMe, Fmoc-His, and the tripeptide, Ac-Gly-His-Gly-OMe, and only a slight change in fluorescence was observed upon the addition of His-

OMe. Using the **344-Zn^{2+}** probe, a limit of detection for Cys of 846 ppb was found in blood serum samples.

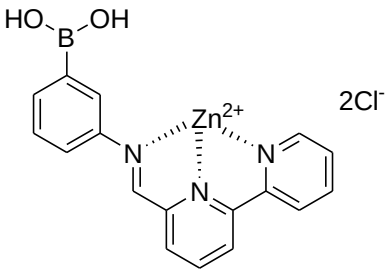

345

Fig. 167 Chemical structure of receptor **345**.

Zhang et al. prepared the metallo-receptor (**345**) which contains two binding sites: i.e. a metal centre and a boronic acid (see Fig. 167).[218] The sensing ensemble was completed by adding the fluorescent dye Alizarin Red S (**ARS**). H_2O solutions of the sensing ensemble, buffered at pH 7.4, presented two emission bands: one centred at 554 nm arising from the interaction between **ARS** and the boronic acid moiety in **345**; and another at 619 nm, produced by the interaction between **ARS** and the metal centre. Partial dye displacement by simple analytes led to different signatures. In particular, the addition of an aqueous solution of a phosphosugar (ribose-5-phosphate), capable of binding the two coordination sites, determined the concomitant decrease of the two fluorescent bands. Otherwise, the addition of a simple sugar, such as fructose or ribose, determined only the decrease in the 554 nm band and a minor increase in the 619 nm band. The authors also found that addition of $P_2O_7^{4-}$ to **345** increased the intensity of both emission bands. In spite of the result obtained upon $P_2O_7^{4-}$ addition, the authors did not report the emission behaviour of the **345-ASR** ensemble in the presence of other inorganic anions.

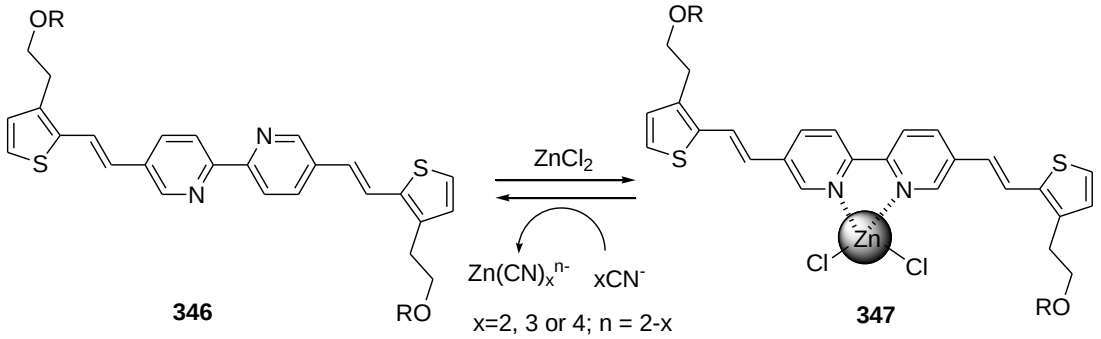

346 **347**

Fig. 168 Binding mode of receptor **346** with Zn^{2+} and CN^--signalling mechanisms.

Divya et al. reported the use of fluorophore **346** and also its fluorescent zinc complex **347** for the detection of endogenous CN^- in natural products (see Fig. 168).[219] Addition of $ZnCl_2$ to a solution of **346** resulted in a colour change from colourless to yellow, along with a shift of the emission maximum from 480 nm to 530 nm due to the formation of zinc complex **347**. Addition of CN^- to **347** in CH_3CN:H_2O 4:1 v/v (HEPES, pH 7.2) resulted in the regeneration of the

original absorption and emission maxima as a result of the decomplexation of Zn^{2+} from **347**, thus regenerating probe **346**. The selectivity of **347** for CN^- was determined by treating the probe with different anions (i.e., I^-, Cl^-, Br^-, F^-, N_3^-, HSO_4^-, $HClO_4^-$ and AcO^-). In all these cases, the green fluorescence of **347** was maintained with no detectable change. Other possible common biological interferents such as phosphates, amino acids and thiols were tested, and but none gave changes in the optical properties of **347**. The authors used probe **347** for the detection of CN^- in the latex of commonly used cassava varieties such s *H226*, *H97*, *MNgal*, *Sreeprabha* and *Sreevishakam*.

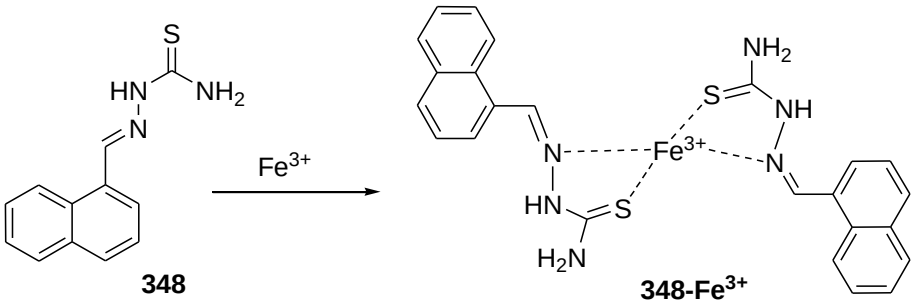

Fig. 169 Binding mode of receptor **348** with Fe^{3+}.

Ssolution of **348** in DMSO-H_2O 3:7 v/v (HEPES, pH 7.2) displayed a significantly increased absorption intensity at 348 nm upon the addition of increasing amounts of Fe^{3+} concomitantly with a quenching of emission band at 400 nm and the formation of a new weak band at around 440 nm. [220] Job´s plot studies confirmed the formation of 2:1 ligand-to-metal complexes (see Fig. 169). With the addition of F^- to **348-Fe^{3+}**, a significant increase of the emission intensity was observed. This response was rationalised as a displacement reaction in which the harder F^- replaced the neutral ligands and captured Fe^{3+} to form $[FeF_x]^{n-}$species. No significant changes in either fluoresce or absorbance were observed when other anions (Cl^-, Br^-, I^-, ClO_4^-, SCN^-, NO_2^-, NO_3^-, AcO^- and N_3^-) were added.

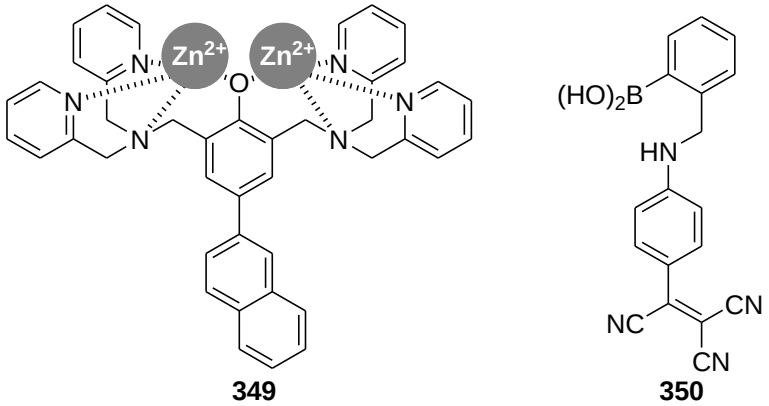

Fig. 170 Chemical structures of receptors **349** and **350**.

Binuclear Zn^{2+} complex **349** and boronic acid **350** (see Fig. 170) were used in a fluorogenic displacement assay for the selective recognition of $P_2O_7^{4-}$ and nucleoside triphosphates (NTPs).[221] Aqueous solutions of complex **349** (CAPS buffer, pH 10.5) presented an intense

emission band at 440 nm (excitation at 317 nm), which was partially quenched upon the addition of increasing quantities of dye **350**. This quenching was ascribed to the formation of a weak emissive **349**-**350** ensemble in which the boronic acid in **350** coordinated with both Zn^{2+} centres in **349**. Addition of $P_2O_7^{4-}$ to the aqueous-sensing ensemble **349**-**350** induced a remarkable 8-fold enhancement of emission intensity due to the formation of **349**-$P_2O_7^{4-}$ and the subsequent release of **350** to the solution. However, addition of NTPs (ATP, CTP, GTP and UTP) led to the complete quenching of the emission of ensemble **349**-**350**. This complete quenching in the presence of NTPs was ascribed to the formation of ternary complexes **349**-**350**-NTP in which the two Zn^{2+} centres coordinated the phosphate moieties of the NTPs and the boronic acid moiety of **350** reacted with the hydroxyl groups of the sugar. Finally, the **349**-**350** sensing ensemble was able to selectively recognise $P_2O_7^{4-}$ in the presence of selected NTPs.

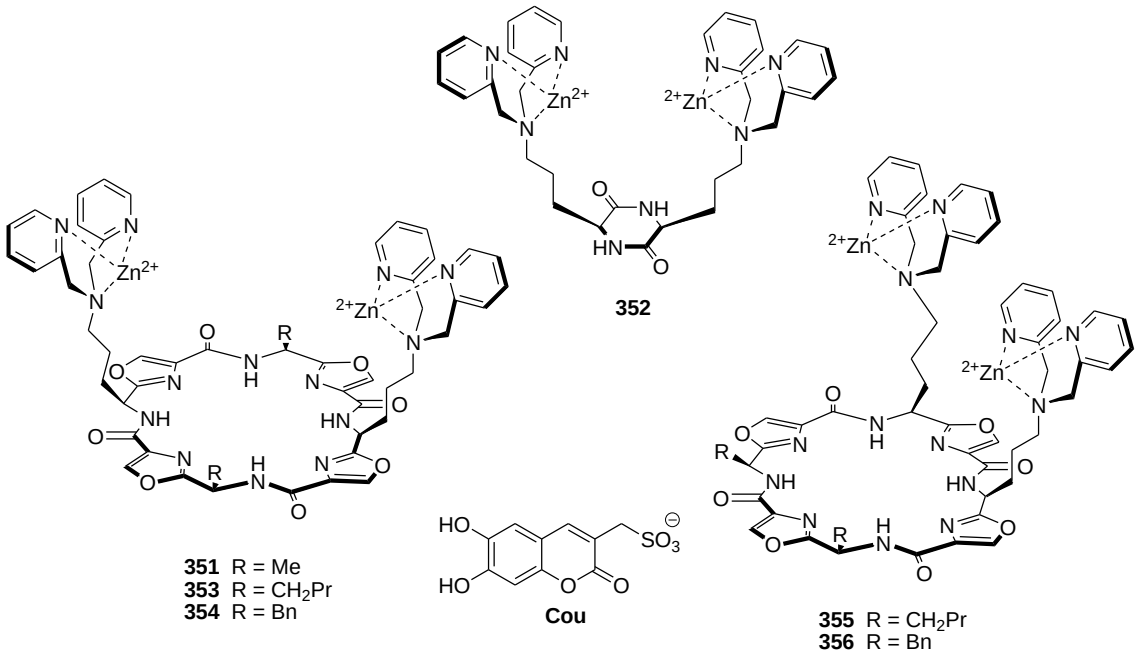

Fig. 171 Chemical structures of the Zn(II) complex **351-356**.

A family of novel backbone modified cyclic peptides, bearing dipicolylamine (DPA) side chains for metal complexation (see Fig. 171) and subsequent anion binding studies, was reported.[222] These Zn(II) complexes formed weakly fluorescent-sensing ensembles (1:1 stoichiometry) with the **Cou** fluorophore. Upon titration of **(351-356)-Cou** ensembles (HEPES buffer at pH 7.4) with $P_2O_7^{4-}$, ATP and ADP, an increase in fluorescence emission was shown (due to a preferential coordination of these anions with receptors **351-356** and the subsequent release of **Cou** to the solution), while no significant changes were observed with the addition of $H_2PO_4^-$, suggesting the selectivity of these receptors for di- and tri-phosphate anions to monophosphate anions with some differences found in the sensing behaviour depending on the used receptor. For instance, while **351-Cou** showed selectivity for $P_2O_7^{4-}$ over ATP and ADP, ensembles **(352-356)-Cou** displayed an increased discrimination between $P_2O_7^{4-}$ and ATP or ADP in accordance with the distance of the binding sites. For example; the phenylalanine-derived ensemble **354-Cou** showed a similar affinity to $P_2O_7^{4-}$, ATP and ADP, whereas **356-Cou**, bearing the same side

chains, but with the two DPAs at proximal distances, bound $P_2O_7^{4-}$ with a greater affinity than either ATP or ADP.

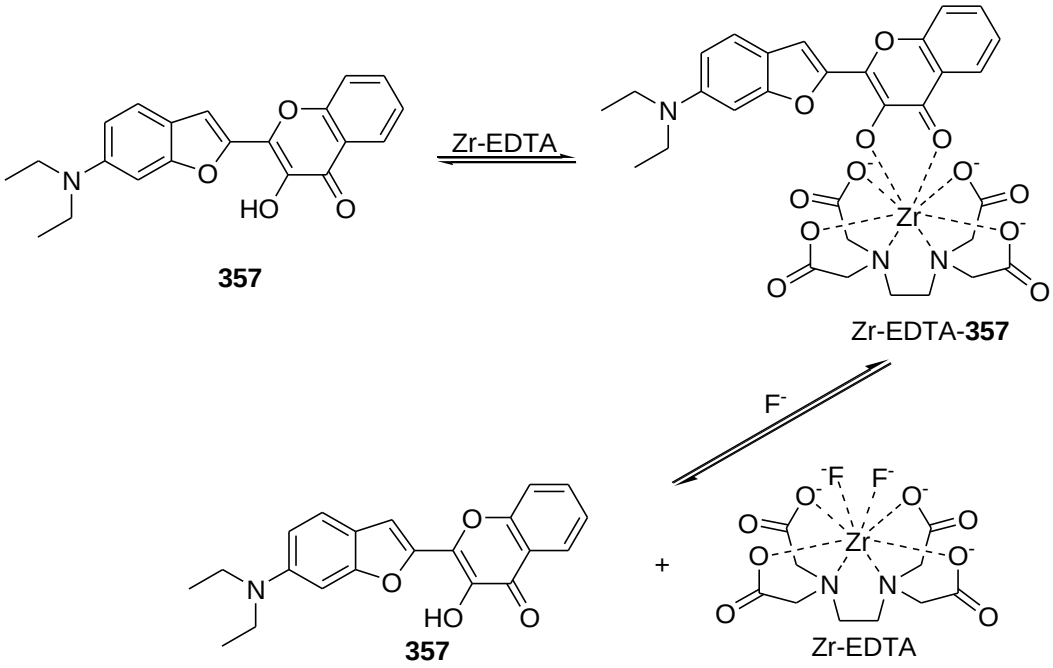

Fig. 172 Proposed signalling mechanism of F^- using receptor **357**.

Wang et al. prepared a new probe for anion F^- based on an excited-state intramolecular proton transfer (ESIPT) phenomenon (see Fig. 172).[223] CH_3OH:H_2O 6:4 v/v solutions of **357**, buffered at pH 7.0, presented an emission band at 570 nm (ESIPT emission) upon excitation at 420 nm. Addition of Zr-EDTA to aqueous solutions of **357** induced a red shift of the emission at 570 nm to 610 nm (with slight loss of intensity), together with the appearance of a new fluorescence at 470 nm. These changes were ascribed to the formation of the Zr-EDTA-**357** ensemble. Addition of F^- to the Zr-EDTA-**357** system induced the quenching of the 470 nm band, together with the regeneration of the emission at 570 nm due to the preferential coordination of this anion with Zr-EDTA and the subsequent release of **357** into the solution. For the practical applications of this sensor, selectivity in the presence of typical competitive anions such as Cl^-, Br^-, I^-, NO_3^-, HSO_4^-, AcO^-, and $H_2PO_4^-$ was evaluated, but none interfered with F^- detection.

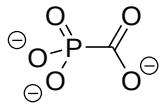

358

Fig. 173 Chemical structure of phosphonoformate anion **358**

Phosphonoformate anion (**358**, see Fig. 173), this being a simple antiviral drug, was selectively detected through a colorimetric and fluorimetric displacement assays with pyrocatechol violet (**PV**) and 6,7-dihydroxy-4-methylcoumarin (**ME**) (see dyes in Fig.30).[224] In particular, Yb^{3+} cation coordinated with the catechol subunit in **PV** to form a 1:1 complex which presented an absorption band at 605 nm in HEPES buffer at pH 7. Addition of **358** to the Yb^{3+}-**PV** complex markedly lowered the absorbance at 605 nm with the concomitant growth of a new band

centred at 444 nm (change in colour from blue to yellow). This new absorption was ascribed to the free **PV,** which was released to the solution due to the formation of Yb^{3+}-**358** complexes. A similar approach was used for the fluorogenic recognition of **358**. In this case, H_2O solutions of **ME,** buffered at pH 7.0, presented an intense emission band at 455 nm (excitation at 375 nm), which was quenched upon the addition of Cu^{2+} cation to form a Cu^{2+}-**ME** complex. Addition of **358** restored the original **ME** emission due to the formation of the Cu^{2+}-**358** complex with the subsequent release of the fluorophore. The sensitivity of the fluorescent displacement assay can be finely tuned by adding aromatic amines (such as 2-(aminomethyl)pyridine and phenanthroline) to form ternary complexes with Cu^{2+} and **ME**.

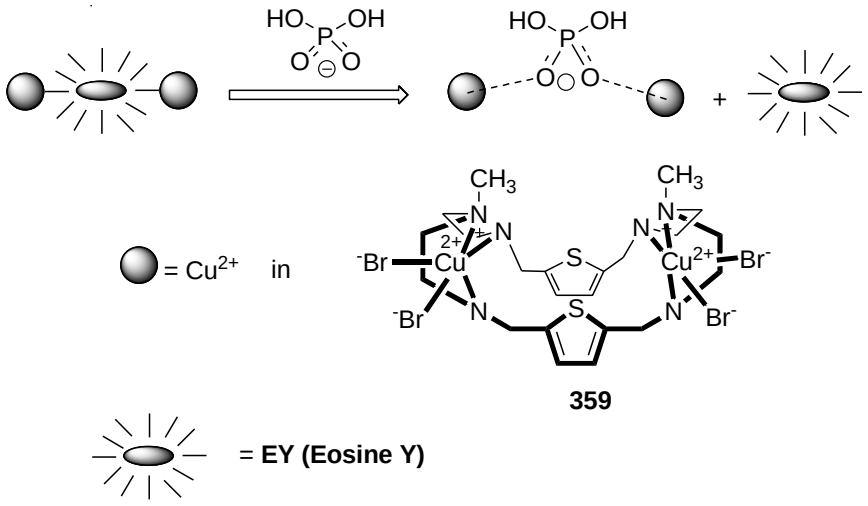

Fig. 174 Squematic representation of a displacement assay using the dinuclear complex **359**.

Saeed et al. designed a displacement assay for anions using the dinuclear ligand **359** (see Fig. 174) and Eosine Y (**EY**) as fluorescent dye (see Fig. 30).[225] By increasing the addition of **359** to a solution of **EY** (HEPES at pH 7.0), the fluorescence intensity of **EY** gradually decreased to finally result in an almost complete quenching due to the formation of the corresponding complex between **359** and the anionic dye. The change in fluorescence intensity gave the best fit for a 1:1 binding model. When adding $H_2PO_4^-$ to **359**-**EY** solutions a fluorescence increase was observed due to the displacement of the dye (**EY**). Under identical conditions, addition of others anions, including F^-, Cl^- , Br^-, I^-, SO_4^{2-}, NO_3^- and ClO_4^-, did not enhance fluorescence.

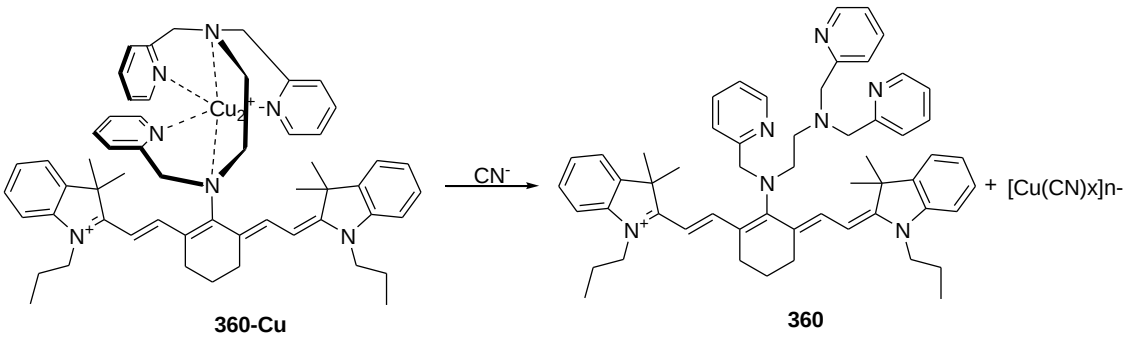

Fig. 175 Reaction of receptor **360-Cu^{2+}** with CN^-

Chen et al. described an NIR fluorescent probe able to selectively sense CN^- in aqueous solution.[226] Ligand **360** (see Fig. 175) comprises an N_5-donor coordination sphere showing strong affinity for Cu^{2+}. In the presence of copper, the fluorescence of **360** was quenched due to the short distance between the fluorophore moiety and the metal binding site. Other metal centres were tested by the authors to determine possible interference. However, negligible effects were observed with cations other than Cu. When CN^- was added to the solution containing the **360-Cu^{2+}** complex, the 748 nm emission band increased due to the removal of the copper ion given the formation of $[Cu(CN)_x]^{n-}$ complexes. The authors used the *nematode C. elegans* (a three-blast microorganism) to test the probe and they demonstrated the possibility to sense CN^- in these microorganisms when infected with Pseudomonas Aeruginosa (responsible for the infection of CN^- in living organisms) and when contamined with exogenous CN^-.

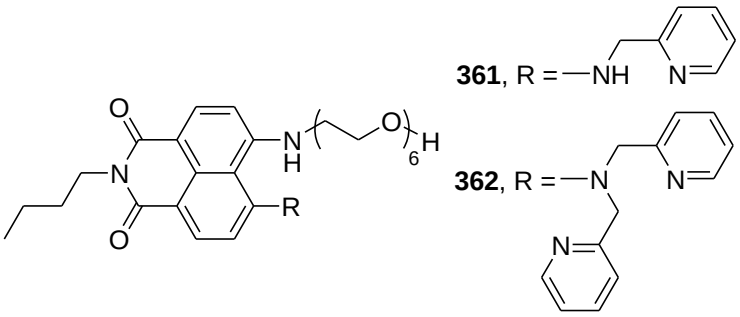

Fig. 176 Chemical structures of probes **361** and **362**.

4,5-disubstituted-1,8-naphthalimide derivatives **361** and **362** were able to fluorimetrically detect CN^- anion by a displacement assay (see Fig. 176).[227] HEPES solutions of **361**, buffered at pH 7.4, showed the typical naphthalimide fluorescence band centered at 534 nm (upon excitation at 458 nm). Addition of Cu^{2+} induced the progressive quenching of the emission at 534 nm with the concomitant growth of a new blue-shifted emission band at 478 nm ascribed to the formation of the **361-Cu^{2+}** complex. Dealing with **362**, HEPES solutions of this receptor showed a broad emission band at 550 nm (excitation at 458 nm) that was completely quenched upon addition of Cu^{2+} cation due to the formation of the **362-Cu^{2+}** complex. Both Cu^{2+} complexes were used for the fluorescent sensing of CN^- because addition of this anion induced the revival of the fluorescence of **361** and **362** due to the formation of $Cu(CN)_2$. Other anions tested (i.e., F^-, Cl^-, Br^-, I^-, NO_3^-, SO_4^{2-} and $H_2PO_4^-$) induced negligible changes in the emission of the **361-Cu^{2+}** and **362-Cu^{2+}** complexes.

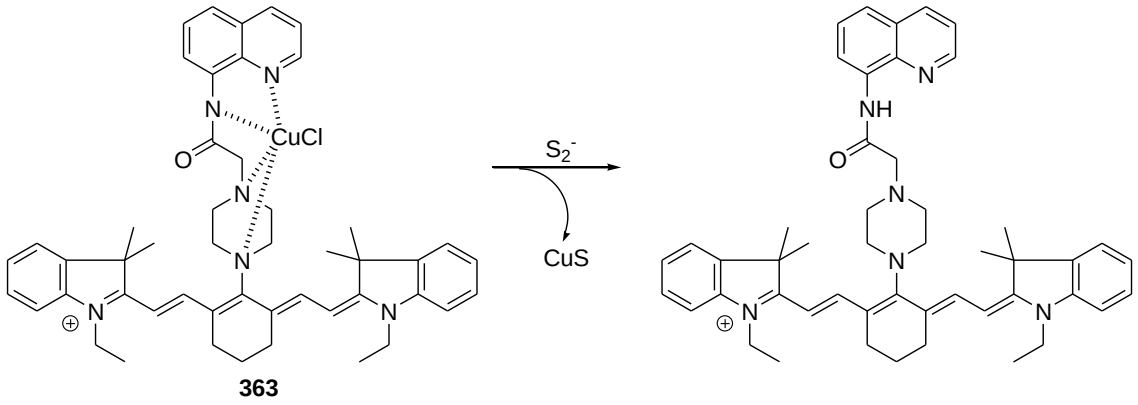

363

Fig. 177 Chemical reaction of complex **363** with the S^{2-} anion.

The Cu^{2+} complex containing a cyanine dye **363** was used as an efficient, selective fluorogenic probe for the S^{2-} anion (see Fig. 177).[228] H_2O:CH_3OH 6:4 v/v (HEPES buffer at pH 7.0) solutions of **363** showed negligible fluorescence upon excitation at 740 nm. Addition of the S^{2-} anion to solutions of **363** led to the appearance of an emission band at 794 nm (27-fold enhancement), whereas the other anions tested (i.e., F^-, Cl^-, Br^-, NO_3^-, NO_2^-, N_3^-, SO_4^{2-}, CO_3^{2-}, PO_4^{3-}, AcO^- and CN^-) induced negligible changes. The emission enhancement observed upon addition of S^{2-} was ascribed to the precipitation of CuS which induced the release of a highly fluorescent cyanine dye.

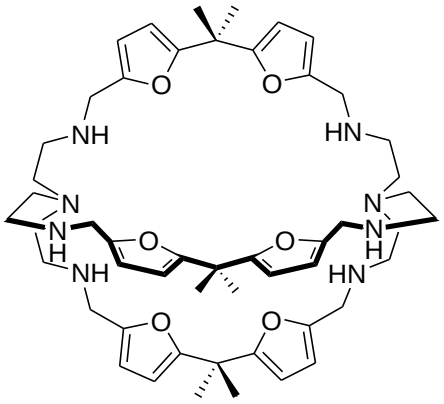

364

Fig. 178 Chemical structure of receptor **364**.

Cryptate **364** (see Fig. 178) formed thedinuclear complex **364-(Cu^{2+})$_2$** which was used in a displacement assay with 6-carboxyfluorescein (**CF**) for the selective detection of GMP.[229] CH_3OH:H_2O 50:50 v/v solutions of **CF** at pH 7.0 showed an intense broad emission at 516 nm when excited at 492 nm. Addition of increasing quantities of the **364-(Cu^{2+})$_2$** complex induced the complete quenching of the **CF** emission due to the consecutive formation of 1:1 (the fluorophore included within the two Cu^{2+} centres inside the cryptate cavity) and 2:1 (the fluorophore binds with the Cu^{2+} atoms of two different cryptates) **364-(Cu^{2+})$_2$-CF** ensembles, in which the emission of the fluorophore was quenched by Cu^{2+} cations. Adding increasing quantities of GMP to the ensemble induced the progressive appearance of the **CF** emission due to the displacement of the fluorophore into the solution as a result of the formation of **364-**

$(Cu^{2+})_2$-GMP complexes. The fluorescence response was selective for GMP and other nucleotides (i.e., TMP, UMP, CMP and AMP) induced negligible emission enhancements. This selective response was ascribed to the fact that GMP matches the distance between the two Cu^{2+} ions inside the cryptate.

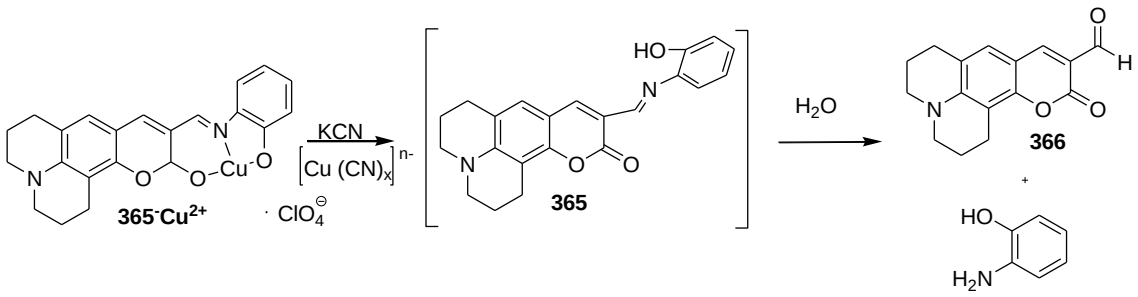

Fig. 179 Squematic representation of the recognition of CN^- with **365-Cu^{2+}**.

Chromogenic sensing ensemble **365-Cu^{2+}** was able to recognise CN^- from other anionic species, showing a marked fluorescence enhancement in aqueous environments.[230-231] Addition of CN^- induced demetalation from the non-fluorescent **365-Cu^{2+}** due to the formation of stable $[Cu(CN)_x]^{n-}$ complexes. Released compound **365** was additionally hydrolysed to give a strongly emissive coumarinaldehyde **366**, providing "turn-on" fluorogenic sensing (see Fig. 179). In particular, addition of the CN^- anion to **365-Cu^{2+}** induced a 57-nm hypsochromic shift of the absorption maximum from 521 to 464 nm, as well as a colour change from orange-red to green. Besides, the fluorescence intensity at 514 nm was concomitantly enhanced. The emission of **365-Cu^{2+}** in H_2O:DMSO 1:99 v/v solution (PBS buffer, pH 7.4) in the presence of various anions commonly found in biological media (F^-, Cl^-, Br^-, I^-, AcO^-, H_2PO4^-, HSO_4^{2-}, NO_3^-, ClO_4^-, HCO_3^-, SCN^-, OH^-, CO_3^{2-}, HPO_4^{2-}, PO_4^{3-}, AMP, ADP, and ATP) was studied. Flourescence enchancement was observed only in the presence of CN^-. Competitive assays also confirmed the selective response to CN^-. A limit of detection as low as 1.0×10^{-8} mol L^{-1} in aqueous solutions was determined. Finally, CN^- detection with **365-Cu^{2+}** was also tested in HepG2 cells.

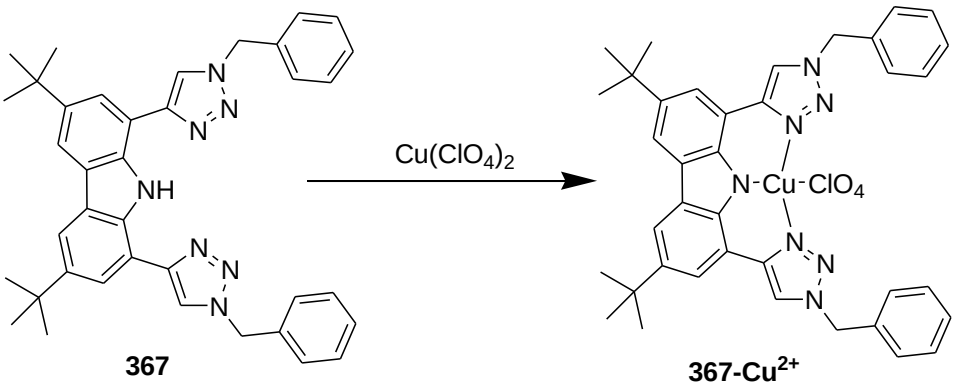

Fig. 180 Chemical structure of **367** and the corresponding Cu(II) complex.

The fluorescent derivative (**367**) containing two triazole groups, which are conjugated with a carbazole moiety, was used for the detection of anion CN^- via fluorescence enhancement by Cu^{2+} complex ligand exchange (see Fig. 180).[232] Solutions of **367** in CH_3CN show two absorption

bands at 300 and 370 nm and an emission band at 385 nm. Upon the addition of Cu^{2+}, bsorption bands shifted to 326 and 405, whereas emission was completely quenched as the result of the formation of the corresponding 1:1 **367-Cu^{2+}** complex. Addition of CN^- to solutions of **367–Cu^{2+}** resulted in the restoration of the absorption and emission profile of **367** due to the demetallation of **367–Cu^{2+}** driven by the formation of very stable $Cu(CN)_2$ or $Cu(CN)_4$ complexes. No significant changes were observed in the presence of the other anions (F^-, Cl^-, Br^-, I^-, ClO_4^-, $H_2PO_4^-$, HSO_4^-, NO_3^-, and AcO^-) evaluated.

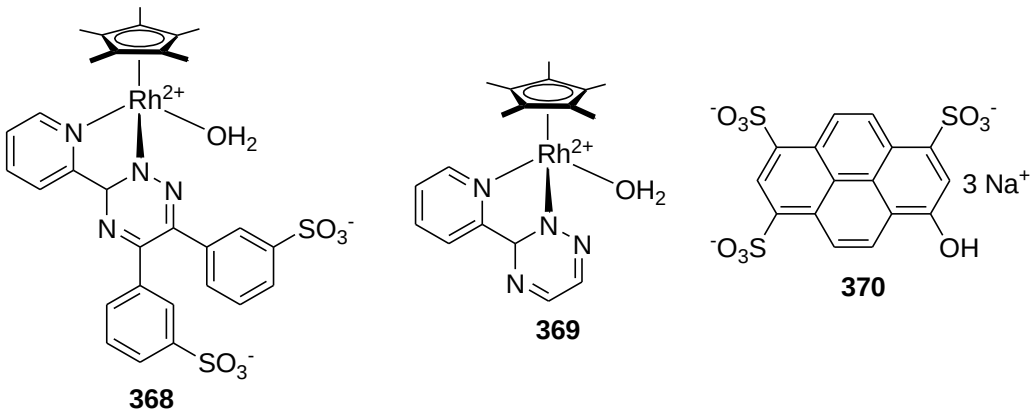

Fig. 181 Chemical structures of compounds **368**-**370**.

The same authors designed and prepared a chemosensing ensemble (see Fig. 181 for the structures of **368**, **369** and **370**) for the fluorimetric detection of Cl^- in buffered H_2O solution (MOPS at pH 7.0).[233] Aqueous solutions of **370** showed an intense emission band at 510 nm upon excitation at 480 nm. Addition of complexes **368** and **369** to this solution induced a signiticant emission quenching (to 25% and 10% of the initial intensity for **368** and **369,** respectively). This quenching was ascribed to the formation of the **368**-**370** and **369**-**370** sensing ensembles, in which the fluorophore interacted with the complexes through the coordination of their hydroxyl group with the Rh(II) centre through electrostatic forces and π-π dispersive interactions. Both the chemosensing ensembles were employed for the fluorescent recognition of anions. Of all the anions tested (Cl^-, F^-, NO_3^-, AcO^-, $H_2PO_4^-$, $H_3P_2O_7^-$, HCO_3^-, SO_4^{2-} and salicylate), only Cl^- was able to induce a remarkable enhancement in the emission at 510 nm due to the preferential coordination with the Rh(II) centre, which allowed the release of **370**. Addition of the AcO^- anion to the **368**-**370** and **369**-**370** sensing ensembles induced a moderate enhancement of the emission band at 510 due to a partial displacement of **370**. The limit of detection for Cl^-, using the **368**-**370** and **369**-**370** sensing ensembles, was 3.0×10^{-4} and 1.5×10^{-4} mol L^{-1}, respectively.

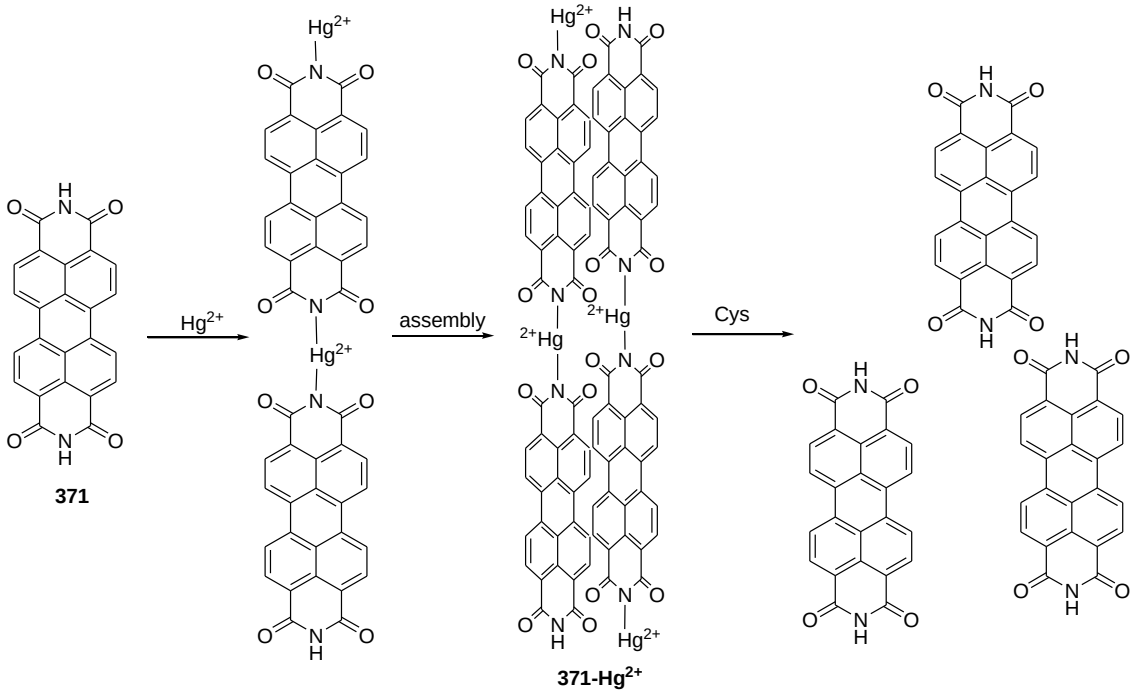

Fig. 182 Schematic representation of Cys detection with **371-Hg^{2+}**.

Ruan and coworkers developed a new method based on specific Hg^{2+}-mediated perylene bisimide (**371**) aggregation for the highly sensitive detection of thiol-containing amino acids (see Fig. 182).[234] This system was based in the non-covalent chemical ensemble **371-Hg^{2+}**. When DMF:H_2O 9:1 v/v solutions of **371** were titrated with increasing Hg^{2+} concentrations, the fluorescence at 532 nm gradually decreased and was almost completely quenched. With increasing Cys concentrations, fluorescence was restored. Given the much stronger Hg–S interaction compared to that of Hg–N, non-fluorescent aggregates **371-Hg^{2+}** dissociated into monomers in the presence of Cys. The **371-Hg^{2+}** ensemble was tested with 19 other natural amino acids, HCys, GSH, DTT, mercapto acetic acid (MMA) and 2-mercaptoethylamine (MEA). As expected,only the thiol-containing amino acids were able to give a fluorescent response.

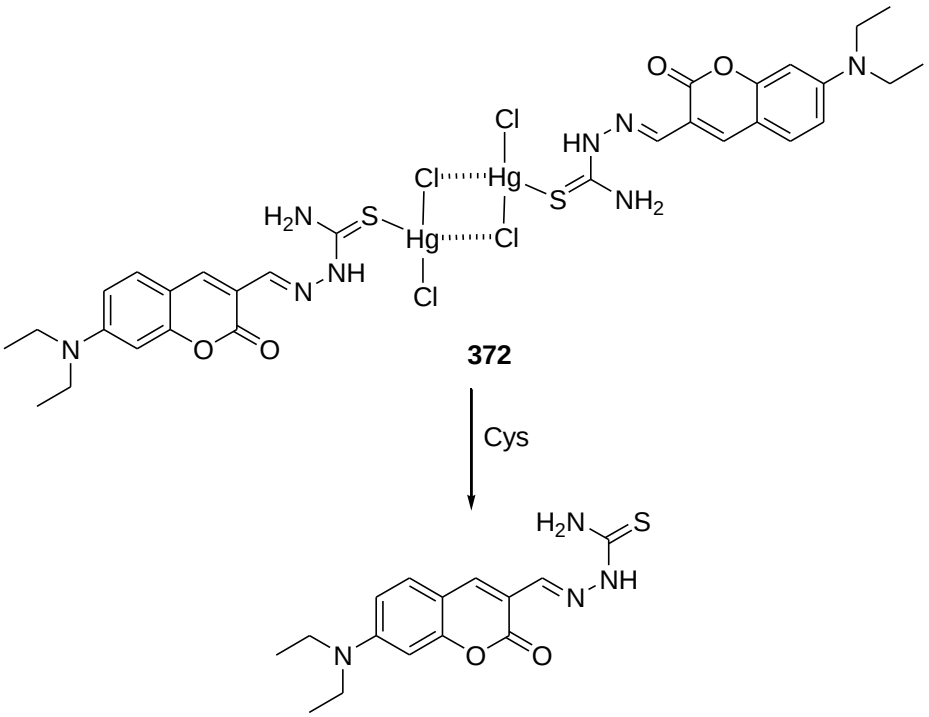

Fig. 183 Schematic representation of Cys detection with **372**.

The next example also involved a displacement assay using Hg^{2+} complexes for the fluorogenic recognition of thiol-containing derivatives. In particular, Wang and co-workers developed complex **372** for the selective fluorogenic sensing of thiol-containing compounds (see Fig. 183).[235] DMSO:H_2O 1:99 v/v solutions of **372** showed a very weak emission band (quantum yield of 0.031) at 520 nm (excitation at 450 nm) due to the heavy atom effect exerted by the Hg^{2+} cation on the coumarin fluorophore. Addition of Cys to solutions of **372** induced a progressive enhancement in the emission band (ca. 30-fold with a final quantum yield of 0.5), which was assigned to a displacement of the Hg^{2+} cation from the complex with the subsequent release of the highly fluorescent coumarin derivative. Practically the same response was obtained in the presence of other SH-containing derivatives, such as Hcy and GSH. Addition of other amino acids (i.e., Gly, Ala, Val, Leu, Ilc, Met, Pro, Tyr, Lys, His, Ser and Trp) induced negligible enhancements in emission intensity.

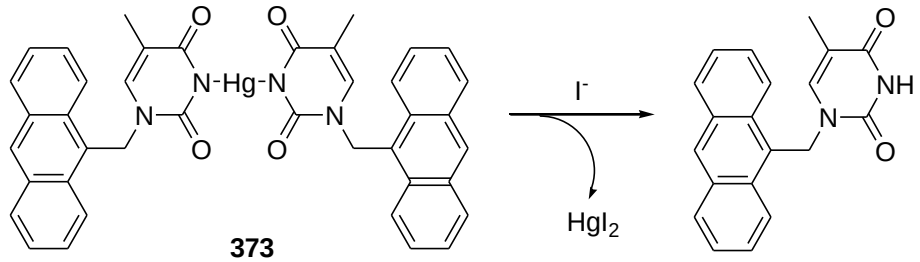

Fig. 184 Chemical reaction of receptor **373** with I^-.

The thymine-Hg^{2+} complex **373** (see Fig. 184) was used for the selective fluorogenic sensing of anion I^-.[236] H_2O-THF 99.5:0.5 v/v solutions of **373,** buffered at pH 7.4, showed a weak emission band centred at 418 nm (excitation at 370 nm) due to the presence of a PET process between

the bonded Hg^{2+} cation and the anthracene fluorophore. Addition of anion I^- to solutions of **373** induced a marked increase (6-fold) of the emission intensity due to the release of thymine-anthracene fluorophore upon the formation of HgI_2. None of the other anions tested (i.e., F^-, Cl^-, Br^-, SO_4^{2-},HCO_3^-, CO_3^{2-}, $H_2PO_4^-$, HPO_4^{2-}, PO_4^{3-}, AcO^- and NO_3^-) induced changes in the emission band. This complex was successfully used for the determination of I^- contents in urine samples.

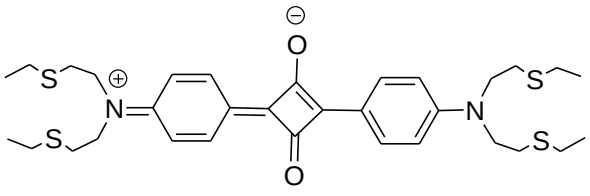

374

Fig. 185 Chemical structure of squaraine **374**.

Squaraine **374** (Fig. 185) underwent absorption and fluorescence bleaching upon Hg^{2+} binding and was used as a turn-off/on system for the colorimetric and fluorescent detection for thiol-containing amino acids.[237] After adding Hg^{2+} to solutions of **374** in CH_3CN:H_2O 2:1 v/v,the absorption band of **374** at 636 nm decreased until complete bleaching. The same occurred with the emission band of **374** centred at 678 nm. This emission quenching was ascribed to the formation of the 1:1 **374-Hg^{2+}** ensemble that disrupts the π-conjugation of **374**. The sensing properties of the **374-Hg^{2+}** complex were tested in the presence of 21 amino acids and short peptides. Only Cys, Hcy, GSH and His induced the appearance of the emission band centred at 678 nm due to a preferential coordination of these species with Hg^{2+} which restored the free **374**.

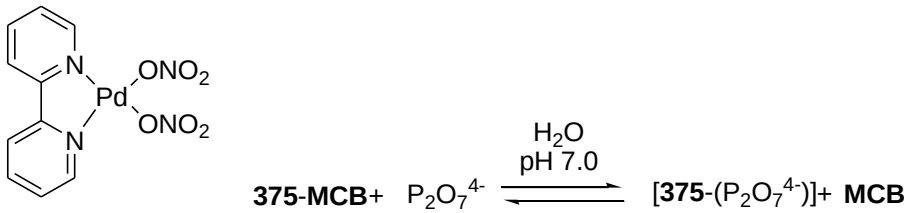

375

Fig. 186 Structure and chemical reaction of receptor **375** with $P_2O_7^{4-}$.

Gao and coworkers discovered the possibility of using the $[Pd(NO_3)_2(bipy)]$ complex (**375**) as a fluorogenic probe for $P_2O_7^{4-}$ (see Fig. 186).[238] Firstly, the authors did a complete study on the interaction of $P_2O_7^{4-}$ with the palladium complex. In aqueous solutions (HEPES at pH 7), $P_2O_7^{4-}$ formed both 1:1 and 2:1 Pd:$P_2O_7^{4-}$ complexes. In the case of the 1:1 complex, $P_2O_7^{4-}$ was suggested to act as a bidentate chelate ligand by replacing the two weakly bound nitrates opposite the bipy N-donor ligand. For the creation of an indicator displacement assay for $P_2O_7^{4-}$, the authors prepared the **375-MCB** sensing ensamble (MCB = Methylcalcein blue). A buffered H_2O solution of **MCB** and **375** showed weak fluorescence when excited at 410 nm. In the presence of $P_2O_7^{4-}$, however, the original strong emission at 440 nm of **MCB** fully recovered. This sensing ensemble displayed very good selectivity for $P_2O_7^{4-}$ over other anions.

This was demonstrated by recording the fluorescence spectra of solutions containing a large excess of F^-, Cl^-, Br^-, $H_2PO_4^-$, ClO_4^-, SO_4^{2-}, AcO^-, HCO_3^-, NO_3^- and salycilate. Only the addition of $H_2PO_4^-$ and ClO_4^- resulted in a minor increase in fluorescence.

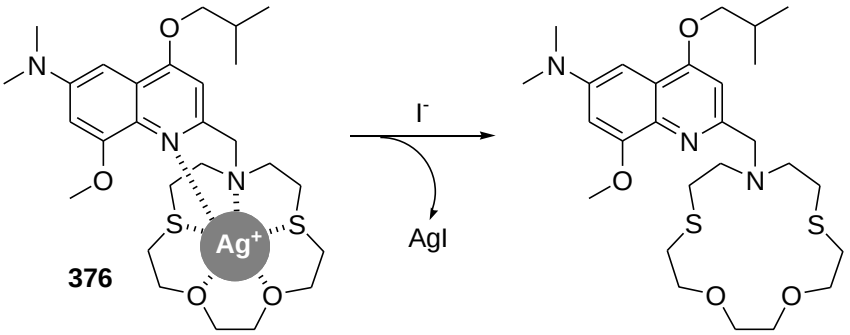

Fig. 187 Schematic representation of a displacement assay using **376** for I^- sensing.

Jiang et al developed a displacement assay for the fluorimetric sensing of anion I^- (see Fig. 187).[239] In particular, water solutions of complex **376** (MES buffer at pH 6.0) showed an intense emission band at 481 nm upon excitation at 405 nm. Addition of anion I^- induced a dramatic quenching of the fluorescence at 481 nm with the simultaneous appearance of a new emission band at 565 nm. These changes were ascribed to the release of the Ag^+ cation from complex **376**, due to the formation of highly insoluble AgI. The new emission at 565 nm was assigned to the quinaldine fluorophore located in the marcocycle. The response to anion I^- was highly sensitive (limit of detection of 0.9 ppm) and selective; that is, F^-, Cl^-, Br^-, HSO_4^-, CO_3^{2-}, $H_2PO_4^-$, AcO^-, SCN^-, CN^- and S^{2-} induced negligible changes in the emission profile of **376**.

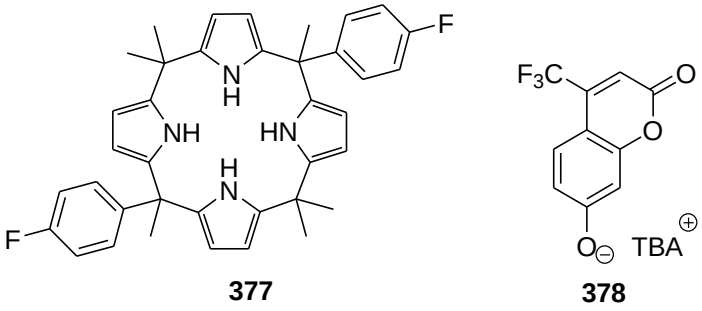

Fig. 188 Chemical structures of **377** and **378**.

CH_3CN solutions of coumarin derivative **378** produced an intense emission band at 500 nm upon excitation at 410 nm.[240] Addition of calix[4]pyrrole **377** induced progressive emission quenching due to the formation of 1:1 complexes between both compounds through hydrogen-bonding interactions (see Fig. 188 for the chemical structures of **377** and **378**). Emission quenching was ascribed to a PET process from the calix[4]pyrrole to the bonded **378**. The sensing ensemble **377**-**378** was used as selective fluorescent probe for the F^- anion. Specifically, addition of F^- to the **377**-**378** complex induced an immediate enhancement of the emission at 500 nm due to the preferential coordination of the anion with **377** and the release of **378** into the solution. The fluorogenic response was highly selective for F^- (limit of detection of 2.3 ppb) and other anions tested (i.e., Cl^-, Br^-, I^-, HSO_4^-, PF_6^-, $H_2PO_4^-$, $HP_2O_7^{3-}$, AcO^-, PhO^-, SCN^-, CN^- and NO_3^-) were unable to induce the displacement of **378** from the sensing ensemble.

Moreover, the complex between **377** and F^- could be disrupted by the addition of the Li^+ cation. This allowed the regeneration of the sensing ensemble **377**-**378** which could be reused in another sensing cycle.

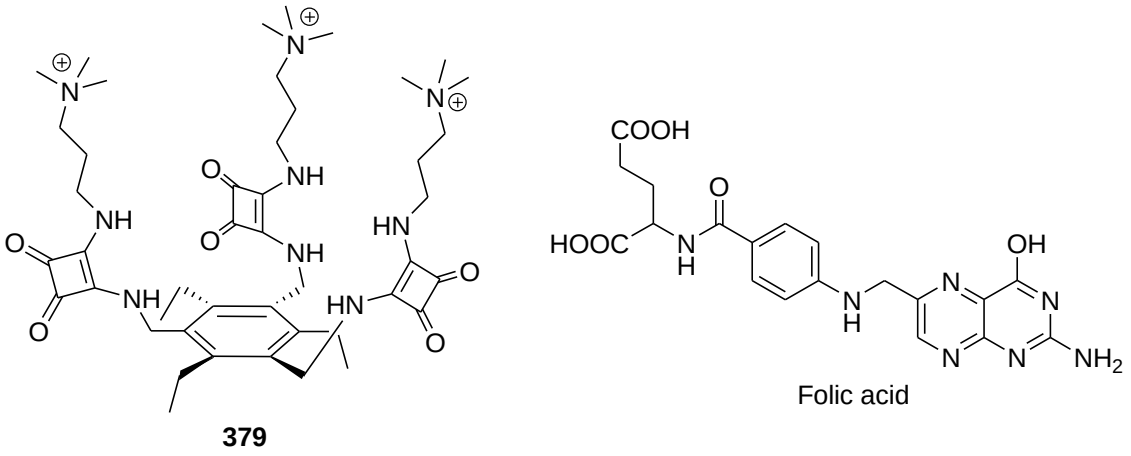

Fig. 189 Chemical structure of receptor **379** and folic acid.

Tripodal squaramido-based receptor **379** (see Fig. 189) was used together with 5-carboxyfluorescein (**5-CF**) for the development of a displacement assay for the recognition of the folate anion.[241] Water solutions of **5-CF** buffered at pH 9.0 showed the typical emission band of the fluorophore at 525 nm upon excitation at 365 nm. Emission was quenched gradually upon the addition of increasing quantities of **379,** leading to the formation of 1:1 complexes. Addition of folate anion to the sensing ensemble induced an increase in the emission intensity at 525 nm due to the formation of complexes between **379** and folate with the subsequent release of **5-CF** to the solution. The sensing ensemble was used for the determination of folic acid in pills with fine results.

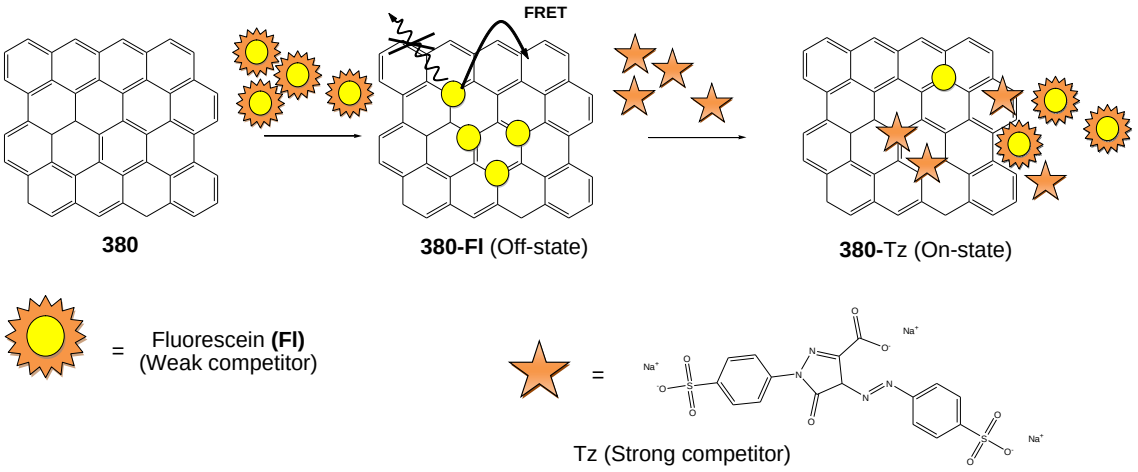

Fig. 190 Representation of the label-free turn-on fluorescent method for the detection of tartrazine with **380**.

A novel and label-free turn-on fluorescent method for the detection of tartrazine (Tz) was developed based on the use of a reduced graphene oxide-fluorescein ensamble (**380-Fl**, see

Fig. 190).[242] Solutions of **Fl** (AcOH-AcONa buffer at pH 5.03) in the presence of **380** showed a remarkable quenching of the fluorescein emission due to an active FRET process between **Fl** and **380**. Upon the addition of increasing amounts of Tz to the **380-Fl** mixture, fluorescence enhancement took place due to the displacement of **Fl**. A similar phenomenon also happened when using 2,7-dichloro-fluoresceine (**DCFl**) and eosin Y (**EY**) as halogenated fluoresceine derivatives. Under optimal conditions, a limit of detection for Tz was estimated to be 0.53 ng mL^{-1}. The fluorescent sensor was tested with common food product-based additives (i.e., NaCl, KI, NaH_2PO_4, $CaCl_2$, $NH_4Fe(SO_4)_2$, fructose, glucose, sucrose, lactose, citric acid, sodium citrate, vitamin C, carboxymethyl cellulose (CMC), and sodium benzoate) and it was fund that only a high concentration of sucrose, sodium benzoate or CMC interfered with Tz detection.

3.3.- Chemodosimeter approach

As also observed for the chromogenic systems, there is an increasing interest in the design of chemodosimeter for the fluorogenic detection of anions. Most examples are related with the detection of F^-, CN^- and thiol-containing amino acids. Other interesting examples for NO_2^-, ClO^- and HS^- have also been reported.

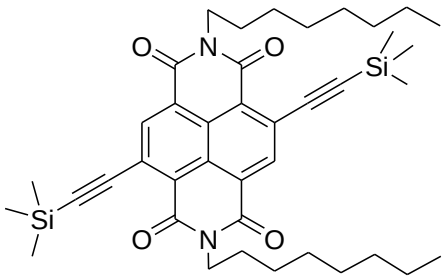

381

Fig. 191 Chemical structure of **381**.

Core-substituted naphthalene diimide (c-NDI) **381** bearing trimethylsilylacetylene (TMS) moieties for the colorimetric and fluorogenic detection of F^-, based on a desilylation reaction, was reported (see Fig. 191).[243] A significant change, visible to the naked eye from yellow to dark brown, was observed, but only when adding F^- in CH_2Cl_2, whereas the addition of other anions, such as Cl^-, Br^-, HSO_4^-, AcO^- and $H_2PO_4^-$, resulted in no distinct changes. When the F^- concentration was increased up to 2 equiv., there was a remarkable shift of the original absorption bands of **381** at 289, 382, 414 and 439 nm to new bands at 275, 376, 396 and 419 nm, respectively. CH_2Cl_2 solutions of receptor **381** showed two weak emission peaks at 329 and 455 nm upon excitation at 289 nm. Only the addition of anion F^- induced a moderate emission enhancement of both bands.

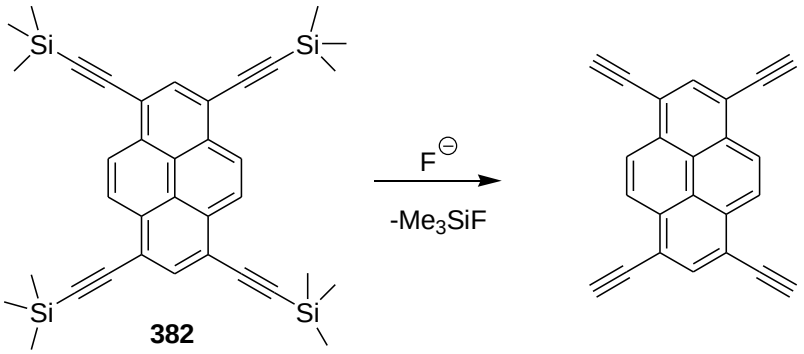

Fig. 192 Chemical reaction of the pyrene derivative **382** with the F^- anion.

The pyrene derivative **382** (see Fig. 192) containing four trimethylsilylethynyl substituents was used as a fluoro-chromogenic chemodosimeter for F^- in THF.[244] **382** showed high sensitivity and specific selectivity to the F^- anions when compared to other anions (i.e., Cl^-, Br^-, ClO_4^-, HPO_4^-, and $H_2PO_4^-$), resulting in a colour change from light green to colourless and in an emission change from blue to purple. These changes were attributed to the elimination of trimethylsilyl (TMS) substituents through a strong interaction between the F^- anion and the silicon atoms, which increased the energy gap between HOMO and LUMO due to the lack of s–p interactions between silicons and the pyrene. TD-DFT calculations also confirmed this mechanism. Finally, a portable test paper containing **382** was prepared to detect F^- in water with a limit of detection of 1 ppm.

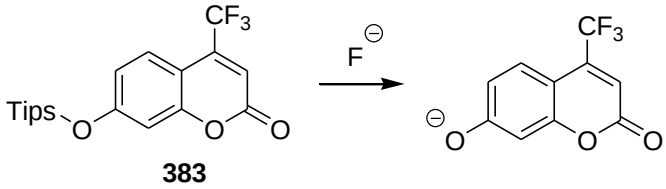

Fig. 193 Deprotection reaction of **383** by F^-.

A 'turn-on' chromo-fluorogenic probe (**383**) for F^- in CH_3CN and in H_2O through a silyl deprotection reaction was reported.[245] Compound **383** (see Fig. 193) showed a band at 330 nm in CH_3CN and it was non-fluorescent. Upon the addition of F^-, a new intense absorption band at 434 nm and a green emission peak at 500 nm were found, accompanied by the development of a bright yellow colour. A limit of detection for F^- of 50 x 10^{-9} mol L^{-1} was determined by fluorescence. Addition of other anions (i.e., Cl^-, Br^-, I^-, CN^-, NO_3^-, $PhCO_2^-$, SCN^-, AcO^-, HSO_4^-, and $H_2PO_4^-$) to **383** had no effect on either absorbance or fluorescence. The deprotection reaction was extremely fast in pure CH_3CN, but the increase of H_2O content significantly delayed the cleavage reaction. Nevertheless the experiments done in HEPES buffer at pH 7.4 using **383** were able to detect 0.3 ppm of F^- by fluorescence. Finally, the authors prepared a test paper that was able to detect F^- in aqueous media.

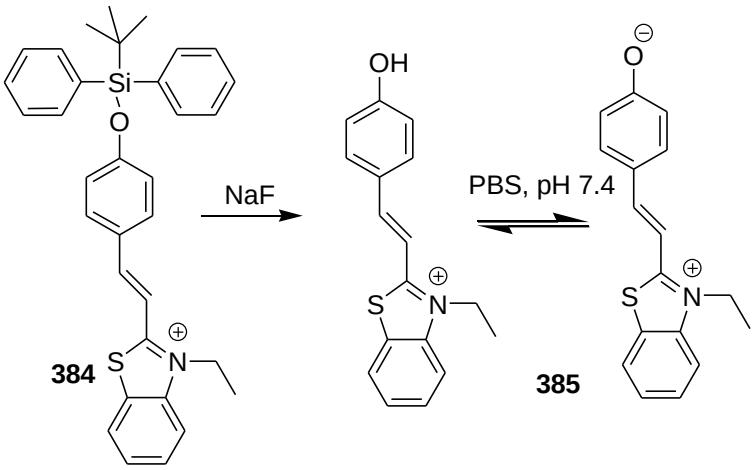

Fig. 194 Chemical reaction of **384** with NaF and the formation of **385**.

Another work detecteding F^- ions using the strong affinity of F^- to silicon was that reported by Zhang et al.[246] Chemodosimeter **384** (see Fig. 194) was employed for the ratiometric determination of F^- in buffered H_2O solution and living systems. The F^- anion was able to cleavage the Si-O bond and to release compound **385**, which was highly fluorescent. The determination of F^- with **384** was investigated in CH_3OH:H_2O 3:7 v/v mixtures (phosphate-buffered saline PBS at pH 7.4). In this medium, **384** displayed one major absorption band at 407 nm. When F^- was gradually added, the maximum absorption peak showed a 110 nm red shift and the colour of the solution turned from pale yellow to orange. In the emission spectrum, the maximum emission peak underwent a red shift from 500 to 558 nm. A limit of detection of 0.08 x 10^{-3} mol L^{-1} was calculated for F^-. **384** exhibited high F^- selectivity over various anions and biorelevant analytes such as CO_3^{2-}, SO_4^{2-}, SCN^-, NO_3^-, N_3^-, Cl^-, Br^-, I^-, Cys, GSH, BSA, and HSA. Finally, the authors demonstrated the ability of chemodosimeter **384** to image F^- in RAW 264.7 macrophage cells.

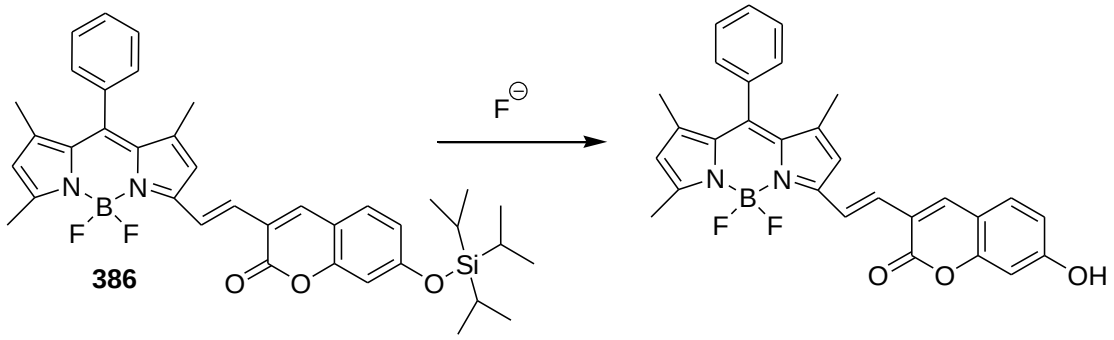

Fig. 195 Chemical reaction of the coumarin-BODIPY derivative **386** with the F^- anion.

In this work, the autors detected the F^- anion by using the new coumarin-BODIPY derivative **386** and a deprotection mechanism via the reaction of F^- with the triisopropylsilyl group (see Fig. 195).[247] The sensor exhibited a large red shift (88 nm) in absorption and a drastic ratiometric fluorescent response (I_{472}/I_{606} = 17.4, λ_{exc} = 450 nm) in the presence of F^- anions in DMSO, showing a colour change from pink to red and an emission colour change from orange to blue. The limit of detection for F^- was 0.12 x 10^{-6} mol L^{-1}. The response of F^- under

competition of relevant analytes showed no influence on the fluorescence detection of F^-. Density function theory and time-dependent density function theory calculations were also conducted by the authors to rationalise the sensor's optical response.

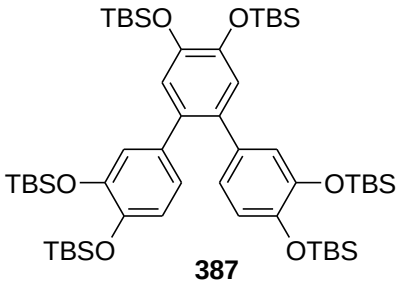

387

Fig. 196 Chemical structure of terphenyl derivative **387**.

Terphenyl derivative **387** (see Fig. 196) was used as a probe for F^- detection.[248] UV-Vis experiments were carried out in THF solutions in the presence of selected anions (i.e., F^-, Cl^-, Br^-, I^-, NO_3^-, AcO^-, CN^-, $H_2PO_4^-$ and HSO_4^-). Of all the anions tested, only the addition of F^- induced a bathochromic shift of the initial band at 295 to 342 nm together with the appearance of a new absorption at 663 nm (change in colour from colourless to violet). On further addition of F^-, the absorption at 663 nm decreased and three new bands appeared at 879, 526 and 287 nm (287 nm was a characteristic band for the triphenylene moiety). The spectral changes in the presence of F^- were due to the cleavage of the Si-O bond, which increased the negative charge on the phenolate oxygen followed by cyclisation to triphenylene. THF solutions of **387** showed a broad emission band at 393 nm when excited at 294 nm. Addition of small quantities of F^- induced a 32-nm red shift of the emission together with a moderate enhancement in intensity (32%), whereas further addition of this anion led to quenching. Initial enhancement was ascribed to the hydrolysis of the Si-O bonds, whereas the final quenching was attributed to an electron transfer process in the final product from the phenolate oxygens to the triphenylene moiety. The other anions tested induced negligible changes in neither the absorption nor the emission profiles.

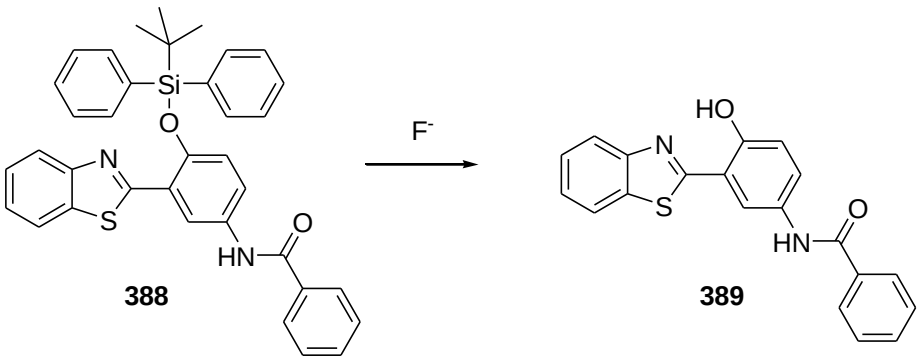

388 **389**

Fig. 197 Chemical reaction of **388** with the F^- anion and the formation of **389**.

R. Hu and co-workers reported the synthesis of a new sylil ether-based chromo-fluorogenic sensor (**388**) for the rapid detection of the F^- anion in water solutions (see Fig. 197).[249] Receptor **388** was not water-soluble and, in order to test its behaviour towards anions in aqueous environments, the authors used a cationic surfactant (cetyltrimethylammoium

bromide, CTAB). Specifically, a stable sensing system was prepared by rapidly injecting a solution of **388** in THF into a micellar solution of CTAB in H_2O. These micellar solutions of receptor **388** presented an emission at 418 nm upon excitation at 350 nm. In the presence of F^- anions, the emission band at 418 nm disappeared progressively with the simultaneous appearance of a new fluorescence centred at 560 nm. The observed fluorogenic response was ascribed to the hydrolysis of the *t*-butyldiphenilsilyl moiety, which yielded the highly emissive **389**. The other anions tested (i.e., Cl^-, Br^-, AcO^-, NO_3^-, $H_2PO_4^-$ and HSO_4^-) induced negligible changes in the emission profile of **388**. Furthermore, in order to confer the system more applicability, the authors prepared test papers of **388** by immersing a filter paper into the THF solution of the receptor and then drying it by exposure to air. Simple immersion in aqueous solutions containing F^- resulted in colorimetric detection.

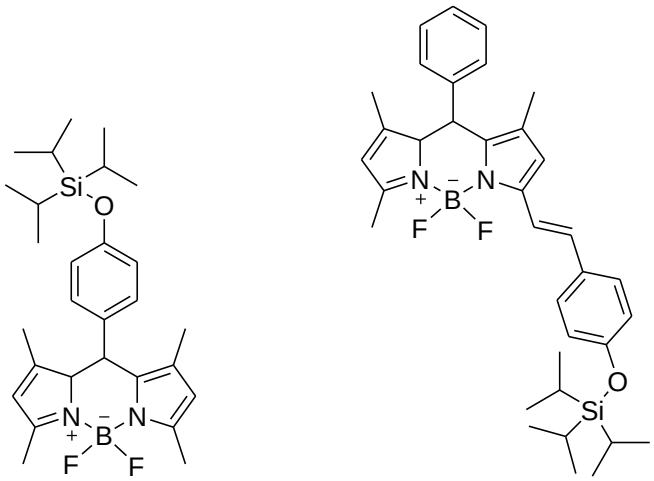

Fig. 198 Chemical structure of probes **390** and **391**.

Probes **390** and **391** (see Fig. 198) for the selective sensing of F^- anion in CH_3CN were described.[250] As in the cases above, the reactive site was a phenolic –OH-protected with a triisopropylsilyl moiety and was, in this case, conjugated with a fluorophore (BODIPY). Both compounds were highly emissive in CH_3CN solutions, showing bands at 507 (excitation at 480 nm) and 580 nm (excitation at 550 nm) for **390** and **391,** respectively. Addition of the F^- anion to solutions of both receptors induced dramatic emission quenching due to the deprotection of the silyl ether moiety, which generated a phenolate anion. This phenolate anion quenched the emission of the BODIPY dye through a PET process. In the case of **391**, the reaction with F^- was additionally accompanied by a strong batochromic shift of the absorption band (from 560 to 682 nm), resulting in a purple to green colour change. Addition of AcO^-, Br^-, Cl^-, CN^-, $H_2PO_4^-$, HSO_4^-, I^- and NO_3^- induced negligible changes in the absorption and emission profiles. To complete their work the authors prepared PMMA films impregnated with probes **390** and **391**, which were able to respond to F^- in CH_3CN-H_20 4:1 solution.

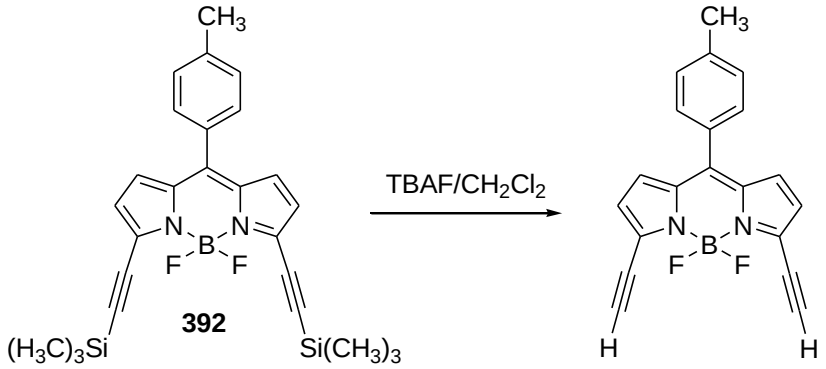

Fig. 199 Chemical reaction of **392** with the F^- anion.

The BODIPY-based chemodosimeter **392** (see Fig. 199) was used for the chromo-fluorogenic recognition of the F^- anion.[251] CH_2Cl_2 solutions of chemodosimeter **392** presented an absorption band at 571 nm that was adscribable to the BODIPY subunit. Besides, solutions of **392** were highly fluorescent with an emission band centred at 584 nm upon excitation at 425 nm. Of all the anions tested (i.e., F^-, Cl^-, Br^-, I^-, HPO_4^{2-} and ClO_4^-), only F^- was able to induce a chromo-fluorogenic response. Addition of F^- anion reduced the intensity at 571 nm together with the appearance of a new band at 551 nm, whereas the emission at 584 nm diminished with the simultaneous growth of a new fluorescence at 564 nm. These changes were attributed to the removal of the electron-rich trimethylsilyl protective groups induced by F^-, yielding the corresponding electron-deficient ethyne groups.

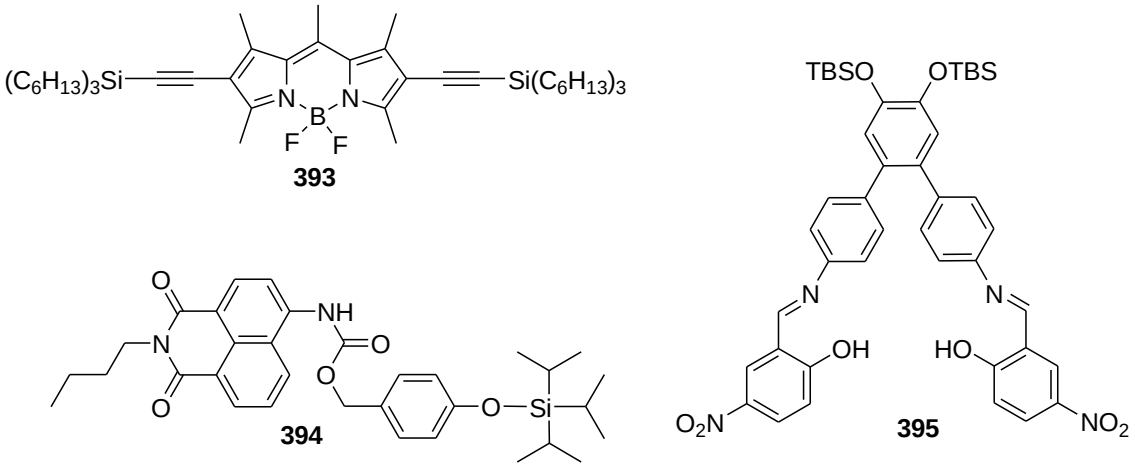

Fig. 200 Chemical structures of probes **393-395**.

BODIPY-functionalized receptor **393** (see Fig. 200) presented a silylether moiety conjugate to the fluorophore through a triple bond and was used for the selective chromo-fluorgenic recognition of the F^- anion.[252] CH_3COCH_3 solutions of **393** showed an absorption at 555 nm which shifted to 538 nm upon the addition of F^-. Besides, **393** was characterised by an emission band at 571 nm, which was also blue-shifted to 554 nm upon the addition of increasing amounts of the F^- anion. The authors determined a limit of detection for F^- of 67.4 nM. Addition of the Cl^-, Br^-, I^-, NO_3^-, $H_2PO_4^-$, SO_4^{2-}, CO_3^{2-} AcO^-, ClO_4^- and NO_2^- anions induced negligible changes in both the emission and absorption profiles. The optical changes observed were ascribed to the F^--induced hydrolysis of the Si-C bonds.

Chemodosimeter **394** (see Fig. 200) was prepared and used for the chromo-fluorogenic sensing of the F^- anion.[253] In this case, the sensor was based on a naphtalenamide fluorophore functionalised with a silyl ether moiety as the reactive site. CH_3CN solutions of **394** showed an absorption at 365 nm which, upon the addition of small amounts of F^-, decreased while a new band centred at 421 nm with a shoulder at 487 nm appeared. When the F^- concentration increased, the shoulder gradually disappeared. The authors explained these changes by a first deprotonation reaction of the amide N-H (at low F^- concentrations), followed by a deprotection of the silyl ether moiety when the added F^- concentration increased. F^--induced spectral changes were also studied by fluorescence spectroscopy under the same conditions. In this case, when F^- was added, the emission intensity at 449 nm (excitation at 365 nm) decreased, while a new fluorescence at 508 nm appeared. Addition of AcO^- and $H_2PO_4^-$ only induced a partial quenching of the emission at 449 nm. The other anions tested (i.e., Cl^-, Br^-, I^-, HSO_4^-, NO_3^-, PF_6^- and ClO_4^-) induced negligible changes in neither UV-Vis nor the fluorescence spectra.

Terphenyl-based bifunctional fluorescent chemosensor **395** (see Fig. 200) showed a selective optical recognition of the F^- anion.[254] In particular, THF solutions of **395** exhibited two absorption bands at 265 and 342 nm, which lowered in intensity with the concomitant appearance of a new red-shifted peak at 447 nm (change in colour from colourless to yellow) upon the addition of the F^- anion. Receptor **395** was also fluorescent and presented a broad emission at 517 nm upon excitation at 360 nm. Addition of F^- induced a progressive quenching of this emission with the appearance of a blue-shifted band at 478 nm. The changes in the emission profile upon the addition of F^- were ascribed to a deprotonation process and also to the hydrolysis of the silyl ether groups. With **395** in use, a limit of detection of 1.0×10^{-8} mol L^{-1} for F^- was measured. Addition of anions Cl^-, Br^-, I^-, HSO_4^-, NO_3^-, and $H_2PO_4^-$ induced negligible changes in the UV-visible and fluorescence profiles.

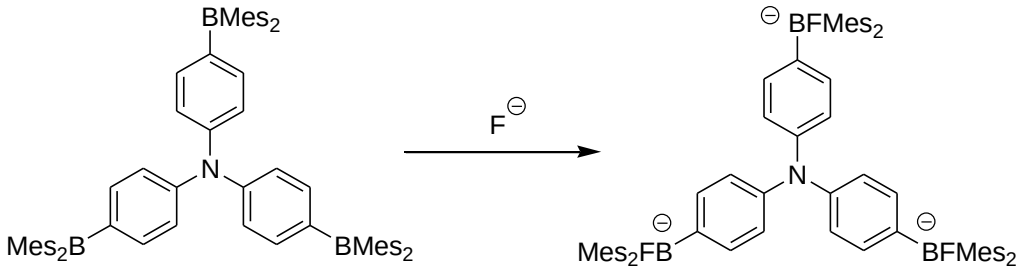

396

Fig. 201 Chemical reaction of **396** with the F^- anion.

The boron-containing derivative (**396**) with three binding sites for the recognition of F^- anions was investigated by optical absorption, luminescence, and (^1H, ^{11}B, ^{13}C, ^{19}F) NMR spectroscopy in CH_2Cl_2 solutions.[255] The binding of F^- to boron atoms occurred in three clearly identifiable steps. Consequently, the initially bright blue emission was red-shifted and decreased in intensity until it was quenched completely in the presence of F^- in excess (see Fig. 201 for the proposed mechanism). Furthermore, the absorption band at 400 nm in **396** was red-shifted to 435 nm upon the addition of F^-.

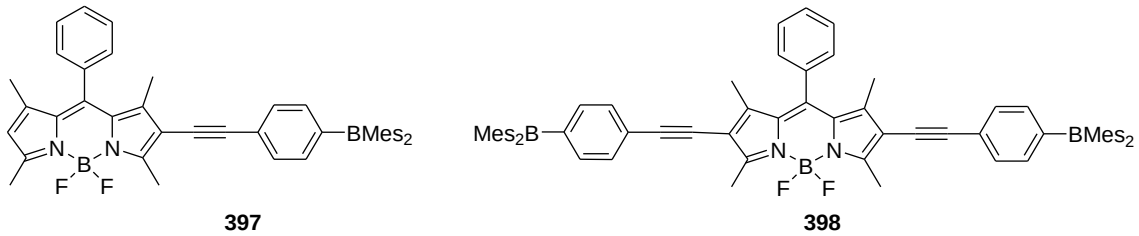

Fig. 202 Chemical structures of probes **397** and **398**.

The two novel BODIPY dyes **397** and **398** (see Fig. 202), which contained bulky substituent [(4-dimesitylboryl)phenyl]ethynyl at the2- and 2,6-positions, acted as sensing systems for F^- and CN^-.[256] These two compounds displayed intense fluorescence in solution and also in the solid state. In THF solution, BODIPY dye **397** exhibited an absorption at 535 nm and a strong orangish-yellow emission at 570 nm. A red shift *ca.* 40 nm in relation respect to **397** was observed in the absorption and the emission of **398** as a result of a more extended conjugation in the latter. In the solid state, the films of **397** and **398** (obtained by spin-coating) in THF exhibited a red shift (7 nm for **397**; 8 nm for **398**), but only in the absorption spectra. Addition of F^- anions led to a decrease in the emission band, whereas excess F^- induced a blue shift of the emission of 28 nm and a blue-shift absorption to 448 nm. Moreover, although the addition of CN^- anions also diminished fluorescence, excess of CN^- did not induce any additional effect. BODIPY dyes displayed this sensitive response to the F^- and CN^- anions through a reaction with the boron centre of the boryl group and the subsequent decomposition of the BODIPY core.

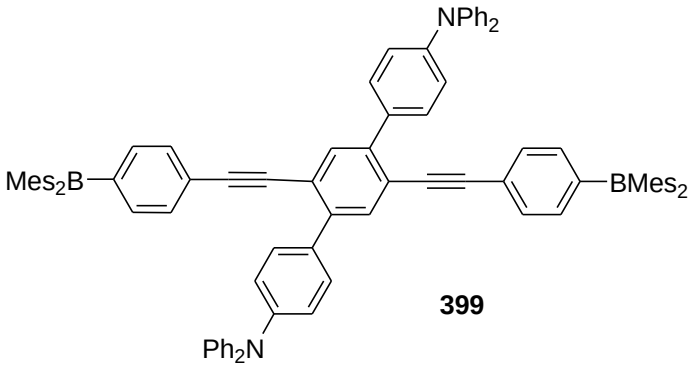

Fig. 203 Chemical structure of probe **399**.

A similar work was reported by the same group.[257] In this case, they prepared a tri-coordinate organoboron compound **399** (see Fig. 203), which displayed a characteristic intramolecular charge transfer transition and was additionally highly emissive in both THF and the solid state, showing an emission centred at 540 nm (excitation at 365 nm). Complexation with F^- ions gradually decreased the band centred at 540 nm, whereas a new blue-shifted band appeared at 442 nm. A response to F^- ions was also observed in the solid state.

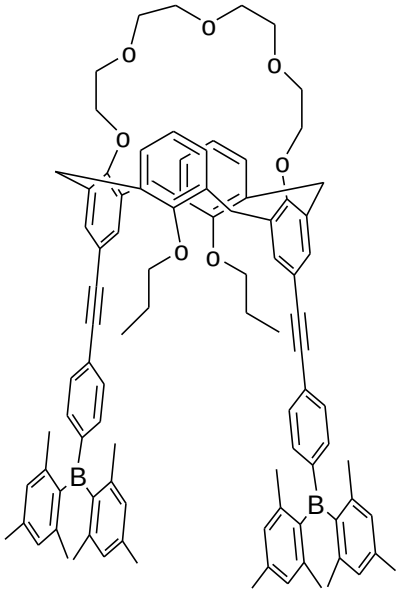

400

Fig. 204 Chemical structure of probe **400**.

The novel calix[4]crown derivative **400** (see Fig. 204) was used as a luminescent probe for F^- with high sensitivity and selectivity.[258] CH_2Cl_2 solutions of **400** showed a strong absorption band at 342 nm. Addition of F^- anion induced the disappearance of the 342 nm band with the concomitant growth of a new absorbance at 300 nm. Addition of anions Cl^-, Br^-, I^-, $H_2PO_4^-$ and AcO^- induced negligible changes in the UV-visible profile of **400**. In addition, the F^- anion quenched the emission band of **400** centred at ca. 425 nm. Absorption and emission changes were the direct result of the F^- anion binding with the boron atoms of **400**. This reaction interrupted the π-conjugation through the boron atom in the chromophore, and eliminated the intramolecular charge transfer process that was active in the receptor alone.

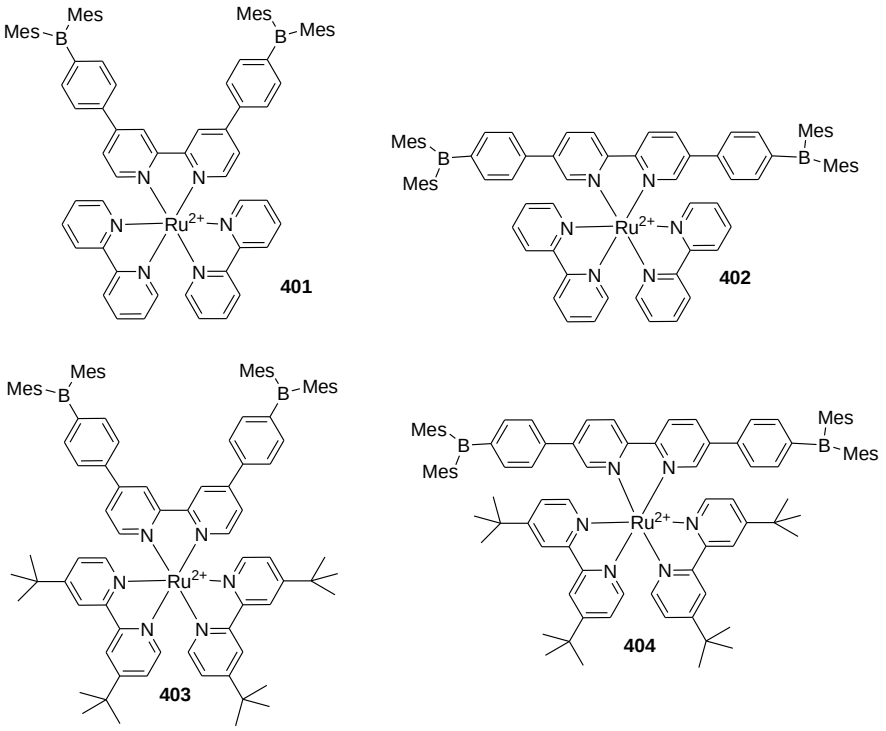

Fig. 205 Chemical structures of Ru^{2+} complexes **401-404**.

New Ru^{2+} complexes **401-404** (see Fig. 205) were used as probes for the recognition of F^- or CN^- in CH_2Cl_2.[259] Compounds **401-404** displayed absorption bands in the 360-370 nm region and were luminescent in both solution and the solid state, showing emissions in the 600-630 nm range. Addition of F^- or CN^- induced a decrease of the absorption band at ca 360 nm, whereas new emissions appeared at ca. 585-600 nm. The changes in absorption and in emission spectra were ascribed to an addition reaction of both nucleophilic anions to the boron centrrs of the receptors.

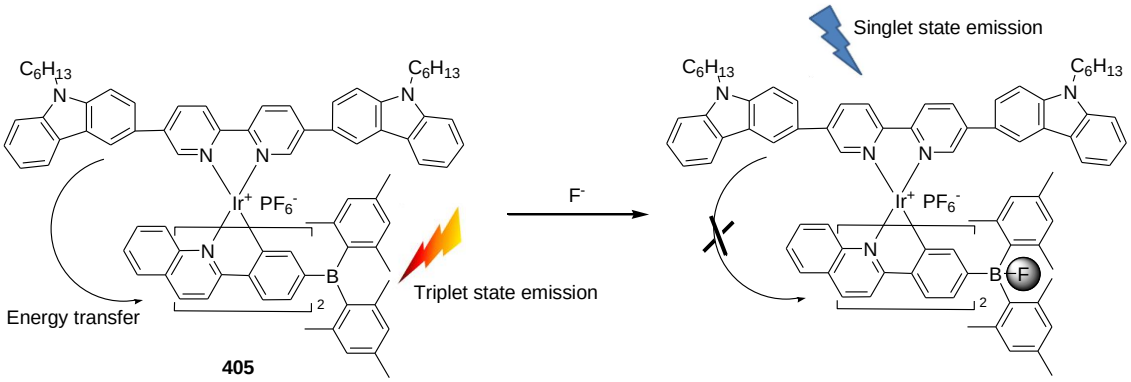

Fig. 206 Chemical reaction between the Ir^{3+}-containing complex **405** and the F^- anion.

Xu and coworkers prepared the Ir^{3+} complex **405** (see Fig. 206) containing both triarylboron and carbazole moieties for ratiometric F^- sensing based on switchable triplet-singlet emission.[260] CH_3CN solutions of complex **405** showed phosphorescence emission at 583 nm upon excitation at 379 nm in the carbazole moiety due to an energy transfer process from the heterocyclic fluorophore to the Ir^{3+} complex. Addition of increasing amounts of the F^- anion induced a progressive decrease of the phosphorescence band at 583 with the concomitant growth of the typical carbazole emission at 458 nm. The binding of the F^- anion with the

triarylboron moiety inhibited the energy transfer process and the emission of the carbazole was observed. Addition of other anions (i.e., Cl^-, Br^-, I^-, NO_3^-, ClO_4^-, $H_2PO_4^-$ and AcO^-) induced negligible changes in the emission profile of chemodosimeter **405**.

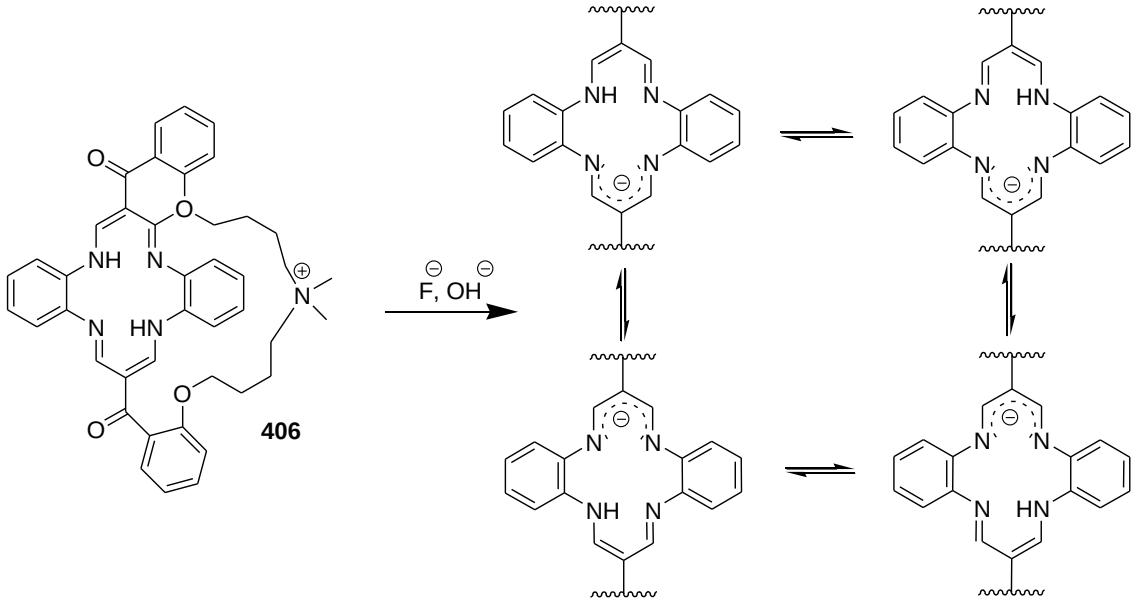

Fig. 207 Proposed reaction mode between **406** and the F^- anion and the formation of zwitterionic species.

Cationic derivative **406** (see Fig. 207) was used for the recognition of the F^- anion.[261] The UV-Vis spectrum of the compound underwent distinct changes in band positions and intensities upon the addition of F^- and OH^- in DMSO (colour change from orange to red), whereas an orange luminescence at 576 nm (excitation at 380 nm) was also observed. The authors demonstrated that the deprotonation of the macrocycle took place in the presence of F^- (and OH^-). DFT calculations support the conclusion that the spectral changes induced by OH^- and F^- resulted from deprotonation. Addition of Cl^-, Br^-, NO_3^- and HSO_4^- was unable to induce any optical response.

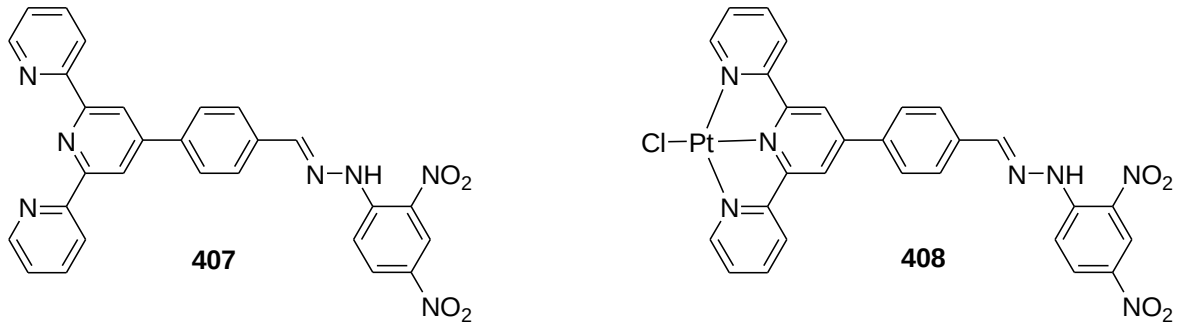

Fig. 208 Chemical structures of probes **407** and **408**.

Zhang and co-workers developed two new probes for basic anions based on terpyridine moieties and 2,4-diphenylhydrazone groups.[262] Both probes **407** and **408** (see Fig. 208) were characterised by intense absorption bands at 404 and 430 nm, respectively, in DMSO solutions. Upon the addition of basic anions, such as F^-, AcO^-, $H_2PO_4^-$, the main absorption band gradually

decreased, while a new band was formed at 525 and 580 nm for **407** and **408**, producing a colour change from yellow to purple and blue, respectively. The explanation of the chromogenic changes was demonstrated by NMR studies and was based on the deprotonation of hydrozonic –NH. Moreover, both **407** and **408** were weakly fluorescent and their emission bands (centred at 550 for both receptors with excitation wavelengths of 404 and 430 nm for **407** and **408,** respectively) were clearly quenched upon the deprotonation event. Finally, the authors treated both **407** and **408** under the same conditions with non-basic anions (i.e., Cl^-, Br^-, I^-, NO_3^- and HSO_4^-) and observed that none was able to induce any detectable chromo-fluorogenic response.

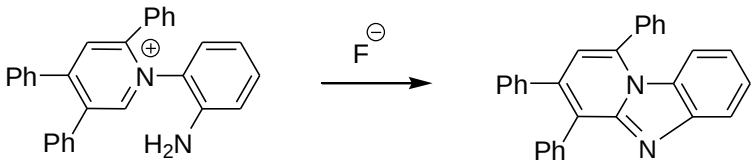

409 **410**

Fig. 209 Chemical reaction of pyridinium derivative **409** with the F^- anion.

Pyridinium derivative (**409**) was used as a probe to detect F^- ions due to an efficient fluoride-induced intramolecular cyclisation in CH_3CN that yielded the highly fluorescent 1,3,4-triphenylpyrido[1,2-a]benzimidazole **410** (see Fig. 209).[263] The absorption spectrum of **409** was characterised by three peaks at 237, 263, and 306 nm. Upon the addition of F^-, these absorption bands gradually decreased, and two new absorptions at 256 and 370 nm belonged to compound **410** appeared simultaneously. On the other hand, compound **409** presented a rather weak fluorescence at 469 nm (λ_{exc} = 366 nm). After adding F^-, a new fluorescence band appeared at 481 nm, which was in accordance with the characteristic emission of **410**. A limit of detection of 2.72 x 10^{-6} mol L^{-1} was determined for F^-. Other anions, such as Cl^-, Br^-, I^-, NO_3^-, AcO^-, and $H_2PO_4^-$, induced no response.

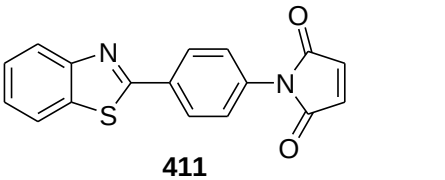

411

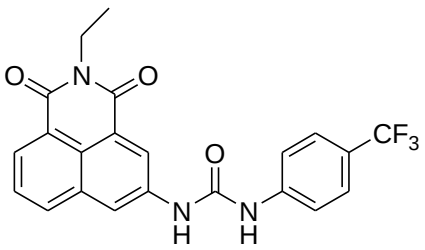

412

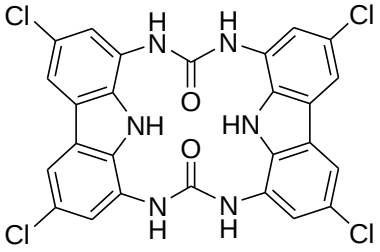

413

Fig. 210 Chemical structures of probes **411-413**.

Probe **411** (see Fig. 210) was able to sense F^- by exploiting both its nucleophilic and basic character.[264] Addition of F^- to compound **411** in DMSO induced a colour change from light yellow to dark red, which vanished concomitantly with the appearance of a precipitate due to the polymerisation of **411**. In particular, the F^- anion was able to add on the α,β-unsaturated system of **411** to form an enolate that initiated the polymerisation reaction by the nucleophilic addition to another receptor molecule. The final elimination of an HF molecule induced the formation of a highly conjugated enolate polymer (red) which, with time, protonated to give a colourless precipitate. On the other hand, a turn-on of fluorescence at 412 nm (10-fold, λ_{exc} = 365 nm) nm was observed. A limit of detection of 50 x 10^{-6} mol L^{-1} was determined for F^-. The authors were also able to determine the F^- content in DMSO:H_2O 1:9 v/v solutions. Detection of F^- was selective from other basic anions, such as AcO^-, OH^- or CN^-, and halogenides. The response of F^-, among other halogenides, was explained by taking into account that only basic anionic nucleophilic species can induce a response, whereas differentiation of F^- and CN^- was due to the fact that the latter was more nucleophilic, but less basic than the former.

Compound **412** (see Fig. 210) in DMSO proved to be a chromo-fluorogenic probe for F^-.[265] The sensing system consisted of a naphthalimide fluorophore which incorporated a trifluromethyl aryl urea into the 3-position as an anion recognition site. **412** in DMSO presented two bands at 394 nm and 340 nm relating to an ICT transition, whereas excitation at these wavelengths produced a broad emission at 453 nm. Addition of $H_2PO_4^-$ and AcO^- induced only minor changes, whereas addition of F^- led to an increase in the absorption at 340 nm and a minor bathochromic shift (4 nm). Addition of F^- anions in excess produced the formation of an absorption band at 490 (colour change from yellow to red) and fluorescence quenching. Changes were due to the formation of hydrogen-bonding complexes with the urea receptor (at a low F^- concentration), followed by deprotonation (at higher F^- concentrations).

Cyclo-bis(urea-3,6-dichlorocarbazole) **413** (see Fig. 210) was used as a probe for certain basic anions.[266] Solutions of **413** in DMSO:H_2O 99.5:0.5 v/v showed an absorption band at 372 nm. Upon the addition of several anions (F^-, Cl^-, Br^-, I^-, HSO_4^-, $H_2PO_4^-$, $HP_2O_7^{3-}$, AcO^-), a perceptible colour change from colourless to yellow (due to the appearance of two new absorptions at 407 and 432 nm) was observed, but only in the presence of F^- and $HP_2O_7^{3-}$. Moreover, **413** showed an intense emission at 387 nm (excitation at 365 nm) that was completely quenched upon the addition of $HP_2O_7^{3-}$ and F^-, whereas AcO^- induced partial deactivation. No significant changes were found for Cl^-, Br^-, I^-, $H_2PO_4^-$ and HSO_4^-. The optical changes were ascribed to the anion-induced deprotonation of the urea moieties.

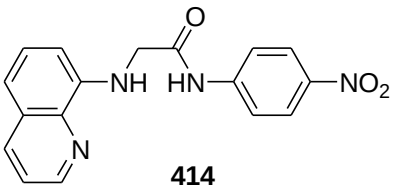

414

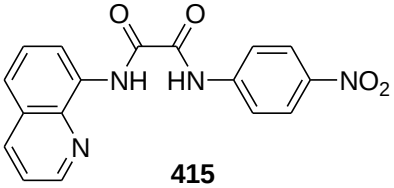

415

Fig. 211 Chemical structures of probes **414** and **415**.

DMSO solutions of receptor **414** (see Fig. 211) presented an absorption band at 333 nm which udnerwent a red shift to 440 nm upon the addition of F^- anions.[267] The other anions tested (i.e., Cl^-, Br^-, I^-, AcO^-, BzO^-, $H_2PO_4^-$, HSO_4^-, ClO_4^- and NO_3^-) induced no colour variations. Change in colour (from colourless to yellow) was attributed to a deprotonation of the amide N-H fragment. The increased acidity of receptor **415**, when compared with **414**, accounted for the fact that F^-, AcO^-, BzO^- and $H_2PO_4^-$ were able to deprotonate the amide groups of the former, leading to colour changes.

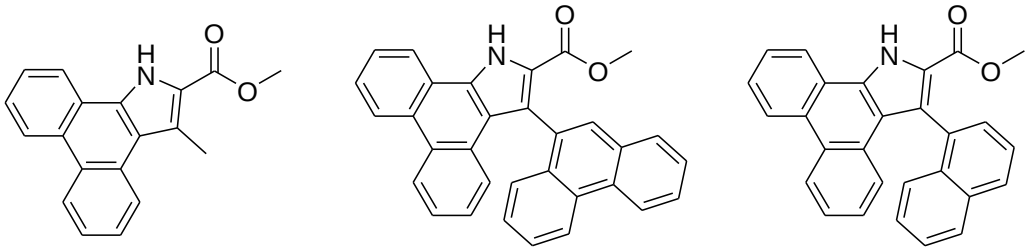

416 **417** **418**

Fig. 212 Chemical structures of indole derivatives **416**-**418**.

Indole derivatives **416**-**418** (see Fig. 212) were used for the fluorescent recognition of the F^- anion.[268] CH_3CN solutions of **416**-**418**, displayed, upon excitation at ca. 330 nm, well-defined emission bands in the 340-420 nm interval. In order to assess the sensing behaviour, changes in the emission spectra of three receptors were evaluated upon the addition of anions F^-, Cl^-, Br^-, AcO^- and HSO_4^-. Only the addition of F^- induced emission quenching in the 340-420 nm range, together with the appearance of a red-shifted band (at 465, 515 and 510 nm for **416**, **417** and **418,** respectively). The new red-shifted emissions were ascribed to the deprotonated form of the receptors induced by the basic F^- anion.

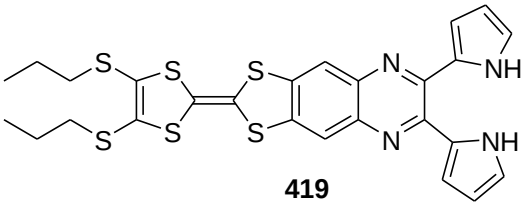

419

Fig. 213 Chemical structure of probe **419**.

Chemodosimeter **419** (see Fig. 213), bearing a dipyrrolyl motif as a recognition site and a tetrathiafulvalene group as an optical unit, showed a selective response to F^- among other anions (Cl^-, Br^-, HSO_4^-, CH_3COO^-, and $H_2PO_4^-$) in CH_2Cl_2 solutions.[269] **419** exhibited three strong absorption bands at 288, 311 and 484 nm with a shoulder at 374 nm. The addition of F^- to **419** causef significant changes in the absorption spectra, with absorption bands decreasing in intensity, while three new bands at 290, 323 and 503 nm appeared with a shoulder at 384 nm. On the other hand, **419** showed an emission band at 662 nm (λ_{exc} = 446 nm) which increased in intensity upon the addition of F^-. ^{1}H-NMR studies suggested a deprotonation of the dipyrrole receptor as a sensing mechanism that induced increased rigidity of **419,** causing fluorescence enhancement. On the other hand, the electrochemical behaviour of compound **419** remained largely unaffected upon the addition of F^-.

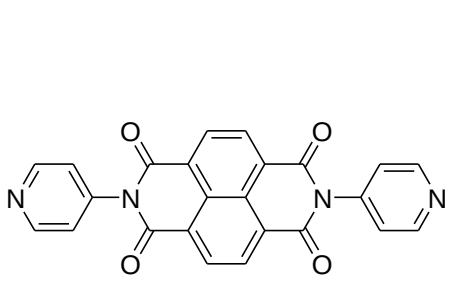

420

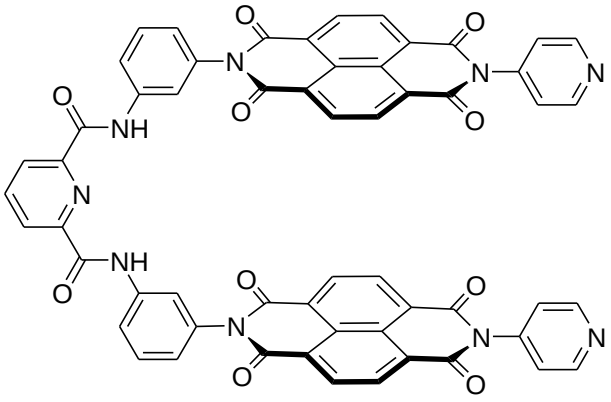

421

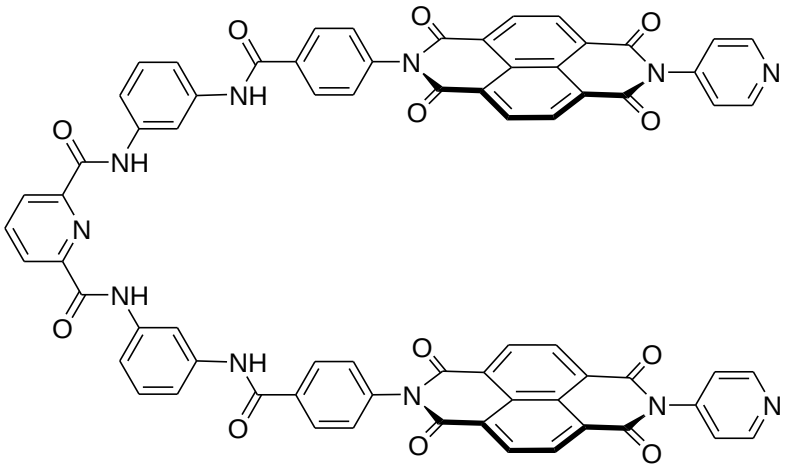

422

Fig. 214 Chemical structures of probes **420**-**422**.

Naphthalene diimides **420**-**422** (see Fig. 214) were used for the colorimetric and fluorimetric sensing of anion F^-.[270] DMSO solutions of **420** displayed characteristic naphthalene diimide (NDI) absorption peaks at 343, 361 and 381 nm. Addition of anion F^- gradually bleached the NDI absorptions, producing new peaks at 475, 605, 711 and 791 nm (change in colour from colourless to orange). Upon the addition of F^- in excess, the latter peaks disappeared with the emergence of a new absorption at 542 nm (change in colour from orange to pink). The first change in colour was ascribed to the binding of F anion with the NDI group through anion-π and the charge-transfer interactions that facilitated an F^-→NDI electron transfer which generated the orange $NDI^{\bullet-}$. The second change in colour was ascribed to the F^--induced reduction of $NDI^{\bullet-}$ to NDI^{2-}. The observed chromogenic response was highly selective and the addition of Cl^-, Br^-, I^-, NO_2^-, NO_3^-, N_3^-, AcO^- and $H_2PO_4^-$ induced negligible changes. Moreover, DMSO solutions of **420** upon excitation at 381 nm showed an emission band at 430 nm. Addition of anion F^- induced the appearance of a new emission at 465 nm. Similar changes were obtained with receptors **421** and **422,** but with best sensitivity due to the preorganisation of the two NDI subunits that improved F^- interaction.

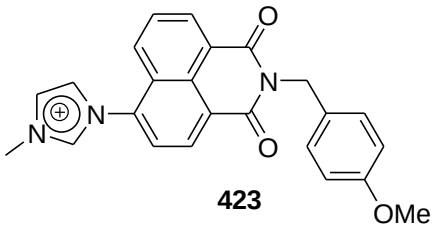

423

Fig. 215 Chemical structure of probe **423**.

Receptor **423** (see Fig. 215), which incorporated a naphthalimide fluorophore linked with an acidic imidazolium ring, was used as chromo-fluorogenic sensor for F^- anion.[271] DMSO solutions of **423** showed an intense absorption at 340. Addition of F^- induced a marked colour change from light yellow to purple due to the appearance of a new absorption at 585 nm. This chromogenic response was selective for anion F^-, whereas addition of Cl^-, Br^-, I^-, HSO_4^-, AcO^-, SCN^- and NO_3^- induced negligible colour changes. The new band was ascribed to an internal charge transfer (ICT) process, which was active upon the F^--induced deprotonation of the C-H fragment in the imidazolium ring. The sensor was also used for the fluorogenic sensing of anion F^-. Excitation at 353 nm of DMSO solutions of **423** induced the appearance of an emission at 373 nm, typical of the naphthalimide fluorophore. Addition of Cl^-, Br^-, I^-, HSO_4^-, AcO^-, SCN^- and NO_3^- induced negligible changes, whereas the presence of F^- promoted the progressive quenching of this band with the appearance of two new emissions at 438 and 545 nm. The former wavelength emission was ascribed to the radiative return of the $\pi \rightarrow \pi^*$ state, whereas the band at 545 nm arose from an ICT emission.

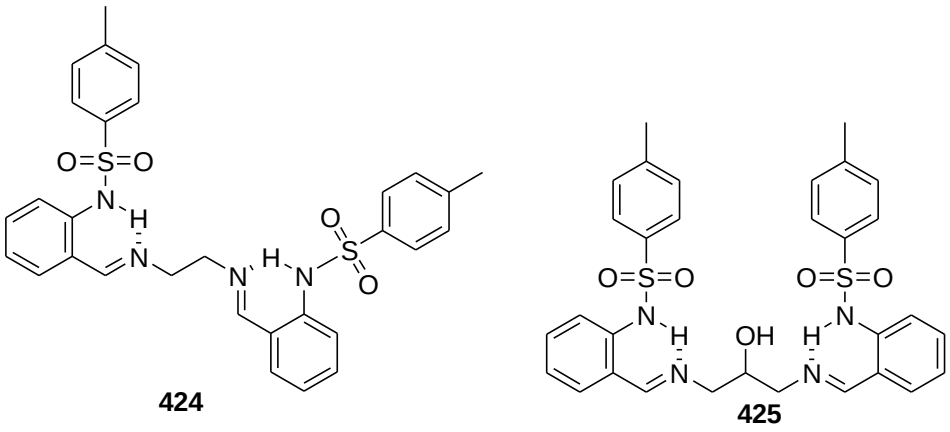

Fig. 216 Chemical structures of probes **424** and **425**.

Sulphonamide-based receptors **424** and **425** (see Fig. 216) were used for the chromo-fluorogenic detection of anion F^-.[272] Acetonitrile solution of both receptors showed an absorption band at 316 nm, which was red-shifted to 361 nm upon the addition of anion F^-. The formation of the red-shifted band was ascribed to a deprotonation of one of the sulphonamide moieties promoted by basic F^-. Addition of AcO^- and $H_2PO_4^-$ induced very slight changes in the UV-visible profiles, indicating that both anions were unable to deprotonate **424** and **425**. The other anions tested (i.e., Cl^-, Br^-, I^-, NO_3^- and HSO_4^-) were unable to induce any spectral change. Upon the excitation of acetonitrile solutions of **424** and **425** at 313 nm, a weak emission at 454 (for **424**) and 461 (for **425**) nm was observed. Of all the anions tested, only F^- was able to enhance the emission bands of both receptors. The authors indicated that one advantage of using this kind of receptors was that the presence of the imine group as an intramolecular H-bond acceptor enhanced the selectivity of these probes to F^- by minimising possible interferences by other basic anions (e.g., AcO^- and $H_2PO_4^-$).

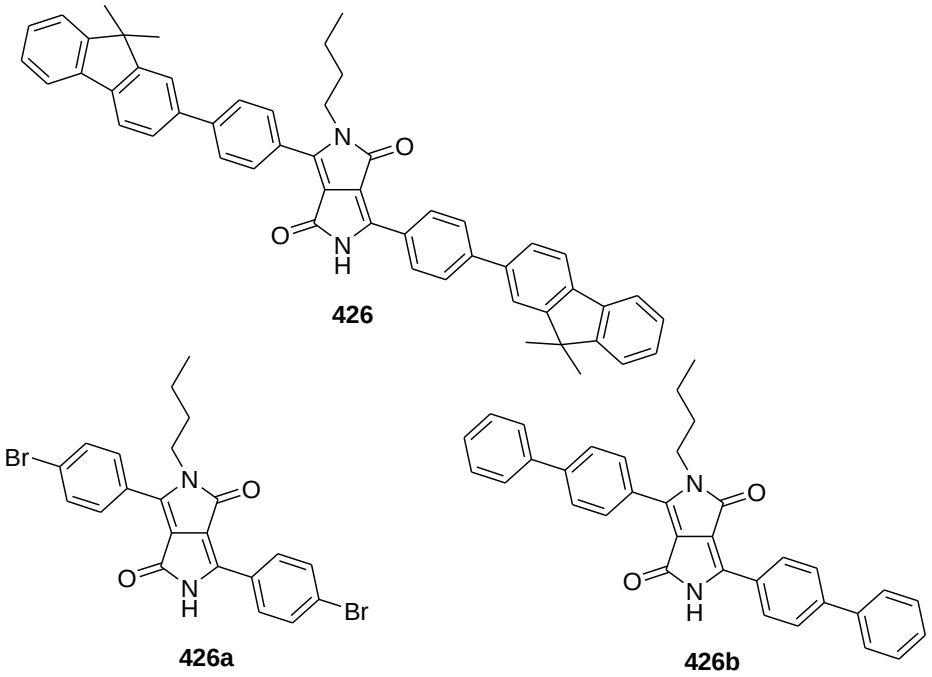

Fig. 217 Chemical structures of diketopyrrolopyrrole derivatives **426**, **426a** and **426b**.

The deprotonation of the lactamic –NH of diketopyrrolopyrrole derivatives **426**, **426a** and **426b** (see Fig. 217) were used as suitable probes for F^- sensing.[273] CH_2Cl_2 solutions of receptor **426** showed an intense absorption band at 497 nm. Of all the anions tested (F^-, Cl^-, Br^- and I^-), only F^- induced a marked decrease in this absorption, together with the appearance of a new band at 594 nm (change in colour from orange to purple). Anion F^- was also able to selectively quench the fluorescence emission of **426** at 563 nm (excitation at 497 nm). The changes observed in the absorption and emission bands were ascribed to F^--induced deprotonation of the lactamic N-H in **426**. Virtually the same changes were observed upon the addition of anion F^- for CH_2Cl_2 solutions of receptors **426a** (shift of the visible band from 477 to 571 nm and quenching of the emission band at 531 nm) and **426b** (shift of the visible band from 485 to 585 nm and quenching of the emission band at 545 nm).

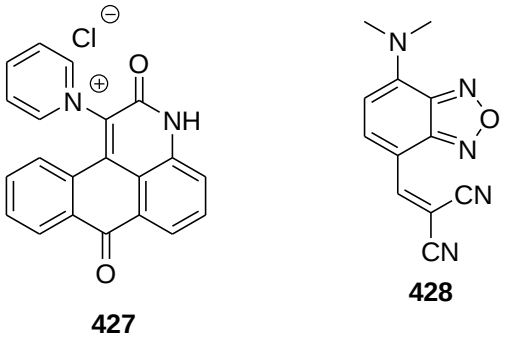

Fig. 218 Chemical structures of probes **427** and **428**.

Luxami and co-workers prepared and studied the new dual-channel concentration-dependent chromo-fluorogenic fluoride chemodosimeter **427** (see Fig. 218).[274] CH_3CN:DMSO 20:1 v/v solutions of **427** showed an absorption band at 410 nm. Addition of small quantities of anion F^- induced a decrease in this absorption with the concomitant increase of a new band at 490 nm (change in colour from pale yellow to dark pink). With a further addition of F^-, three new absorption bands at 355, 445 and 630 nm appeared (change in colour from dark pink to bright green). The presence of other anions such as Cl^-, Br^-, I^-, CN^-, HPO_4^{2-}, NO_3^-, AcO^-, ClO_4^- and HSO_4^- did not induce any noticeable change. The authors rationalised these chromogenic changes by NMR studies and stated that the first (pale yellow to pink) chromatic change was due to the deprotonation of the pyridone N-H, whereas the chromogenic change occurring when reaching a higher fluoride concentration was related to the aggregation of F^- anions around the positively quaternary nitrogen atom of receptor **427**. Probe **427** was also fluorescent and showed a very weak emission at 510 nm upon excitation at 400 nm. The gradual addition of anion F^- induced a significant enhancement of the emission band, whereas no emission enhancements were found when the other selected anions were added.

Dicyanovinyl-substituted benzofurazan derivative (**428**) was used as an efficient ratiometric chemosensor for anion CN^- (see Fig. 218).[275] Solution of **428** in CH_3CN:H_2O 95:5 v/v exhibited two main absorption bands at 391 and 513 nm and a moderate fluorescence (Φ = 0.7%) at 581 nm (λ_{ex} = 485 nm). Upon the addition of CN^-, a drastic reduction of the absorption intensities was observed, accompanied by the appearance of a new absorption at 441 nm and a visual change of colour from pink to colorless, while the maximum emission band underwent a blue shift to 526 nm. No significant spectral changes were observed in the presence of the other anions (F^-, Cl^-, Br^-, I^-, AcO^-, $H_2PO_4^-$, SCN^-, OCN^-, and HS^-) evaluated. The colormetric and fluorometric sensing behaviour of **428** with CN^- was attributed to a nucleophilic addition of this anion to the α-position of the dicyanovinyl moiety.

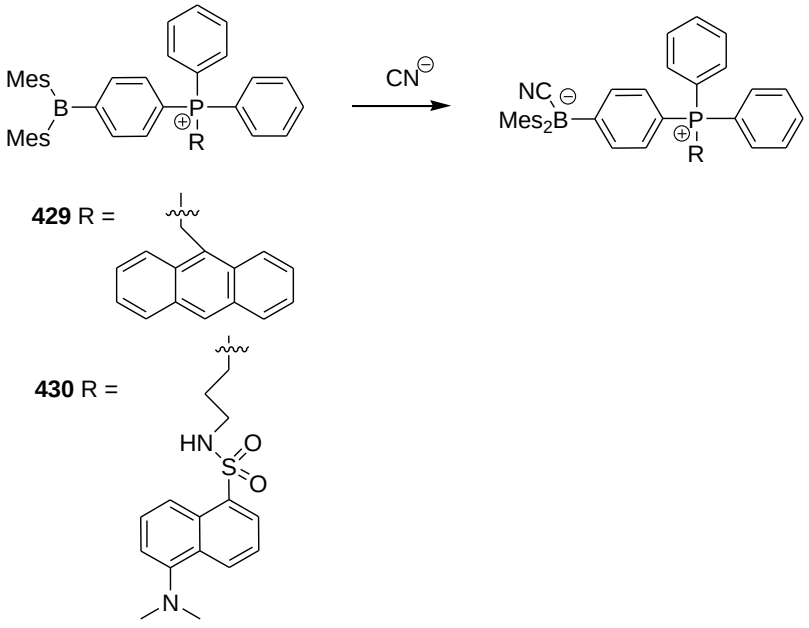

Fig. 219 Chemical structures of probes **429** and **430** and the reaction with anion CN^-.

A turn-on fluorescence probe for anion CN^- in aqueous solution was developed using *para*-phenylene phosphonium borane/fluorophore conjugates **429** and **430** (see Fig. 219).[276] These compounds gave absorption bands at 340 nm (**429**) and 335 nm (**430**) in CH_3CH_2OH, whereas they were weakly fluorescent with emissions at 427 nm (**429**, λ_{ex} = 347 nm) and 501 nm (**430**, λ_{ex} = 347 nm). Addition of CN^- to **429** and **430** in CH_3OH resulted in noticeable increased fluorescence intensity due to the reaction of CN^- with the $B(Mes)_2$ moiety. These observations, as well as the absence of charge-transfer bands in the absorption spectrum of these conjugates, suggest that the fluorescence enhancement of **429** and **430** occurred through the inhibition of an intramolecular PET from the excited state of the fluorophore to the electron-deficient phosphonium borane upon the reaction with cyanide. On the other hand, **429** and **430** showed no detectable affinity for other anions, such as Cl^-, Br^-, I^-, NO_3^-, $H_2PO_4^-$, SO_4^{2-} and AcO^-, whereas F^- was able to react with **429** and **430** with a lower binding constant when compared with CN^-. Compounds **429** and **430** were tested in aqueous solutions. Compound **429** showed an irreversibly decomposition in H_2O:CH_3OH 6:4 v/v, but compound **430** remained stable for at least one hour. CN^- addition to **430** at pH 7 in this mixture led to a decreased absorbance at 333 nm, and a limit of detection for CN^- of 1.0 x 10^{-6} mol L^{-1} was determined.

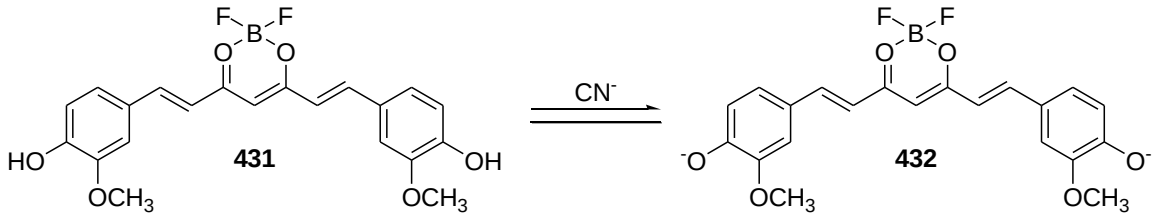

Fig. 220 Chemical reaction of probe **431** with CN^- to give **432**.

Chemodosimeter **431** (see Fig. 220) was able to selectively detect anion CN^- by changes in colour and in fluorescence emission.[277] CH_3CN:H_2O 4:1 v/v solutions of **431** presented an absorption band at 507 nm. Of all the anions tested (i.e., F^-, Cl^-, Br^-, I^-, CN^-, AcO^-, BzO^- and $H_2PO_4^-$), only CN^- induced a colour change from red to deep blue due to the appearance of a strong absorption at 649 nm. Moreover, CH_3CN:H_2O 4:1 v/v solutions of **431** displayed a very weak emission in the 500-800 nm range, whereas addition of anion CN^- induced the appearance of a strong emission at 750 nm. The authors reported a limit of detection of 0.14 μM for CN^-. The colour and fluorescence changes were ascribed to a CN^--induced deprotonation reaction of the two *p*-phenolic –OH of **431,** which yielded **432**.

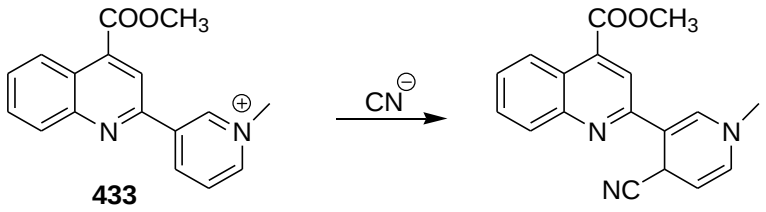

Fig. 221 Chemical reaction of probe **433** with CN^-.

The absorption spectrum of **433** (see Fig. 221) displayed a maximum at 330 in DMSO:H_2O 7:3, v/v buffered solutions at pH 7.0. The addition of various anions, such as F^-, AcO^-, SCN^-, HSO_4^-,

NO_3^-, Cl^-, Br^-, I^- and $H_2PO_4^-$, induced no changes, whereas the presence of CN^- resulted in a colour modulation from colourless to deep yellow owing to the generation of a new band at 406 nm.[278] In addition, the emission spectrum of **433** (λ_{ex} = 345 nm) presented a broad emission at 435 nm, and an off-on response upon the addition of CN^- (a limit of detection of 1.6 x 10^{-6} mol L^{-1} was observed). Finally, NMR analysis confirmed the regioselective addition of CN^-.

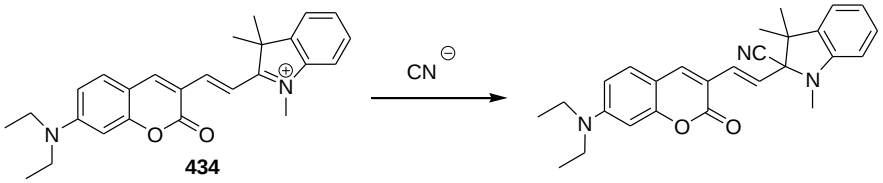

Fig. 222 Chemical reaction of probe **434** with anion CN^-.

A ratiometric fluorescent CN^- probe was developed based on a hybrid coumarin–hemicyanine dye (**434**).[279] The UV-Vis spectra of **434** (see Fig. 222) exhibited an absorption band at 570 in CH_3OH:H_2O 1:1 v/v (Tris buffer at pH 9.3) due to the expanded π-conjugation, and it was attributed to a strong ICT from the coumarin moiety to the hemicyanine group. Upon the addition of CN^-, the intensity of the absorption band at **434** decreased, whereas a new peak appeared at 415 nm. An obvious change from purple to pale yellow was observed. Moreover, the fluorescence spectrum of **434** with CN^- showed a decreased in the intensity of the emission band at 630 nm, whereas an increase in the fluorescence at 514 nm was seen. These changes were attributed to a CN^- nucleophilic attack to the indolium group, resulting in an interruption of the π-conjugation which blocked the ICT process and led to a recovery of the emission of the coumarin moiety. Using emission changes, a limit of detection of 0.6 x 10^{-6} mol L^{-1} was determined for CN^-. Finally, studies with other anions (i.e., F^-, Cl^-, Br^-, I^-, AcO^-, SCN^-, N_3^-, ClO_4^-, NO_3^-, SO_4^{2-}, PO_4^{3-}, CO_3^{2-}, HCO_3^-, HSO_4^-, S^{2-} and $H_2PO_4^-$ and Cys) did not lead to any significant optical change.

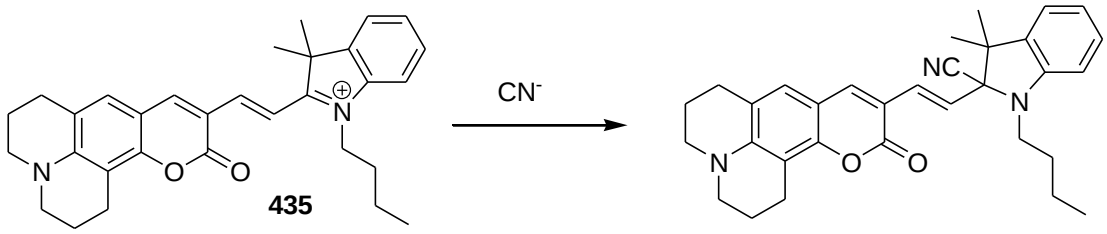

Fig. 223 Chemical reaction of probe **435** with CN^-.

The next example shows a similar probe for CN^- detection.[280] Compound **435** (see Fig. 223) presents a characteristic UV-Vis absorbance at 609 nm in H_2O:CH_3CN 5:95 v/v. In the presence of CN^-, the absorption at 610 nm disappeared with the concomitant growth of a new band at 409 nm. Fluorescence measurements displayed a remarkable increase in the emission at 484 nm (λ_{ex} = 410 nm) upon the addition of CN^-. As before, optical changes were attributed to a nucleophilic attack of CN^- to the indole group. Addition of other anions (i.e., F^-, Cl^-, Br^-, I^-, AcO^-, HSO_4^-, HPO_4^{2-}, HCO_3^-, NO_3^-, ClO_4^- and SCN^-) induced no response.

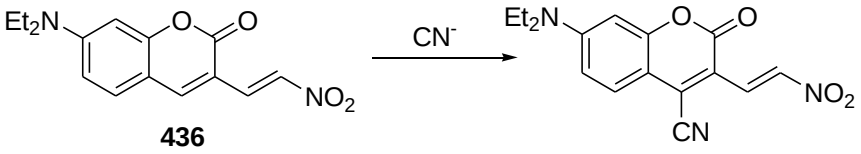

436

Fig. 224 Chemical reaction of probe **436** with anion CN^-.

Coumarin-based chemodosimeter **436** (see Fig. 224) was used for the chromo-fluorogenic sensing of anion CN^- in CH_3CN.[281] Solutions of **436** presented an intense absorption band at 468 nm, whereas it was weakly fluorescent with an emission maximum at 468 nm when excited at 390 nm. The authors studied the UV-visible and fluorescent behaviour in the presence of selected anions (i.e., F^-, Cl^-, Br^-, I^-, CN^-, N_3^-, HPO_4^{2-}, AcO^-, and HSO_4^-). Of all the anions tested, only CN^- was able to induce a marked decrease in the absorbance band, while a new maximum at 550 nm appeared (colour change from pale yellow to pink). In addition, a 5-fold enhancement in the emission was also observed. Optical changes were ascribed to a Michael addition.

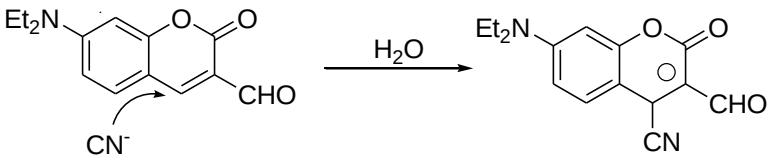

437

Fig. 225 Chemical reaction of receptors **437** with anion CN^-.

A Michael addition was also used for the sensing of CN^- using coumarinyl aldehyde **437** (see Fig. 225).[282] H_2O solutions of receptor **437**, buffered at pH 7.4, showed an intense absorption at 446 nm, which decreased and vanished after 120 minutes upon the addition of anion CN^-. Moreover, the emission intensity of **437** at 503 nm (excitation at 455 nm) was quenched (25-fold) with the addition of CN^-. The response obtained was highly selective and the other anions tested (i.e., F^-, Cl^-, Br^-, I^-, N_3^-, HPO_4^{2-}, AcO^-, and HSO_4^-) were unable to induce any noticeable optical response.

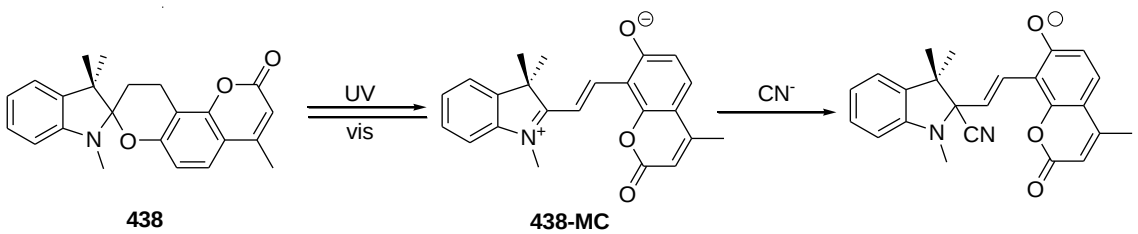

438 **438-MC**

Fig. 226 Proposed chemical reaction mechanism of probe **438** with anion CN^-.

Shirashi and co-workers reported the use of spirobenzopyran **438** (see Fig. 226) for the selective detection of anion CN^-.[283] H_2O:CH_3CN 8:2 v/v solutions of **438** buffered at pH 9.3 and irradiated at 334 nm presented an intense absorption band at 528 nm due to the formation of

merocyanine isomer **438-MC**. Of all the anions tested (i.e., CN^-, F^-, Cl^-, Br^-, I^-, $H_2PO_4^-$, HSO_4^-, AcO^-, ClO_4^- SCN^- and NO_3^-), only CN^- was able to induce a marked decrease of the absorption band with a change in colour from pink to colourless. This change in colour was ascribed to a nucleophilic addition to the spyrocyclic carbon. Additionally, **438-MC** was weakly emissive (upon excitation at 309 nm), but the addition of CN^- induced the appearance of an intense emission at 453 nm which was ascribed to the coumarin moiety.

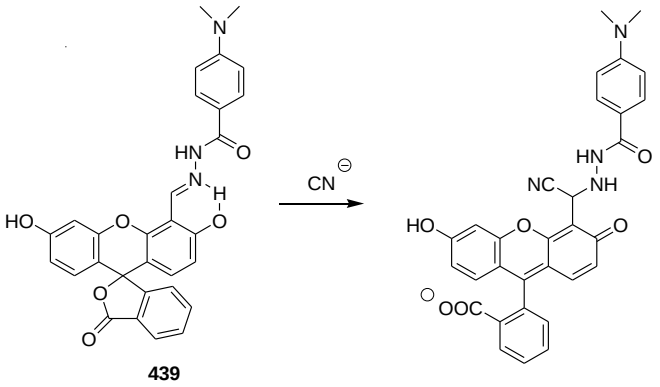

439

Fig. 227 Chemical reaction of probe **439** with anion CN^-.

Probe **439** (see Fig. 227) was designed to involve three parts: a 4-(*N*,*N*-dimethylamino)benzamide energy donor, a salicylaldehyde hydrazone binding unit; a fluorescein spirolactone unit (a potential energy acceptor).[284] CN^- detection using **439** was achieved in DMF:H_2O 9:1 v/v solutions in a pH range from 4 to 8. In the absence of CN^-, the fluoresceine moiety adopted a closed non-fluorescent form, showing an absorption band at 350 nm. The addition of CN^- induced a marked decrease of the 350 nm band, whereas the absorption at 515 nm increased. The fluorescence spectrum of **439** exhibited a blue emission of the donor at 450 nm and a weak yellow emission of the acceptor at 530 nm. Addition of CN^- induced a decrease in the donor emission at 450 nm and an increase of the emission of the acceptor. The changes observed were induced by a nucleophilic CN^- addition to the activated hydrazone. This was followed by a fast proton transfer of the acidic phenol proton to the nitrogen anion, which led to a ring-opening in the fluoresceine spirolactone. A limit of detection of 4.4 x 10^{-7} mol L^{-1} was observed for CN^-. Compound **439** was evaluated in the presence of other anions (F^-, Cl^-, Br^-,I^-, AcO^-, SCN^-, N_3^-, ClO_4^-, NO_3^-, SO_4^{2-} and $H_2PO_4^-$), yet only F^-, AcO^- and $H_2PO_4^-$ induced minor optical changes.

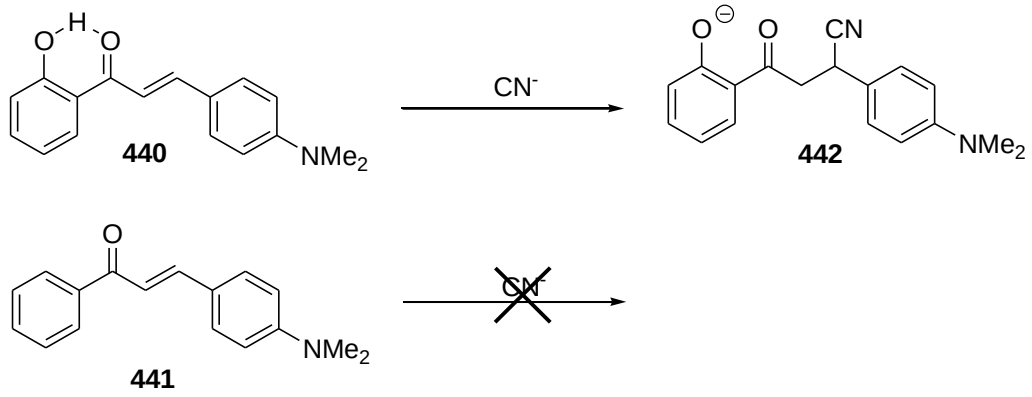

440 **442** **441**

Fig. 228 Chemical structures of receptors **440**-**441** and the reaction product (**442**) of **440** with anion CN^-.

S. Park and co-workers developed a new chemodismeter for the cyanide anion based on the turn-on of fluorescence upon a Michael addition reaction.[285] In particular, acetonitrile solutions of **440** (see Fig. 228) showed an absorption band at 430 nm which, upon the addition of increasing amounts of anion CN^-, decreased with the concomitant appearance of a new band at 260 nm (the colour of the solution changed from yellow to colourless). Acetonitrile solutions of **440** were non-fluorescent (excitation at 272 nm). However, addition of anion CN^- induced the growth of an emission at 469 nm. The presence of other selected anions (i.e., F^-, Cl^-, Br^-, I^-, N_3^-, HPO_4^-, HSO_4^- and AcO^-) induced negligible optical changes. The α,β-unsaturated carbonyl group (activated by an intramolecular hydrogen bond with the *o*-hydroxyl moiety) played a crucial role as a Michael acceptor and reacted fast with anion CN^- to afford an intermediate enol, which tautomersed to yield the highly fluorescent compound **442**. In fact, compound **441**, which did not bear the –OH moiety, was unable to react with cyanide.

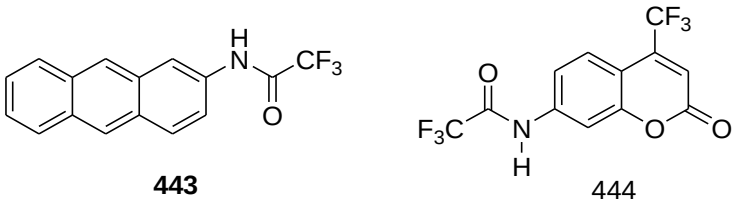

443 444

Fig. 229 Chemical structures of probes **443** and **444**.

Chemosensor **443** (see Fig. 229) was used as a ratiometric fluorescent sensor for anion CN^-.[286] CH_3CN solutions of **443** presented the typical broad structured emission of the anthracene fluorophore in the 375-450 nm range (upon excitation at 350 nm). Addition of increasing quantities of anion CN^- induced a marked decrease in anthracene emission with the simultaneous appearance of a new band at 503 nm. This optical change was attributed to the formation of two fluorescent derivatives: (i) one obtained upon a CN^- nucleophilic addition reaction with the amide carbonyl moiety (ii) and a second one arising from the CN^--induced deprotonation of the N-H amide group. Addition of HPO_4^{2-}, PO_4^{3-}, CO_3^{2-} and S^{2-} also induced the appearance of the emission band at 503 nm, but it was of lower intensity than that obtained for CN^-. The authors attributed this effect to some partial deprotonation of **443**. Meanwhile, addition of oxalate, AcO^-, Cl^-, ClO_4^-, $H_2PO_4^-$, HSO_3^-, SO_3^{2-}, SO_4^{2-} and I^- induced negligible changes in the emission profile.

A colorimetric and fluorescent CN^- probe based on 7-(trifluoroacetamido)coumarin **444** (see Fig. 229) was reported.[287] When several anions (i.e., CN^-, F^-, Cl^-, Br^-, I^-, AcO^- , $H_2PO_4^-$, HSO_4^-, ClO_4^- , NO_3^-, NO_2^-) were added to solutions of **444** in CH_3CN, only CN^-, F^-, AcO^- and $H_2PO_4^-$ induced the appearance of a new absorption at 389 nm, along with a concomitant decrease of the band at 327 nm. However, addition of Cl^-, Br^-, I^-, and HSO_4^- only led to minor hypochromic effects in the 327 nm band. Moreover, when the same anions were in the presence of **444** in CH_3CN:H_2O 4:1 v/v, only CN^- induced changes in the absorption and emission spectra, with decreased absorption at 327 nm and the formation of a new red-shifed band at 365nm. An increase in the emission intensity (30-fold) at 505 nm (λ_{ex} = 388 nm) was also observed. Job´s plots indicated the formation of 1:1 complexes. The limit of detection for CN^- was determined as

0.29 x 10^{-6} mol L^{-1} by fluorescent assays and of 1.18 x 10^{-6} mol L^{-1} by absorption studies. The changes in colour and fluorescence were ascribed to a nucleophilc addition reaction of anion CN^- to the carbonyl moiety of the trifluoroacetamido group.

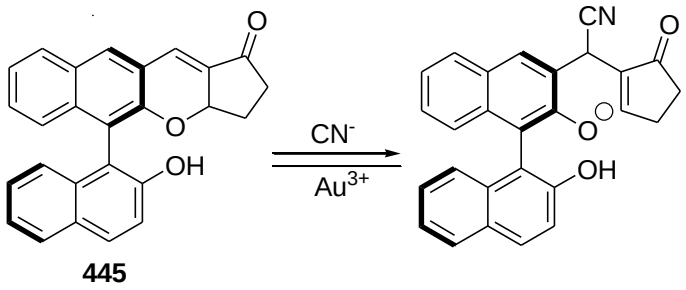

445

Fig. 230 Chemical reaction of probe **445** with anion CN^-.

Dong and co-workers prepared and studied the photochemical properties of a new reversible chemodosimeter for anion CN^- based on a BINOL signalling unit (**445**).[288] Specifically, when acetonitrile solutions of **445** (see Fig. 230) were treated with a series of different anions (i.e., F^-, Cl^-, Br^-, I^-, HSO_4^-, NO_3^-, AcO^-, $H_2PO_4^-$, N_3^-, ClO_4^-, BF_4^-, SCN^-, CN^-, $CF_3SO_3^-$, Cys and Hcy), only CN^- was able to induce appreciable changes in the absorption and emission spectra. CH_3CN solutions of **445** showed a band at 334 nm which was red-shifted to 375 nm upon the addition of CN^-. In addition, the emission band at 364 nm (excitation at 295 nm) of **445** was quenched by anion CN^-. The sensing mechanism, confirmed by NMR and MS studies, was based on the nucleophilic attack of the cyanide anion to a double bond of **445,** inducing a conjugated ring-opening reaction. Finally, the author demonstrated the reversibility of the sensing process through the addition of Au^{3+}, which induced an intramolecular oxa-S_N2' cyclisation reaction to once again yield **445**.

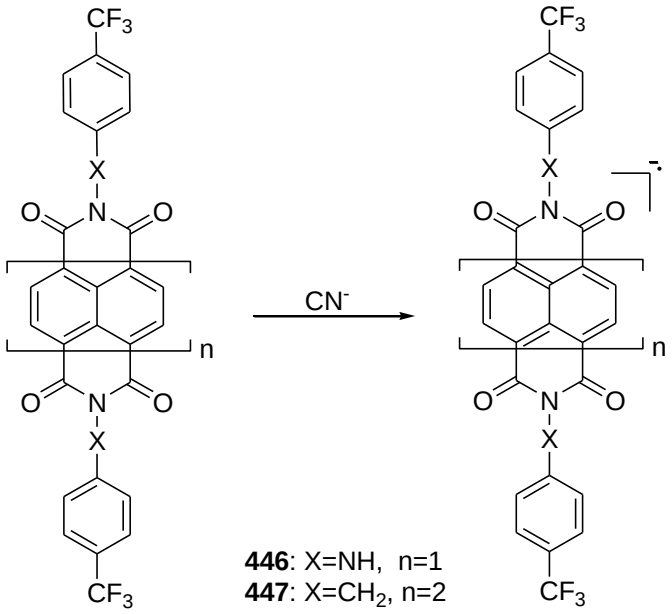

Fig. 231 Chemical reaction of probes **446** and **447** with anion CN^-.

S. Yadav and S. Ghosh reported the design of low-LUMO (LL) probes using naphthalene diimide (**446**) and perylen diimide (**447**) as receptors (see Fig. 231) for the detection of anion CN^-.[289] In

both receptors, addition of CN^- yielded an air stable radical due to a SOMO-LUMO electron transfer (from cyanide to the LL of the probe). In particular, when DMF:H_2O 97:3 v/v solutions of **446** were treated with CN^-, a change from colourless (358 and 377 nm absorption bands) to dark brown (470, 603, 701, 786 and 1100 nm absorption bands) was observed. Besides, addition of CN^- to THF:H_2O 97:3 v/v solutions of **447** resulted in a colour change from orange (485 nm) to turquoise blue (absorption bands at 699, 761, 794, 952 and 1100 nm) and in complete fluorescence quenching (broad emission bands in the 500-700 nm interval upon excitation at 485 nm were observed for **447**). Both ligands were also treated with other reducing anions such as $S_2O_3^{2-}$, $S_2O_4^{2-}$, $Fe(CN)_6^{4-}$, NO_2^- and SO_3^{2-} to assess selectivity to cyanide. Finally, the authors prepared thin films of **447** by vapour deposition onto glass surfaces and used the probe to detect cyanide in non-polar and aqueous solvents.

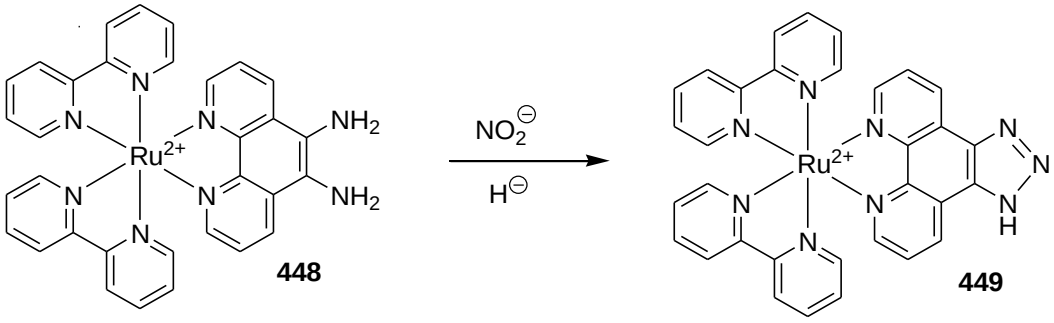

Fig. 232 Chemical reaction of the Ru^{2+}-polypyridyl-based complex **444** with anion NO_2^-.

The Ru^{2+}-polypyridyl-based complex (**448**) was used for the detection of ion NO_2^- in aqueous solution and NO in the gas phase (see Fig. 232).[290] In acid media, anion NO_2^- produced N_2O_3, whereas NO was converted into N_2O_3 in the presence of O_2. N_2O_3 could react with **448** to form the triazole-based complex **449**. In order to detect NO_2^-, N_2O_3 gas produced by reacting a saturated solution of $NaNO_2$ and 1 N HCl, was allowed to pass through a 1 N hydrochloric acid solution of complex **448** (CH_3CN:H_2O 1:9 v/v) in a closed glass vessel; a colour change from orange to brown was visually detected. Moreover, through the changes of the emission intensity at 620 nm (λ_{exc} = 440 nm), a limit of detection of 2 x 10^{-3} mol L^{-1} was calculated. Detection of NO gas was assayed by purging gas onto an acidic solution of complex **448** in the same solvent, which produced the same optical change. Other analytes (H_2O_2, OCl^-, NO_3^-, $ONOO^-$, O_2^-) were tested and no optical modulations were observed.

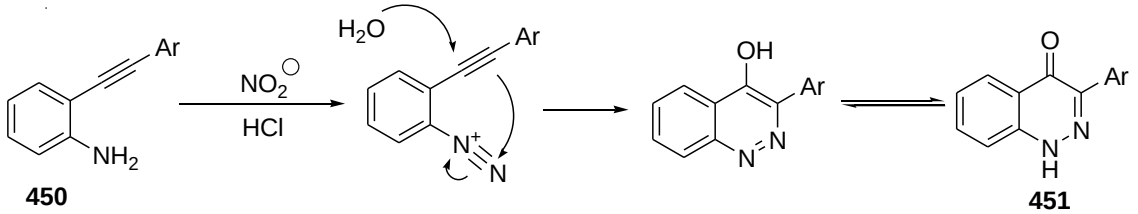

Fig. 233 Chemical reaction of 2-arylethynyl aniline derivative **450** with anion NO_2^-.

A new method for the detection of anion NO_2^- using a family of 2-arylethynyl aniline derivatives (**450**) was reported.[291] The authors exploited the ability of anion NO_2^- to form diazonium salts in an acidic ambient which, in this case, was additionally coupled with the subsequent intramolecular annulation reaction to give the final 4(1*H*)-cinnolone derivative **451**

(see Fig. 233). An acidic solution and low temperatures were required to produce these reactions. In a typical experiment, a water solution of **450** was first treated with HCl 2N (temperature in the 0-5°C range) and then anion NO_2^- was added to observe a colour change from colourless to yellow due to the formation of **451**. The other anions tested (i.e., F^-, Cl^-, Br^-, I^-, NO_3^-, AcO^-, N_3^-, SCN^-, SO_4^{2-} and PO_4^{3-}) induced no colour changes. Moreover, if the aryl group in **450** was a methoxynaphthyl moiety, the starting aryl ethynyl aniline showed a strong fluorescence emission at 401 nm (excitation at 315 nm), which was selectively quenched by anion NO_2^-. A limit of detection of less than 1 ppm was calculated.

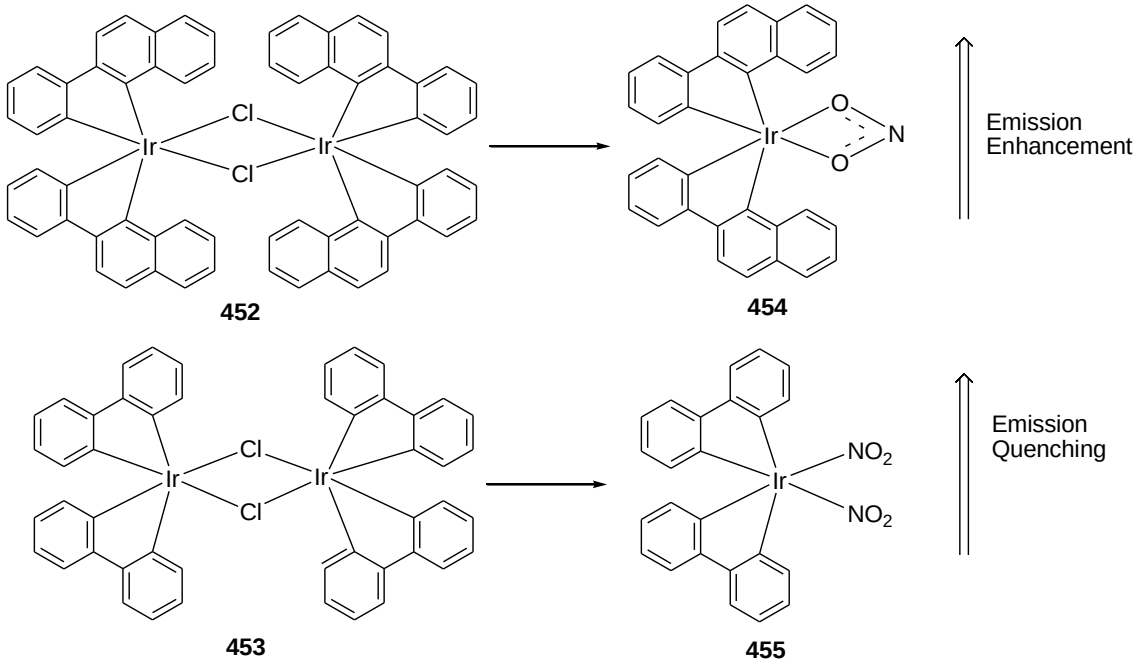

Fig. 234 Chemical structures and reactions of diiridium complexes **452** and **455** with anion NO_2^-.

Tetrakis(2-phenylquinoline-C_2,N')(μ-dichloro)diiridium complexes (**452** and **455**, see Fig. 234) were used to sense anion NO_2^-.[292] The chromo-fluorogenic behaviour of **452** and **453** towards selected anions (F^-, Cl^-, Br^-, I^-, NO_3^-, $H_2PO_4^-$, SO_4^{2-}, CO_3^{2-} and NO_2^-) was studied in CH_3CN:H_2O 1:1 v/v solutions buffered at pH 7.1. Both receptors presented a broad absorption band at 430 and 380 nm for **452** and **453**, respectively. Of all the anions tested, only NO_2^- induced the appearance of new absorptions at 353 (for **452**) and 360 nm (for **453**). Moreover, CH_3CN:H_2O 1:1 v/v solutions of **452** upon excitation at 430 nm showed an emission at 567 nm which was enhanced upon the addition of anion NO_2^-. These changes were ascribed to the coordination of one NO_2^- anion with the metal that yielded compound **454**. For receptor **453**, the emission band at 550 nm was quenched upon the addition of anion NO_2^- due to the formation of **455**.

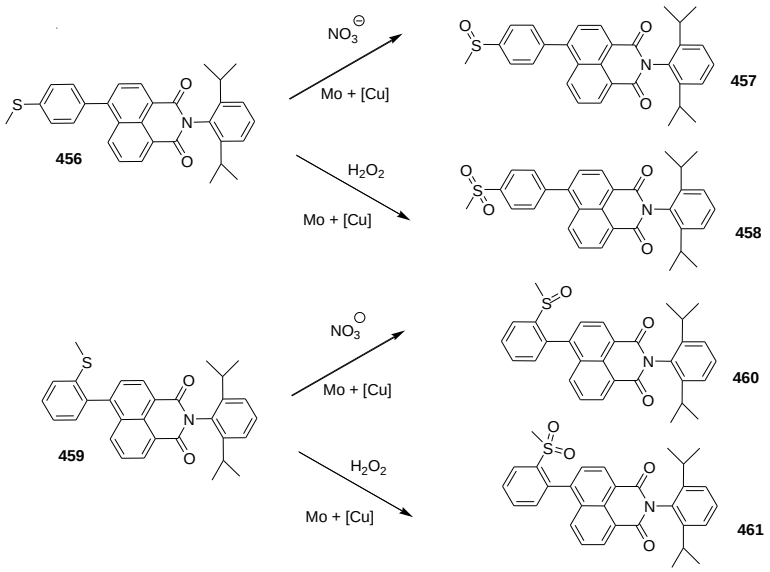

Fig. 235 Chemical structures of compounds **456-461** and reactions of probes **456** and **459** with anion NO_3^-.

Two thioether-based chemosensors (**456** and **459**, see Fig. 235) were used as probes for nitrate via a nitrate-induced selective sulphoxidation of the thioether groups (through an oxygen-transfer reaction) in the presence of a catalyst containing Cu^{2+} and Mo^{6+} (Mo-Cu).[293] By following this strategy, discrimination between nitrate salts and other oxidants such as H_2O_2 was achieved. The absorption and fluorescence spectra of **4526** showed bands at 370 nm and 540 nm, respectively, whereas compound **457** respectively displayed absorption and emission bands at 350 nm and 425 nm in CH_3CN. Addition of NO_3^- to a CH_3CN solution containing the Mo-Cu system produced the conversion of **456** into **457**. All nitrate salts induced the same result, whereas nitrite salts and common explosives such as TNT or RDX showed no response. Addition of H_2O_2 produced sulphone **458** with an emission band at 411 nm closely overlapping the emission of **457** at 425 nm. In order to avoid this problem, compound **459** was prepared. In this case, the nitrate-based oxidation of **459** to sulphoxide **460** revealed a significant red shift in the emission spectrum from 425 nm to 492 nm, unlike the blue-shift response observed in the sulphoxidation of **456**. Furthermore, oxidation of **459** to sulphone **461** using H_2O_2 led to a major reduction in the fluorescence emission.

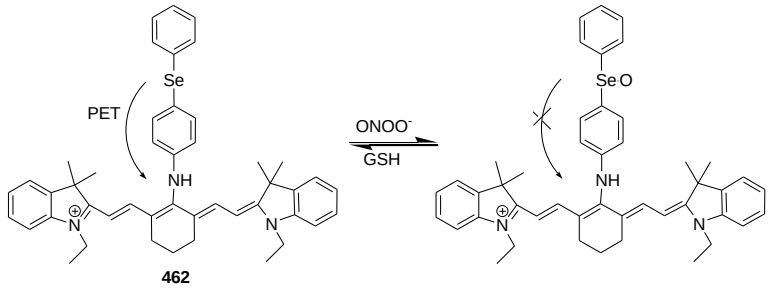

Fig. 236 Chemical reaction of receptor **462** with the peroxynitrite anion.

The authors designed a near-IR reversible fluorescent probe containing an organoselenium functional group for the reversible detection of peroxynitrite ($ONOO^-$) under physiological conditions.[294] The probe (**462**, see Fig. 236), containing a cyanine dye as a signal transducer and a 4-(phenylselenyl)aniline as a modulator, displayed absorption and weak fluorescence at

758 and 800 nm in PBS (pH 7.4), respectively. The fluorescence in **462** was quenched as a result of a PET between the modulator and the transducer. In the presence of $ONOO^-$, the Se atom was oxidised, causing an increase in the intensity and a blue shift of the fluorescence emission from 800 nm to 775 nm. High selectivity was observed to $ONOO^-$ vs. other reactive oxygen species and thiols. A reversible oxidation-reduction cycle was achieved with the addition of $ONOO^-$ and glutathione (GSH) as an oxidising and reducing agent, respectively. Finally, the authors used probe **462** to monitor $ONOO^-$ in living cells.

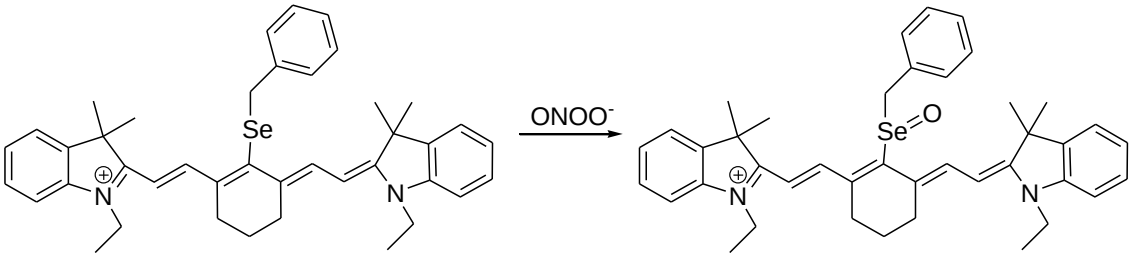

463

Fig. 237 Chemical reaction of probe **463** with the peroxynitrite anion.

Other authors independently used a similar compound (**463**, see Fig. 237) to detect $ONOO^-$ in water and in living cells by means of a similar mechanism to that described above.[295] The aqueous solutions of **463,** buffered at pH 7.4, showed an intense emission band at 800 nm (excitation at 700 nm), which was quenched selectively by anion $ONOO^-$ (5-fold).

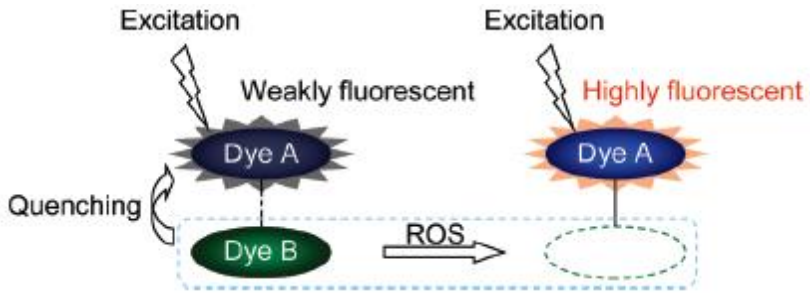

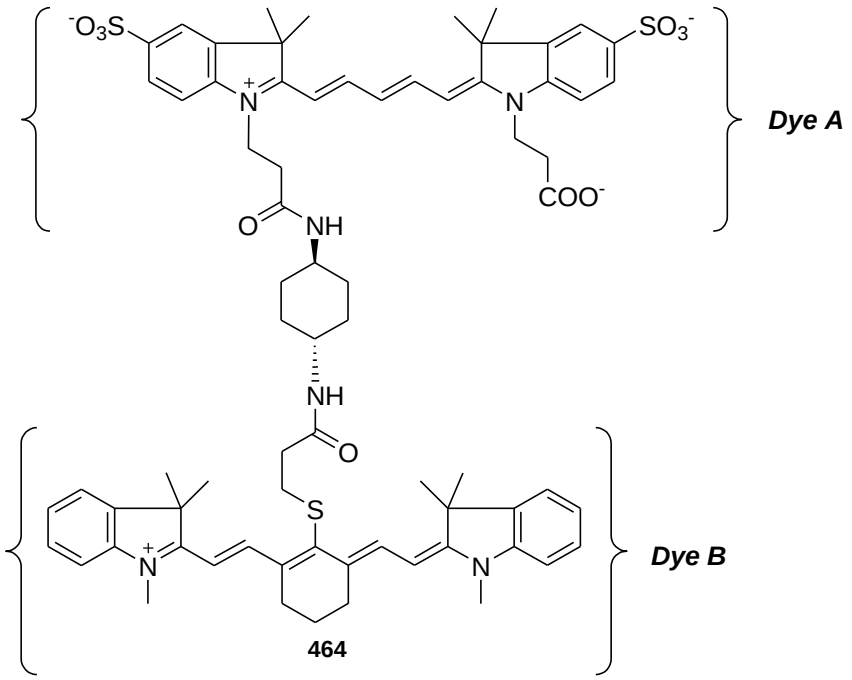

Fig. 238 Chemical structure of **464** and its use as a sensing probe for ROS.

Oushiki and co-workers developed a new off-on NIR-fluorescent chemodosimeter for the *in-vivo* imaging of ROS (Reactive Oxygen species).[296] Specifically, the authors developed a sensor (**464**) based on the coupling of two different cyanine dyes showing a different reactivity towards ROS (see Fig. 238). The designed probe consisted of two main components, a less ROS-susceptible dye (dye A) as a fluorophore and a highly ROS-susceptible dye (dye B) as a ROS-sensitive fluorescence modulator, connected by a linker. Aqueous solutions of receptor **464**, buffered at pH 7.4, showed a very weak emission at 668 nm upon excitation at 645 nm. The very weak emission of **464** was ascribed to the quenching of dye A by dye B via a FRET mechanism. Addition of ROS ($^{\cdot}OH$, $ONOO^-$, ^-OCl, $^1O_2$, $^-$ and $O_2^{\cdot-}$) induced a remarkable emission enhancement at 668 nm (ascribed to dye A) due to the inhibition of the FRET process resulting from the reaction of the target analytes with dye B. Having demonstrated the *in vitro* reactivity of **464**, the authors tested the probe for the intra-cellular imaging of ROS and also for the *in vivo* imaging of oxidative stress.

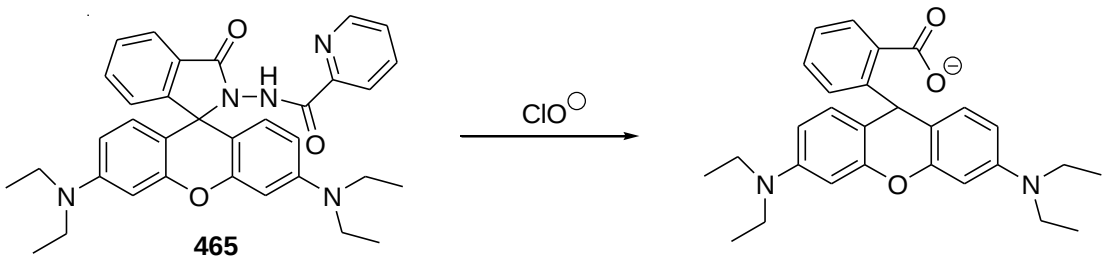

Fig. 239 Chemical structures of probe **465** and the reaction with anion ClO^-.

Chemosensor **465** (see Fig. 239), containing a signalling rhodamine B unit and a diacylhydrazine reactive moiety for ClO^- sensing, was described.[297] $CH_3CH_2OH:H_2O$ 7:3 v/v (buffered at pH 12.0) solutions of **465** showed a very weak emission at 580 nm (due to the spirolactam form of the rhodamine fluorophore) upon excitation at 515 nm. Addition of ClO^- induced a 420-fold increase in the emission intensity at 580 nm due to the opening of the spirolactam ring, which yielded the corresponding highly fluorescent carboxylate derivative. A limit of detection as low as 1 x 10^{-9} mol L^{-1} was determined for ClO^-. The other anions (i.e. ,Cl^-, NO_3^-, SiO_3^{2-}, SO_4^{2-}, AcO^-, $H_2PO_4^-$, ClO_3^- and MnO_4^-) induced no response.

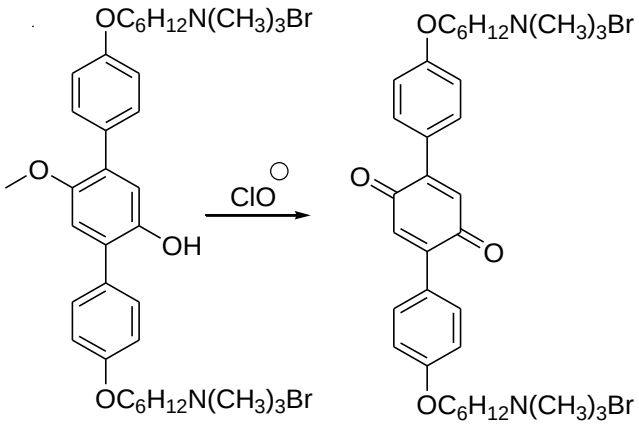

466

Fig. 240 Chemical structure of probe **466** and the reaction with anion ClO^-.

The authors reported ClO^- signalling by using a simple oxidation of a *p*-methoxyphenol derivative (**466**) in PBS (pH 7.4), which resulted in both colorimetric and fluorescent changes (see Fig. 240).[298] **466** exhibited a band centred at 314 nm, which decreased upon the addition of ClO^-, with the concomitant appearance of a new absorbance at 393 nm (colour change from colourless to yellow). Moreover, **466** displayed a decreased emission intensity at 388 nm (λ_{exc} = 320 nm) after adding ClO^-. A limit of detection of 0.8 x 10^{-6} mol L^{-1} was reported for ClO^-. The oxidation of p-methoxyphenol to benzoquinone by ClO^- was confirmed by ^{1}H-NMR studies. Finally, reactivity of **466** to other ROS (H_2O_2, $O_2^{\cdot-}$, NO, $^{\cdot}OH$, $ONOO^-$) was studied, but none induced any noticeable optical change.

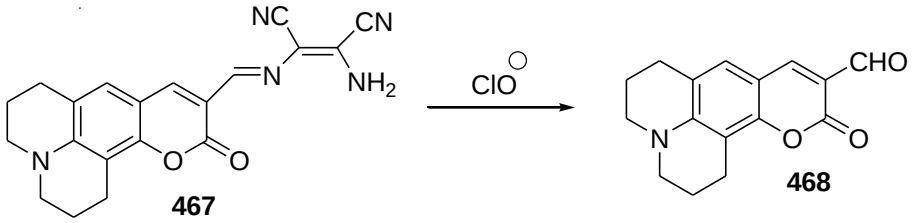

467 **468**

Fig. 241 Chemical reaction of probe **467** with with anion ClO^-.

A novel ClO^- probe (**467**), based on a diaminomaleonitrile elimination reaction selectively mediated by this anion, was described (see Fig. 241).[299] The free probe in PBS:DMF 8:2 v/v (pH 7.4) displayed an emission peak at 585 nm (λ_{exc} 540 nm). Upon the titration with ClO^-, emission intensity gradually decreased with the simultaneous appearance of a new blue-shifted

fluorescence at 505 nm. This blue shift was also observed in the absorption spectra. Transformation of probe **467** into compound **468** was confirmed by ^{1}H-RMN studies. In the presence of several anions (i.e., F^-, SO_4^{2-}, HCO_3^-, NO_2^-, NO_3^-, SO_3^{2-}, Cl^-, I^- and PO_4^{3-}) and cations, the probe did not show optical changes, whereas ROS species (H_2O_2, $OH^·$ and CH_3CO_3H) induced a very modest response. Finally, the probe was tested for the ratiometric imaging of ClO^- in living cells.

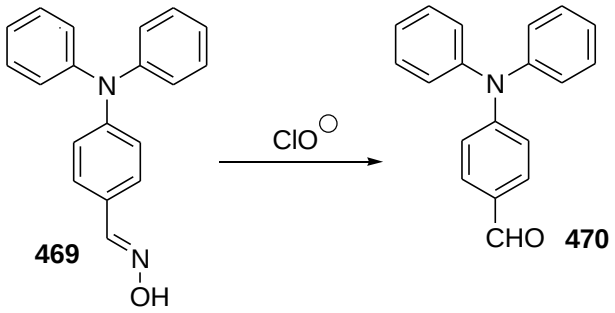

Fig. 242 Chemical structure of probe **469** and the reaction with anion ClO^-.

A new chemosensor for the detection of ClO^- was reported based on the reaction of this anion with triphenylamine derivative **469**, whose oxime moiety was able to react with hypochlorite to give the corresponding aldehyde **470** (see Fig. 242).[300] DMF:potassium phosphate buffer (pH 9.0) 4:1 v/v solutions of **469** showed an intense emission at 458 nm upon excitation at 339 nm. Addition of ClO^- induced significant fluorescence intensity quenching with a moderate blue shift of the band. Addition of ClO_4^-, NO_2^-, Cl^-, AcO^-, ClO_3^-, CO_3^{2-} and SO_4^{2-} induced negligible changes in the emission profile.

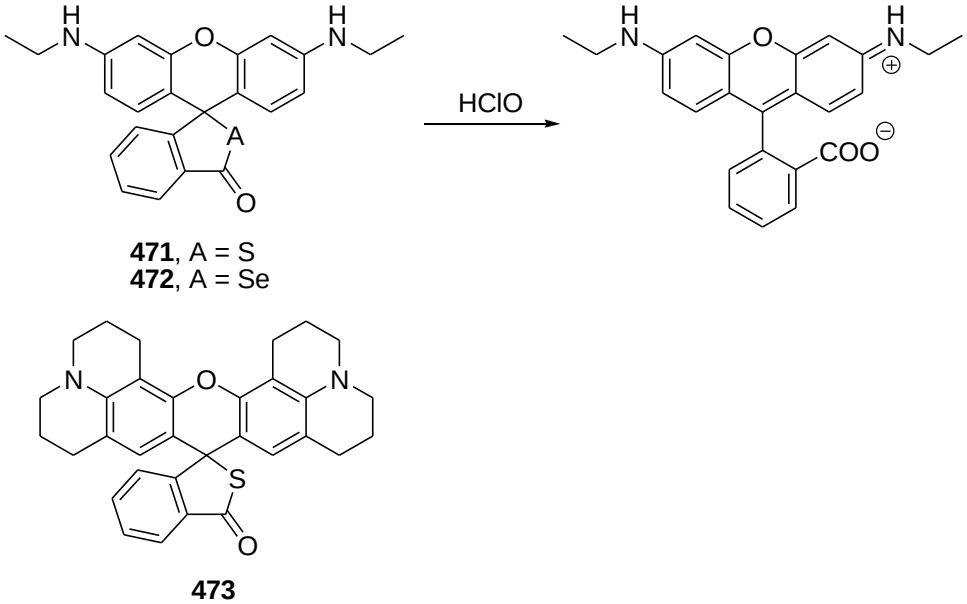

Fig. 243 Chemical structures of probe **471-473** and the reaction of **471** and **472** with ClO^-.

Rhodamine derivatives **471**-**473** were used for the detection of ClO^- (Fig. 243).[301] H_2O-CH_3CN 99:1 v/v solutions (buffered at pH 5.5 with KH_2PO_4) of receptor **471** were non-emissive upon

excitation at 515 nm. Of all the reactive oxygen species added (ClO^-, H_2O_2, NO·, ·OH, ROO·, $ONOO^-$ $\cdot O_2^-$ and $^1O_2$) only ClO^- is able to induce the appearance of a broad emission band at 550 nm. The new emission band was ascribed to the ClO^--induced thiolactone ring opening. The same selective emission enhancement upon addition of ClO^- was observed for chemodosimeters **472** and **473**. Finally, **471** was used for the visualization of phagosomal and mucosal ClO^- production in a variety of cellular contexts.

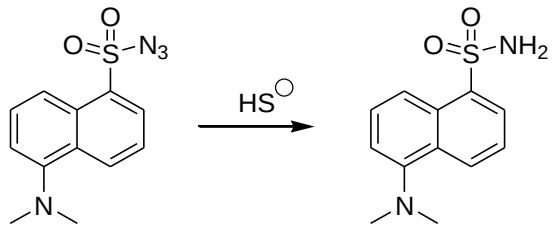

474

Fig. 244 Chemical structure of probe **474** and the reactions with anion HS^-.

Probe **474** (see Fig. 244) was able to detect HS^- in aqueous solutions, and also in blood serum and whole blood samples.[302] **474** itself was non-fluorescent. However, upon the addition of HS^- a strong fluorescence enhancement at 493 nm (λ_{exc} 340 nm) in phosphate buffer (pH 7.5, 0.5% Tween-20) was found. Besides, **474** was very selective for HS^- among the other anions tested (i.e., F^-, Cl^-, Br^-, I^-, OH^-, AcO^-, CN^-, N_3^-, NO_2^-, HCO_3^-, HSO_3^-, SO_4^{2-}, $S_2O_3^{2-}$, $S_2O_5^{2-}$, HPO_4^{2-} and citrate), with a limit of detection of 1×10^{-6} mol L^{-1}. Finally, **474** was used to detect HS^- in mouse blood using a C57BL6/J mouse model.

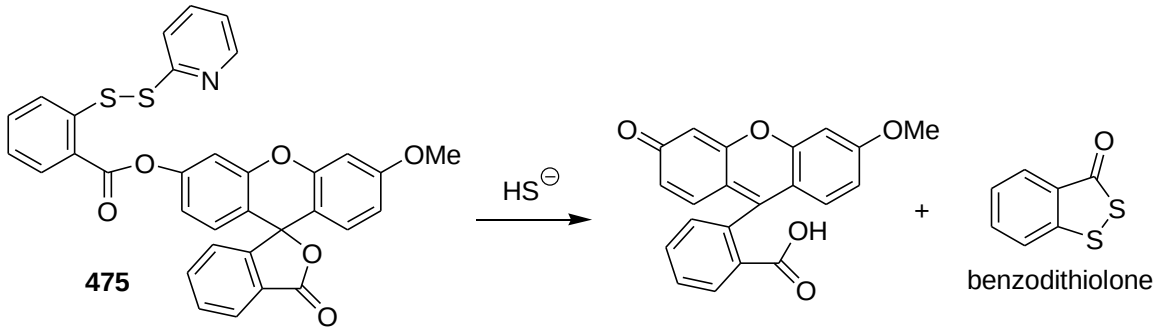

475

Fig. 245 Chemical structure of probe **475** and the reaction with anion HS^-.

Derivative **475** (see Fig. 245) was also designed to detect HS^-.[303] The probe contained an electrophile capable of reacting with anion HS^- and an ester group in a suitable position, which underwent spontaneous cyclisation, leading to the release of a fluorophore. This reaction was selective for HS^- and did not proceed with other biological thiols such as Cys and GSH. Particularly, aqueous solutions of **475,** buffered at pH 7.4, showed a weak fluorescence band at 515 nm when excited at 465 nm. Addition of HS^- induced a 77-fold enhancement of emission intensity. The efficiency of this probe for HS^- detection was demonstrated in both plasma and cells (COS7). Using this strategy, the HS^- concentration can be not only measured by the fluorescence signal, but also assessed with the analysis of the benzodithiolone product.

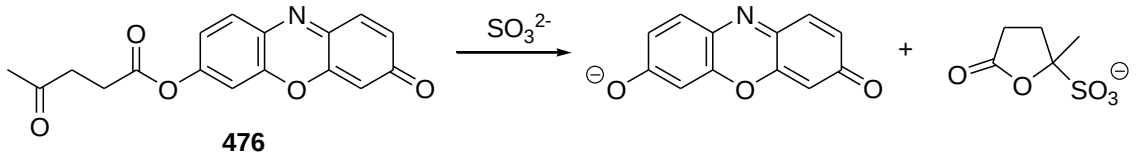

Fig. 246 Chemical reaction between **476** and anion SO_3^{-}.

The resorufin levulinate derivative (**476**) acted as a selective fluorogenic probe for SO_3^{2-} (see Fig. 246).[304] H_2O:CH_3CN 98:2 v/v solutions of **476** at pH 7 presented two absorption bands at 359 and 456 nm. The UV-vis behaviour of receptor **476** in the presence of selected anions (F^-, Cl^-, Br^-, I^-, SO_4^{2-}, HPO_4^{2-}, NO_3^-, N_3^-, AcO^-, ClO_4^-, HSO_4^- and SO_3^{2-}) was studied, but only SO_3^{2-} induced the appearance of a new red-shifted band at 571 nm (change in colour from yellow to pink). The same selectivity to SO_3^{2-} was found when fluorescence measurements were taken. The excitation of aqueous solutions of **476** at 487 nm yielded a weak emission band at 584 nm, which was enhanced (55-fold) and moderately red-shifted (4 nm) in the presence of anion SO_3^{2-}. The operation principle of this probe relied on the ability of SO_3^{2-} to selectively deprotect **476**. The cleavage of levulinate was affected by the initial attack of SO_3^{2-} to the carbonyl carbon at the 4-position of levulinate with the formation of a tetrahedral intermediate and subsequent intramolecular cyclisation leading to the cleavage of the ester function and to the generation of the resorufin fluorophore.

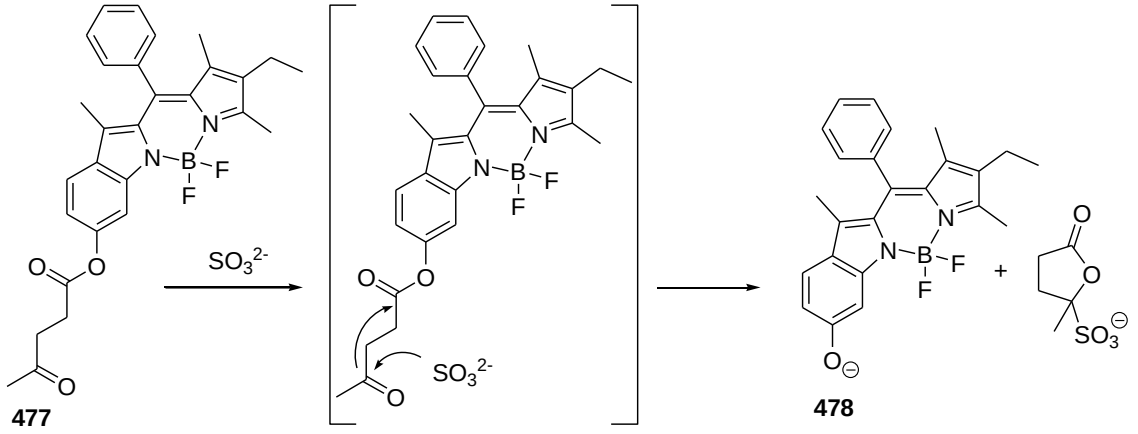

Fig. 247 Chemical reaction of probe **477** with anion SO_3^{-} and the formation of **478**.

Gu and co-workers prepared chromo-fluorogenic probe **477** for SO_3^{2-} which was based on a similar reaction (see Fig. 247). In this case, an indole-BODIPY was used as the signalling subunit, which was functionalised with a levulinate group as the reactive site (**477**).[305] **477** in H_2O:DMSO 1:1 v/v solutions showed an intense band at 510 nm which, upon addition of anion SO_3^{2-}, diminished together with the formation of a new absorption at 620 nm (change in colour from red to blue). Moreover, **477** showed intense emission at 553 nm which was gradually quenched with the concomitant appearance of a new fluorescence band at 647 nm upon the addition of anion SO_3^{2-}. By means of fluorescence measurements, the authors determined a limit of detection of 5.8×10^{-5} mol L^{-1} for SO_3^{2-}. None of the other anions tested (i.e., F^-, Cl^-, Br^-,

I^-, SO_4^{2-}, NO_3^-, HCO_3^-, SCN^-, $H_2PO_4^-$, N_3^-, NO_2^-, Cys and GSH) induced changes in either colour or emission. The selective cleavage of the levulinate ester induced by SO_3^{2-} yielded product **478,** which was responsible for the optical changes observed.

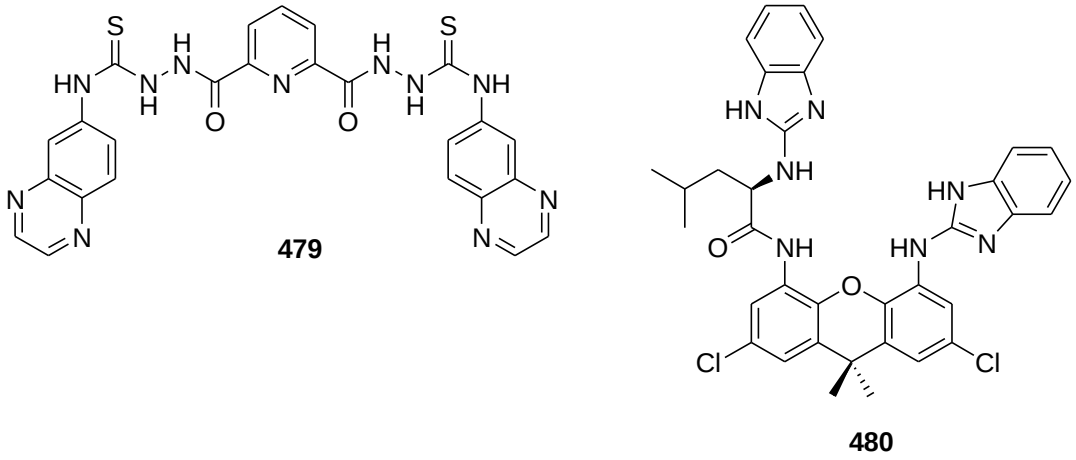

Fig. 248 Chemical structure of probes **479** and **480**.

Quinoxaline-containing probe **479** (see Fig. 248) was used for the chromo-fluorogenic sensing of AcO^-.[306] CH_3CN:DMSO 99:1 v/v solutions of **479** showed an absorption band due to the quinoxaline chromophore, centred at 338 nm. Addition of AcO^- induced an increase in the absorption together with a bathochromic shift to 490 nm. Excitation of **479** at 338 nm resulted in an emission at 464 nm, which was gradually quenched upon the addition of anion AcO^-. These spectroscopic changes were ascribed to a deprotonation of the thiourea N-H protons in **479** by the basic anion AcO^-. Unfortunately, the authors did not report anything about the optical response of receptor **479** in the presence of other anions.

Xanthene-benzimidazole receptor **480** (see Fig. 248) was used together with anthracenecarboxylic acid for the fluorescent sensing of anion Cl^-.[307] **480** and anthracenecarboxylic acid formed a weakly fluorescence 1:1 ensemble with an emission band centred at 470 nm in $CHCl_3$. Addition of Cl^- induced an hypsochromic shift of the emission band (20 nm) owing to an anion-induced proton transfer from anthracenecarboxylic acid to **480,** which yielded a ternary complex (anthracenecarboxylate-**480**-H^+-Cl^-). Addition of Br^- and I^- was unable to induce any change in the emission profile of the **480**-anthracenecarboxylic acid ensemble.

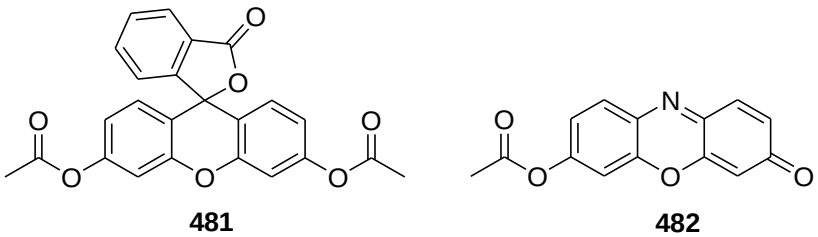

Fig. 249 Chemical structures of resorufin derivatives **481** and **482**.

Fluoresceine and resorufin derivatives **481** and **482** (see Fig. 249) were used as chromo-fluorgenic probes for anion BO_3^-.[308] H_2O:CH_3CN 9:1 v/v solutions (pH 4.8) of **481** presented

almost no absorption bands above 400 nm. Addition of anion BO_3^- induced the appearance of strong absorption at 491 nm with a colour change from colourless to bright yellow. Upon excitation of aqueous solutions of receptor **481** at 470 nm, an intense emission at 517 nm was observed. In this case, addition of anion BO_3^- induced a pronounced emission intensity enhancement. Adding other anions, such as F^-, Cl^-, Br^-, I^-, SO_4^{2-}, HPO_4^-, NO_3^-, N_3^-, AcO^-, ClO_4^- and HCO_3^-, resulted in negligible changes in the absorption and emission bands. The signalling mechanism took place by the BO_3^--induced deprotection of the diacetate moieties of **481**. The chromo-fluorogenic response of **482** was very similar to that shown by **481**. Addition of BO_3^- to H_2O:CH_3CN 9:1 v/v solutions (pH 4.8) of receptor **482** induced a colour change from amber (absorption band at 453 nm) to pink (new absorption band at 572 nm) and the appearance of a strong emission band at 590 nm (excitation at 487 nm).

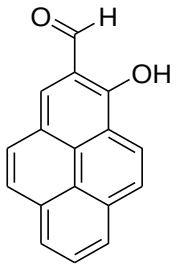

483

Fig. 250 Chemical structure of probe **483**.

The pyrene-based chromo-fluorogenic probe **483** (see Fig. 250) was used for the selective recognition of Lys.[309] In particular, H_2O:CH_3CN 9:1 v/v solutions of **483,** buffered at pH 7.4, presented the typical pyrene absorptions in the 250-350 nm range. Addition of Lys induced the formation of a broad absorption band in the 380-550 nm interval, which induced a colour change from yellow to pink. Addition of other amino acids (i.e., His, Ile, Met, Thr, Trp, Tyr, Val, Phe, Ser, Ala, Arg, Asn, Asp, Gln, Glu, Gly, Cys and Leu) induced negligible changes in the colour of **483** solutions. Moreover, Lys was also able to induce an increase in the emission intensity of **483** (band at 465 nm upon excitation at 380 nm), while other amino acids were unable to do this. Optical changes were ascribed to a reaction between Lys and the aldehyde moiety of **483,** which yielded an imine derivative.

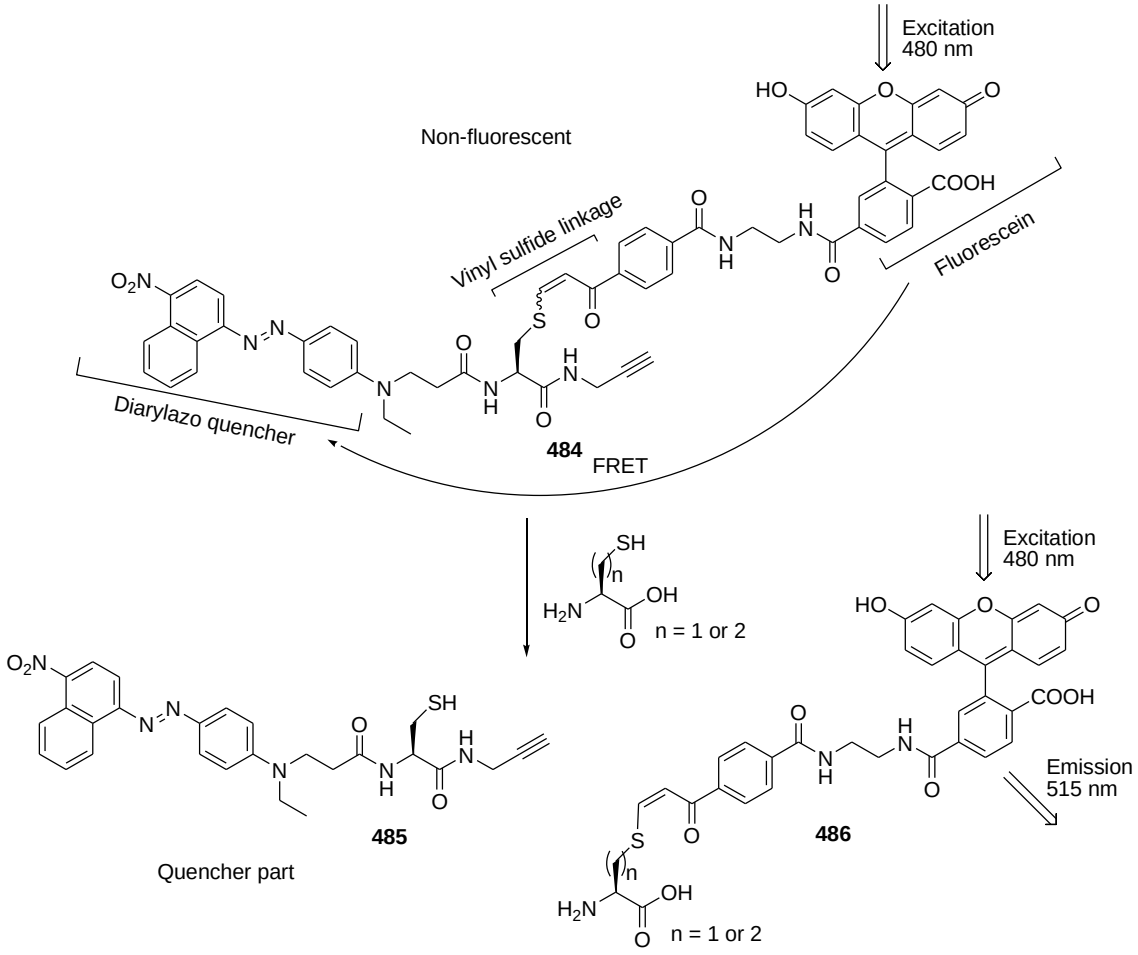

Fig. 251 Schematic representation of the FRET-based sensing system for the detection of Cys and Hcy using **484**.

Shiu et al. developed a FRET-based fluorescent system for the detection of Cys and Hcy[310] using compound **484** (see Fig. 251), which contained a fluorescent group (fluoresceine) and a quencher (diarylazo moiety) connected via a vinyl sulphide linkage. The fluorescence of **484** was very weak due to an active intramolecular fluorescent resonance energy transfer (FRET) mechanism. After treatment with thiols, the quencher unit was disconnected from the fluorescent probe through the cleavage of the vinyl sulphide linkage, via 1,4-addition of thiols to the α,β-unsatured vinyl sulphide bond. Consequently, fluorescence was turned on (30-fold increase in the emission at 515 nm). The rate of the conjugate addition to the vinyl sulphide double bond was dependent on the steric bulk of the nucleophilic thiol. Thus for instance, Hcy, which had a less hindered thiol, gave a stronger fluorescent signal than Cys. The authors performed all the sensing tests in H_2O:DMSO 9:1 v/v solution (buffered at pH 8.1) and determined that other amino acids, metal ions, reducing agents (NADH) and glucose did not result in any emission enhancement in **484**. In addition, the authors successfully applied probe **484** to sense Cys/Hcy in human blood and demonstrated the possibility of intracellular thiol determination.

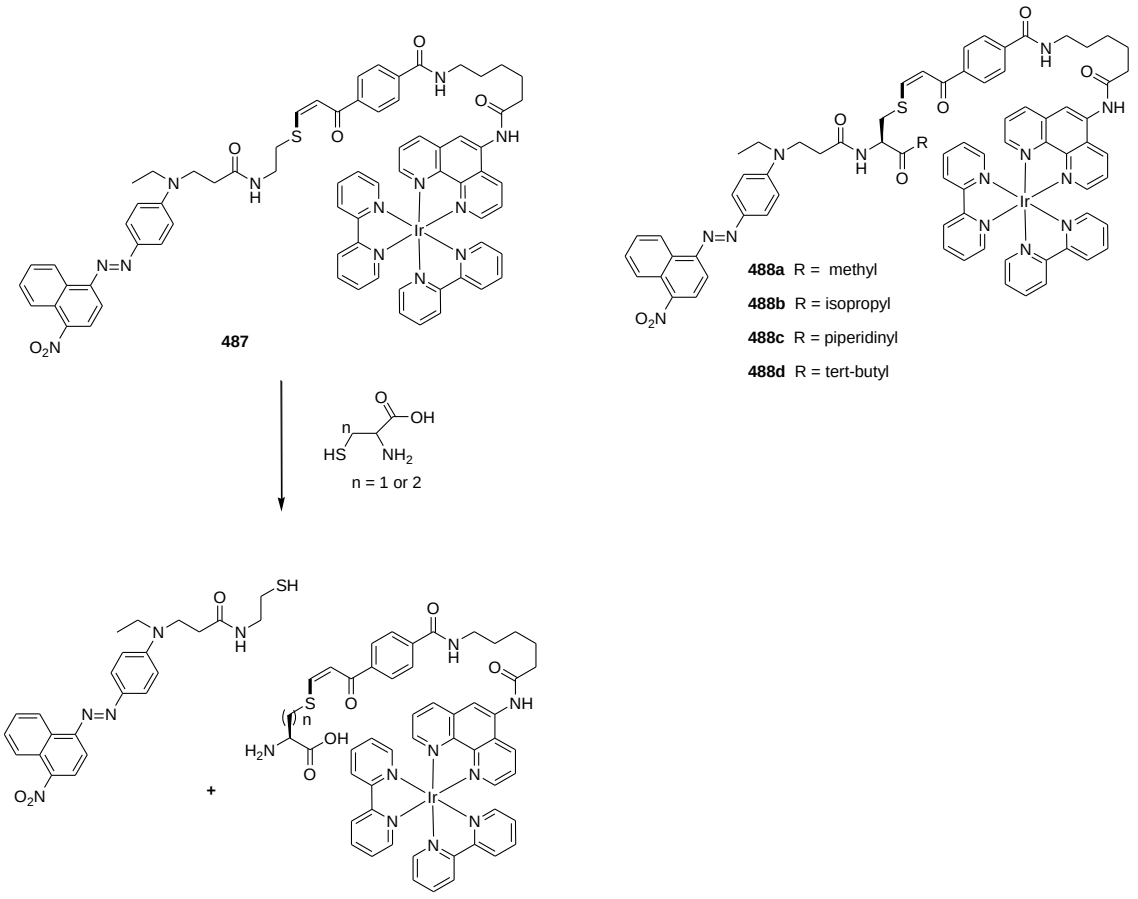

Fig. 252 Schematic representation of the elimination reaction using **487** for the detection of Cys and Hcy.

The same authors used a similar mechanism to detect Cys and Hcy, in this case by also coupling the addition of thiols to a vinyl sulphide linkage with a quencher elimination reaction.[311] Probe **487** (see Fig. 252) was weakly emissive, but addition of Cys/Hcy resulted in an enhanced emission at 590 nm (λ_{exc} 360 nm) in PBS:CH_3CN 1:3 v/v (pH 8.1). The emission maximum was observed after 15 min. Selectivity of the probe to thiols was tested in the presence of amino acids Cys, Hcy and GSH, and the emission enhanced in the order of Hcy > Cys >>> GSH in accordance with the steric bulkiness of these thiols. Based on these findings, the authors prepared probes **488a-d** to increase the steric hindrance of the environment around the reactive moiety. With these probes, Hcy was able to produce a much greater enhancement in emission intensity than Cys (for instance, a ratio of fluorescence Hcy:Cys of 5:1 was found using **488d**). Finally, the authors used the probes to detect Hcy and Cys in human blood plasma.

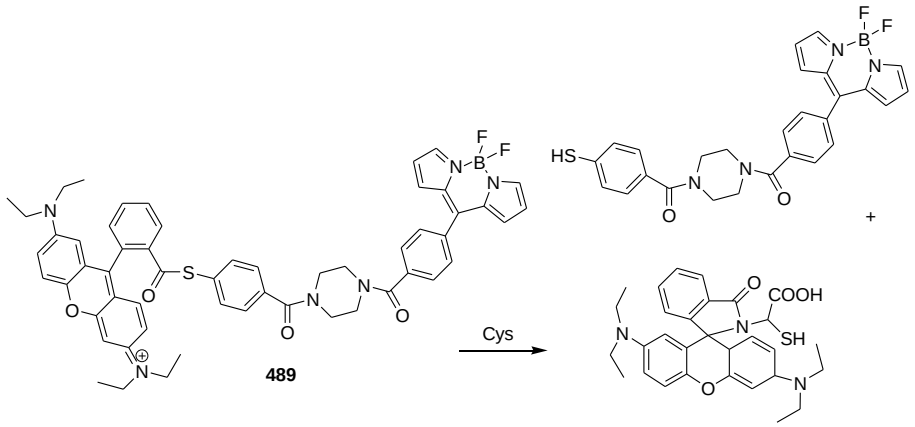

Fig. 253 Reaction of **489** with Cys.

Another FRET-based ratiometric thiol probe was designed by Yuan et al.[312] The probe contained a rhodamine dye, a thioester group, a piperazyl moiety and a BODIPY dye (**489**, see Fig. 253). The two dyes were selected by the authors after bearing in mind the strong overlap of the BODIPY emission with the absorption of rhodamine (forming a suitable FRET dyad), whereas the thioester group was used as a reactive site for thiols. The absorption spectrum of the probe in H_2O:CH_3CN 55:45 v/v (buffered at pH 7.4) presented the two typical bands centred at 500 nm and 562 nm for BODIPY and rhodamine, respectively, whereas only the emission of rhodamine at 590 nm (excitation at 470 nm) was observed. Upon the addition of Cys, the intensity of the rhodamine emission at 590 nm gradually decreased and the emission band of BODIPY at 510 nm was found, indicating that the FRET was inhibited. Furthermore, the fluorescence intensity ratios at 510 and 590 nm changed from 0.09 to 275 with the addition of Cys, showing a limit of detection of 8.2×10^{-8} mol L^{-1}. Selectivity of the probe to thiols over other biologically relevant species, such as amino acids (Phe, Ala, Gly, Glu, Arg, Lys, Tyr, Leu, Ser and Val), reactive oxygen species (H_2O_2) and NADH, was demonstrated. The authors used the probe to detect thiol-containing species in living cells.

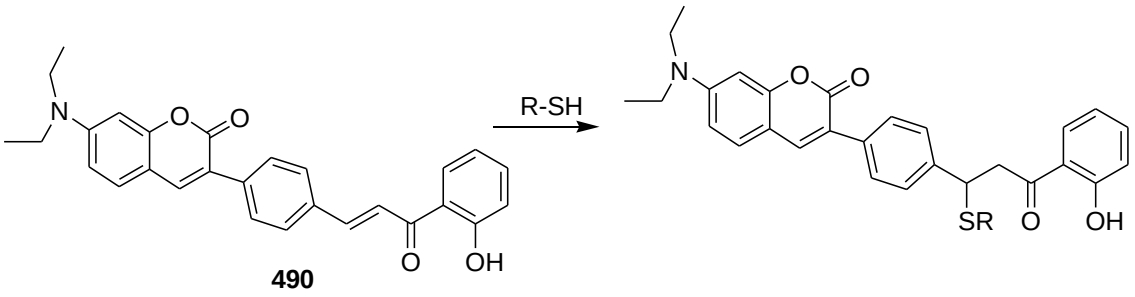

Fig. 254 Representation of the Michael addition reaction for the detection of GSH and Cys using **490**.

Coumarin-3-phenyl enone (**490**) was used for the selective and ratiometric detection of GSH and Cys over other natural amino acids through a Michael addition reaction (see Fig. 254).[313] **490** displayed an absorption band at 434 nm and a weak emission at 480 nm (λ_{exc} = 365 nm) in DMF:H_2O 3:1 v/v (buffered at pH 7.4). Upon the addition of GSH, the **490**-GSH conjugate

triggered a hypsochromic shift of the absorption band to 404 nm (with a colour change from yellow to colourless), whereas the emission intensity at 480 nm was enhanced. Cys also induced a significant fluorescence enhancement, but other amino acids (i.e., Pro, Ala, Val, Phe, His, Ser, Asp, Asn, Lys and Arg) gave no significant response. The limit of detection for GSH was 0.18 x 10^{-3} mol L^{-1}. Finally, probe **490** was able to visualise cellular GSH levels effectively.

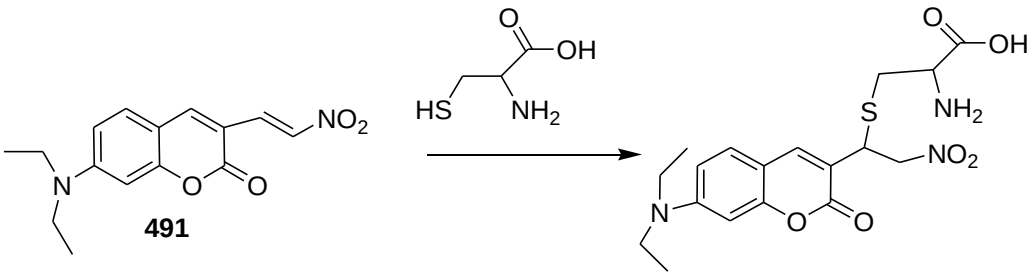

Fig. 255 Representation of the Michael addition reaction for the detection of bio-thiols using **491**.

Following a similar procedure, coumarin derivative **491** (see Fig. 255) was designed to detect bio-thiols using the Michael addition reaction to a nitroolefin.[314] In this case, a blue shift in the absorption of **491** from 483 nm to 400 nm was observed in CH_3CN:H_2O 1:1 v/v, (buffered at pH 7.4) upon the addition of Cys. Moreover, an enhancement in the emission intensity at 480 nm was also observed (λ_{exc} = 365 nm). A limit of detection of 8.6 x 10^{-7} mol L^{-1} for Cys was determined. The probe also exhibited a fast response and high selectivity to bio-thiols over other natural amino acids (i.e., Ala, Arg, Asn, Glu, Gln, Gly, His, Ile, Leu, Lys, Met, Phe, Pro, Ser, Thr, Trp, Tyr and Val). The probe was also used to image thiols in living cells.

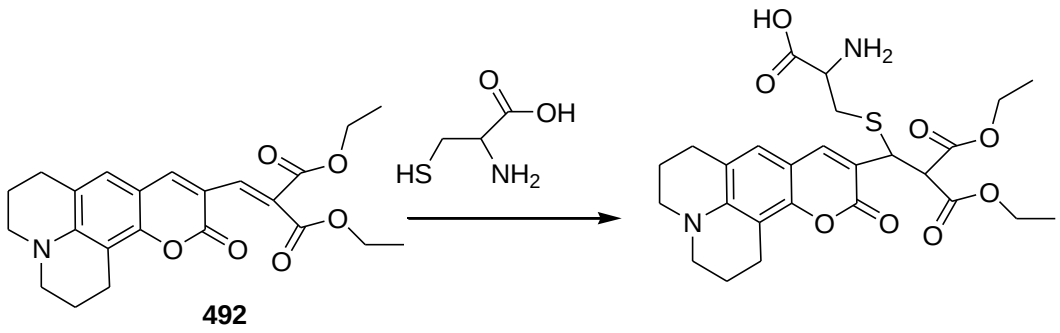

Fig. 256 Schematic representation of the Michael addition reaction for the detection of bio-thiols using **492**.

Another work, which also employed a coumarin-based probe for thiols, was reported by Kim et al.[315] In this case, addition of Cys to **492** (see Fig. 256) in H_2O:DMSO 9:1 v/v, buffered at pH 7.4, induced a 62-nm hypsochromic shift of the absorption maximum at 426 nm, resulting in a colour change from dark orange to green, while the fluorescence maximum at 502 nm (λ_{exc} = 440 nm) was enhanced by ca. 107-fold. A comparison of the reactivity of **492** to Cys, Hcy and GSH showed that **492** preferred Cys to the other biological thiols. This selectivity arose from

the lower pK_a value and the lower steric hindrance of Cys when compared with Hcy and GSH. Finally, probe **492** was tested to detect intracellular thiols by confocal microscopy.

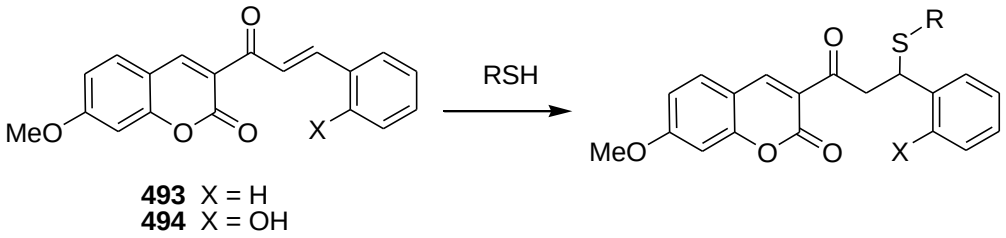

493 X = H
494 X = OH

Fig. 257 Schematic representation of the Michael addition reaction for the detection of bio-thiols using **493** and **494**.

Following the same mechanism, Pavez et al. tested a series of coumarin-based derivatives containing a chalcone-like moiety that reacted with biothiols through a Michael addition reaction in H_2O buffered at pH 7.4 (see Fig. 257).[316] The authors observed that the reactivity of the tested biothiols with the probes (**493** and **494**) followed the order of Cys > GSH > Hcy > Cys-Gly. The authors also saw that **493** was less reactive than **494**. The greater reactivity of **494**, when compared with **493**, was a result of the proton transfer by the hydroxyl group of the former probe to the vinyl carbon neighbouring the carbonyl group. This made the reaction site more prone to a nucleophilic attack by thiols. Upon excitation at 340 nm, probes **493** and **494** displayed a highly selective fluorescence enhancement at 430 nm (**493**) and 435 nm (**494**) with thiols. Finally, these probes were utilised for fluorimetric GSH determination in SH-SY5Y cells upon the addition of *N*-acetylcysteine, an agent capable of stimulating GSH synthesis.

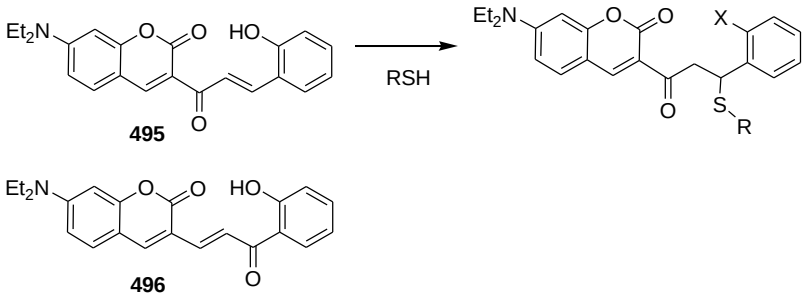

495

496

Fig. 258 Schematic representation of the Michael addition reaction for the detection of bio-thiols using **495** and **496**.

A similar paradigm for thiol detection was observed using chemosensors **495** and **496** (see Fig. 258).[317] In order to compare the reactions rates between probes, the UV-kinetics at 466 nm were monitored with the addition of GSH in DMSO:HEPES buffer 4:1, v/v (pH 7.4). Probe **496** (with a hydroxyl moiety at the orto position of the carbonyl group) exhibited the fastest response. However, given its good solubility in HEPES (0.1 mol L^{-1} pH 7.4), probe **495** was used for GSH detection. In this case, the absorption at 510 nm diminished, whereas a new band at 450 nm appeared upon the addition of GSH. Moreover, fluorescence was enhanced at 500 nm (λ_{exc} = 470 nm) with the addition of GSH, showing a limit of detection of 0.14 x 10^{-6} mol L^{-1}. In addition, competitive studies with **495** showed good selectivity for GSH. The reaction

mechanism was investigated by ^{1}H-RMN confirming a Michael addition reaction which was responsible for the emission and colour changes observed.

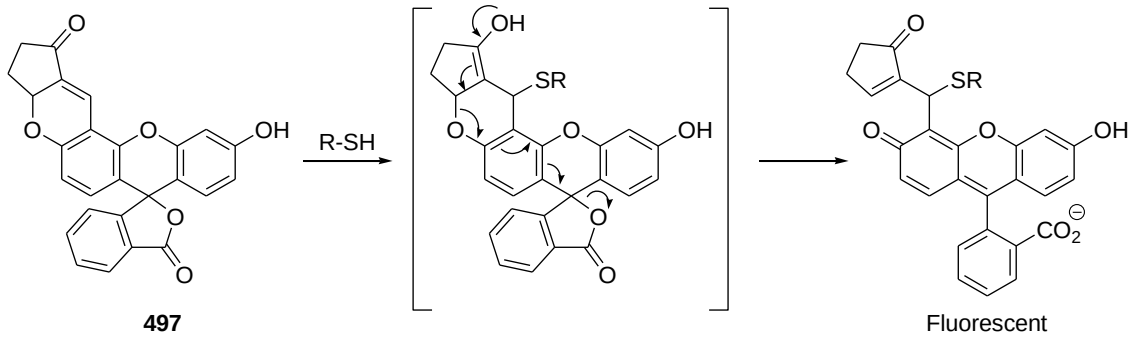

Fig. 259 Schematic representation of the reaction used for the detection of bio-thiols using **497**.

Fluoresceine derivative **497** (see Fig. 259) was used as a chemodosimeter for the selective recognition of Cys, Hcy and GSH.[318] Probe **497** was non-fluorescent in H_2O:CH_3CN 99:1 v/v solutions buffered at pH 7.4. However, addition of Cys, GSH and Hcy induced the appearance of a strong emission at 520 nm upon excitation at 485 nm (the quantum yield increased from 0.04 to 0.91, 0.65 and 0.47 for Cys, GSH and Hcy, respectively). The other amino acids tested (i.e., Gly, Phe, Ser, Glu, Lys, Arg, His, Ala, Gln, Met and Tyr) induced negligible changes. The detection mechanism consisted in a 1,4-addition of the thiol moiety to an α,β-unsaturated ketone in **497**, followed by the spiro ring opening of fluoresceine.

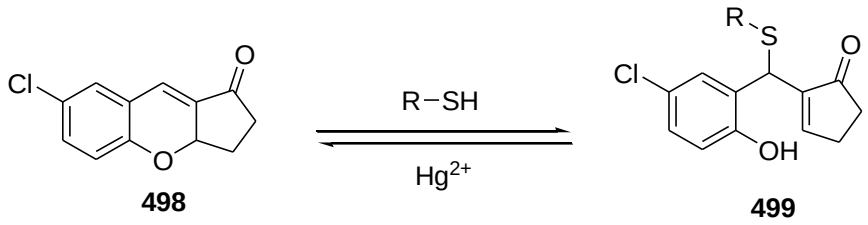

Fig. 260 Regenerative fluorescence on-off-on probe **498** for thiols and Hg^{2+}.

Huo and co-workers reported a new regenerative, fluorescence on-off-on probe for thiols and Hg^{2+} (**498**).[319] Aqueous solutions of receptor **498** (see Fig. 260), buffered at pH 8.0, presented three absorption bands at 250, 302 and 377 nm, which gradually decreased upon the addition of Cys. With the excitation of the aqueous solutions of **498** at 380 nm, a broad emission band at 550 nm was observed, which was quenched (10-fold intensity reduction) after adding Cys. Addition of Hcy and GSH induced the same changes, whereas the other amino acids tested (i.e., Ala, Arg, Asn, Asp, Gln, Glu, Gly, His, Ile, Leu, Lys, Met, Phe, Pro, Ser, Thr, Trp, Tyr and Val) were unable to produce any modification in the absorption and emission bands. Optical changes were ascribed to a Michael addition of Cys to **498**, yielding non-fluorescent derivative **499**. Moreover, the Hg^{2+} cation was able to induce the rupture of the C-S bond in **499**, followed by a subsequent intramolecular nucleophilic attack of the phenolic oxygen to the cyclopentenone moiety, which resulted in the regeneration of probe **498**.

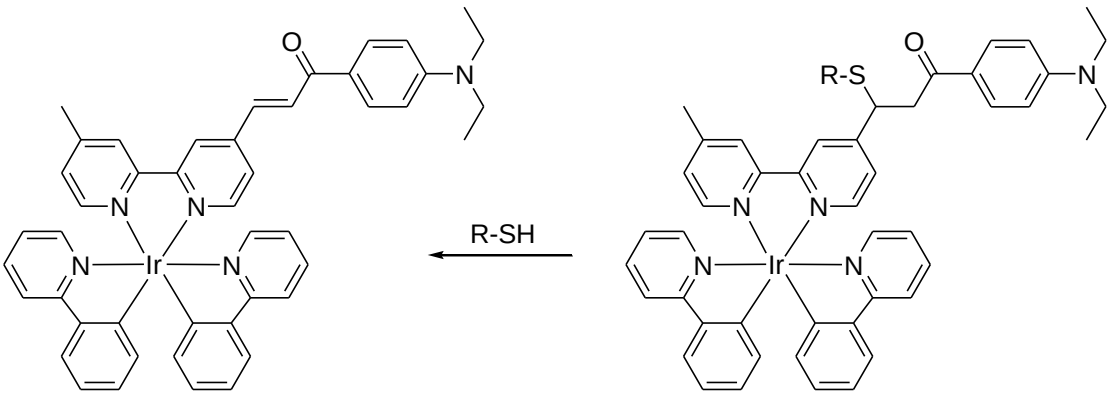

500

Fig. 261 Schematic representation of the detection of bio-thiols using **500**.

Zhao and co-workers reported phosphorescent thiol probe **500** (see Fig. 261) based on a cyclometallated iridium (III) complex with 2,2'-bipyridyl ligands containing an α,β-unsatured ketone as reactive site for thiol-containing amino acids.[320] DMF:H_2O 4:1 v/v solutions of **500** buffered at pH 7.2, showed an intraligand charge transfer (ILCT) band at 450 nm, which underwent a blue shift to 350 nm upon the addition of Cys (change in colour from yellow to colourless). Virtually the same changes were observed with the addition of Hcy and GSH, whereas the other amino acids tested (i.e., Pro, His, Ile, Met, Thr, Trp, Tyr, Val, Phe, Ser, Ala, Arg, Asn, Asp, Gln, Glu, Gly, Lys and Leu) induced negligible changes. Colour variations were ascribed to a 1,4-addition reaction of thiol groups to the α,β-unsatured ketone, which induced the suppression of the ILCT transition. Moreover, solutions of **500** were weakly emissive but, when Cys was added, an intense emission band at 587 nm was obtained (20-fold enhancement). The weak emission of compound **500** was assignable to an ILCT transition form of the HOMO (π) resident on the electron-rich fragment $-C(O)C_6H_4N(C_2H_5)_2$ to the LUMO (π^*), localised on the 2,2'-bipyridyl moiety in the functionalised 2,2'-bipyridyl ligand. Upon the addition of thiols, the thioether was obtained by making the ILCT significantly suppressed, whereas the [π(ppy)$\rightarrow\pi^*$(L)] LLCT and [5d(Ir) $\rightarrow\pi^*$(L)] MLCT transitions were most likely converted into the lowest energy excited states, thus conferring highly enhanced luminescence.

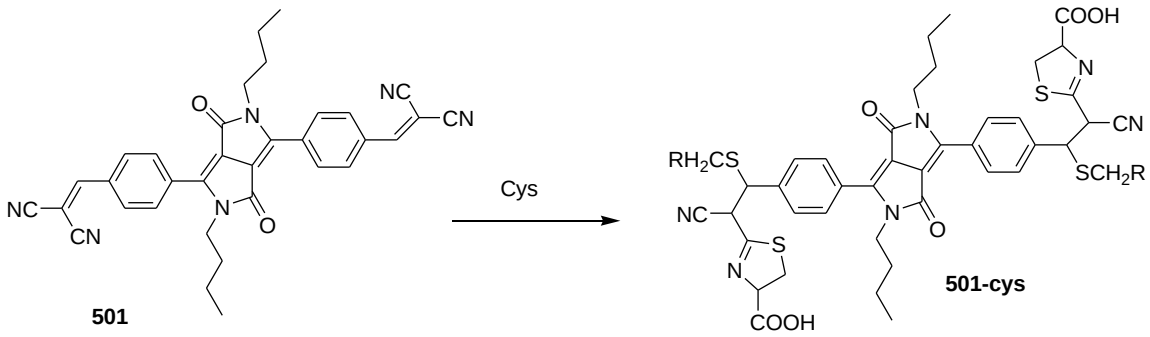

501 **501-cys**

Fig. 262 Schematic representation of the detection of Cys using **501**.

In this work, the authors designed a probe for the selective detection of thiols in CH_3CN:H_2O 4:1 v/v based on the Michael multiaddition of thiols to C=C bonds and to the -CN groups of the malonitrile moiety.[321] Probe **501** (see Fig. 262) showed absorption and emission bands at 523 and 666 nm (λ_{exc} = 490 nm), respectively. In the presence of thiols, such as Cys, the absorption and emission bands shifted to 479 and 540 nm, respectively. Correspondingly, the colour of the probe solution changed from purple to yellow. The limit of detection of probe **501** for Cys was determined to be 6.02 x 10^{-7} mol L^{-1}. **501** was used for the fluorescence imaging of intracellular thiols, and the mechanism response of **501** was rationalised by DFT calculations. The authors claimed that this probe was the first thiol probe based on the malonitrile/Michael addition mechanism to show simultaneous colorimetric and ratiometric fluorescence changes.

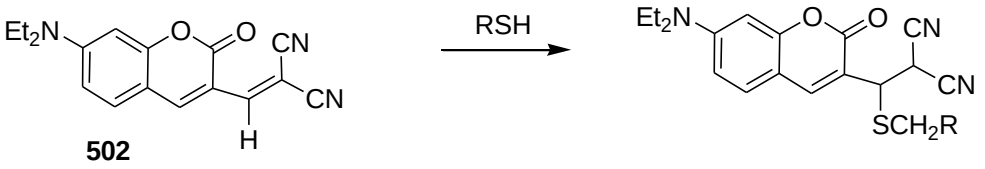

502

Fig. 263 Schematic representation of the detection of bio-thiols using **502**.

Also based on a Michael addition of thiols to the malonitrile moiety, Kim el al. designed a coumarin-malonitrile conjugate for the recognition of biothiols Cys, Hcy and GSH in DMSO:HEPES 1:2 v/v (pH 7.4) (see Fig. 263).[322] Upon the addition of these thiols to solutions of **502**, a peak at 524 nm disappeared and a new absorbance at around 406 nm appeared. In addition, strong fluorescence was observed at 475 nm (λ_{exc} = 394 nm). The other amino acids (i.e., Ala, Ser, Met, Ser, Asp, His and Lys) induced no response. Moreover, the authors used probe **502** for the detection of biothiols in cells.

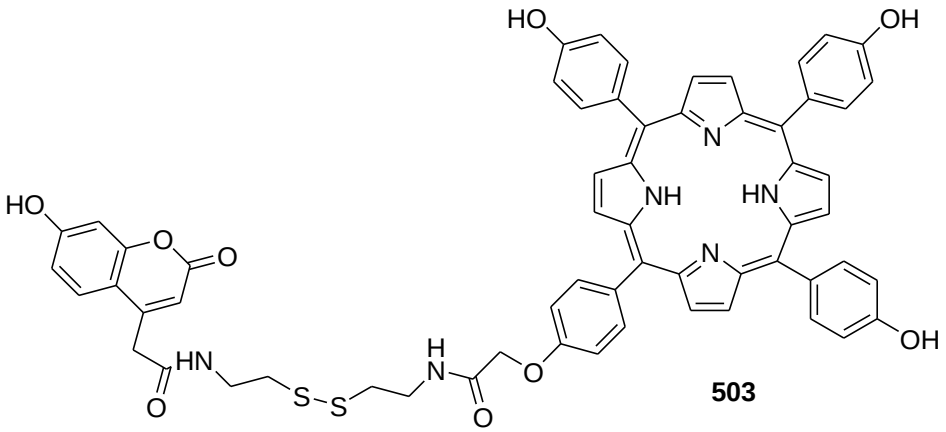

503

Fig. 264 Chemical structure of probe **503**.

In this work, the authors designed a new ratiometric fluorescent probe (**503**) for thiols in PBS buffer:CH_3OH 1:1 v/v (pH 7.4).[323] The free probe (see Fig. 264) showed a characteristic emission of the porphyrin fragment at 658 nm (λ_{exc} 350 nm), but did not display the coumarin emission at 459 nm, indicating that the fluorescence of the coumarin dye was quenched due to a FRET mechanism from the coumarin donor to the porphyrin acceptor. Addition of Cys

induced a cleavage on the disulphide bond, the FRET was turned off and fluorescence enhancement occurred at 459 nm, but almost no changes were observed at 658 nm. A limit of detection for Cys of 0.73 x 10^{-6} mol L^{-1} was calculated. The signalling mechanism was confirmed by ^{1}H NMR and mass spectroscopy studies. Selectivity of the probe to thiols over other amino acids (i.e., Ala, Arg, Gly, Leu, Pro, Phe, Tyr, Val and Lys) was confirmed. Only small molecular-weight thiols (Cys, Hcy, GSH) induced a significant ratiometric response. Finally, the probe was used for imaging thiols in living cells.

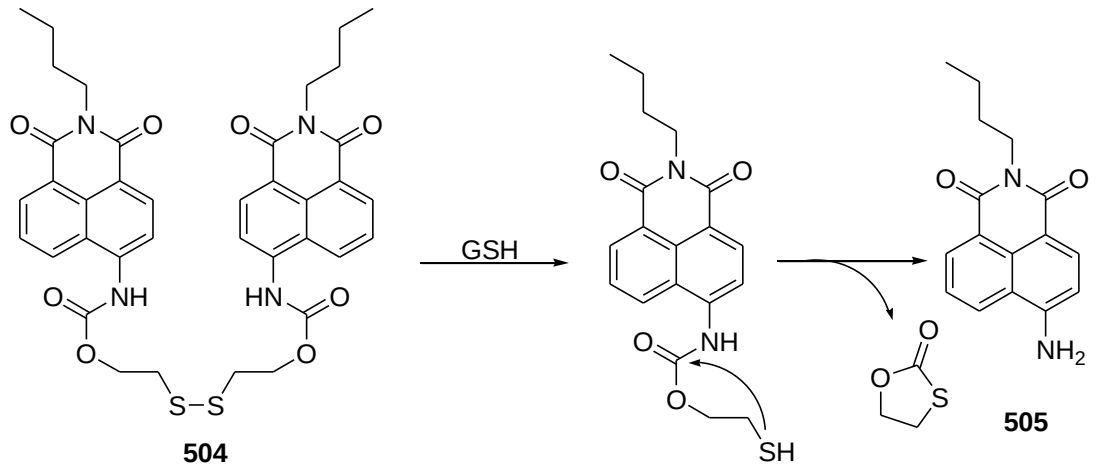

Fig. 265 Reaction of **504** with GSH to give **505**.

B. Zhu and co-workers prepared a new switch-on fluorescence-based probe **504** for the detection of thiols. [324] $CH_3CH_2OH:H_2O$ 1:9 v/v solutions of **504** (see Fig. 265) at pH 7.4 presented an absorption band at 350 nm which underwent a 85 nm bathochromic shift upon addition of GSH (change in colour from colourless to yellow). Moreover, solutions of **504** displayed intense emission at 485 nm (excitation at 400 nm), which underwent a red shift to 533 upon the addition of GSH. By using **504**, a limit of detection of 2.8 x 10^{-5} mol L^{-1} was achieved. The colour and emission changes were ascribed to a reaction of **504** with the thiol group in GSH, which triggered the cleavage of the disulphide-based carbamate-protecting group, yielding the highly fluorescent compound **505**. No fluorescence changes were observed in the presence of other the other amino acids (i.e., Arg, Ala, Tyr, Lys, His, Asp, Val, Leu, Try, Met, Pro, Phe, Ser, Thr, Glu and Gly) or upon the addition of ascorbic acid (a physiological reducing agent). However, low molecular-weight thiols, such as DTT, Cys, β-mercaptothylamine, thioglycerol and thioglycolic acid, induced the same optical changes as GSH. Chemodosimeter **504** was employed for imaging thiols in HeLa cells.

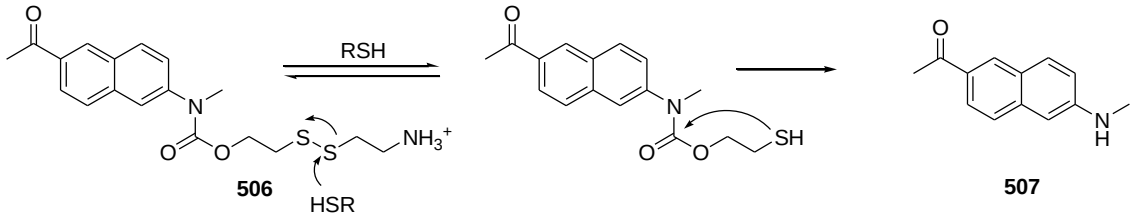

Fig. 266 Chemical structures of **506** and **507** and the reaction used for the detection of biothiols.

A similar reaction was used in receptor **506** (see Fig. 266) for the fluorogenic recognition of thiols.[325] Aqueous solutions of **506** (MOPS buffer, pH 7.2) showed a weak emission at 450 (excitation at 321 nm). Addition of Cys and GSH induced the appearance of a new emission band at 503 nm, which was ascribed to compound **507** generated upon the nucleophilic attack of the thiol groups at the disulphide moiety, followed by the cleavage of the C-N bond. Furthermore, **506** showed strong response to dithiothreitol (DTT), 2-mercaptoethanol (2-ME), and 2-aminoethanethiol (2-AET), and a negligible response to other amino acids (i.e., Glu, Ser, Val, Met, Ala and Ile), metal ions (i.e., Ca^{2+}, K^{+}, Na^{+}, Fe^{3+}, Zn^{2+}, Mg^{2+}) and H_2O_2. Having demonstrated the correct operation *in vitro,* the system was used for the intracellular detection of thiols.

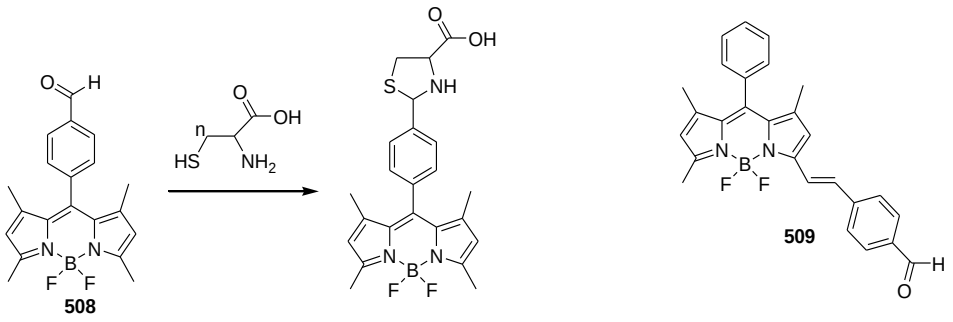

Fig. 267 Chemical structures of **508** and **509** and the reaction between **508** and biothiols.

Two BODIPY fluorophores containing an aldehyde group for the detection of Hcy and Cys were reported.[326] **508** (see Fig. 267) was tested in the presence of various amino acids (Gly, Arg, Thr, Ala, Hcy and Cys) and GSH in HEPES:CH_3CN 2:3 v/v (pH 7.4). Of these, only Hcy or Cys were able to induce fluorescence enhancement at 513 nm (λ_{exc} 498 nm). Addition of Hcy or Cys induced the transformation of the aldehyde group into a stable ring of thiazinane or thiazolidine, respectively, as a key element for their selective recognition. Moreover, the authors found that compound **509** did not undergo changes in fluorescence under similar conditions, indicating that the reaction of **509** with Hcy or Cys did not take place and suggesting the importance of the exact location of the aldehyde-phenly group. This effect was attributed to the difference in electropositivity of the carbon atom in aldehydes of **508** and **509**.

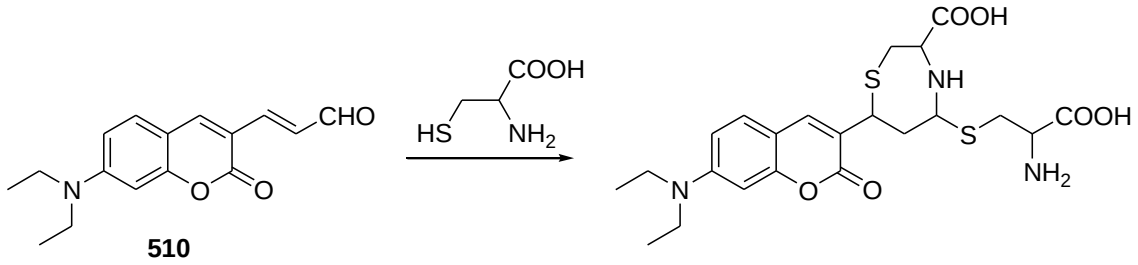

Fig. 268 Chemical reaction for detection of Cys using **510**.

Probe **510** was used for the specific detection of Cys over Hcy and GSH based on a drastic distinction in the kinetics of the reaction shown in Fig. 268.[327] **510** displayed an emission band at 557 nm (λ_{exc} = 435 nm) whose intensity diminished with the concomitant enhancement of a

new fluorescence at 487 nm upon the addition of Cys. The emission ratio between both bands was proportional to the amount of Cys and a limit of detection of 7.5 x 10^{-7} mol L^{-1} in PBS:CH_3CN 9:1 v/v (pH 7.4) was achieved. Moreover, **510** was seen to be highly selective to Cys. A study of the time-dependent emission ratio changes for **510** upon treatment with Cys, Hcy and GSH revealed that the second-order rate constant for Cys was around 1,000 and 20,000 faster than that for Hcy and GSH, respectively. Finally, the probe was applied for the ratiometric imaging of Cys levels in living cells.

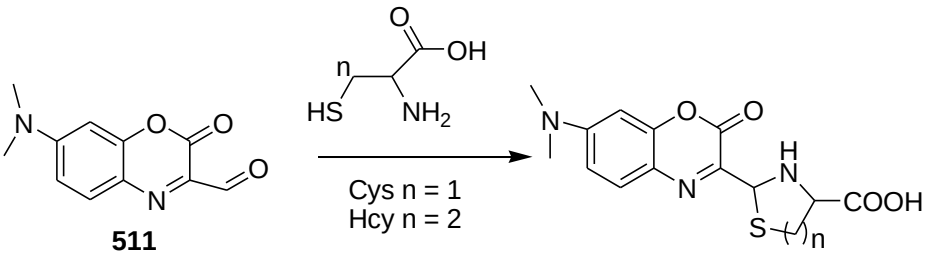

511

Fig. 269 Reaction for the detection of Cys and Hcy using **511**.

Fluorescent chemodosimeter **511** (see Fig. 269) for the recognition of Cys and Hcy in CH_3CN:HEPES 3:7 v/v (pH 7.4) was reported.[328] Upon the addition of Cys/Hcy, **511** exhibited an enhancement of the fluorescence intensity at 560 nm (λ_{exc}=500 nm). Additionally, a major absorption shift from 500 to 430 nm and a visual colour change from orange to yellow were also observed. The sensing mechanism involved a cyclisation of the thiol-containing biomolecules with the aldehyde in **511**. This detection mechanism was proved by ^{1}H-NMR, mass spectrometry analysis and Gaussian calculations. Finally, **511** was used for the bioimaging of Cys/Hcy in living cells and for their detection in human plasma.

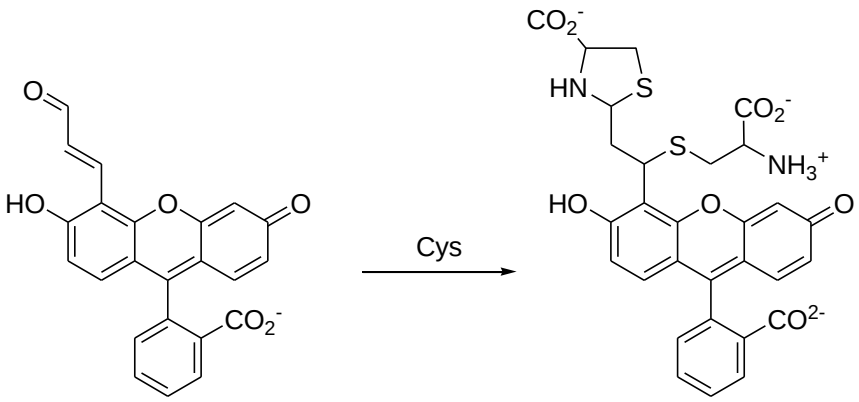

512

Fig. 270 Reaction between probe **512** and Cys.

S. Lim and co-workers prepared a new selective chemodosimeter (**512**) for the detection of Cys and Hcy in water (see Fig. 270).[329] Aqueous solutions of **512** (pH 7.4) presented an emission at 524 nm upon excitation at 508 nm, which underwent a remarkable 41-fold enhancement upon the addition of Cys. This emission enhancement was ascribed to the reaction of two Cys molecules with the α,β-unsaturated aldehyde moiety in **512**, leading to a conjugate addition and thiazolidine ring formation. The mechanism was confirmed by NMR and ESI-TOF-HRMS. The same response, but with lesser emission intensity enhancement, was obtained when Hcy

was added. This selective response to Cys was due to the faster reaction of this amino acid with **512** when compared with Hcy. Addition of structurally similar analogues (penicillamine, L-cysteic acid, 3-mercaptopropionic acid and 2-mercaptoethanol) induced negligible changes in the emission profile of **512**.

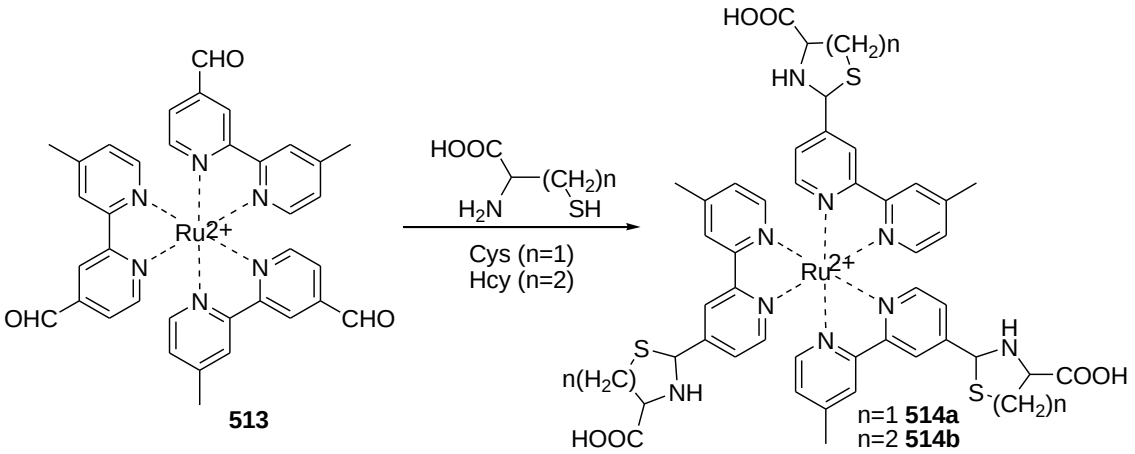

Fig. 271 Chemical structure of **513** and the reaction used for the detection of Cys and Hcy.

Zhang and co-workers prepared a Ru(II) complex-based luminescent probe (**513**) for the selective recognition of Cys and Hcy (see Fig. 271).[330] DMSO:H_2O 9:1 v/v solutions of **513**, buffered at pH 7.0, showed a very weak MLCT emission at 720 nm (excitation at 485 nm) due to the presence of three aldehyde electron withdrawing moieties that quenched the emission of the ruthenium complex. However, addition of Cys and Hcy induced a major blue shift (from 720 to 635 nm) with significantly increased emission intensity. These changes were ascribed to the reaction of the aldehydes with Cys/Hcy, yielding the corresponding electron donor thiazoline/thiazinane heterocycles (**514a** and **514b**). Addition of Gly, Leu, Asp, Pro, Arg, Lys, Tyr, Val, GSH, Thr, Ser, Ala, His, Met and Trp induced negligible changes in the emission of **513**.

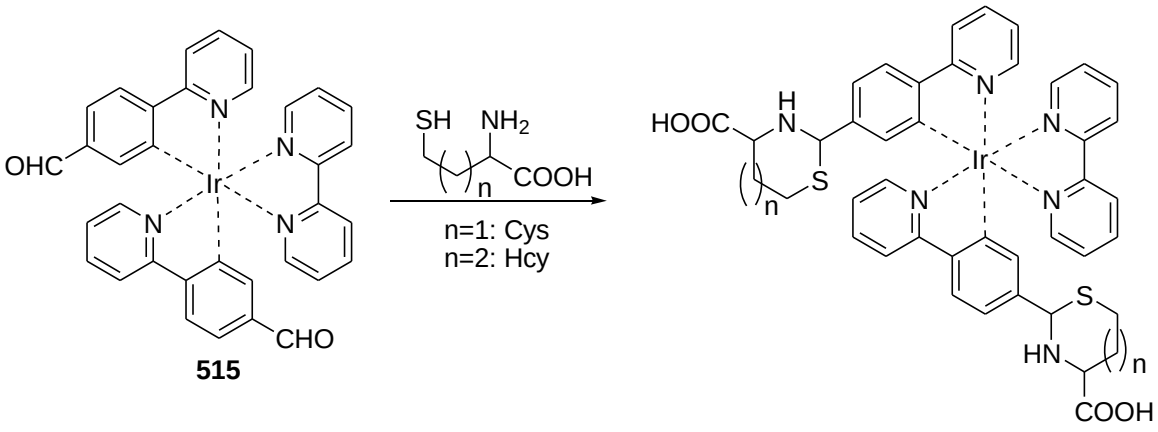

Fig. 272 Chemical structure of **515** and the reaction used for the detection of Cys and Hcy.

Following a similar approach, Xiong and co-workers prepared **515** (see Fig. 272) as a luminescent probe for the detection of Cys and Hcy.[331] In this case, an Ir(III) complex was used

as a signalling subunit, whereas aldehyde moieties were selected as reactive sites. DMSO:H_2O 9:1 v/v solutions of **515**, buffered at pH 7.2, showed a phosphorescence band at 547 nm upon excitation at 360 nm, which was ascribed to an ^{3}MLCT transition. Addition of Cys/Hcy induced a red shift of emission to 586 nm together with a slight quenching of its intensity. Cys and Hcy reacted with the aldehyde moieties of **515**, yielding the corresponding thiazolidine and thiazinane Selectivity of **515** to Cys and Hcy was assessed and the addition of other amnio acids (i.e., Gly, Leu, Asp, Pro, Arg, Lys, Tyr, Val, GSH, Thr, Ser, Ala, His, Met and Trp) induced negligible optical changes. Finally, **515** was used for the intracellular imaging of Cys and Hcy in KB cells with fine results.

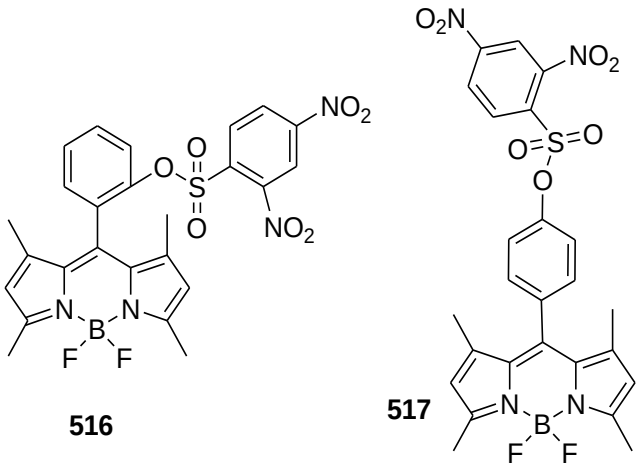

Fig. 273 Chemical structure of thiol probes **516** and **517**.

In this work, the authors designed two highly selective off-on green-emitting fluorescent thiol probes (**516** and **517**).[332] Probe **516** (see Fig. 273) in CH_3CH_2OH:H_2O 4:1 v/v (pH 7) showed a 300-fold enhancement of emission intensity in the presence of Cys at 516 nm with a limit of detection for this amino acid of 4.0 x 10^{-7} mol L^{-1}. The sensing mechanism directly resulted from the nucleophilic aromatic substitution of the arene-sulphonate ester with Cys, which generated a fluorescent derivative. This mechanism was also rationalised by DFT/TDDFT calculations. Moreover, the longer distance between BODIPY and the 2,4-dinitrobenzenesulphonyl groups in probe **517** induced lesser florescence enhancement (54-fold). Other biologically related analytes, such as GSH and ROS, were also tested against probe **516**, and only $OH^{\cdot}$ showed some response. Finally, the authors employed probes **516** and **517** for the fluorescent imaging of intracellular thiols.

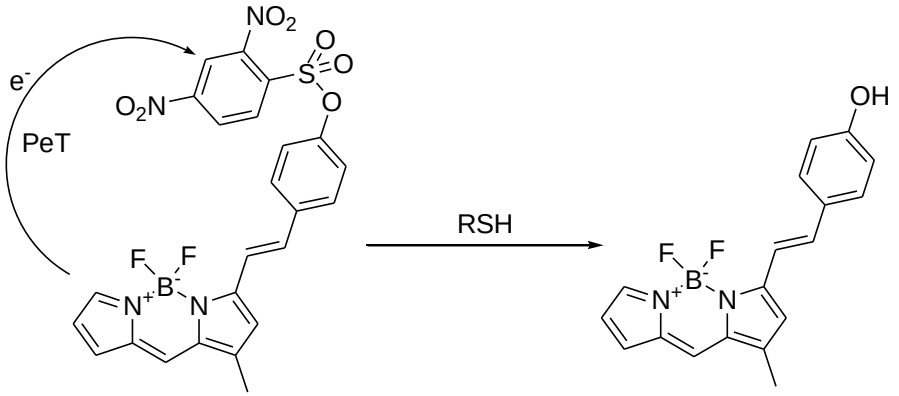

518 **519**

Fig. 274 Reaction of **518** with biothiols to give **519**.

X. Li and co-workers developed a similar probe, which was also based on the reactivity of the 2,4-dinitrobenzensulphonate groups to nucleophilic aromatic substitution with thiols (see Fig. 274).[333] Probe **518** consisted of a 2,4-dinitrobenzensulphonate unit conjugated to a fluorophore (BODIPY). $CH_3CN:H_2O$ 1:99 v/v (buffered at pH 7.3) solutions of receptor **518** showed a weak emission at 500 nm (excitation at 360 nm). This low emission was ascribed to a PET process from the donor BODIPY dye to the 2,4-dinitrobenzenesulphonate acceptor moiety. Addition of Cys to aqueous solutions of **518** induced the appearance of a strong emission at 570 nm as a result of the nucleophilic aromatic substitution of the arenesulfonate ester with Cys, which generated derivative **519**. Addition of GSH induced the same emission enhancement, whereas other amino acids induced negligible changes. Finally, the authors successfully employed the probe for the intracellular imaging of thiols.

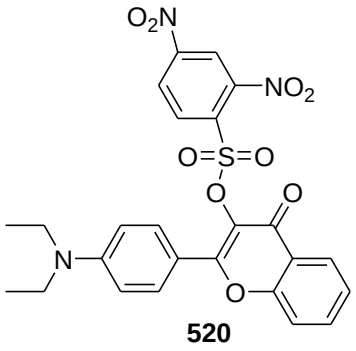

520

Fig. 275 Chemical structure of probe **520**.

Another probe using a similar mechanism (**520**) for thiols sensing was also reported (see Fig. 275).[334] Solutions of **520** in $CH_3OH:H_2O$ 4:6 v/v, buffered at pH 7.4, were non-fluorescent due to a strong PET process from the 4'-(diethylamino)-3-hydroxyflavone fluorophore to the 2,4-dinitrobenzenesulphonyl moiety. Addition of increasing amounts of Cys induced the appearance of a strong emission band at 534 nm (λ_{ex} = 405 nm) with a 180-fold enhancement. Similar enhancements were observed upon the addition of Hcy and GSH. No significant changes in absorbance and fluorescence were shown by other amino acids (i.e., Ala, Arg, Asp, Glu, Gly, Ile, Leu, Lys, Met, Ser, Thr, Trp, Tyr and Val). As in the above case, emission enhancement was ascribed to a suppression of the PET process upon the reaction of the thiol-

containing biomolecules with the 2,4-dinitrobenzenesulphonyl moiety. Confocal laser scanning microscopy imaging of biological thiols in living HeLa cells was also performed.

3.4.- Nanostructures and polymers

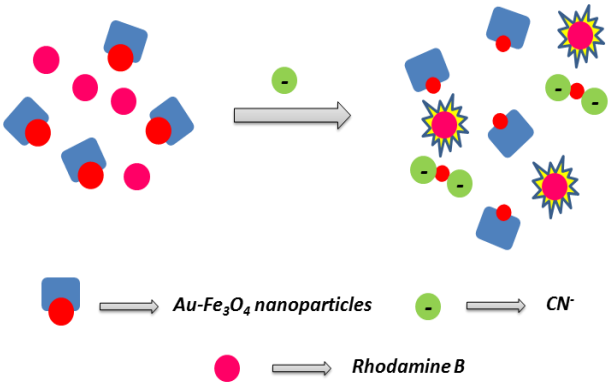

Fig. 276 Schematic representation of a probe for CN^- by using Au-Fe_3O_4 nanoparticles combined with rhodamine B.

Bifunctional Au-Fe_3O_4 nanoparticles combined with rhodamine B (**RB**) for the sensitive and selective turn-on fluorescent detection of CN^- were reported (see Fig. 276).[335] **RB** presented an intense emission band at 577 nm when excited at 450 nm in water (phosphate buffer at pH 10.5). Addition of Au–Fe_3O_4 to **RB** induced a marked quenching of fluorophore emission. This quenching was due to a strong overlapping between the absorption bands of the nanoparticles, centered at 548 nm, with the emission spectra of the fluorophore. Addition of CN^- to these suspensions resulted in the dissolution of Au from Au-Fe_3O_4 nanoparticles and the formation of $Au(CN)_2^-$ complexes. Due to this erosion of Au, the absorption at 548 decreased and, subsequently, **RB** emission at 577 nm was restored. Fluorescence gradually increased with the CN^- concentration, showing a limit of detection of 2.0 x 10^{-13} mol L^{-1}. The application of this method to detect CN^- in tap water, ground water and lake water was achieved.

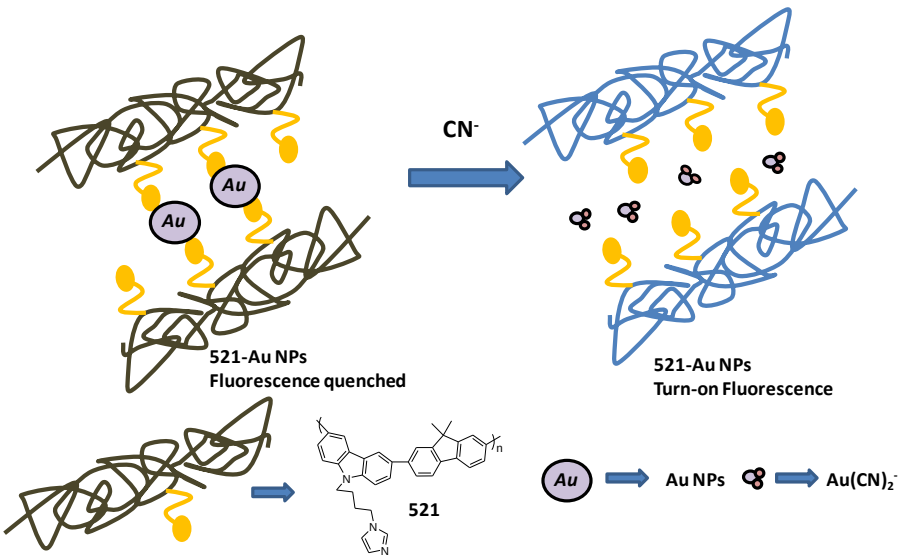

Fig. 277 Schematic representation of CN^- detection using **521-Au NPs**.

Another work that also describes a sensitive and selective fluorescent detection of CN^- was reported by Li et al.[336] The sensing protocol was based on the cyanide-promoted dissolution of gold from a polymer containing Au nanoparticles (see Fig. 277). The nitrogen atoms of the imidazole moieties in **521** showed an affinity for the Au surface and, as a result, the hybrid polymer **521-Au NPs** complex was formed. **521-Au NPs** showed a brown colour in solution and was practically non-fluorescent because of the Au-induced quenching of the **521** emission at 402 nm (λ_{exc} = 355 nm). When CN^- was added, AuNPs were dissolved to form the soluble $[Au(CN)_2]^-$ complex, the brown colour of the solution changed to coloruless and bright blue fluorescence was observed due to the recovery of **521** emission. A limit of detection of 3.0 x 10^{-7} mol L^{-1} was achieved for CN^-. The other anions tested (i.e., Cl^-,CO_3^{2-}, $EDTA^{2-}$, F^-, HCO_3^-, I^-, NO_2^-, NO_3^-, SCN^-, SO_3^{2-}, SO_4^{2-}, $C_2O_4^{2-}$, AcO^-, $S_2O_8^{2-}$, $P_2O_7^{4-}$, PO_4^{3-}, HPO_4^{2-} and Br^-) induced negligible changes in the emission profiles. The authors tested this sensing method in real water samples, including local groundwater, tap water, boiled water and lake water, with fine results.

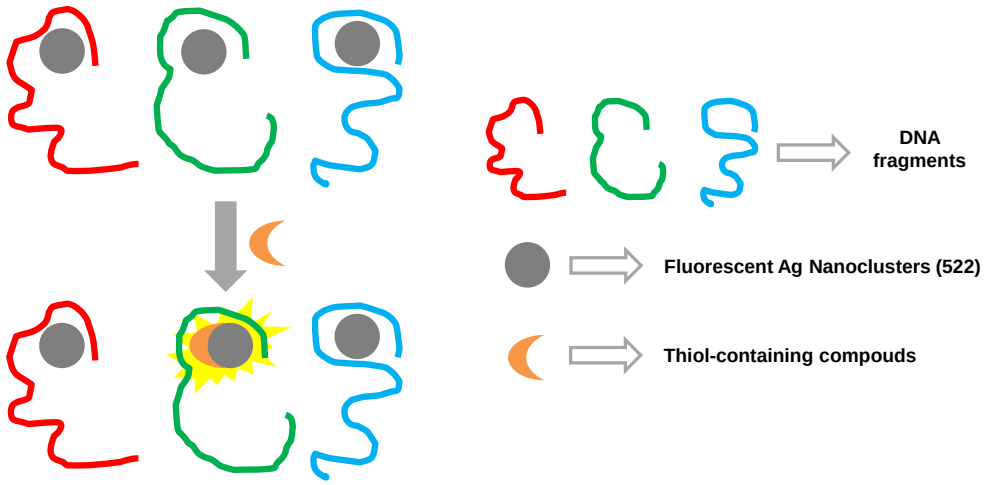

Fig. 278 Schematic representation of DNA-based Ag nanoclusters (**DNA-522**) for sensing thiol-containing compounds.

DNA-based Ag nanoclusters (**DNA-522**) were used for the fluorogenic recognition of thiol-containing compounds (see Fig. 278).[337] The emission response of different **DNA-522** conjugates to biothiols (Cys, Hys and GSH) was tested and the best results in terms of selectivity and sensitivity were found for **dC_{12}-522** (containing the dCCCCCCCCCCCC DNA fragment). Water solutions of **dC_{12}-522,** buffered at pH 6.9, presented a weak emission band at 615 nm upon excitation at ca. 560 nm, which increased gradually upon the addition of Cys, Hcy and GSH. Limit of detections of 6.2, 2.1 and 1.5 x 10^{-9} mol L^{-1} for GSH, Cys and Hcy were respectively found. The fluorescence responses of **dC_{12}-522** to other 19 amino acids showed no obvious fluorescence enhancement. The authors ascribed the emission enhancements to a charge transfer process from the ligands to the metal centre through the Ag-S bonds. Finally,the authors tested the detection of thiols in human plasma using **dC_{12}-522** particles.

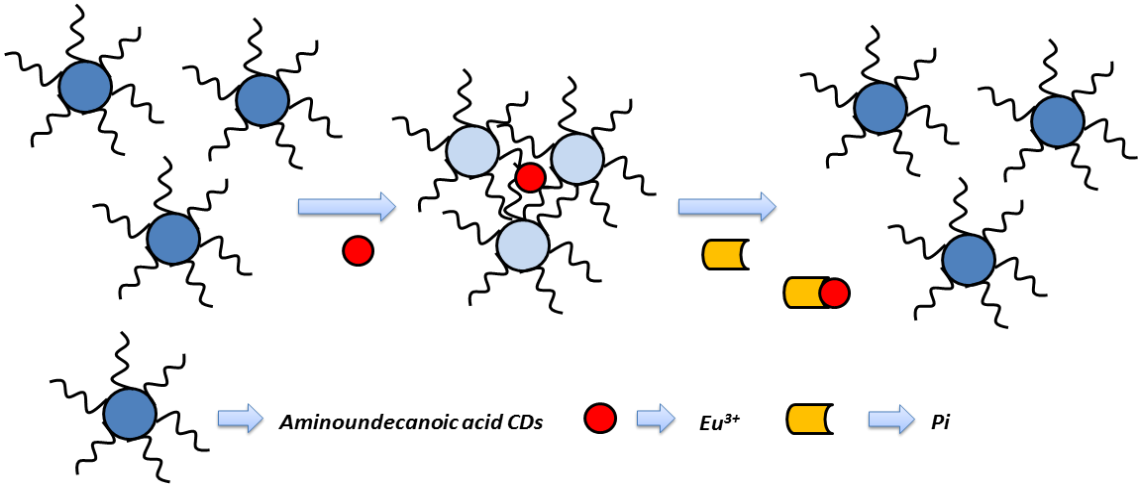

Fig. 279 Schematic representation of HPO_4^{2-} detection using carboxylate modified carbon dots (CDs).

A simple method for HPO_4^{2-} detection was developed using an off-on fluorescence probe consisting in carboxylate modified carbon dots (**CD**s) complexed with Eu^{3+} cations (see Fig. 279).[338] In particular, Tris-HCl solutions of carboxylate-modified **CD**s, pH 7.8, showed an intense emission at 420 nm when excited at 320 nm. This emission band was intrinsic of the **CD**s. Addition of Eu^{3+} induced a marked decrease in the emission band as a result of an aggregation of the **CD**s upon the coordination of Eu^{3+} with the carboxylate moieties on the **CD**s surface. Addition of HPO_4^{2-} induced the recovery of the emission band, which was ascribed to a disaggregation process because of the preferential coordination of Eu^{3+} with HPO_4^{2-}. A limit of detection of 5.1 x 10^{-8} mol L^{-1} was achieved for HPO_4^{2-}. The probe showed much higher selectivity to HPO_4^{2-} when compared with other anions (i.e., SO_4^{2-}, SO_3^{2-}, NO_3^-, NO_2^-, ClO_3^-, ClO^-, BrO_3^-, S_2^-,Cl^-, Br^-, $S_2O_3^{2}$, F^-, I^-, Hcy, Ser, Glu and Arg). Besides, this sensing method was successfully applied to the detection of HPO_4^{2-} in artificial wetland systems.

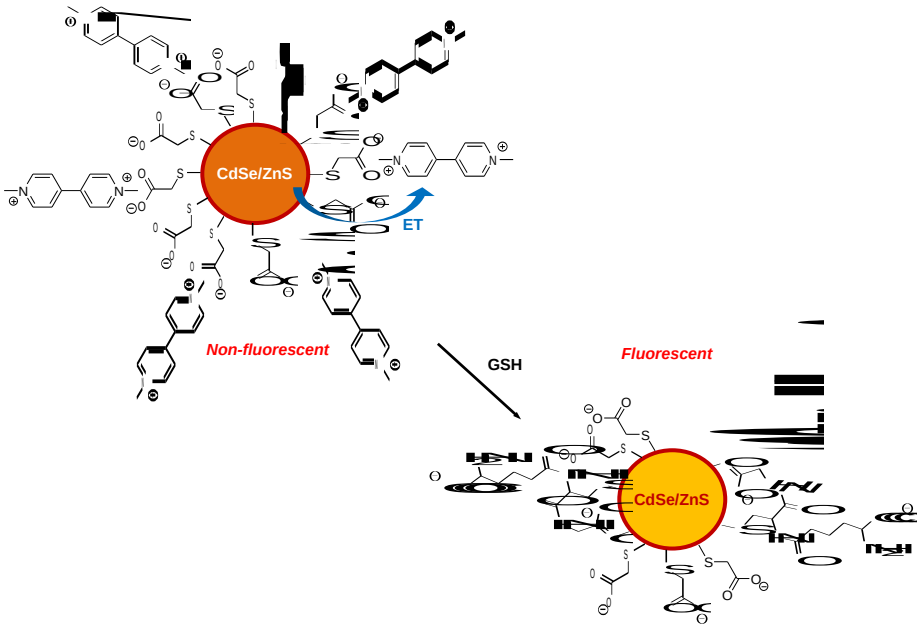

Fig. 280 Schematic representation of the use of CdSe-ZnS quantum dots (**QDs**) for the fluorescent sensing of GSH.

Liu et al. designed and developed a new off-on fluorescence probe for glutathione (GSH).[339] The system was based on an electron transfer quenching mechanism of mercaptotriacetic acid (TGA) capped CdSe-ZnS quantum dots (**QDs**) paired electrostatically with methyl viologen (1,1'-dimethyl-4,4'-bipyridinium chloride, MV^{2+}) (see Fig. 280). Specifically MV^{2+}, in the proximity of **QDs,** rendered the fluorescence of QDs in the "off" state due to an efficient electron transfer process. However, the addition of GSH effectively displaced the TGA ligands, restoring the native luminescence of the QDs to the "on" state. The strong selectivity of GSH was conferred by GSH's capability to chelate metal ions in QDs with more than one thiol binding site. Furthermore, the major steric hindrance effect created by GSH enhanced the stability of the complexes. The authors found that the fluorescence restoration capability followed this order: GSH >> Hcys > Cys.

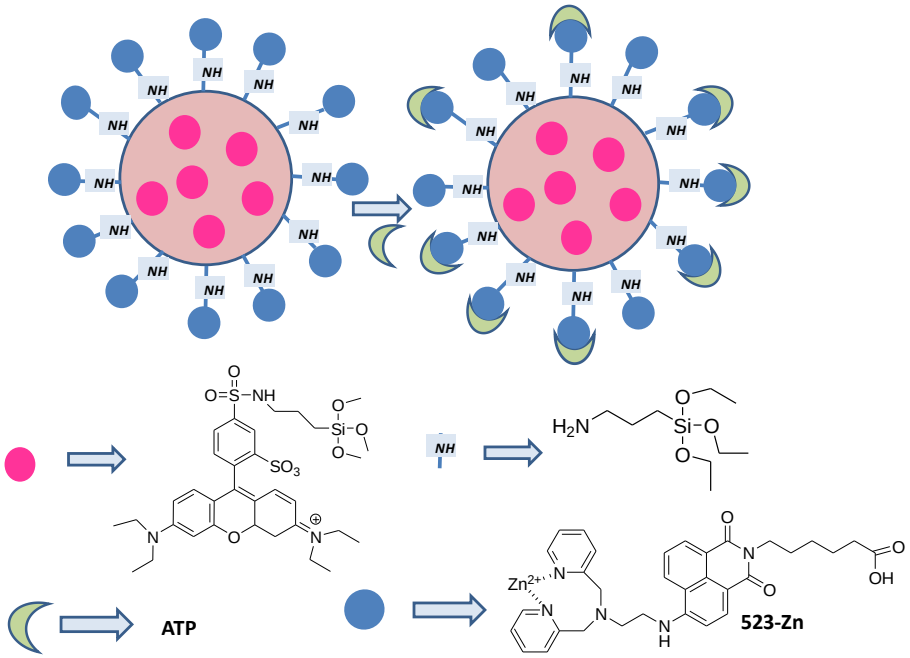

Fig. 281 Schematic representation of a probe for ATP by using fluorescent silica nanoparticles with the rhodamine and dipicolylamine-naphthalimide units complexed with Zn(II) (**523-Zn**).

Silica nanoparticles functionalised with two fluorescent dyes, these being a dipicolylamine-naphthalimide unit complexed with Zn(II) (**523-Zn**) and a rhodamine derivative used as reference, were employed for the detection of ATP (see Fig. 281).[340] Aqueous suspensions of the hybrid nanoparticles buffered at pH 7.4 showed emission at 530 nm upon excitation at 450 nm, which was ascribed to the **523-Zn** unit. Addition of ATP induced moderate emission enhancement, whereas the signal of the reference dye (rhodamine) remained unaffected. Selectivity assays in the presence of other nucleotides (GTP, UTP and CTP) exhibited how ATP induced a considerably stronger response. Finally, the potential of the fluorescent nanoparticles for biomedical applications was evaluated using epithelial normal rat kidney (NRK) cells. These studies revealed the non-toxicity of the hybrid nanoparticles, at concentrations ranging from 0.1 to 0.4 mg mL^{-1}, and their localisation in the cytoplasm by measuring the emission of both fluorophores by confocal microscopy.

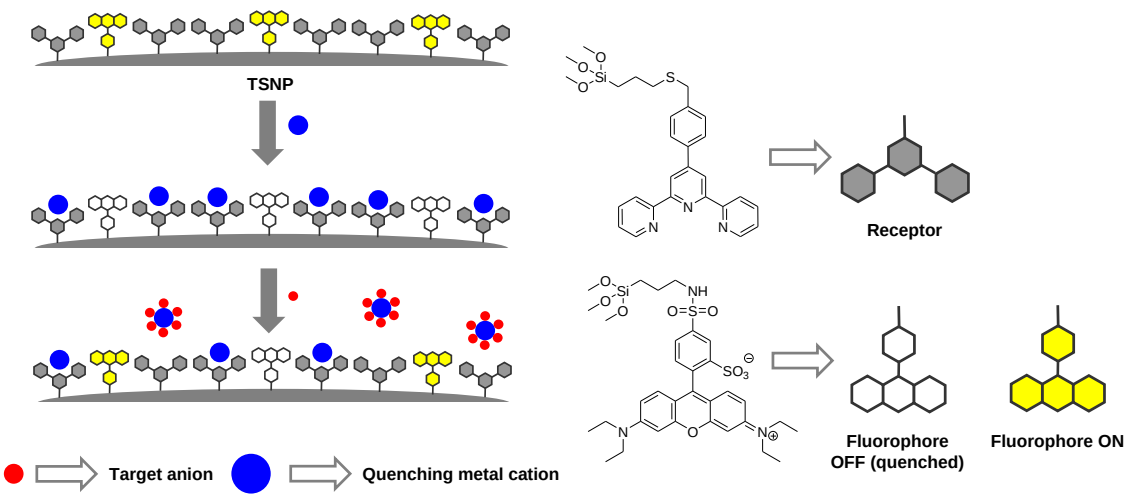

Fig. 282 Schematic representation of a probe for anions using silica nanoparticles functionalised with terpyridines and sulphorhodamine B units.

Silica nanoparticles (**TSNP**) functionalised with terpyridines, as binding sites for metal cations, and sulphorhodamine B, as the fluorophore, were used for the fluorescent recognition of certain anions (see Fig 282).[341] In particular, addition of metal cations (Cu^{2+}, Fe^{3+}, Hg^{2+}, Ni^{2+} and Pb^{2+}) to acetonitrile suspensions of the hybrid nanoparticles induced several degrees of quenching of grafted sulphorhodamine B through an energy or electron transfer process from the terpyridine-bound cation to the excited fluorophore. Addition of inorganic anions (i.e., $H_2PO_4^-$, HSO_4^-, F^-, Cl^-, Br^-, I^- and NO_3^-) to the metal complexes induced the partial recovery of the sulphorhodamine B emission due to the formation of cation-anion complexes. The best response was obtained with Pb^{2+}. In this case, of all the anions tested, only $H_2PO_4^-$ was able to induce the recovery of the sulphorhodamine B emission. With the other metal cations, unselective changes were found. However as a general trend, addition of $H_2PO_4^-$ and F^- induced remarkable fluorescence enhancements, addition of Cl^-, Br^- and HSO_4^- led to moderate increases, whereas the addition of I^- and NO_3^- produced minimial fluorescence changes.

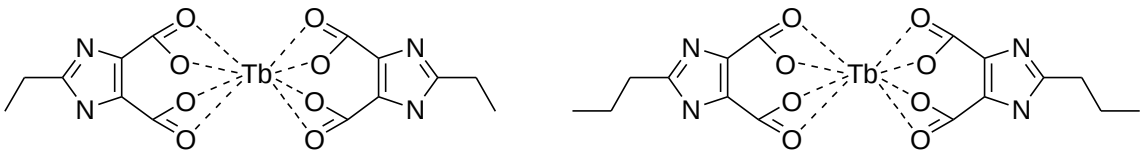

524 **525**

Fig. 283 Chemical structure of terbium complexes **524** and **525.**

Two novel composite materials, based on terbium luminescent polyelectrolyte hydrogels for the detection of $H_2PO_4^-$ and HSO_4^-, were prepared (see Fig. 283).[342] During a first step, xerogels containing complexes **524** and **525** were prepared and then a sol-gel technique was used to prepare the **CM-524** and **CM-525** hydrogels from the corresponding xerogels. Solutions containing **CM-524** and **CMb-525** in H_2O displayed green luminescence. Upon the addition of $H_2PO_4^-$ or HSO_4^-, the emission of **CM-524** at 545 nm, excited at 286 nm, gradually decreased and was finally quenched. No pronounced reduction (less than 20%) was observed in the

fluorescent spectra with the other anions (F^-, Cl^-, Br^-, and I^-) evaluated. Very similar results were obtained with solutions of **CM-525**. Reusability of both luminescent materials was studied by rinsing **CM-524** and **CM-525** with H_2O until the characteristic emission was nearly recovered.

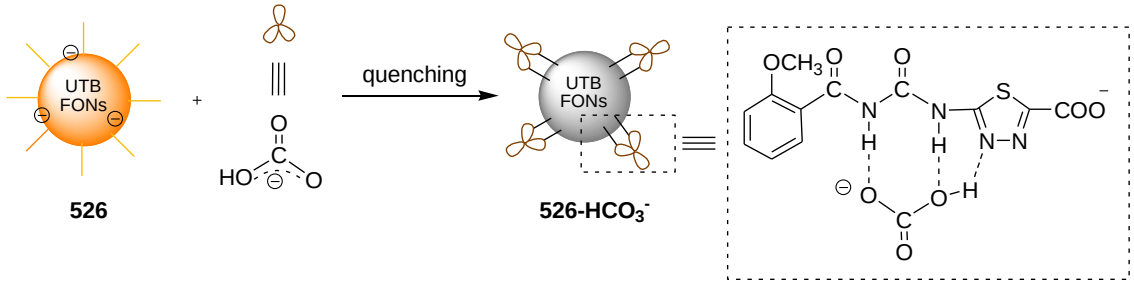

Fig. 284 Schematic representation of a probe for HCO_3^- using fluorescent nanoparticles **526**.

The novel fluorescent turn-off nanosensor **526** (see Fig. 284) was proved to selectively detect HCO_3^- in aqueous solution.[343] The probe was based on urea-thiadiazole-benzene (UTB) molecules, which in CH_3CN:H_2O 3:7 v/v, self-assembled into colloidal fluorescent nanoparticles (**519**) with an average diameter of 100 nm. Of all the anions tested (i.e., AcO^-, $H_2PO_4^-$, HPO_4^{2-}, $C_2O_4^{2-}$, HSO_3^-, NO_3^- and HCO_3^-) with aqueous suspensions of **526,** only HCO_3^- was able to induce a noticeable quenching of the emission band in **526** centred at 396 nm. This selectivity was explained in terms of the preferential coordination on **526** of the plane triangular HCO_3^- over other non-planar anions. The formation of the **526-HCO_3^-** complexes, via hydrogen-bonding interactions, enhanced the electron charge density at the receptor sites, thus enabling a PET process that quenched the emission of the nanoparticles. By using **526,** a limit of detection of 5.57×10^{-7} mol L^{-1} was determined for HCO_3^-.

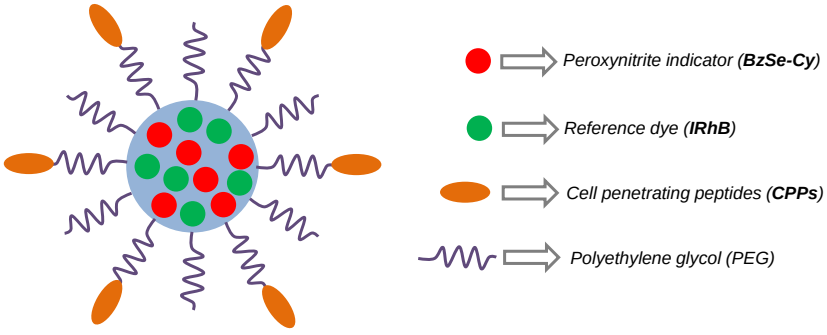

Fig. 285 Schematic representation of a hybrid polypeptide-polymer micelle-based fluorescent nanoprobe.

A hybrid polypeptide-polymer micelle-based fluorescent nanoprobe for the ratiometric detection and imaging of $ONOO^-$ in living cells was reported (see Fig. 285).[344] The nanoprobe was based on a polymeric micelle containing a hydrophobic core of polylactic acid (PLA), which encapsulated inside two dyes: benzylselenide-tricarbocyanine (**BzSe-Cy**) as $ONOO^-$ indicator and isopropylrhodamine B (**IRhB**) as the reference. The hydrophilic nanoprobe shell consisted in polyethylene glycol (PEG), which was linked to the hydrophobic core and conjugated with

cell-penetrating peptides (**CPPs**). Aqueous suspensions, PBS-buffered at pH 7.4, of the nanoprobe showed an intense emission at 810 nm upon excitation at 788 nm, arising from the **BzSe-Cy** dye. Besides, excitation at 555 nm induced the appearance of a broad emission at 575 nm, which was ascribable to **IRhB**. Addition of increasing quantities of $ONOO^-$ induced significant emission quenching at 810 nm due to a reaction between the **BzSe-Cy** dye and the anion in which $ONOO^-$ oxidided Se^{2+} to Se^{4+}, whereas the fluorescence at 575 nm remained unaltered. This allowed a ratiometric detection of $ONOO^-$ with a limit of detection of 50 x 10^{-9} mol L^{-1}. The presence of various interfering agents (i.e. H_2O_2, $^1O_2$, $O_2^{\cdot-}$, $^{\cdot}NO$, NO_2^-, NO_3^-, $ROO^{\cdot}$, $^{\cdot}OH$, ClO^- and HRP) was unable to induce any noticeable emission change. The authors used the nanoprobe to image $ONOO^-$ in living macrophages (RAW 264.7), normal human liver cells (HL-7702), and human hepatoma cells (HepG2) to obtain low toxicity and good membrane permeability.

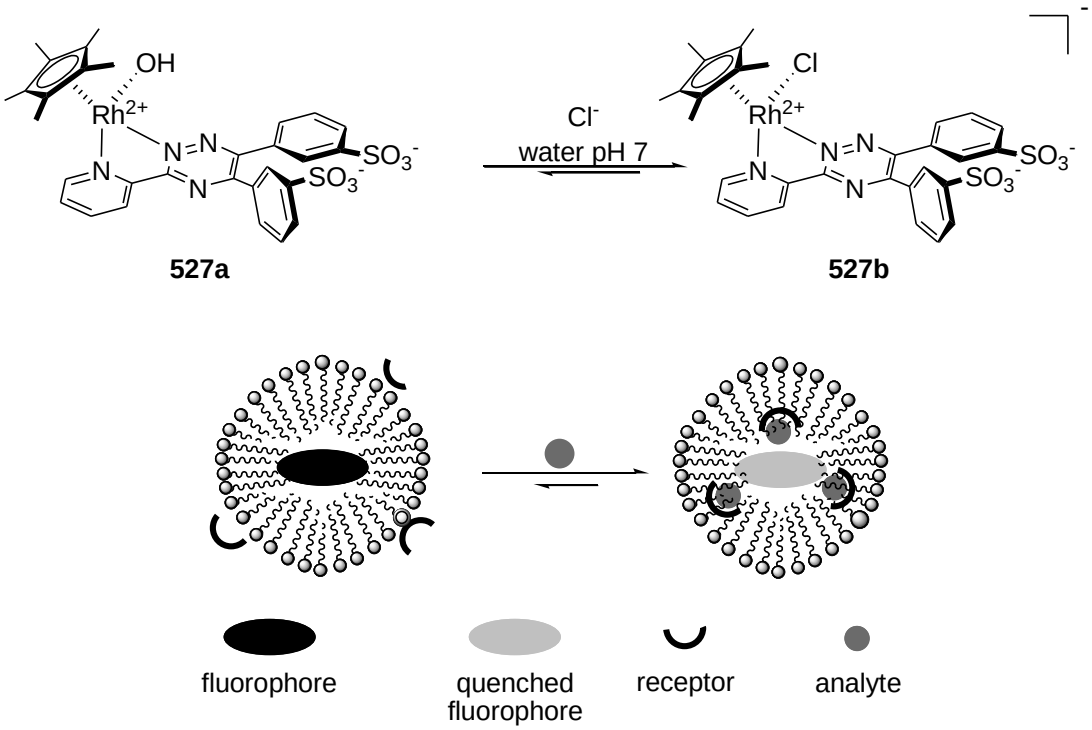

Fig. 286 Schematic representation of a micelle-based chemosensing system for the detection of Cl^- using **527**.

Johannessen et al. developed a micelle-based chemosensing system using the commercially available fluorophore (8-hydroxypyrene-1,3,6-trisulfonate, HPTS), a surfactant (cetyltrimethylammonium, CTA) and a Rh^{3+}-based receptor (see Fig. 286).[345] The system was able to work in buffered aqueous solutions (MOPS at pH 7.0) and proved selective for the detection of anion Cl^-. The micelle dispersion provided both a secondary pseudo-phase in which the receptor-Cl^- complex was selectively stabilised and a platform upon which the receptor and the reporter units for signalling transduction juxtaposed. The general operational principle of this system was that in the presence of the correct concentration of surfactant (CTA), dye (HPTS) and receptor (**527a**), a micelle containing the dye and with the receptor on the surface would form. Upon the addition of Cl^-, the more amphiphilic complex (**527b**) was obtained and internalised in the micelle, where it quenched the fluorescence of the HPTS dye.

This system was largely unresponsive to other tested anions. Nevertheless, the sensor did succumb to the usual interference problems with the heavier halides (Br^- and I^-) and the pseudohalide CN^-.

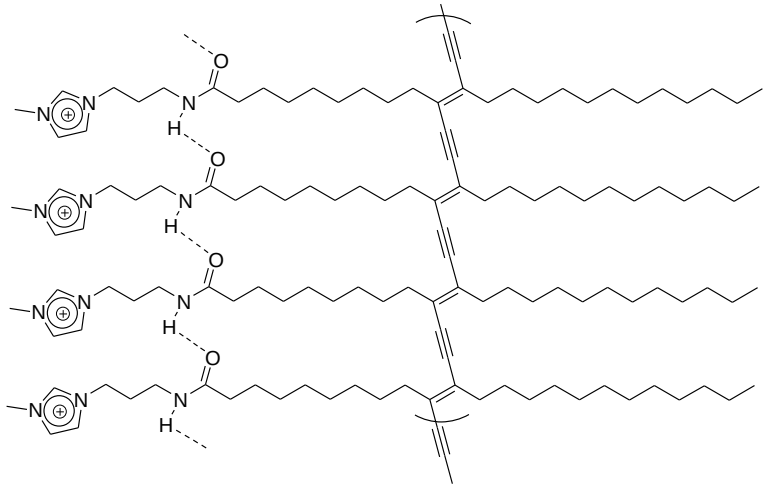

528

Fig. 287 Chemical structure of imidazolium-based polydiacetylene polymer **528**.

Imidazolium-based polydiacetylene polymer **528** (see Fig. 287) was developed as a chemosensor system for anionic surfactants.[346] Aqueous solutions of **528,** buffered at pH 7.4, showed a blue colour due to the presence of a broad absorption band at 620 nm. Changes in colour were studied in the presence of anions (F^-, Cl^-, Br^-, I^-, SO_4^{2-}, CO_3^{2-}, ClO_4^-, CH_3COO^-, NO_3^-, HPO_4^{2-} and SCN^-) and anionic (SDS, SDC, SDP and SDBS), neutral (Triton X-100) and cationic (CTAC) surfactants. Of all the tested species, only anionic surfactants were able to induce colour modulations. SDS induced a blue-to-yellow transition as SDS bound **528** more strongly, whereas SDC and SDP induced a blue-to-orange transition (medium interaction) and SDBS gave a blue-to-red transition as the extent of binding was less. Changes in colour were ascribed to the disruption of ionic hydrogen bonding, which allowed the release of the strain energy imposed on the alkyl side chains generated during polymerisation. Moreover, a 34-fold enhancement in fluorescence intensity at 565 nm was observed when SDS was added to an aqueous solution of **528**, where 56 ppb was the estimated limit of detection.

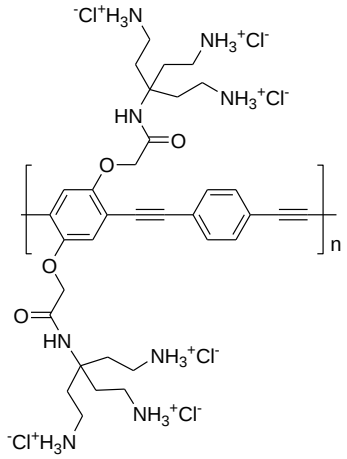

529

Fig. 288 Chemical structure of polymer **529** containing branched polyamine side chains.

Direct detection of $P_2O_7^{4-}$ in aqueous solutions was demonstrated using the cationic poly(phenylene-ethynylene) polymer with branched polyamine side chains **529** (see Fig. 288).[347] Aqueous solutions of polymer **529**, buffered at pH 6.5, showed an absorption band at 400 nm and a strong emission in the 433-455 nm range. Upon the addition of increasing amounts of $P_2O_7^{4-}$, the absorbance at 400 nm decreased and a new band at 430 nm emerged to become the dominating peak. Regarding emission, addition of anion $P_2O_7^{4-}$ induced emission quenching together with the appearance of a new fluorescence at 550 nm. The red shift in the absorption band, in addition to the well-defined isosbestic point at 410 nm, was consistent with an aggregation-induced planarisation of the phenylene-ethynylene backbone. Moreover, the blue-to-green emission change also suggested a conversion between the "free chain state" and the "aggregated state" of the polymer chains. Neither the absorption nor the emission spectra of **529** showed changes in the presence of PO_4^{3-}, CO_3^{2-}, SO_4^{2-}, F^-, Cl^-, Br^-, I^- and AMP, even at high concentrations. However, ADP and ATP should be considered as potential interferents as polymer fluorescence was affected by them. A limit of detection of 3.4 x 10^{-7} mol L^{-1} was estimated for $P_2O_7^{4-}$.

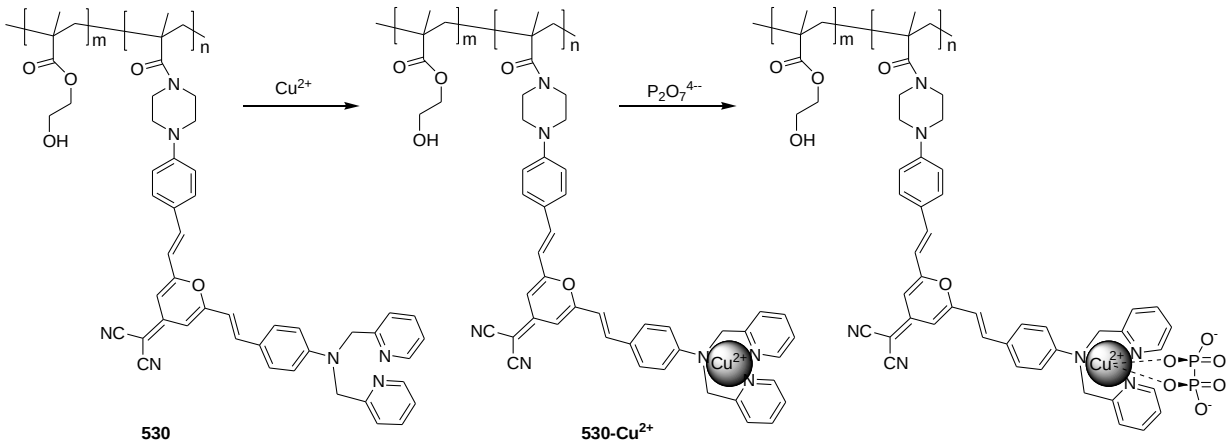

530 **530-Cu^{2+}**

Fig. 289 Schematic representation of the recognition of anion $P_2O_7^{4-}$ using copolymer **530**.

The incorporation of the ion-sensitive fluorescent unit (the dicyanomethylene-4H-pyran group) into a hydrophilic copolymer (**530**) yielded a sensory film for the recognition of anion $P_2O_7^{4-}$ (see Fig. 289).[348] CH_3CH_2OH:H_2O 5:2 v/v solutions of **530** (pH 7.4) showed intense emission at 605 nm upon excitation at 460 nm. Addition of cation Cu^{2+} induced an almost complete quenching of the emission band at 605 nm due to the formation of the corresponding **530-Cu^{2+}** complex. The formation of this complex lessened the electron-donating ability of the amino groups, thus resulting in the observed quenching. Afterwards, the changes in the emission profiles of the **530-Cu^{2+}** complex upon the addition of increasing quantities of anions (F^-, Cl^-, Br^-, I^-, $H_2PO_4^-$, HCO_3^-, HSO_4^-, AcO^-, NO_3^-, HPO_4^{2-}, SO_4^{2-}, CO_3^{2-}, AMP, ADP, ATP, PO_4^{3-} and $P_2O_7^{4-}$) were tested and only the addition of $P_2O_7^{4-}$ induced a 4.8-fold enhancement in the emission band. This enhancement was ascribed to the electrostatic interactions between $P_2O_7^{4-}$ and **530-Cu^{2+}** in which two oxygen atoms of the anion coordinated with the Cu^{2+} centre (see Fig. 281). These electrostatic interactions were able to reduce the electron withdrawal magnitude through a partial neutralisation of charge on the Cu^{2+} ion, thus enhancing the electron-donating character of the amino groups. A thin film of **530-Cu^{2+}** was fabricated on quartz slides and was proved to display a sensitive response to $P_2O_7^{4-}$, showing a turn-on of fluorescence.

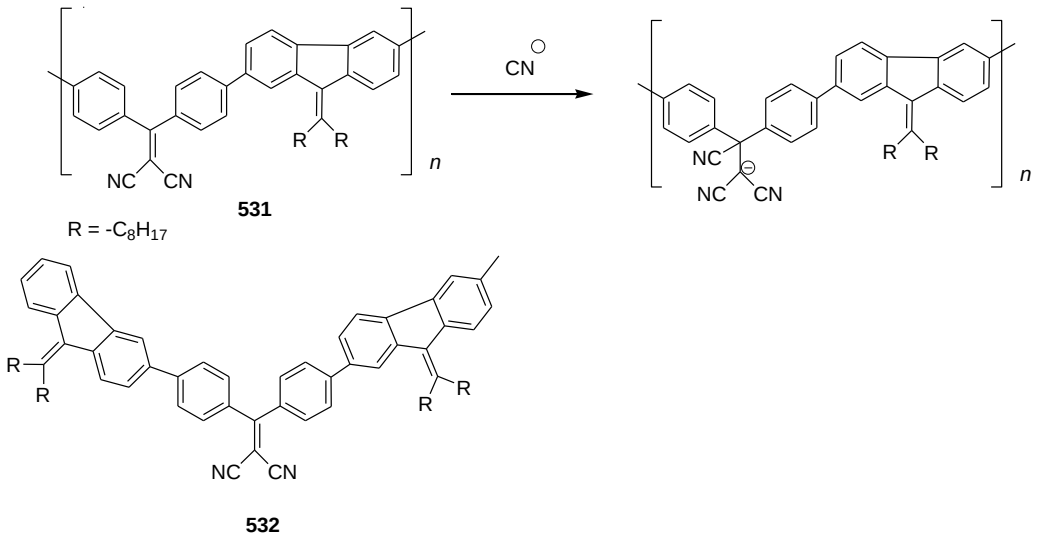

Fig. 290 Schematic representation of the recognition of anion CN^- using dicyano-vinyl-containing conjugated polymer **531**.

The use of a dicyano-vinyl-containing conjugated polymer (**531**) as colorimetric and fluorescent chemosensor for anion CN^- was reported. The authors compared the sensing properties of polymer **531** and its small molecular counterpart **532** (see Fig. 290).[349] Particularly when compared with **532**, **531** exhibited greater sensitivity and selectivity, a wider linear range and a faster response. In DMF, the UV-visible spectrum of **532** showed an absorption maximum at 380, whereas in **531,** the band was red-shifted to 403 nm due to the conjugation of the polymer backbone. The emission spectrum of **532** displayed a major emission peak at 575 nm and very weak emission at 434, whereas in **531,** these peaks were red-shifted to 597 and 455 nm, respectively. Addition of CN^- induced a decrease in the absorption of **531** at 403 nm and the formation of a new band at 338 nm, which corresponded to a colour change from yellow-green to colourless. In the emission spectra, addition of CN^- induced a quenching of the 597 nm band, while the emission at 455 nm remained unchanged. A limit of detection of 0.5 x 10^{-6}

mol L^{-1} was determined when using **531**. The studies with **532** gave a limit of detection of 2.5 x 10^{-6} mol L^{-1}. No colour or fluorescent changes were observed in the presence of other common anions, such as Cl^-, Br^-,I^-, $H_2PO_4^-$, HSO_4^- and AcO^-, and with various nucleophilic reagents. Only the addition of F^- induced slight interference. As in some of the examples above, the colormetric and fluorometric changes upon the addition of CN^- were ascribed to a nucleophilic addition of this anion at the α-position of the dicyanovinyl moiety.

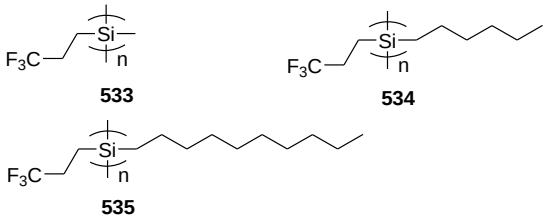

Fig. 291 Chemical structure of polymers **533-535**.

Poly(3,3,3-trifluoropropyl *n*-alkylsilane) polymers with methyl (**533**), hexyl (**534**) and decyl (**535**) groups were used for the fluorogenic recognition of monovalent anions (see Fig. 291).[350] Polysilanes **533-535** showed an absorption band at ca. 310 nm in THF, suggesting the adoption of a 7_3-helix structure. These solutions were also fluorescent and a broad emission at 332 nm was observed upon excitation at 300 nm. Addition of F^-, NO_3^-, Br^-, Cl^-, HSO_4^-, PF_6^- and I_3^- to THF solutions of **533** induced different degrees of quenching that were proportional to the surface charge density of the anion (F^- > NO_3^-, Br^- > Cl^- > HSO_4^- > PF_6^- > I_3^-). Practically the same quenching results were obtained for polymers **534** and **535**. Due to the helicoidal conformation of **533-535**, and as monovalent anions have to pass through the alkyl side chain's clad layers to reach the positively charged Si main chain, the more compact the steric size of the anion, the easier access becomes. Because of this, sensitivity to monovalent anions was modulated by the length of the appended alkyl chains. In particular, the calculation of Stern-Volmer quenching constants (ΔK_{SV}**534** >>>ΔK_{SV}**535** >>ΔK_{SV}**533**) indicated that the best sensitivity was achieved with polymer **534**.

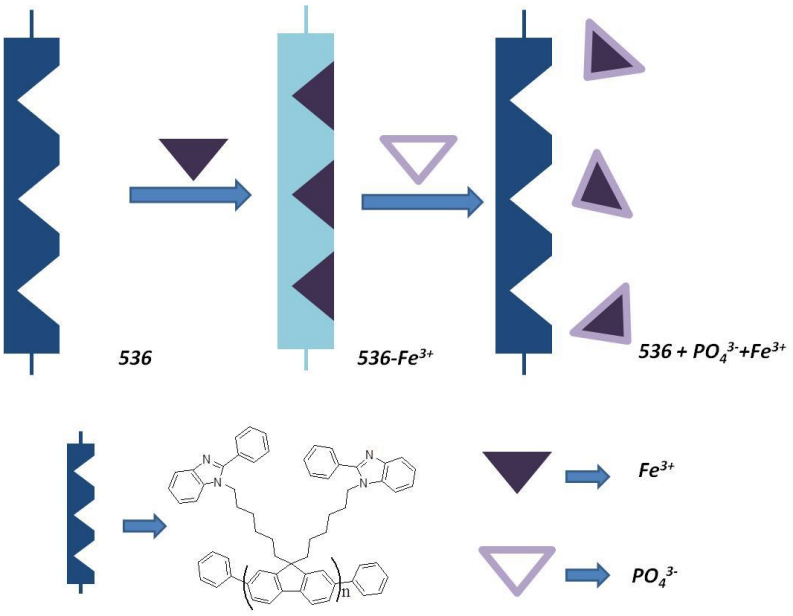

Fig. 292 Schematic representation of the recognition of anion HPO_4^{2-} using polymer **536**.

A material designed for the detection of HPO_4^{2-} was reported by Iyer and co-workers.[351] The probe consisted of a neutral polyfluorene derivative, poly(9,9-bis(6'-benzimidazole)hexyl)fluorene-alt-1,4-phenylene (**536**), containing benzimidazole as cation binding sites and fluorene as the fluorescent signalling subunit (see Fig. 292). Aqueous solutions of **536,** buffered at pH 7.4, revealed an intense emission at 410 nm upon excitation at 370 nm, which was quenched by the addition of cation Fe^{3+}. The observed quenching was ascribed to the formation of **536-Fe^{3+}** complexes, which induced a PET process. Addition of HPO_4^{2-} to a solution of **536-Fe^{3+}** induced the recovery of fluorescence due to the displacement of Fe^{3+} from the polymer backbone. Other anions (i.e., Cl^-, Br^-, I^-, NO_3^-, CO_3^{2-}, NO_2^-, CN^-, SO_4^{2-}, $S_2O_3^{2-}$, $S_2O_5^{2-}$) were unable to induce any effect, whereas studies with inorganic ($P_2O_7^{4-}$, polyphosphate) and organic phosphates (ADP, ATP, G6P, TEP, oPLS) revealed that only inorganic phosphate derivatives produced quenching. Finally, it was possible to detect HPO_4^{2-} and polyphosphates in saliva with a limit of detection of 1.44 x 10^{-3} mol L^{-1}.

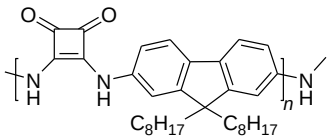

537

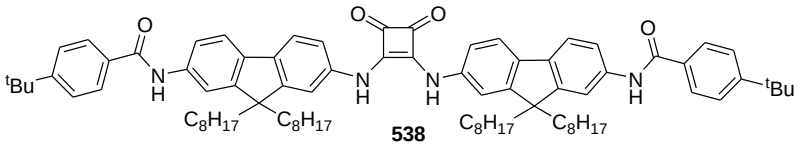

538

Fig. 293 Chemical structures of polymer **537** and model compound **538**.

Solution of polymer **537** (see Fig. 293) in H_2O:*N*-methylpyrrolidinone (NMP) 10:90 v/v showed an increase in emission intensity at 453 nm (λ_{ex} = 415 nm) upon the addition of increasing

amounts of $H_2PO_4^-$.[352] Fluorescence intensity as a function of $H_2PO_4^-$ concentration displayed the characteristic sigmoidal shape of a cooperative anion response, whereas the Hill plot indicated positive cooperativity for the **537**-$H_2PO_4^-$ interaction. In addition, receptor **538** also exhibited an increased fluorescence quantum yield upon the addition of $H_2PO_4^-$, but it was approximately four times less sensitive. Moreover, **538** did not show the cooperative response found for **537**. The fluorescence response of polymer **537** was selective for $H_2PO_4^-$ over other monovalent anions (i.e., F^-, Cl^-, Br^-, I^-, HSO_4^-, NO_3^-, AcO^- and OH^-). In contrast, model compound **538** displayed the greatest fluorescence response to F^-, followed by $H_2PO_4^-$. The authors ascribed the emission enhancements upon $H_2PO_4^-$ binding with both receptors to an intramolecular charge transfer mechanism. The unusual enhancement in affinity and in the selectivity of **537**, when compared with **538**, resulted from polymer aggregation (revealed from TEM studies) upon anion binding.

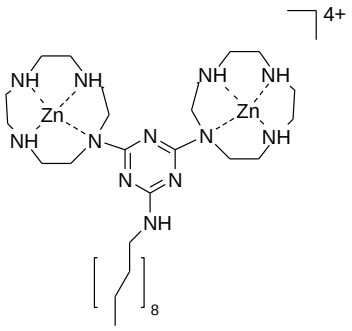

539

Fig. 294 Chemical structure of **539**.

An approach to signal anion binding by the non-covalent co-embedding of amphiphilic binding sites and fluorescent dyes into the membrane of small unilamellar vesicles was described.[353] Luminiscent vesicular receptors (LVR) were prepared by combining **539** (as a binding site for anions, see Fig. 294) and two amphiphilic fluorophores based on carboxyfluoresceine **(CF)** and coumarin **(Cou)**. **LVR-539-Cou** exhibited a strong fluorescence emission with a maximum intensity at 405 nm upon excitation at 349 nm. Addition of $P_2O_7^{4-}$ or phosphoserine anions induced moderate quenching, whereas the other anions tested (SO_4^{2-}, Gly-OMe) induced negligible changes in the emission profile. Vesicular receptor **LVR-539-CF** showed green fluorescence emission with a maximum intensity at 520 nm if excited at 495 nm. Upon addition of $P_2O_7^{4-}$, emission intensity increased.

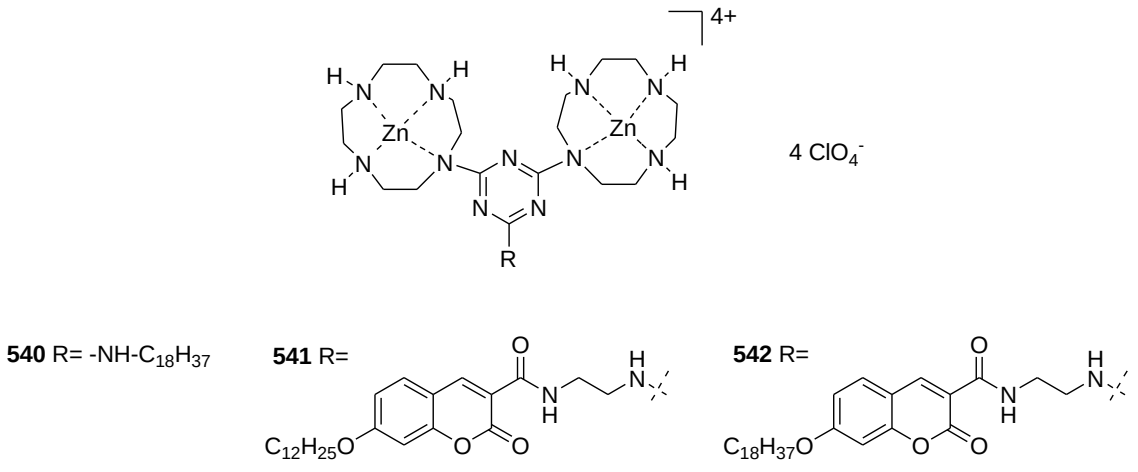

Fig. 295 Chemical structures of bis-Zn(II) cyclen complexes **540**-**542**.

Bis-Zn(II) cyclen complexes **540**-**542** (see Fig. 295) were used to prepare vesicular receptors (**VR-540**, **VR-541** and **VR-542**), which were used for the detection of phosphate derivatives using indicator displacement assays (with **VR-540**) and as luminescent labelled complexes (with **VR-541** and **VR-542**).[354] Aqueous solutions, buffered at pH 7.4, of coumarin methyl sulphonate (CMS) showed an emission band at 480 nm which was progressively quenched upon the addition of **VR-540** due to the formation of an ensemble between the fluorophore and the vesicular receptor. Addition of phosphate derivatives (i.e., UTP, $P_2O_7^{4-}$, GTP, UDP, GDP, PO_4^{3-} phenylphosphate and pSer) induced different enhancements (UTP > $P_2O_7^{4-}$ > GTP > UDP > GDP > PO_4^{3-} > pSer > phenylphosphate) in emission intensity due to coordination of phosphates with the Zn(II) centre with the subsequent release of CMS. Receptors **VR-541** and **VR-542** were composed of bis-Zn(II) cyclen complexes, linked with a coumarin fluorophore. through covalent bonds. Aqueous solutions of **VR-542** showed an emission at 405 nm, which was ascribed to the coumarin group. Addition of ATP, $P_2O_7^{4-}$ and PO_4^{3-} to the aqueous solutions of **VR-542** induced a remarkable quenching of the emission band, whereas the other anions tested (UTP, GDP, GTP, UDP, phenylphosphate and pSer) induced negligible changes. Virtually the same response was observed for **VR-541**.

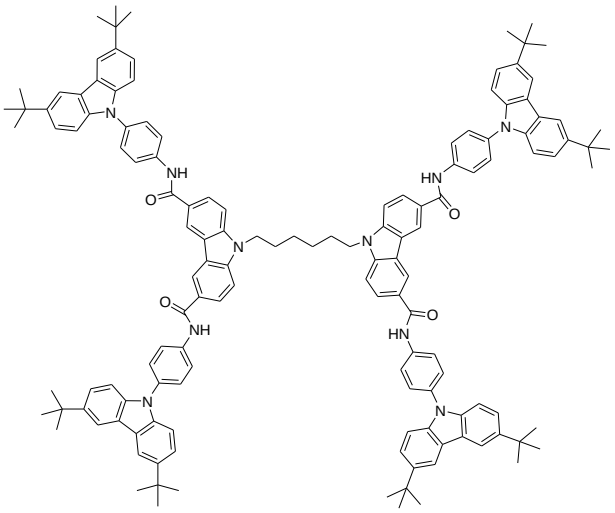

543

Fig. 296 Chemical structures of dendritic gelator **543**.

In this work, the authors prepared a dendritic gelator with carbazole building blocks (**543**), which was able to form a supergel in DMSO (see Fig. 296).[355] H-bonding, between the N-H amide moieties, and π-π interactions played key roles in gel formation, whereas amide groups acted as anion receptors. DMSO solutions of the gel formed by **543** showed an emission band centred at 440 nm upon excitation at 299 nm, ascribed to the formation of *J*-aggregates and the restricted molecular motion in the gel state, which was moderately enhanced upon the addition of F^- anion. This emission enhancement was ascribed to the rupture of the gel structure owing to the formation of 1:4 **543**:F^- complexes in which the anion interacted with the amide moieties via hydrogen-bonding forces. The other anions tested, such as Cl^-, Br^-, I^-, and AcO^-, were unable to interact with the amide groups in **543** due to the steric hindrance imposed by the branched arms and induced negligible changes in the emission band.

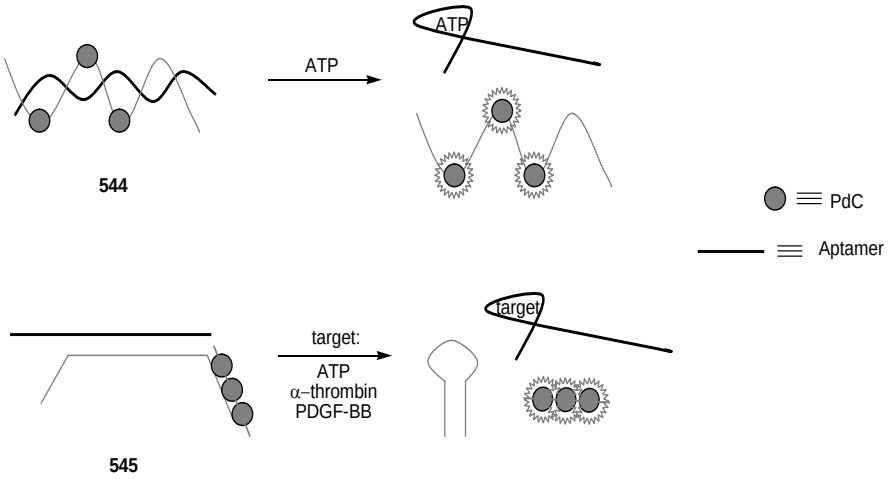

Fig. 297 Schematic representation of the recognition of ATP using a **544-545**.

Two versions of signal-on aptasensors for molecular recognition, which employed unmodified DNA aptamers and signalilng probes containing the fluorescent-based analogue pyrrolo-dC (**PdC**), were developed (see Fig. 297).[356] Both **544** and **545** were based on **PdC**'s property to respond to the structural changes of aptamers caused by the presence of targets. Aptasensor system **544** comprised a 27-base DNA aptamer for target recognition, which initially bound to the three fluorescent **PdC** bases incorporated into the signalling competitor, where its intrinsic fluorescence was strongly quenched. Upon the addition of different ATP concentrations, fluorescence intensity increased owing to the simultaneous formation of **544**:ATP complexes and the free competitor **PdC**-incorporated probe, which was fluorescent. No significant fluorescence increase was observed when GTP was added. A limit of detection of 3.0 x 10^{-7} mol L^{-1} was calculated for ATP. The more sophisticated aptasensor **545** employed three components, including an unmodified aptamer, a hairpin-haped competitor and a **PdC** signalling probe. Initially, aptamer **545** was hybridised with a complementary loop part of the competitor and a stem part of the competitor bound to the universal fluorescent base (**UFB**) probe, a single-strand DNA fragment containing **PdC** signalling probes, leading to the formation of triplex DNA. In the presence of ATP, α-thrombin and platelet-derived growth factor (PDGF-BB), the competitor was displaced from the aptamer, yielding a hairpin structure. The released UFB probe induced an enhanced fluorescence signal. The limits of detection of **545** for ATP, α-thrombin and PDGF-BB were found to be 3.0 x 10^{-7} mol L^{-1}, 4.0 x 10^{-10} mol L^{-1} and 8.0 x 10^{-10} mol L^{-1}, respectively. As a negative control, no significant signals were observed when BSA was employed.

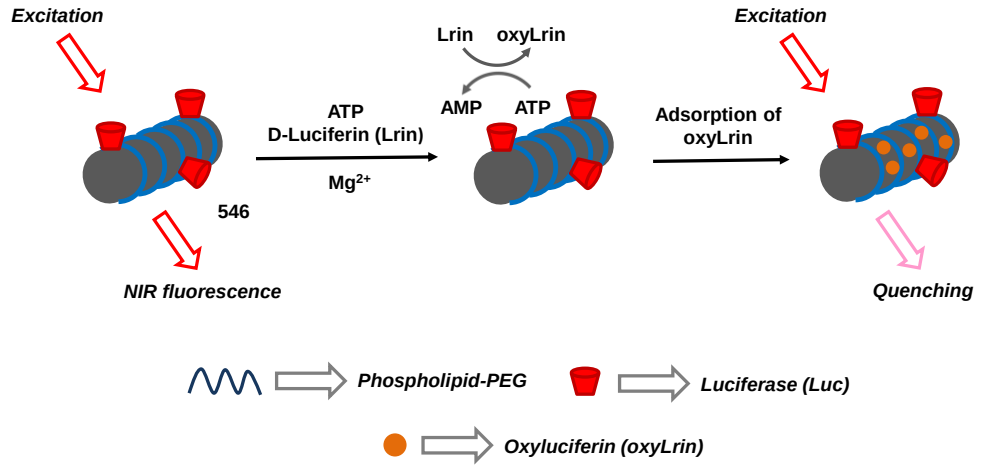

Fig. 298 Schematic representation of the recognition of ATP using **546**.

Single-walled carbon nanotube/luciferase (SWNT/Luc) enzyme conjugate **546** was reported for the near-infrared (NIR) fluorescent detection of cellular ATP (see Fig. 298).[357] When only ATP or D-luciferin (Lrin) was added to the solution of **546,** no fluorescence quenching was observed. The addition of $P_2O_7^{4-}$, H_2O_2, AMP, ADP, CTP and GTP was also unable to induce any change in the emission profile of **546**. However, after adding both ATP and Lrin to a solution of **546** in Tris-HCl buffer, fluorescence quenching was observed. This emission quenching was ascribed to the formation of oxyluciferin (oxyLrin), a product of the Luc-mediated biolumiscent reaction during ATP detection. The formed oxyluciferin quenched the emission of **546** through an electron transfer process. When **546** was employed, a limit of detection of 2.4 x 10^{-7} mol L^{-1} nm

was determined for ATP. Moreover, it was found that **546** was capable of spatially and temporally detecting ATP in HeLa cells.

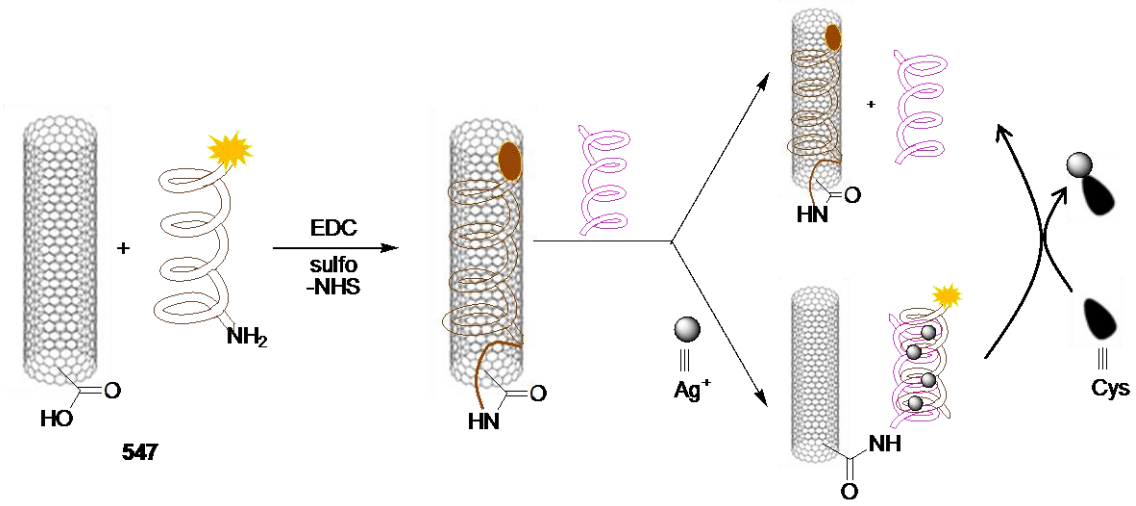

Fig. 299 Schematic representation of the recognition of Cys using reusable DNA single-walled carbon-nanotube-based (SWNT) fluorescent probe **547**.

Reusable DNA single-walled carbon-nanotube-based (SWNT) fluorescent sensor **547** (see Fig. 299) was developed for the sensitive and selective detection of cysteine in aqueous solutions.[358] Given the strong π-π stacking interaction between the ssDNA-F sequence (functionalised with fluoresceine) and SWNTs, the dye emission was quenched completely. However in the presence of Ag^+ and a semicomplementary single strand, a DNA duplex formed (by C-Ag^+-C coordination) with the subsequent suppression of the quenching effect of SWNT. Addition of Cys to this ensemble induced a gradual quenching of the emission intensity (emission at 518 nm upon excitation at 480 nm), which was ascribed to the removal of Ag^+ from C-Ag^+-C base pairs through competitive binding. When **547** was used, a limit of detection of 1.8 x 10^{-8} mol L^{-1} of Cys was achieved. Other amino acids tested (i.e., Ala, Arg, Asn, Asp, Gln, Glu, Gly, His, Ile, Leu, Lys, Met, Phe, Pro, Ser, Thr, Trp, Tyr and Val) induced negligible changes in the emission profile of the hybrid sensory system.

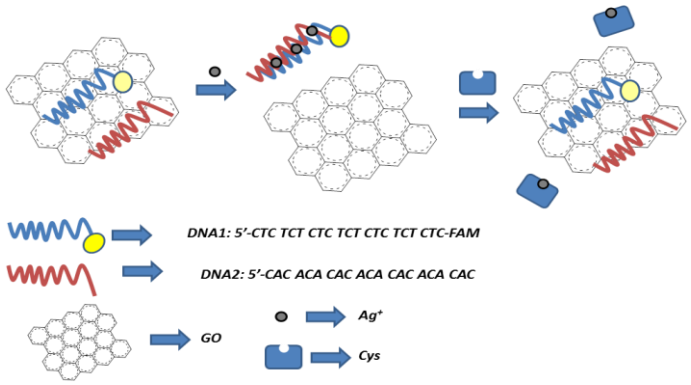

Fig. 300 Schematic representation of the recognition of Cys and Ag^+ using a dual-ouput fluorescent DNA logic gate.

A dual-ouput fluorescent DNA logic gate, capable of detecting Ag^+ ions and Cys based on graphene oxide (GO), was reported (see Fig. 300).[359] In the absence of Ag^+, the two separate C-rich ssDNA silver-specific oligonucleotides (DNA1-F labelled with fluoresceine and DNA2) were

found in a flexible single-strand conformation and formed stable GO/DNA complexes in the aqueous solution due to the stacking interactions between nucleotide bases and GO. Consequently, GO adsorbed the unbound ssDNA sequences and quenched the fluorescence of DNA1-F. In the presence of Ag^+, C-Ag^+-C base pairs were formed and, therefore, fluoresceine fluorescence was recovered. By bearing in mind the competition between C-Ag^+-C base pairs and Cys for the binding to Ag^+, addition of Cys induced remarkable quenching. The limit of detection for Cys using this protocol was 4.4×10^{-8} mol L^{-1}. Practically the same response was obtained upon the addition of Hcy and GSH, whereas addition of Ala, Arg, Asn, Asp, Gln, Glu, Gly, His, Ile, Leu, Lys, Met, Phe, Pro, Ser, Thr, Trp, Tyr and Val induced negligible changes.

4.- Concluding remarks

Nowadays, the chemistry of chromo-fluorogenic anion chemosensors is a well-established area in the anion supramolecular chemistry field. In this review, an account of the examples reported in 2010-2011 related with the design of chromogenic and/or fluorogenic probes for anions has been provided. Most examples reveal different combinations of binding or reactive sites and signalling units coupled in different ways to develop selective systems for different anionic species. In the first part, chromogenic examples have been described, whereas fluorogenic examples have been provided in a second more extense section. Moreover, each section was classified according to the signalling paradigm used; i.e. (i) the binding site - signalling unit protocols, (ii) the displacement approach and (iii) the design of chemodosimeters. In addition, a section with examples using polymers of nanomaterials has also been included.

We published a comprehensive review on chromo-fluorogenic anion chemosensors and reagents in 2003 which embraced all the examples reported in the literature in this field until that year.[1] This 2003 review ncluded a total of 190 reports. In 2010, we published another comprehensive review on chromo-fluorogenic anion chemosensors containing 130 papers published in 2009.[15] This review accounts for a total of 139 examples reported in 2010, wheras 182 papers were published in 2011. This relatively large number of examples (451 in the 2009-2011 period) is a clear indication of the scientific community's interest in designing anion signalling probes. In 2010-2011, a total of 153 examples were related with the binding site-signalling subunit approach, which is still the most widely used approach to develop chromo-fluorogenic anion probes. Thirty-three papers used displacement protocols and 107 followed the chemodosimeter approach. We also found a significant number (40 examples) of new anion signalling concepts which mostly involve the use of nanoparticles or nanostructured scaffoldings. A significant feature observed in this review is that there is still a large number of systems showing optical signalling of anions in non-aqueous environments, whereas increasing interest has been shown in designing probes capable of detecting target anions in complex environmental and biological samples, and a number of new advances in this last field is envisioned.

[1] R. Martínez-Máñez, F. Sancenón, *Chem. Rev.*, 2003, **103**, 4419-4476.

[2] E. A. Katayev, Y. A. Ustynyuk, J. L. Sessler, *Coord. Chem. Rev.*, 2006, **250**, 3004-3037.

[3] C. Suksai, T. Tuntulani, *Chem. Soc. Rev.*, 2003, **32**, 192-202.

[4] S. K. Kim, D. H. Lee, J. –I. Hong, J. Yoon, *Acc. Chem. Res.*, 2009, **42**, 23-31.

[5] P. D. Beer, *Coord. Chem. Rev.*, 2000, **205**, 131-155.

[6] Y. Zhou, Z. Xu, J. Yoon, *Chem. Soc. Rev.*, 2011, **40**, 2222-2235.

[7] T. Gunnlaugsson, M. Glynn, G. M. Tocci, P. E. Kruger, F. M. Pfeffer, *Coord. Chem. Rev.*, 2005, **250**, 3094-3117.

[8] V. Amendola, D. Esteban-Gómez, L. Fabbrizzi, M. Licchelli, *Acc. Chem. Res.*, 2006, **39**, 343-353.

[9] T. Gunnlaugsson, H. P. D. Ali, M. Glynn, P. E. Kruger, G. M. Hussey, F. M. Pfeffer, C. M. G. dos Santos, J. Tierney, *J. Fluoresc.*, 2005, **15**, 287-299.

[10] S. L. Wiskur, H. Aït-Haddou, J. J. Lavigne, E. V. Anslyn, *Acc. Chem. Res.*, 2001, **34**, 963-972.

[11] B. T. Nguyen, E. V. Anslyn, *Coord. Chem. Rev.*, 2006, **250**, 3118-3127.

[12] Z. Xu, X. Chen, H. N. Kim, J. Yoon, *Chem. Soc. Rev.*, 2010, **39**, 127-137.

[13] K. Kaur, R. Saini, A. Kumar, V. Luxami, N. Kaur, P. Singh, S. Kumar, *Coord. Chem. Rev.*, 2012, **256**, 1992-2028.

[14] Y. Zhou, J. Yoon, *Chem. Soc. Rev.*, 2012, **41**, 52-67.

[15] M. E. Moragues, R. Martínez-Máñez, F. Sancenón, *Chem. Soc. Rev.*, 2011, **40**, 2593-2643.

[16] A. Aldrey, C. Núñez, V. García, R. Bastida, C. Lodeiro, A. Macías, *Tetrahedron*, 2010, **66**, 9223-9230.

[17] M. O. Odago, D. M. Colabello, A. J. Lees, *Tetrahedron*, 2010, **66**, 7465-7471.

[18] P. Piatek, *Chem. Commun.*, 2011, **47**, 4745-4747.

[19] X. He, F. Herranz, E. C. -C. Cheng, R. Vilar, V. W. -W. Yam, *Chem. Eur. J.*, 2010, **16**, 9123-9131.

[20] W. -C. Lin, Y. -P. Tseng, C. -Y. Lin, Y. -P. Yen, *Org. Biomol. Chem*., 2011, **9**, 5547-5553.

[21] M. Regueiro-Figueroa, K. Djanashvili, D. Esteban-Gómez, A. de Blas, C. Platas-Iglesias, T. Rodríguez-Blas, *Eur. J. Org. Chem*., 2010, 3237-3248.

[22] I. A. Carasel, C. R. Yamnitz, R. K. Winter, G. W. Gokel, *J. Org. Chem*., 2010, **75**, 8112-8116.

[23] A. Rostami, A. Colin, X. Y. Li, M. G. Chudzinski, A. J. Lough, M. S. Taylor, *J. Org. Chem*., 2010, **75**, 3983-3992.

[24] V. Amendola, G. Bergamaschi, M. Boiocchi, L. Fabbrizzi, M. Milani, *Chem. Eur. J.*, 2010, **16**, 4368-4380.

[25] A. Sola, R. A. Orenes, M. A. García, R. M. Claramunt, I. Alkorta, J. Elguero, A. Tárraga, P. Molina, *Inorg. Chem.*, 2011, **50**, 4212-4220.

[26] D. Y. Lee, N. Sihgh, A. Satyender, D. O. Jang, *Tetrahedron Lett.*, 2011, **52**, 6919-6922.

[27] V. Haridas, S. Sahu, P. P. Praveen Kumar, *Tetrahedron Lett.*, 2011, **52**, 6930-6934.

[28] J. J. Park, Y. H. Kim, S. Rhim, J. Kang, *Tetrahedon Lett.*, 2012, **53**, 247-252.

[29] V. Amendola, L. Fabbrizzi, L. Mosca, F. –P. Schmidtchen, *Chem. Eur. J.*, 2011, **17**, 5972-5981.

[30] J. -M. You, H. Jeong, H. Seo, S. Jeon, *Sens. Actuators B*, 2010, **146**, 160-164.

[31] A. S. F. Farinha, A. C. Tomé, J. A. C. Cavaleiro, *Tetrahedron Lett.*, 2010, **51**, 2184-2187.

[32] G. W. Lee, N-K. Kim, K-S. Jeong, *Org. Lett.*, 2010, **12**, 11, 2634-2637.

[33] P. Bose, P. Ghosh, *Chem. Commun.*, 2010, **46**, 2962-2964.

[*34*] L. Wang, X. He, Y. Guo, J. Xua, S. Shao*, Org. Biomol. Chem.,* 2011, **9**, 752–757.

[35] M. A. Tetilla, M. C. Aragoni, M. Arca, C. Caltagirone, C. Bazzicalupi, A. Bencini, A. Garau, F. Isaia, A. Laguna, V. Lippolis, V. Meli, *Chem. Commun*., 2011, **47**, 3805-3807.

[36] T. Kundu, S. M. Mobin, G. K. Lahiri, *Dalton Trans*., 2010, **39**, 4232-4242.

[37] C. -H. Lee, S. Lee, H. Yoon, W. -D. Jang, *Chem. Eur. J*., 2011, **17**, 13898-13903.

[38] A. N. Swinburne, M. J. Paterson, K. H. Fischer, S. J. Dickson, E. V. B. Wallace, W. J. Belcher, A. Beeby, J. W. Steed, *Chem. Eur. J*., 2010, **16**, 1480-1492.

[39] R. Kannappan, C. Bucher, E. Saint-Aman, J. -C. Moutet, A. Milet, M. Oltean, E. Métay, S. Pellet-Rostaing, M. Lemaire, C. Chaix, *New. J. Chem*., 2010, **34**, 1373-1386.

[40] N. Kumari, S. Jha, S. Bhattacharya, *J. Org. Chem*., 2011, **76**, 8215-8222.

[41] V. Amendola, M. Boiocchi, L. Fabbrizzi, N. Fusco, *Eur. J. Org. Chem*., 2011, 6434-6444.

[42] A. Kumar, V. Kumar, K. K. Upadhyay, *Tetrahedron Lett.*, 2011, **52**, 6809-6813.

[43] X. Bao, Y. Zhou, *Sens. Actuators, B*, 2010, **147**, 434-441.

[44] X. Lou, Y. Zhang, Q. Li, J. Qin, Z. Li, *Chem. Commun*., 2011, **47**, 3189-3191.

[45] X-F. Shang, H. Su, H. Lin, H-K. Lin, *Inorg. Chem*. *Commun.*, 2010, **13**, 999-1003.

[46] J. S. Mendy, M. A. Saeed, F. R. Fronczek, D. R. Poell, Md. A. Hossain, *Inorg. Chem*., 2010, **49**, 7223-7225.

[47] P. Mahato, A. Ghosh, S. K. Mishra, A. Shrivastav, S. Mishra, A. Das, *Inorg. Chem*., 2011, **50**, 4162-4170.

[48] P. Mahato, A. Ghosh, S. K. Mishra, A. Shrivastav, S. Mishra, A. Das, *Chem. Commun.*, 2010, **46**, 9134-9136.

[49] A. D. Cort, G. Forte, L. Schiaffino, *J. Org. Chem*., 2011, **76**, 7569-7572.

[50] P. Das, A. K. Mandal, M. K. Kesharwani, E. Suresh, B. Ganguly, A. Das, *Chem. Commun*., 2011, **47**, 7398-7400.

[51] L. A. Baumes, M. Buaki, J. Jolly, A. Corma, H. Garcia, *Tetrahedron Lett.*, 2011, **52**, 1418–1421.

[52] L. A. Baumes, M. B. Sogo, P. Montes-Navajas, A. Corma, H. Garcia, *Chem. Eur. J*., 2010, **16**, 4489-4495.

[53] H. T. Chifotides, B. L. Schottel, K. R. Dunbar, *Angew. Chem. Int. Ed*., 2010, **49**, 7202-7207.

[54] X. Gu, C. Liu, Y. –C. Zhu, Y. –Z. Zhu, *Tetrahedron Lett.*, 2011, **52**, 5000-5003.

[55] C. Männel-Croisé, C. Meister, F. Zelder, *Inorg. Chem*., 2010, **49**, 10220-10222.

[56] S. Watchasit, A. Kaowliew, C. Suksai, T. Tuntulani, W. Ngeontae, C. Pakawatchai, *Tetrahedron Lett.*, 2010, **51**, 3398-3402.

[57] P. Mateus, R. Delgado, P. Brandão, V. Félix, *Chem. Eur. J*., 2011, **17**, 7020-7031.

[58] Z. -H. Chen, Y. Lu, Y. -B. He, X. -H. Huang, *Sens. Actuators, B*, 2010, **149**, 407-412.

[59] P. -K. Müller-Graff, H. Szelke, K. Severin, R. Krämer, *Org. Biomol. Chem.*, 2010, **8**, 2327-2331.

[60] Z. -Q. Hu, X. -M. Wang, Y. -C. Feng, L. Ding, M. Li, C. -S. Lin, *Chem. Commun.*, 2011, **47**, 1622-1624.

[61] N. Singh, D. O. Jang, *Tetrahedron Lett.*, 2011, **52**, 5094–5097.

[62] K. Ghosh, A. R. Sarkar, *Org. Biomol. Chem.*, 2011, **9**, 6551-6558.

[63] A. K. Atta, I. H. Ahn, A. Y. Hong, J. Heo, C. K. Kim, D. G. Cho, *Tetrahedron Lett.*, 2012, **53**, 575-578.

[64] R. Perry-Feigenbaum, E. Sella, D. Shabat, *Chem. Eur. J.,* **17**, 2011, 12123-12128.

[65] P. Rajamalli, E. Prasad, *Org. Lett.,* 2011, **13**, 3714-3717.

[66] C. Bhaumik, S. Das, D. Maity, S. Baitalik, *Dalton Trans*., 2011, **40**, 11795-11808.

[67] J. Isaad, A. Perwuelz, *Tetrahedron Lett.*, 2010, **51**, 5810-5814.

[68] C. R. Wade, F. P. Gabbaï, *Inorg. Chem*., 2010, **49**, 714-720.

[69] T. Ábalos, D. Jiménez, M. Moragues, S. Royo, R. Martínez-Máñez, F. Sancenón, J. Soto, A. M. Costero, M. Parra, S. Gil, *Dalton Trans.*, 2010, **39**, 3449-3459.

[70] T. Ábalos, S. Royo, R. Martínez-Máñez, F. Sancenón, J. Soto, A. M. Costero, S. Gil, M. Parra, *New J. Chem.*, 2009, **33**, 1641-1645.

[71] S. Sumiya, T. Doi, Y. Shiraishi, T. Hirai, *Tetrahedron*, 2012, **68**, 690-696

[72] Y. Shirashi, M. Itoh, T. Hirai, *Tetrahedron Lett.*, 2011, **52**, 1515-1519.

[73] Y. Shiraishi, M. Itoh, T. Hirai, *Tetrahedron*, 2011, **67**, 891-897.

[74] J. Isaad, A. El Achari, *Tetrahedron*, 2011, **67**, 5678-5685.

[75] J. Isaad, A. El Achari, *Tetrahedron*, 2011, **67**, 4196-4201.

[76] I. S. Park, E. J. Heo, J. M. Kim, *Tetrahedron Lett.*, 2011, **52**, 2454-2457.

[77] X. Tang, W. Liu, W. Zhao, H. Zhang, P. Wang, *Tetrahedron Lett.*, 2011, **52**, 5136-5139.

[78] W. Wei, X. Liang, G. Hu, Y. Guo, S. Shao, *Tetrahedron Lett.*, 2011, **52**, 1422-1425.

[79] K. Cui, D. Zhang, G. Zhang, D. Zhu, *Tetrahedron Lett.*, 2010, **51**, 6052-6055.

[80] M. H. Kim, S. Kim, H. H. Jang, S. Yi, S. H. Seo, M. S. Han, *Tetrahedron Lett.*, 2010, **51**, 4712-4716.

[81] S. Zhang, J. Wang, L. Han, C. Li, W. Wang, Z. Yuan, *Sens. Actuators, B*, 2010, **147**, 687-690.

[82] D.-Q. Feng, G. Liu, W. Zheng, J. Liu, T. Chen, D. Li, *Chem. Commun*., 2011, **47**, 8557-8559.

[83] R. Cao, B. Li, *Chem. Commun*., 2011, **47**, 2865-2867.

[84] C. -Y. Liu, W. -L. Tseng, *Chem. Commun*., 2011, **47**, 2550-2552.

[85] M. Zhang, Y. -Q. Liu, B. -C. Ye, *Chem. Commun*., 2011, **47**, 11849-11851.

[86] H. Li, F. Li, C. Han, Z. Cui, G. Xie, A. Zhang, *Sens. Actuators, B*, 2010, **145**, 194-199.

[87] R. Sakai, S. Okade, E. B. Barasa, R. Kakuchi, M. Ziabka, S. Umeda, K. Tsuda, T. Satoh, T. Kakuchi, *Macromolecules*, 2010, **43**, 7406-7411.

[88] R. Sakai, N. Sakai, T. Satoh, W. Li, A. Zhang, T. Kakuchi, *Macromolecules*, 2011, **44**, 4249-4257

[89] J. Isaad, F. Salaün, *Sensors and Actuators B*, 2011, **157**, 26-33.

[90] J. Isaad, A. E. Achari, *Thetrahedron*, 2011, **67**, 4939-4947.

[91] Z. Yao, H. Bai, C. Li, G. Shi, *Chem. Commun*., 2010, **46**, 5094-5096.

[92] J. Krishnamurthi, T. Ono, S. Amemori, H. Komatsu, S. Shinkai, K. Sada, *Chem. Commun*., 2011, **47**, 1571-1573.

[93] S. Vallejos, P. Estévez, F. C. García, F. Serna, J. L. de la Peña, J. M. García, *Chem. Commun.*, 2010, **46**, 7951-7953.

[94] J. Liu, Y. Liu, Q. Liu, C. Li, L. Sun, F. Li*, J. Am. Chem. Soc*., 2011, **133**, 15276-15279.

[95] E. Climent, C. Giménez, M. D. Marcos, R. Martínez-Máñez, F. Sancenón, J. Soto, *Chem. Commun.*, 2011, **47**, 6873-6875.

[96] M. J. Greaney, M. A. Nuyen, C. -C. Chang, A. Good, L. D. Margerum, *Chem. Commun.*, 2010, **46**, 5337-5339.

[97] A. P. de Silva, H. Q. N. Gunaratne, T. Gunnlaugsson, A. J. M. Huxley, C. P. McCoy, J. T. Rademacher, T. E. Rice, *Chem. Rev.*, 1997, **97**, 1515-1566.

[98] D. Maity, A. Chakraborty, R. Gunupuru, P. Paul, *Inorg. Chim. Acta*, 2011, **372**, 126-135.

[99] M. Kumar, R. Kumar, V. Bhalla, *Tetrahedron Lett.*, 2010, **51**, 5559-5562.

[100] M. Kumar, R. Kumar, V. Bhalla, *Org. Lett.,* 2011, **13**, 366-369.

[101] X. -L. Ni, X. Zeng, C. Redshaw, T. Yamato, *J. Org. Chem.,* 2011, **76**, 5696–5702.

[102] K. Ghosh, D. Kar, P. R. Chowdhury, *Tetrahedron Lett.,* 2011, **52**, 5098–5103.

[103] Z. Zeng, A. A. J. Torriero, A. M. Bond, L. Spiccia, *Chem. Eur. J.*, 2010, **16**, 9154-9163.

[104] D. Thongkum, T. Tuntulani, *Tetrahedron,* 2011, **67**, 8102-8109.

[105] Y. Zhou, J. Y. Jung, H. R. Jeon, Y. Kim, S. –J. Kim, J. Yoon, *Org. Lett.*, 2011, **23**, 2742-2745.

[106] F. Schmidt, S. Stadlbauer, B. König, *Dalton Trans.*, 2010, **39**, 7250-7261.

[107] Z. Xu, D. R. Spring, J. Yoon, *Chem. Asian J.*, 2011, **6**, 2114-2122.

[108] T. –M. Fu, C. –Y. Wu, C. –C. Cheng, C. –R. Yang, Y. –P. Yen, *Sensors Actuators B*, 2010, **146**, 171-176.

[109] W. T. Gong, S. Bao, F. –R. Wang, J. –W, Ye, G. –L. Ning, K. Hiratani, *Tetrahedron Lett.*, 2011, **52**, 630-634.

[110] X. –H. Huang, Y. Lu, Y. –B. He, Z. –H. Chen, *Eur. J. Org. Chem.*, 2010, 1921-1927.

[111] S. K. Lee, H. Kim, S. Jang, J. Kang, *Tetrahedron Lett.,* 2011, **52**, 1977–1980.

[112] S. K. Lee, J. Kang, *Tetrahedron Lett.,* 2011, **52**, 5192–5195.

[113] J. J. Park, Y. H. Kim, C. Kim, J. Kang, *Tetrahedron Lett.*, 2011, **52**, 2759-2763.

[114] M. Shahid, P. Srivastava, A. Misra, *New J. Chem.,* 2011, **35**, 1690–1700.

[115] S. Goswami, N. K. Das, D. Sen, G. Hazra, J. H. Goh, Y. C. Sing, H. K. Fun, *New J. Chem.,* 2011, **35**, 2811–2819.

[116] L. -Y. Yao, L. Qin, T. -Z Xie, Y. -Z Li, S. -Y Yu, *Inorg. Chem.,* 2011, **50**, 6055-6062.

[117] N. Ahmed, B. Shirinfar, I. Geronimo, K. S. Kim, *Org. Lett.*, 2011, **13**, 5476-5479.

[118] H. Kim, J. H. Moon, S. K. Kim, J. Y. Kwon, Y. J. Jang, J. Y. Lee, J. Yoon, *J. Org. Chem.,* 2011, **76**, 3805–3811.

[119] J. R. Jadhav, C. H. Bae, H. -S. Kim, *Tetrahedron Lett.,* 2011, **52**, 1623–1627.

[120] M. Bhuyan, E. Katayev, S. Stadlbauer, H. Nonaka, A. Ojida, I. Hamachi, B. König, *Eur. J. Org. Chem.,* 2011, 2807–2817.

[121] Q. Zou, J. Jin, B. Xu, L. Ding, H. Tian, *Tetrahedron,* 2011, **67**, 915-921.

[122] C. Jia, B. Wu, S. Li, X. Huang, X. –J. Yang, *Org. Lett.*, 2010, **12**, 5612-5615.

[123] J. Wen, Z. Geng, Y. Yin, Z. Zhang, Z. Wang, *Dalton Trans.,* 2011, **40**, 1984-1989.

[124] Mitra, V. K. Hinge, A. Mittal, S. Bhakta, P. Guionneau, C. P. Rao, *Chem. Eur. J.,* 2011, **17**, 8044 – 8047.

[125] K. Ghosh, I. Saha, *New J. Chem.,* 2011, **35**, 1397–1402.

[126] T. D. Thangadurai, G. Chung, O. Kwon, D. Jin, Y. –I. Lee, *Tetrahedron Lett.*, 2011, **52**, 6465-6469.

[127] H. Maeda, Y. Bando, K. Shimomura, I. Yamada, M. Naito, K. Nobusawa, H. Tsumatori, T. Kawai, *J. Am. Chem. Soc*., 2011, 133, 9266-9269.

[128] Q. –S. Lu, J. Zhang, L. Jiang, J. –T. Hou, X. –Q. Yu, *Tetrahedron Lett.*, 2010, *51*, 4395-4399.

[129] L. Yang, S. Qin, X. Su, F. Yang, J. You, C. Hu, R. Xie, J. Lan, *Org. Biomol. Chem.*, 2010, 8, 339-348.

[130] S. Kondo, M. Nagamine, S. Karasawa, M. Ishihara, M. Unno, Y. Yano, *Tetrahedron,* 2011, **67**, 943-950.

[131] C. H. Chen, M. Leung, *Tetrahedron,* 2011, **67**, 3924-3935.

[132] K. M. K. Swamy, N. J. Singh, J. Yoo, S. K. Kwon, S. –Y. Chung, C. –H. Lee, J. Yoon, *J. Incl. Phenom. Macrocycl. Chem.*, 2010, **66**, 107-111.

[133] B. Roy, A. Rao, K. H. Ahn, *Org. Biomol. Chem.,* 2011, **9**, 7774–7779.

[134] X. Chen, H. Wang, X. Jin, J. Feng, Y. Wang, P. Lu, *Chem. Commun*., 2011, **47**, 2628-2630.

[135] C. Park, J. –I. Hong, *Tetrahedron Lett.*, 2010, **51**, 1960-1962.

[136] D. Moreno, J. V. Cuevas, G. García-Herbosa, T. Torroba, *Chem. Commun*., 2011, **47**, 3183–3185.

[137] N. Singh, D. O. Jang, *Tetrahedron Lett.,* 2011, **52**, 2608-2610.

[138] Y. Wu, H. Guo, X. Zhang, T. D. James, J. Zhao, *Chem. Eur. J.,* 2011, **17**, 7632 – 7644..

[139] D. Siebler, C. Förster, K. Heinze, *Eur. J. Inorg. Chem.*, 2010, 523-527.

[140] K. R. Dey, B. M. Wong, M. A. Hossain, *Tetrahedron Lett.*, 2010, **51**, 1329-1332.

[141] V. Bhalla, R. Tejpal and M. Kumar, *Dalton Trans.,* 2012, **41**, 403-407.

[142] H. Szelke, S. Schübel, J. Harenberg, R. Krämer, *Chem. Commun.*, 2010, **46**, 1667-1669.

[143] D. Wang, X. Zhang, C. He, C. Duan, *Org. Biomol. Chem.*, 2010, **8**, 2923-2925.

[144] A. J. Moro, P. J. Cywinsky, S. Kὸrsten, G. J. Mohr, *Chem. Commun.*, 2010, **46**, 1085-1087.

[145] J. Xiong, L. Sun, Y. Liao, G. –N. Li, J. –L. Zuo, X. –Z. You, *Tetrahedron Lett.*, 2011, **52**, 6157-6161.

[146] T. Cheng, T. Wang, W. Zhu, X. Chen, Y. Yang, Y. Xu, X. Qian, *Org. Lett.*, 2011, **13**, 3656-3659.

[147] J. Wang, Y. Hou, C. Li, B. Zhang, X. Wang, *Sensors Actuators B,* 2011, **157**, 586-593.

[148] H. Y. Kuchelmeister, C. Schmuck, *Chem. Eur. J*., 2011, **17**, 5311-5318.

[149] J. Szmytkowski, S.M.K. Brunet, U. Tripathy, J. A. O'Brien, M. F. Paige, R. P. Steer, *Chem. Phys. Lett.,* 2011, **501**, 278–282.

[150] M. R. Rao, M. Ravikanth, *Eur. J. Org. Chem.* 2011, 1335–1345.

[151] A. Dorazco-González, H. Höpfl, F. Medrano, A. K. Yatsimirsky, *J. Org. Chem*., 2010, **75**, 2259-2273.

[152] A. N. Swinburne, M. J. Patterson, A. Beeby, J. W. Steed, *Org. Biomol. Chem.*, 2010, **8**, 1010-1016.

[153] V. Amendola, L. Fabbrizzi, E. Monzani, Chem. Eur. J., 2004, 10, 76-82.

[154] L. M. Jordan, P. D. Boyle, A. L. Sargent, W. E. Allen, *J. Org. Chem.*, 2010, **75**, 8450-8456.

[155] C. Bazzicalupi, A. Bencini, S. Puccioni, B. Valtancoli, P. Gratteri, A. Garau, V. Lippolis, *Chem. Commun*., 2012, **48**, 139–141.

[156] C. Carroll, B. Coombs, S. McClintock, C. Johnson II, O. Berryman, D. Johnson, M. Haley, *Chem. Commun.*, 2011, **47**, 5539–5541.

[157] X. Wanga, C. Zhangb, L. Fengb, L. Zhang, *Sens. Actuators B*, 2011, **156**, 463–466.

[158] R. Koteeswari, P. Ashokkumar, V. T. Ramakrishnan, E. J. P. Malar, P. Ramamurthy, *Chem. Commun.*, 2010, **46**, 3268-3270.

[159] I. Ravikumar, P. Ghosh, *Inorg. Chem.,* 2011, **50**, 4229–4231.

[160] S. Goswami, D. Sen, N. K. Das, *Tetrahedron Lett.*, 2010, **51**, 6707-6710.

[161] C. He, X. Qian, Y. Xu, C. Yang, L. Yin and W. Zhu, *Dalton Trans.,* 2011, **40**, 1034-1037.

[162] C. L. Do-Thanh, M. M. Rowland, M. D. Best, *Tetrahedron,* 2011, **67**, 3803-3808.

[163] M. Alfonso, A. Espinosa, A. Tarraga, P. Molina, *Org. Lett.*, 2011, **13**, 2078-2081.

[164] M. K. Chae, J. –M. Suk, K. –S. Jeong, *Tetrahedron Lett.*, 2010, **51**, 4240-4242.

[165] S. Saha, A. Ghosh, P. Mahato, S. Mishra, S. K. Mishra, E. Suresh, S. Das, A. Das, *Org. Lett.*, 2010, **12**, 3406-3409.

[166] Y. Abraham, H. Salman, K. Suwinska, Y. Eichen, *Chem. Commun.,* 2011, **47**, 6087–6089.

[167] F. Zapata, A. Caballero, A. Tárraga, P. Molina, *J. Org. Chem.*, 2010, **75**, 162-169.

[168] M. Alfonso, A. Tarraga, P. Molina, *Org. Lett.*, 2011, **13**, 6432-6435.

[169] D. Curiel, M. Más-Montoya, G. Sánchez, R. A. Orenes, P. Molina, A. Tárraga, *Org. Biomol. Chem.*, 2010, **8**, 4811-4814.

[170] C. Bejger, J. S. Park, E. S. Silver, J. L. Sessler, *Chem. Commun.*, 2010, **46**, 7745-7747.

[171] A. Helal, H. –S. Kim, *Tetrahedron*, 2010, **66**, 7097-7103.

[172] D. Lee, N. Singh, M. J. Kim, D. Jang, *Org. Lett.*, 2011, **13**, 3024-3027.

[173] F. S. Raad, A. O. El-Ballouli, R. M. Moustafa, M. H. Al-Sayah, B. R. Kaafarani, *Tetrahedron*, 2010, **66**, 2944-2952.

[174] L. –M. Tumir, M. Grabar, S. Tomić, I. Piantanida, *Tetrahedron*, 2010, **66**, 2501-2513.

[175] K. R. Rathikrishnan, V. K. Indirapriyadharshini, S. Ramakrishna, R. Murugan, *Tetrahedron,* 2011, **67**, 4025-4030.

[176] S. Goswami, A. Hazra, M. K. Das, *Tetrahedron Lett.*, 2010, **51**, 3320-3323.

[177] P. Singh, J. Kaur, W. Holzer, *Sensors Actuators B*, 2010, **150**, 50-56.

[178] J. Kaur, P. Singh, *Chem. Commun*., 2011, **47**, 4472–4474.

[179] W. -H. Chen, Y. Xing, Y. Pang, *Org. Lett*., 2011, **13**, 1362-1365.

[180] P. Das, A. Ghosh, M. Kesharwani, V. Ramu, B. Ganguly, A. Das, *Eur. J. Inorg. Chem.,* 2011, 3050-3058.

[181] H. Li, R. Lalancette, F. Jäkle, *Chem. Commun.,* 2011, **47**, 9378–9380.

[182] M. M. M. Raposo, B. García-Acosta, T. Ábalos, P. Calero, R. Martínez-Máñez, J. V. Ros-Lis, J. Soto, *J. Org. Chem.*, 2010, **75**, 2922-2933.

[183] N. Shao, J. Jin, H. Wang, J. Zheng, R. Yang, W. Chan, Z. Abliz, *J. Am. Chem. Soc.*, 2010, **132**, 725-736.

[184] Y. Kurishita, T. Kohira, A. Ojida, I. Hamachi, *J. Am. Chem. Soc.*, 2010, **132**, 13290-13299.

[185] H. J. Kim, J. H. Lee, J. –I. Hong, *Tetrahedron Lett.*, 2011, **52**, 4944-4946.

[186] S. O. Jung, J. Y. Ahn, S. Kim, S. Yi, M. H. Kim, H. H. Jang, S. H. Seo, M. S. Eom, S. K. Kim, D. H. Ryu, S. –K. Chang, M. S. Han, *Tetrahedron Lett.*, 2010, **51**, 3775-3778.

[187] Y. –K. Yang, S. Shim, J. Tae, *Chem. Commun.*, 2010, **46**, 7766-7768.

[188] C. Kaewtong, J. Noiseephum, Y. Uppa, N. Morakot, N. Morakot, B. Wanno, T. Tuntulani, B. Pulpoka, *New J. Chem.*, 2010, **34**, 1104-1108.

[189] K. Sasakura, K. Hanaoka, N. Shibuya, Y. Mikami, Y. Kimura, T. Komatsu, T. Ueno, T. Terai, H. Kimura, T. Nagano, *J. Am. Chem. Soc.* 2011, **133**, 18003–18005.

[190] Z. Xu, N. R. Song, J. H. Moon, J. Y. Lee, J. Yoon, *Org. Biomol. Chem.*, 2011, **9**, 8340-8345.

[191] Z. Xu, N. J. Singh, S. K. Kim, D. R. Spring, K. S. Kim, J. Yoon, *Chem. Eur. J.*, 2011, **17**, 1163-1170.

[192] A. Chakraborty, R. Gunupuru, D. Maity, S. Patra, E. Suresh, P. Paul, *Inorg. Chem. Comm.*, 2010, **13**, 1522-1526.

[193] S. Patra, V. P. Boricha, K. R. Sreenidhi, E. Suresh, P. Paul, *Inorg. Chim. Acta*, 2010, **363**, 1639-1648.

[194] D. Saha, S. Das, C. Bhaumik, S. Dutta, S. Baitalik, *Inorg. Chem.*, 2010, **49**, 2334-2348.

[195] B. Wu, J. Yang, X. Huang, S. Li, C. Jia, X. J. Yang, N. Tang, C. Janiak, *Dalton Trans*. 2011, **40**, 5687-4696.

[196] S. Das, D. Saha, C. Bhaumik, S. Dutta, S. Baitalik, *Dalton Trans.,* 2010, **39**, 4162–4169.

[197] V. Vajpayee, Y. H. Song, M. H. Lee, H. Kim, M. Wang, P. J. Stang, K. W. Chi, *Chem. Eur. J.* 2011, **17**, 7837-7844.

[198] C. Castillo, D. Davies, A. Duhme, K. Singh, S. Singh, *Dalton Trans.* 2012, **41**, 628-635.

[199] M. C. L. Yeung, V. W. W. Yam, *Chem. Eur. J.* 2011, **17**, 11987-11990.

[200] C. Song, Z. Ye, G. Wang, J. Yuan, Y, Guan, *Chem. Eur. J.*, 2010, **16**, 6464-6472.

[201] M. M. G. Dos Santos, A. J. Harte, S. J. Quinn, T. Gunnlaugsson, *Coord. Chem. Rev.*, 2008, **252**, 2512-2527.

[202] T. L. Esplin, M. L. Cable, H. B. Gray, A. Ponce, *Inorg. Chem.*, 2010, **49**, 4643-4647.

[203] R. Tripier, C. Platas-Iglesias, A. Boos, J.-F. Morfinm, L. Charbonnière, *Eur. J. Inorg. Chem.*, 2010, 2735-2745.

[204] S. Shinonda, K. Yano, H. Tsukube, *Chem. Comm.*, 2010, **46**, 3110-3112.

[205] H. P. Wang, H. G. Li, G. N. Lu, N. Tang, W. S. Liu, Y. Tang, *Inorg. Chem. Comm.*, 2010, **13**, 882-886.

[206] J. H. Lee, A. R. Jeong, I. S. Shin, H. J. Kim, J. I. Hong, *Org. Lett.*, 2010, **12**, 764-767.

[207] S. Rochat, K. Severin, *Chem. Commun.*, 2011, **47**, 4391-4393.

[208] R. Villamil-Ramos, A. K. Yatsimirsky, *Chem. Commun.*, 2011, **47**, 2694-2696.

[209] X. B. Zhou, W. H. Chan, A. W. M. Lee, *Tetrahedron Lett.* 2011, **52**, 5431–5434.

[210] A. Mitra, J. P. Chinta, C. P. Rao, *Tetrahedron Lett.*, 2010, **51**, 139-142.

[211] K. Ghosh, I. Saha, G. Masanta, E. B. Wang, C. A. Parish, *Tetrahedron Lett.*, 2010, **51**, 343-347.

[212] K. Dhara, U. C. Saha, A. Dan, S. Sarkar, M. Manassero, P. Chattopadhyay, *Chem. Commun.*, 2010, **46**, 1754-1756.

[213] J. J. Gassensmith, S. Matthys, J. –J. Lee, A. Wojcik, P. V. Kamat, B. D. Smith, *Chem. Eur. J.*, 2010, **16**, 2916-2921.

[214] A. Späth, B. König, *Tetrahedron*, 2010, **66**, 1859-1873.

[215] Y. Zhao, Y. C. Yang, S. M. Chi, H. Shi, Y. Zhao, H. Y. Zhu, Q. L. Li, Y. F. Wang, *Helv. Chim. Acta*, 2010, **93**, 999-1011.

[216] S. D. Taylor, W. Howard, N. Kaval, R. Hart, J. A. Krause, W. B. Connick, *Chem. Commun*., 2010, **46**, 1070-1072.

[217] R. K. Pathak, K. Tabbasum, V. K. Hinge, C. P. Rao, *Chem. Eur. J.* 2011, **17**, 13999 -14003.

[218] S. Zhang, T. E. Glass, *Tetrahedron Lett.*, 2010, **51**, 112-114.

[219] K. P. Diya, S. Sreejith, B. Balakrishna, P. Jayamurthy, P. Anees, A. Ajayaghosh, *Chem. Comm.*, 2010, **46**, 6069-6071.

[220] W. Lu, H. Jiang, F. Hu, L. Jiang, Z. Shen, *Tetrahedron,* 2011, **67**, 7909-7912.

[221] J. H. Lee, A. Reum Jeong, J. –H. Jung, C. –M. Park, J. –I. Hong, *J. Org. Chem.*, 2011, **76**, 417-423.

[222] S. J. Butler, K. A. Jolliffe, *Org. Biomol. Chem.* 2011, **9,** 3471–3483.

[223] F. Wang, J. Wu, X. Zhuang, W. Zhang, W. Liu, P. Wang, S. Wu, *Sensors and Actuators B*, 2010, **146**, 260-265.

[224] E. Gaidamasuskas, D. C. Crans, H. Parker, K. Saejueng, B. A. Kashemirov, C. E. McKenna, *New. J. Chem.*, 2011, **35**, 2877-2883.

[225] M. A. Saeed, D. R. Powell, M. A. Hossain, *Tetrahedron Lett.* , 2010, **51**, 4904-4907.

[226] X. Chen, S. W. Nam, G. H. Kim, N. Song, Y. Jeong, I. Shin, S. K. Kim, J. Kim, S. Park, J. Yoon, *Chem. Commun*, 2010, **46**, 8953-8955.

[227] Z. Xu, J. Pan, D. R. Spring, J. Cui, J. Yoon, *Tetrahedron*, 2010, **66**, 1678-1683.

[228] X. Cao, W. Lin, L. He, *Org. Lett.*, 2011, **13**, 4716-4719.

[229] V. Amendola, G. Bergamarchi, A. Buttafava, L. Fabbrizzi, E. Monzani, *J. Am. Chem. Soc.*, 2010, **132**, 147-156.

[230] H. S. Jung, J. H. Han, Z. H. Kim, C. Kang, J. S. Kim, *Org. Lett.,* 2011, **19**, 5056-5059.

[231] H. S. Jung, J. H. Han, Y. Habata, C. Kang, J. S. Kim, *Chem. Commun.,* 2011, **47**, 1622-1624.

[232] H. Gee, C. Lee, Y. Jeong, W. Jang, *Chem. Commun.,* 2011, **47**, 11963-11965.

[233] T. Riis-Johannessen, K. Schenk, K. Severin, *Inorg. Chem.*, 2010, **49**, 9546-9553.

[234] Y. B. Ruan, A. F. Li, J. S. Zhao, J. S. Shen, Y. B. Yao, *Chem. Commun*, 2010, **46**, 4938-4940.

[235] J. Wu, R. Sheng, W. Liu, P. Wang. J. Ma, H. Zhang, X. Zhuang, *Inorg. Chem.*, 2011, **50**, 6543-6551.

[236] B. Ma, F. Zeng, F. Zheng, S. Wu, *Chem. Eur. J.*, 2011, **17**, 14844-14850.

[237] C. Luo, Q. Zhou, B. Zhang, X. Wang, *New J. Chem.*, 2011, **35**, 45–48.

[238] J. Gao, T. R. Johannessen, R. Scopelliti, X. Qian, K. Severin, *Dalton Trans.*, 2010, **39**, 7114-7118.

[239] H. Wang, L. Xue, H. Jiang, *Org. Lett.*, 2011, **13**, 3844-3847.

[240] P. Sokkalingam, J. Yoo, H. Hwang, P. H. Lee, Y. M. Jung, C. –H. Lee, *Eur. J. Org. Chem.*, 2011, 2911-2915.

[241] D. Quiñonero, K. A. López, P. M. Deyà, M. N. Piña, J. Morey, *Eur. J. Org. Chem.*, 2011, 6187-6194.

[242] S. Huang, Y. Shi, N. Li, H. Luo, *Chem. Commun*., 2012, **48**, 747–749.

[243] D. Buckland, S. v. Bhosale, S. J. Langford, *Tetrahedron Lett.,* 2011, **52**, 1990-1992.

[244] H. Lu, Q. Wang, Z. Li, G. Lai, J. Jiang, Z. Shen, *Org. Biomol. Chem.,* 2011, **9**, 4558-4562.

[245] P. Sokkalingam, C-H. Lee, *J. Org. Chem.*, 2011, **76**, 3820-3828.

[246] B. Zhu, F. Yuan, R. Li, Q. Wei, Z. Ma, B. Du, X. Zhang, *Chem. Commun.*, 2011, **47**, 7098-7100.

[247] X. Cao, W. Lin, Q. Yu, J. Wang, *Org. Lett.*, 2011, **13**, 6098-6101.

[248] V. Bhalla, H. Singh, M. Kumar, *Org. Lett.*, 2010, **12**, 628-631.

[249] R. Hu, J. Feng, D. Hu, S. Wang, S. Li, Y. Li, G. Yang, *Angew. Chem. Int. Ed.*, 2010, **49**, 4915-4918.

[250] O. A. Bozdemir, F. Sozmen, O. Buyukcakir, R. Gulyev, Y. Cakmak, E. U. Akkaya, *Org. Lett.*, 2010, **12**, 1400-1403.

[251] M. R. Rao, S. M. Mobin, M. Ravikanth, *Tetrahedron*, 2010, **66**, 1728-1734.

[252] L. Fu, F. L. Jiang, P. D. Harvey, Y. Liu, *Chem. Commun.*, 2011, **47**, 5503-5505.

[253] J. F. Zhang, C. S. Lim, S. Bhuniya, B. R. Cho, J. S. Kim, *Org. Lett.*, 2011, **13**, 1190-1193.

[254] V. Bhalla, R. Tejpal, M. Kumar, *Tetrahedron*, 2011, **67**, 1266-1271.

[255] H.C. Schmidt, L. G. Reuter, J. Hamacek, O. S. Wenger, *J. Org. Chem.*, 2011, **76**, 9081-9085.

[256] G.-L. Fu, H. Pan, Y.-H.-Zhao, C.-H. Zhao, *Org. Biomol. Chem.*, 2011, **9**, 8141-8146.

[257] Y.-H.-Zhao, H. Pan, G.-L. Fu, J.-M. Lin, C.-H. Zhao, *Tetrahedron Lett.*, 2011, **52**, 3832-3835.

[258] X. He, V. W.-W. Yam, *Org. Lett.*, 2011, **13**, 2172-2175

[259] Y. Sun, Z. M. Hudson, Y. Rao, S. Wang, *Inorg. Chem.*, 2011, **50**, 3373-3378.

[260] W. J. Xu, S. J. Liu, X. Y. Zhao, S. Sun, S. Cheng, T. C. Ma, H. B. Sun, Q. Zhao, W. Huang, *Chem. Eur. J.*, 2010, **16**, 7125-7133.

[261] L. Dudek, J. Grolik, A. Kazmierska, E. Szneler, A. Eilmes, K. Stadnicka, J. Eilmes, *Tetrahedron Lett.*, 2011, **52**, 3597-3601.

[262] B. Zhang, Y. Li, W. Su, *Eur. J. Inorg. Chem.*, 2011, 4964-4969.

[263] G. Li, W-T. Gong, J-W. Ye, Y. Lin, G.-L. Ning, *Tetrahedron Lett.,* 2011, **52**, 1313-1316.

[264] C. Padié, K. Zeitler, *New J. Chem.,* 2011, **35**, 994-997.

[265] R. M. Duke, T. Gunnlaugsson, *Tetrahedron Lett.,* 2011, **52**, 1503-1505.

[266] N. Ahmed, I. Geronimo, I. C. Hwang, N. J. Singh, and K. S. Kim, *Chem. Eur. J.* 2011, **17**, 8542-8548.

[267] J. J. Park, Y. –H. Kim, C. Kim, J. Kang, *Tetrahedron Lett.*, 2011, **52**, 3361-3366.

[268] G. Pereira, E. M. S. Castanheira, P. M. T. Ferreira, M. –J. R. P. Queiroz, *Eur. J. Org. Chem.*, 2010, 464-475.

[269] S. Rivadehi, E. F. Reid, C. F. Hogan, S. V. Bhosale, S. J. Langford, *Org. Biomol. Chem.*, 2012, **10**, 705-709.

[270] S. Guha, S. Saha, *J. Am. Chem. Soc.*, 2010, **132**, 17674-17677.

[271] S. H. Mashraqui, R. Betkar, M. Chandiramani, D. Quiñonero, A. Frontera, *Tetrahedron Lett.*, 2010, **51**, 596-599.

[272] M. V. López, M. R. Bermejo, M. E. Vázquez, A. Taglietti, G. Zaragoza, R. Pedrido, M. M. Calvo, *Org. Biomol. Chem.*, 2010, **8**, 357-362.

[273] Y. Qu, J. Hua, H. Tian, *Org. Lett.*, 2010, **12**, 3320-3323.

[274] V. Luxami, A. Kumar, M. S. Hundal, S. Kumar, *Sensor and Actuators B*, 2010, **145**, 1-6.

[275] Z. Liu, X. Wang, Z. Yang, W. He, *J. Org. Chem.* 2011, **76**, 10286−10290.

[276] Y. Kim, H-S. Huh, M. H. Lee, I. L. Lenov, H. Zhao, F. P. Gabbai, *Chem. Eur. J.,* 2011, **17**, 2057–2062.

[277] A. Chaicham, S. Kulchat, G. Tumcharern, T. Tuntulani, B. Tomapatanaget, *Tetrahedron*, 2010, **66**, 6217-6223.

[278] S. H. Mashraqui, R. Betkar, M. Chandiramani, C. Estarellas, A. Frontera, *New J. Chem.,* 2011, **35**, 57-60.

[279] X. Lv, J. Liu, Y. Liu, Y. Zhao, Y.-Q. Sun, P. Wang, W. Guo, *Chem. Commun.,* 2011, **47**, 12843-12845.

[280] H. J. Kim, K. C. Ko, J. H. Lee, J. Y. Lee, J. S. Kim, *Chem. Commun.,* 2011, **47**, 2886-2888.

[281] G. J. Kim, H. J. Kim, *Tetrahedron Lett.*, 2010, **51**, 185-187.

[282] G. J. Kim, H. J. Kim, *Tetrahedron Lett.*, 2010, **51**, 2914-2916.

[283] Y. Shirashi, S. Sumiya, T. Hirai, *Chemm. Commun.*, 2011, **47**, 4953-4955.

[284]X. Lv, J. Liu, Y. Liu, Y. Zhao, M. Chen, P. Wang, W. Guo, *Org. Biomol. Chem.,* 2011, **9**, 4954–4958.

[285] S. Park, H. J. Kim, *Chem. Commun.*, 2010, **46**, 9197-9199.

[286] H. Yu, Q. Zhao, Z. Jiang, J. Qin, Z. Li, *Sensors Act. B*, 2010, **148**, 110-116.

[287] H. Li, B. Li, L. Y. Jin, Y. Kan, B. Yin, *Tetrahedron,* 2011, **67**, 7348-7353.

[288] Y. M. Dong, Y . Peng, M. Dong, Y. W. Wang, *J. Org. Chem.*, 2011, **76**, 6962-6966.

[289] S. Yadav, S. Ghosh, *Org. Lett.*, 2010, **12**, 2646-2649.

[290] A. Ghosh, P. Das, S. Saha, T. Banerjee, H. B. Bhatt, A. Das, *Inorg. Chim. Acta*, 2011, **372**, 115-119.

[291] R. Dey, T. Chatterjee, B. C. Ranu, *Tetrahedron Lett.*, 2011, **52**, 461-464.

[292] S. Quinghai, J. W. Bats, M. Schmittel, *Inorg. Chem.*, 2011, **50**, 10531-10533.

[293] H. Marom, Y. Popowski, S. Antonov, M. Gozin, *Org. Lett.,* 2011, **13**, 5532-5535.

[294] F. Yu, P. Li, G. Zhao, T. Chu, K. Han, *J. Am. Chem. Soc.,* 2011, **133**, 11030-11033.

[295] K. Xu, H. Chen, J. Tian, B. Ding, Y. Xie, M. Qiang, B. Tang, *Chem. Commun.,* 2011, **47**, 9468-9470.

[296] D. Oushiki, H. Kojima, T. Terai, M. Arita, K. Hanaoka, Y. Urano, T. Nagano, *J. Am. Chem. Soc.*, 2010, **132**, 2795-2801.

[297] Y. Lin, Y. Sun, J. Du, X. Lv, Y. Zhao, M. Chen, P. Wang, W. Guo, *Org. Biomol. Chem.,* 2011, **9**, 432-437.

[298] W. Zhang, C. Guo, L. Liu, J. Qin, C. Yang, *Org. Biomol. Chem.,* 2011, **9**, 5560-5563.

[299] L. Yuan, W. Lin, J. Song, Y. Yang, *Chem. Commun.,* 2011, **47**, 12691-12693.

[300] J. Shi, Q. Li, X. Zhang, M. Peng, J. Qin, Z. Li, *Sensors and Actuators B*, 2010, **145**, 583-587.

[301] X. Chen, K. A. Lee, E. –M. Ha, K. M. Lee, Y. Y. Seo, H. K. Choi, N. N. Kim, C. –S. Cho, S. Y. Lee, W. –J. Lee, J. Yoon, *Chem. Commun.*, 2011, **47**, 4373-4375.

[302] H. Peng, Y. Cheng, C. Dai, A. L. King, B. L. Predmore, D. J. Lefer, B. Wang, *Angew. Chem. Int. Ed.,* 2011, **50**, 9672-9675.

[303] C. Liu, J. Pan, S. Li, Y. Zhao, L.Y. Wu, C. E. Berkman, A. R. Whorton, M. Xian, *Angew. Chem. Int. Ed.,* 2011, **50**, 10327-10329.

[304] M. G. Choi, J. Hwang, S. Eor, S. K. Chang, *Org. Lett.*, 2010, **12**, 5624-5627.

[305] X. Gu, C. Liu, Y. C. Zhu, Y. Z. Zhu, *J. Agr. Food. Chem.*, 2011, **59**, 11935-11939.

[306] R. M: Duke, T. Gunnlaugsson, *Tetrahedron Lett.*, 2010, **51**, 5402-5405.

[307] F. M. Muñiz, V. Alcázar, F. Sanz, L. Simon, A. L. Fuentes de Arriba, C. Raposo, J. R. Morán, *Eur. J. Org. Chem.*, 2010, 6179-6185.

[308] M. G. Choi, S. Cha, J. E. Park, H. Lee, L. Jeon, S. K. Chang, *Org. Lett.*, 2010, **12**, 46, 1468-1471.

[309] Y. Zhou, J. Won, J. Y. Lee, Y. Yoon, *Chem. Commun.*, 2011, **47**, 1997-1999.

[310] H. Y. Shiu, H. C. Chong, Y. C. Leung, M. K. Wong, C. M. Che , *Chem. Eur. J.*, 2010, **16**, 3308-3313.

[311] H.-Y. Shiu, M.-K. Wong, C.-M. Che, *Chem. Commun.,* 2011, **47**, 4367-4369.

[312] L. Long, W. Lin, B. Chen, W. Gao, L. Yuan, *Chem. Commun.*, 2011, **47**, 893-895.

[313] S.-Y. Lim, S. Lee, S. B. Park, H.-J. Kim, *Tetrahedron Lett.,* 2011, **52**, 3902-3904.

[314] Y.-Q. Sun, M. Chen, J. Liu, X. Lv, J.-F. Li, W. Guo, *Chem. Commun.,* 2011, **47**, 11029-11031.

[315] H. S. Jung, K. C. Ko, G.-H. Kim, A.-R. Lee, Y.C. Na, C. Kang, J. Y. Lee, J. S. Kim, *Org. Lett.,* 2011, **13**, 1498-1501.

[316] O. García-Beltrán, N. Mena, E. G. Pérez, B. K . Cassels, M. T. Nuñez, F. Werlinger, D. Zavala, M. E. Aliaga, P. Pavez, *Tetrahedron Lett.,* 2011, **52**, 6606-6609.

[317] H.-J. Ha, D.-H. Yoon, S. Park, H.-J. Kim, *Tetrahedron,* 2011, **67**, 7759-7762.

[318] X. Chen, S. –K. Ko, M. J. Kim, J. Yoon, *Chem. Commun.*, 2010, **46**, 2751-2753.

[319] F. J. Huo, Y. Q. Sun, J. Su, Y. U. Yang, C. X. Yin, J. B. Chao, *Org. Lett.*, 2010, **12**, 4756-4759.

[320] N. Zhao, Y. H. Wu, L. X. Shi, Q. P. Lin, Z. N. Chen, *Dalton Trans.*, 2010, **39**, 8288-8295.

[321] L. Deng, W. Wu, H. Guo, J. Zhao, S. Ji, X. Zhang, X. Yuan, C. Zhang, *J. Org. Chem.*, 2011, **76**, 9294-9304.

[322] H. Kwon, K. Lee, H. J. Kim, *Chem. Commun.,* 2011, **47**, 1773-1775.

[323] X. Cao, W. Lin, Q. Yu, *J. Org. Chem.,* 2011, **76**, 7423-7430.

[324] B. Zhu, X. Zhang, Y. Li, P. Wang, H. Zhang, X. Zhuang, *Chem. Commun.*, 2010, **46**, 5710-5712.

[325] J. H. Lee, C. S. Lim, Y. S. Tian, J. H. Han, B. R. Cho, *J. Am. Chem. Soc.*, 2010, **132**, 1216-1217.

[326] Y. Yue, Y. Guo, J. Xu, S. Shao, *New J. Chem*., 2011, **35**, 61-64.

[327] L. Yuan, W. Lin, Y. Yang, Che, *Chem. Commun.,* 2011, **47**, 6275-6277.

[328] M. Hu, J. Fan, H. Li, K. Song, S. Wang, G. Cheng, X. Peng, *Org. Biomol. Chem.,* 2011, **9**, 980-983.

[329] S. Lim, J. O. Escobedo, M. Lowry, X. Xu, R. Strongin, *Chem. Comm.*, 2010, **46**, 5707-5709.

[330] R. Zhang, X. Yu, Z. Ye, G. Wang, W. Zhang, J. Yuan, *Inorg. Chem.*, 2010, **49**, 7898-7903.

[331] L. Xiong, Q. Zhao, H. Chen, Y. Wu, Z. Dong, Z. Zhou, F. Li, *Inorg. Chem,* 2010*,* **49**, 6402-6408.

[332] H. Guo, Y. Jing, X. Yuan, S. Ji, J. Zhao, X. Li, Y. Kan, *Org. Biomol. Chem.,* 2011, **9**, 3844-3853.

[333] X. Li, S. Qian, Q. He, B. Yang, J. Li, Y. Hu, *Org. Biomol. Chem.*, 2010, **8**, 3627-3630.

[334] M. Lan, J. Wu, W. Liu, H. Zhang, W. Zhang, X. Zhuang, P. Wang, *Sens. Act. B*, 2011, **156**, 332–337.

[335] Y. Zhai, L. Jin, P. Wang, S. Dong, *Chem. Commun.*, 2011, **47**, 8268-8270.

[336] X. Lou, Y. Zhang, J. Qin, Z. Li, *Chem. Eur. J.*, 2011, **17**, 9691-9696.

[337] Z. Huang, F. Pu, Y. Lin, J. Ren, X. Qu, *Chem. Commun.*, 2011, **47**, 3487-3489.

[338] H. X. Zhao, L. Q. Liu, Z. D. Liu, Y. Wang, X. J. Zhao, C. Z. Huang, *Chem. Commun.*, 2011, **47**, 2604-2606.

[339] J. Liu, C. Bao, X. Zhong, C. Zhao, L. Zhu, *Chem. Commun.*, 2010, **46**, 2971-2793.

[340] A. J. Moro, J. Schmidt, T. Doussineau, A. Lapesta-Fernandez, J. Wegener, G. J. Mohr, *Chem. Commun.*, 2011, **47**, 6066-6068.

[341] P. Calero, M. Hecht, R. Martínez-Máñez, F. Sancenón, J. Soto, J. L. Vivancos, K. Rurack, *Chem. Commun.*, 2011, **47**, 10599-10601.

[342] C. Tan, Q. Wang, *Inorg. Chem*., 2011, **50**, 2953–2956.

[343] H. Yan, H. Li, *Sens. Actuators, B*, 2010, **148**, 81-86.

[344] J. Tian, H. Chen, L. Zhuo, Z. Xie, N. Li, B. Thang, *Chem. Eur. J.*, 2011, **17**, 6626-6634.

[345] T. Riis-Johanssenn, K. Severin, *Chem. Eur. J.*, 2010, **16**, 8291-8295.

[346] X. Chen, S. Kang, M. J. Kim, J. Kim, Y. S. Kim, H. Kim, B. Chi, S-J Kim, J. Y. Lee, J. Yoon, *Angew. Chem. Int. Ed.*, 2010, **49**, 1422-1425.

[347] X. Zhao, K. Schanze, *Chem. Commun*., 2010, **46**, 6075-6077.

[348] Z. Guo, W. Zhu, H. Tian, *Macromolecules*, 2010, **43**, 739-744.

[349] X. Wu, B. Xu, H. Tong, L. Wang, *Macromolecules*, 2011, **44**, 4241-4248.

[350] M. Naito, M. Nakamura, K. Terao, T. Kawabe, M. Fujiki, *Macromolecules*, 2010, **43**, 7919-7923.

[351] G. Saikia, P. K. Iyer, *Macromolecules*, 2011, **44**, 3753-3758.

[352] A. Rostami, C. J. Wei, G. Gurin, M. S. Taylor, *Angew. Chem. Int.,* 2011, **50**, 2059 –2062.

[353] B. Gruber, S. Stadlbauer, A. Späth, S. Weiss, M. Kalinina, B. König, *Angew. Chem. Int. Ed*., 2010, **49**, 7125-7128.

[354] B. Gruber, S. Stadlbauer, K. Woinaroschy, B. König, *Org. Biomol. Chem*., 2010, **8**, 3704-3714.

[355] D. Xu, X. Liu, R. Lu, P. Xue, X. Zhang, H. Zhou, J. Jia, *Org. Biomol. Chem*., 2011, **9**, 1523-1528.

[356] T. Li, R. Fu, H. G. Park, *Chem. Commun.,* 2010, **46**, 3271-3273.

[357] J. -H. Kim, J. -H. Ahn, P. W. Barone, H. Jin, J. Zhang, D. A. Heller, M. S. Strano, *Angew. Chem. Int. Ed*., 2010, **49**, 1456-1459.

[358] C. Zhao, K. Qu, Y. Song, C. Xu, J. Ren, X. Qu, *Chem. Eur. J.,* 2010, **16**, 8147-8154.

[359] W. Y. Xie, W. T. Huang, N. B. Li, H. Q. Luo, *Chem. Commun.*, 2012, **48**, 82-84.